



Tibetan pasture degradation under the impact of global change:
Consequences for carbon and nutrient cycles and recovery strategies

Dissertation

to obtain the Doctor of Philosophy (Ph.D.)

within the doctoral degree program

of the Faculty of Forest Sciences and Forest Ecology

of the Georg-August University of Göttingen

by

Shibin Liu

born in 1987 in Henan

Göttingen, 2013-2017

Members of the thesis committee (supervisors):

1. Prof. Dr. Yakov Kuzyakov, Department of Soil Science of Temperate Ecosystems and Department of Agricultural Soil Science, Georg-August University of Göttingen
2. Prof. Dr. Michaela Dippold, Department of Biogeochemistry of Agroecosystems, Georg-August University of Göttingen
3. Prof. Dr. Sandra Spielvogel, Institute of Geography, University of Bern
4. Prof. Dr. Bruno Glaser, Department of Soil Biogeochemistry, Martin-Luther-University of Halle-Wittenberg
5. Prof. Dr. Christoph Leuschner, Department of Plant Ecology and Ecosystems Research, Georg-August University of Göttingen
6. Prof. Dr. Christian Ammer, Silviculture and Forest Ecology of the Temperate Zones, Georg-August University of Göttingen

Day of the doctoral defense: 13th July, 2017

To My Wife—Yanling Shang

Summary

The Tibetan Plateau hosts the world's largest alpine pastoral ecosystems, dominated by the endemic sedge *Kobresia pygmaea* C.B. Clarke. Overgrazing on the Tibetan Plateau has caused severe degradation of vegetation and soils over the past 30-50 years. Due to the very harsh environment and nitrogen (N) and phosphorus (P) limitations in soils, these pastoral ecosystems are particularly sensitive to disturbances (e.g. anthropogenic activities and climate change) and exhibit slow recovery.

The objectives of this thesis were to 1) summarize the mechanisms of pasture degradation, 2) elucidate the effect of pasture degradation on carbon (C) and nutrient cycles and 3) assess the impacts of recovery strategies on degraded Tibetan pastures.

Laboratory chamber incubation experiments were established to investigate the effects of pasture degradation on C and N cycles, the response of Tibetan pastures to the simulated warming and increased precipitation and the impacts of manure application strategies on plant growth. A literature review was conducted to summarize the consequences of pasture degradation on soil organic carbon (SOC), N and P stocks across the entire Tibetan plateau, in order to evaluate the primary mechanisms of the SOC and nutrient losses. Additionally, the impacts of recovery strategies on degraded pastures were also summarized accordingly.

Tibetan pastures at the intermediate degradation stage exhibited the highest C loss as CO₂ emission and DOC leaching, while the highest N loss occurred in the extreme degradation stage of Tibetan pastures. These are primarily explained by the gradual disappearance of living plants and the decrease of C stocks, along with the more serious Tibetan pasture degradation. The simulated warming increased the activities of all enzymes relating to C, N and P cycles. Similarly, simulated increases in precipitation enhanced CO₂ emission from pasture soils. These results indicated that both simulated environmental factors (i.e. increased temperature and precipitation) prompted nutrient release and CO₂ emission, inducing greater loss of C and nutrients from Tibetan pastures. The literature review showed that degradation on the Tibetan Plateau has triggered significant loss of SOC ($-42 \pm 2 \%$), N ($-33 \pm 6 \%$) and P ($-17 \pm 4 \%$) contents compared to non-degraded pastures. While losses of total N and plant biomass were

found to be accompanied by SOC losses, total P loss was resistant to decreasing SOC content because of its precipitation as $\text{Ca}_3(\text{PO}_4)_2$. While various strategies have been implemented to cease and even reverse the degradation processes, their effects on soil quality are still ambiguous, and restoration of soil fertility and ecosystem stability is infeasible due to very slow pedogenic processes, slow vegetation restoration, as well as continuously increasing anthropogenic pressures and global climate change. As a result of the rapid losses of SOC and nutrients and the very slow recovery potential, natural *Kobresia* root mats will disappear in the coming decades. This will dramatically destabilize these unique alpine ecosystems and have broader negative impacts on global environmental changes.

Zusammenfassung

Das Tibetische Plateau beherbergt die weltweit größten alpinen pastoralen Ökosysteme, dominiert von der endemischen Sedge *Kobresia pygmaea* C.B.Clarke. Die Überweidung auf dem Tibetischen Plateau hat in den vergangenen 30-50 Jahren einen starken Abbau von Vegetation und Böden verursacht. Aufgrund der sehr harten Umwelt und die Einschränkung der Stickstoff (N) und Phosphorus- (P) in Böden sind diese pastoralen Ökosysteme besonders gegenüber Störungen (z. B. anthropogene Aktivitäten und Klimawandel) empfindlich und sie zeigen eine langsame Erholung.

Daher waren die Ziele dieser Arbeit wie folgt: 1) die abbau-Mechanismen der *Kobresia* pastoralen zusammenzufassen, 2) die Wirkungen des *Kobresia* pastoralen abbau auf Kohlenstoff- (C) und Nährstoff-zyklen zu ermitteln und 3) die Auswirkungen von Rückgewinnungs strategien auf abgebaute Tibetischer *Kobresia* pastoralen zu beurteilen.

Laborator-Inkubationsexperimente wurden durchgeführt, um die Wirkungen des *Kobresia* abbau auf C- und N-Zyklen zu untersuchen. Außerdem, wurde die Reaktion der Tibetischen *Kobresia* auf die simulierte Erwärmung und die Niederschlag erhöhung beurteilt und die Auswirkungen der anwendungsstrategien der Dünger auf das Pflanzenwachstum untersucht. Zuerst wurde eine Literaturrecherche durchgeführt um die abbau-folgen der *Kobresia* auf organischen Kohlenstoff (SOC) des Bodens, N- und P-Beständen auf dem gesamten Tibetischen Plateau zusammenzufassen und die primären Mechanismen des SOC und der Nährstoffverluste zu bewerten. Darüber hinaus wurden auch die Auswirkungen von Erholungsstrategien auf abgebaute *Kobresia* entsprechend zusammengefasst.

Tibetische *Kobresia* in der mittlerenabbauphase zeigten die höchsten C-Verluste als CO₂-Emission und DOC-Auslaugung und die höchsten N-Verluste traten in der extremen Abbaustufe der Tibetischen *Kobresia* auf. Diese werden vor allem durch das allmählich Verschwinden der lebenden Pflanzen und den Rückgang der C-Bestände erklärt da die ernsteren Tibetischen *Kobresia* abbau diese Prozesse schon intensiviert hat. Die simulierte Erwärmung erhöhte die Aktivitäten aller Enzyme in Bezug auf die Zyklen der C, N und P. Ebenso verbesserte die simulation der Niederschlag Erhöhung

die CO₂-Emission von *Kobresia* bedeckte Böden. Diese Ergebnisse zeigten, dass simulierte Umwelteinflüsse (d.h. erhöhte Temperatur und Niederschlag) Nährstofffreisetzung und CO₂-Emissionen veranlassten, wodurch größere Verluste an C und Nährstoffen aus Tibetischen *Kobresia* hervorgerufen wurden. Die Literaturrecherche ergab, dass der *Kobresia* Abbau auf dem Tibetischen Plateau signifikante Verluste an SOC ($-42 \pm 2\%$), N ($-33 \pm 6\%$) und P ($-17 \pm 4\%$) im Vergleich zu nicht abgebauten Weiden ausgelöst hat. Während die Verluste an Gesamte N und Pflanzen-Biomasse mit SOC-Verlusten begleitet wurden, war der Verlust der Gesamte P unabhängig der abnehmenden SOC-Gehalt weil P als Ca₃(PO₄)₂ ausfallen kann. Obwohl verschiedene Strategien schon implementiert wurden um die Abbauprozesse einzustellen oder sogar umzukehren, sind ihre Auswirkungen auf die Bodenqualität immer noch zweideutig. Da die Wiederherstellung der Bodenfruchtbarkeit und der Ökosystemstabilität durch sehr langsame pedogene Prozesse, langsame Vegetationswiederherstellung, kontinuierlich zunehmende Anthropogenen Drucke und globaler Klimawandel undurchführbar sind. Infolge der schnellen Verluste von SOC und Nährstoffen und dem sehr langsamen Erholungspotential werden die natürliche Kobresienwurzelmatte in den kommenden Jahrzehnten verschwinden und so wird diese einzigartigen alpinen Ökosysteme dramatisch destabilisieren und in folge verstärken die negative Auswirkungen auf globale Umweltveränderungen.

Table of Contents

Summary	II
Zusammenfassung	IV
Table of Contents.....	VI
List of Tables	IX
List of Figures	X
Acknowledgements.....	XIII
Abbreviations	XIV
1 Extended Summary.....	1
1.1 Introduction	1
1.1.1 Overview of Grassland and its worldwide degradation	1
1.1.2 Overview of Grassland and its degradation status across the whole Tibetan Plateau	1
1.1.3 Classification and Definition of degradation in the Tibetan Plateau	2
1.1.4 Unknown or unclear questions related to pasture degradation	3
1.2 Objectives	4
1.2.1 Identification of the mechanisms of pasture degradation to	4
1.2.2 Elucidation of the effect of degradation on C and nutrient cycles to.....	4
1.2.3 Assessment of the recovery strategies of degraded Tibetan pastures to.....	4
1.3 Material and Methods.....	4
1.3.1 Sampling sites.....	5
1.3.2 Incubation experiments	5
1.3.3 Data collection for review (Study 1).....	7
1.4 Main results and discussion	7
1.4.1 Mechanisms of pasture degradation.....	7
1.4.2 Effect of pasture degradation on C and nutrient cycles.....	9
1.4.3 Recovery strategies of degraded Tibetan pastures	11
1.5 Conclusions	13
1.6 References.....	14
1.7 Contributions to the included manuscripts.....	16
2 Publications and Manuscripts.....	18
2.1 Study 1: Degradation of Tibetan grasslands: Consequences for carbon and nutrient cycles	18
2.1.1 Abstract.....	18
2.1.2 Introduction	20

2.1.3 Materials and Methods.....	23
2.1.4 Results and discussion.....	25
2.1.5 Synthesis	33
2.1.6 Conclusions	39
2.1.7 Acknowledgements	40
2.1.8 References.....	40
2.1.9 Supporting information	45
2.2 Study 2: Hot experience for cold-adapted microorganisms: Temperature sensitivity of soil enzymes	48
2.2.1 Abstract.....	48
2.2.2 Introduction	50
2.2.3 Material and methods.....	53
2.2.4 Results.....	57
2.2.5 Discussion.....	61
2.2.6 Acknowledgements	64
2.2.7 References.....	65
2.2.8 Supporting information	68
2.3 Study 3: Carbon and nitrogen losses from soil depend on degradation of Tibetan <i>Kobresia</i> pastures.....	70
2.3.1 Abstract.....	70
2.3.2 Introduction	71
2.3.3 Materials and Methods.....	73
2.3.4 Results.....	77
2.3.5 Discussion.....	81
2.3.6 Conclusions	85
2.3.7 Acknowledgements	86
2.3.8 References.....	86
2.4 Study 4: Responses of degraded Tibetan <i>Kobresia</i> pastures to N addition	89
2.4.1 Abstract.....	89
2.4.2 Introduction	90
2.4.3 Materials and Methods.....	92
2.4.4 Results.....	97
2.4.5 Discussions.....	100
2.4.6 Conclusions	107
2.4.7 Acknowledgements	108

2.4.8 References.....	108
2.4.9 Supporting information	112
2.5 Study 5: Spatio-temporal patterns of enzyme activities after manure application reflect mechanisms of niche differentiation between plants and microorganisms.....	113
2.5.1 Abstract.....	113
2.5.2 Introduction	115
2.5.3 Materials and methods.....	117
2.5.4 Results.....	122
2.5.5 Discussion.....	128
2.5.6 Conclusions	133
2.5.7 Acknowledgements	133
2.5.8 References.....	134
2.5.9 Supporting information	137
3 Abstracts of additional studies.....	140
3.1 The <i>Kobresia pygmaea</i> ecosystem of the Tibetan highlands – origin, functioning and degradation of the world’s largest alpine pastoral ecosystem.....	140
3.1.1 Abstract.....	141
3.2 Mechanisms and consequences of Tibetan grassland degradation.....	142
3.2.1 Abstract.....	142
Appendix.....	143
Curriculum vitae	143
Declarations.....	145

List of Tables

Extended Summary:	1
Table 1 Factors and drivers of pastures degradation on Tibetan Plateau	8
Study 1:	18
Table 1 Factors, drivers and consequences of pastures degradation on Tibetan Plateau*	36
Table S1 Classification of pasture degradation (adapted from Ma <i>et al.</i> , 2002)	45
Study 2:	48
Table 1 Basic information of the sampling site	53
Table 2 Description of soil properties.....	54
Table S1. K_m and catalytic efficiency (V_{max}/K_m) of β -glucosidase, xylanase and leucine aminopeptidase	68
Study 3:	70
Table 1 Distribution of carbon and nitrogen in pools of soil, root and microbial biomass	77
Study 4:	89
Table 1 Characteristics of soil, root and microbial biomass	99

List of Figures

Extended Summary	1
Figure 1 Classification of Tibetan pasture degradation.....	3
Figure 2 Longitudinal section of chamber (left) and origin of three <i>Kobresia</i> root mat types (right).	6
Figure 3 Rhizoboxes with barley growing under three manure application strategies: No manure (left), manure homogenized with the whole soil (middle), and manure localized in the soil layer between 1.0 and 2.5 cm below the soil surface (right).....	6
Figure 4 Enzyme activity as a function of temperature demonstrates a gradual increase for cellobiohydrolase (top), tyrosine aminopeptidase (middle) and acid phosphomonoesterase (bottom) within the range of nine temperatures.	9
Figure 5 Correlation between soil moisture content (% dw) and nighttime CO ₂ efflux during the second experiment.	9
Figure 6 Conceptual diagram of C and N losses from <i>K. pygmaea</i> pastures depending on degradation stages.	10
Figure 7 Relations between foliar ¹⁵ N uptake and total N in the leachate (top) and N ₂ O efflux (bottom).	10
Figure 8 Effect sizes of SOC content, nutrient content, plant biomass, soil bulk density (BD) and soil pH for four degradation stages compared to non-degraded pastures.	11
Figure 9 Response of aboveground biomass (AGB) to single and combined additions of N and P.....	12
Figure 10 Plant biomass and shoot/root ratio under three manure application strategies: 1) No manure, 2) Homogenized manure and 3) Localized manure..	12
Figure 11 Synthesis of the main results of the studies.....	14
Study 1:	18
Figure 1 Degradation of pastures on the Tibetan Plateau.....	20
Figure 2 Classification of Tibetan pasture degradation.	22
Figure 3 Effect sizes of SOC content, nutrient content, plant biomass, soil bulk density (BD) and soil pH for four degradation stages compared to non-degraded pastures.	26
Figure 4 Relationships between vegetation coverage (in % of area) and stocks of soil organic carbon: SOC (top), total nitrogen: TN (middle) and total phosphorus: TP (bottom) for three depth intervals (0-10, 10-20 and 20-30 cm).	28
Figure 5 Soil organic carbon (SOC) and nutrient contents, belowground biomass (BGB) and soil properties depending on depths.....	32
Figure 6 Response of aboveground biomass (AGB) to single and combined additions of N and P.....	38
Figure S1 Relationships between content and stocks of soil organic carbon: SOC (top), total nitrogen: TN (middle) and total phosphorus: TP (bottom) in a 10 cm depth intervals.	45
Figure S2 Indicators of degradation of vegetation and soil fertility: Sensitivity of nutrient losses in plant biomass (top row) and soil (bottom row) to SOC losses.....	46
Figure S3 Response of vegetation coverage (%) and SOC content (g C kg ⁻¹) to thickness of the	

active layer of permafrost (m).....	46
Figure S4 Decadal development of socio-economic factors affecting pasture degradation: livestock numbers in Qinghai (top left) and Tibet (top right), length of highways (bottom left) and tourists (bottom right) in Qinghai and Tibet.	47
Study 2:	48
Figure 1 Enzyme activity as a function of temperature demonstrates a gradual increase for cellobiohydrolase (top), tyrosine aminopeptidase (middle) and acid phosphomonoesterase (bottom) within the range of nine temperatures.	57
Figure 2 Temperature sensitivity of maximal reaction rate ($V_{max} \cdot Q_{10}$) and substrate affinity ($K_m \cdot Q_{10}$) of six enzymes as a function of temperature with 5 °C increments.	58
Figure 3 The activation energy (E_a) of all tested enzymes at two temperature ranges: low (0-20 °C) and high (25–40 °C).	59
Figure 4 K_m and catalytic efficiency (V_{max}/K_m) of cellobiohydrolase (top), tyrosine aminopeptidase (middle) and acid phosphomonoesterase (bottom).....	60
Figure 5 Generalized thermal responses of enzyme catalytic properties to a temperature increase.	63
Figure S1 Examples of Michaelise Menten kinetics (enzyme activity as a function of substrate concentration) in response to increasing temperature for cellobiohydrolase (top), tyrosine aminopeptidase (middle), acid phosphomonoesterase (bottom) measured at nine temperatures.	69
Study 3:	70
Figure 1 Longitudinal section of chamber (left) and origin of three <i>Kobresia</i> root mat types (right).	72
Figure 2 Relations between microbial biomass carbon (MBC) and nighttime CO ₂ efflux (top) and DOC concentration in the leachate (bottom) at Day 114.	77
Figure 3 Nighttime (top) and daytime (bottom) CO ₂ efflux of three <i>Kobresia</i> root mat types.	78
Figure 4 Correlation between cumulative CO ₂ -C for all replicates and their final soil organic carbon (SOC) contents. “Living” = living root mat; “Dying” = dying root mat; “Dead” = dead root mat.	79
Figure 5 Correlation between soil moisture content (% dw) and nighttime CO ₂ efflux during the second experiment.	79
Figure 6 Change of soil moisture content (top) and response of nighttime CO ₂ efflux (bottom) in living and dead root mats to increased moisture.	80
Figure 7 Concentrations of DOC (top), DON (middle) and NO ₃ ⁻ -N (bottom) in the leachate of three <i>Kobresia</i> root mat types during the leaching experiment.	81
Figure 8 Conceptual diagram of C and N loss from <i>K. pygmaea</i> pastures depending on degradation stages.	85
Study 4:	89
Figure 1 Aboveground biomass (AGB, top left), foliar N content (top right), foliar N stock (bottom	

left) and ^{15}N uptake (bottom right) by <i>K. pygmaea</i>	97
Figure 2 Total N concentration in the leachate of living (top left), dying (top right) and dead (bottom left) root mats and comparison among three N-added root mats (bottom right).	99
Figure 3 DOC concentrations averaged over 101 days in the leachate of three root mats.....	99
Figure 4 ^{15}N recovery in plant and soil pools of three non-added and N-added root mats 91 days after labelling.	101
Figure 5 Relations between foliar ^{15}N uptake and total N in the leachate (top) and N_2O efflux (bottom).	105
Figure 6 Total N stock and N fluxes in the three root mats during the growing season.....	106
Figure S1 N_2O efflux from living (top), dying (middle) and dead (bottom) root mats during the incubation.	112
Study 5:	113
Figure 1 Rhizoboxes with barley growing under three manure application strategies: No manure (left), manure homogenized with the whole soil (middle), and manure localized in the soil layer between 1.0 and 2.5 cm below the soil surface (right).....	116
Figure 2 Response of phosphomonoesterase (top), β -glucosidase (middle) and chitinase (bottom) activities to manure application strategies over time.....	123
Figure 3 Examples of zymograms for phosphomonoesterase activities.....	124
Figure 4 Effects of manure application strategies on phosphomonoesterase (top), β -glucosidase (middle) and chitinase (bottom) activities in the whole soil.....	125
Figure 5 The detritosphere extension for phosphomonoesterase (left) and β -glucosidase activities (right) from the initial manure layer at the top (presented as the shaded area between 1.0 and 2.5 cm) over time.....	126
Figure 6 Ratio of E_R to E_H for phosphomonoesterase (top), β -glucosidase (middle) and chitinase (bottom).	127
Figure 7 Plant biomass and shoot/root ratio under three manure application strategies: 1) No manure, 2) Homogenized manure and 3) Localized manure.	128
Figure 8 General responses and localization of soil enzyme activities to manure application strategies over time.	130
Figure S1 Example of detecting the boundaries of three categories of enzyme activities: Low activity, Medium activity, and Hotspots.....	137
Figure S2. Examples of zymograms for β -glucosidase activity.....	138
Figure S3 Examples of zymograms for chitinase activity.	139

Acknowledgements

During my PhD study in the Department of Soil Science of Temperate Ecosystems in University of Göttingen, I really enjoy the time working in our group - great supervisor, super-friendly international friends, nice academic atmosphere and so on. This is a great and memorable period for my whole life. Before it ends, I would like to thank people who support, teach and understand me.

First of all, I would like to thank Prof. Yakov Kuzyakov for his supervision during my PhD study. Prof. Kuzyakov patiently helped me and gave me all the advice that he can give during our discussions. During these years, I not only learnt knowledge and good research attitude but also knew what characters a great scientist should have. Besides, I also want to thank Prof. Michaela Dippold for her great help especially during these recent months. Without her assistant, I cannot imagine how my dissertation will be. I also would like to thank Prof. Sandra Spielvogel, Prof. Bruno Glaser and Prof. Christoph Leuschner for their suggestions for my dissertation and for their attendance to my defense. I also want to thank PD Dr. Evgenia Blagodatskaya for her great and creative suggestions about this study.

I am very thankful to the colleagues and members in our group, department of agricultural soil science and department of soil hydrology for their help during my PhD. I also would like to thank all the colleagues in the Priority Programme 1372: Tibetan Plateau: Formation-Climate-Ecosystems (Project KU 1184/14-2) for their help.

I want to especially thank my international friends - Kazem Zamanian, Bahar S. Razavi, Amit Kumar, Duyen Hoang, DeeJay Maranguit, Menuka Maharjan and Josh Bostic. I also thank my Chinese friends. They really help and support me a lot not only during my study but also for my life. We together have lots of fun and they all are the treasures of my life.

I would like to thank my family for their understanding during my PhD study. At the end, I want to especially give most of my thanks to my wife. She gives me most of the understanding and patience in these 4 years to support my study. Without her support, I cannot finish this study.

Abbreviations

SOC	Soil organic carbon
SOM	Soil organic matter
N	Nitrogen
P	Phosphorus
K	Potassium
BD	Bulk density
AGB	Aboveground biomass
BGB	Belowground biomass
MBC	Microbial biomass carbon
MBN	Microbial biomass nitrogen
DOC	Dissolved organic carbon
DON	Dissolved organic nitrogen
WHC	Water holding capacity
Living	Living root mat
Dying	Dying root mat
Dead	Dead root mat

1 Extended Summary

1.1 Introduction

1.1.1 Overview of Grassland and its worldwide degradation

Grasslands, covering around 40% of the total global terrestrial area (Suttie et al., 2005), support the livelihoods of around 800 million people worldwide and also provide forage for livestock and wildlife. Grasslands store ca. 30% of the global soil carbon (Tennigkeit and Wilkies, 2008), and nutrients (nitrogen (N) and phosphorus (P)). These carbon and nutrient statuses matter not only for soil fertility, forage production and climate change, but also have important feedbacks in soil water condition, plant community composition and biodiversity. However, in recent decades, global grassland ecosystems have experienced serious degradation, which incurred dramatic repercussions for ecosystem functioning and socio-economic development. For instance, 20-35 % of grasslands have been affected by degradation (Bai et al., 2008; FAO, 2010). A meta-analysis of 55 studies by Dlamini et al., (2016) found that 4-14% of soil organic carbon (SOC) stock in grasslands has already been lost due to various intensities of degradation. Grassland degradation also induced loss of global livestock productivity, with an estimated economic cost of around 6.8 billion US \$ in 2007 (Kwon et al., 2015). Degradation-induced nutrient losses also resulted in eutrophication of rivers and soil erosion resulting from strong sand storms and land desertification.

1.1.2 Overview of Grassland and its degradation status across the whole Tibetan Plateau

Tibetan pastures, hotspots of global grassland research, are the world's largest pastoral alpine ecosystems, covering around 450,000 km². More than 4.0% of the world's grassland soil carbon (C) is stored in soils under Tibetan pastures (ca. 10.7 Pg C; Ni, 2002). Around 920 Tg of nitrogen (N) is preserved in Tibetan pastures soils, which represents 0.7-1.0 % of the total global N storage (Tian et al., 2006) and is required for sufficient forage production. Over the last half century, Tibetan pastures have provided an important basis for livestock (i.e. 12 million of yaks, 30 million of sheep and goats; Suttie et al., 2015), thus ensuring the livelihood of Tibetan herders (Harris, 2010). Additionally, several major Asian rivers originate from the Tibetan Plateau and pass

through Tibetan pastures. These rivers collectively constitute the primary water sources for billions of people in the surrounding regions of southeastern Asia (Fan and Hou, 2016). The Tibetan pastures play a critical role in ecological security, such as conservation of water and soil as well as the protection of biodiversity. In total, the values of these ecosystem services from Tibetan pastures were estimated to reach approximately 25.3 billion dollars (Squires et al., 2009; Xie et al., 2003), accounting for more than 62% of the entire economic output of the Tibetan grasslands. Therefore, due to their undisputed importance, the status of Tibetan pastures matters considerably for socio-economic development and ecological security in China and the surrounding Asian region (Sun et al., 2012; Babel et al., 2014; Zhong et al., 2006).

Tibetan pastures remained stable throughout the last millennia of nomadic animal husbandry. However, these ecosystems have been intensively exploited in recent decades due to the high demands of socio-economic developments, e.g., overgrazing, land use change and infrastructure construction. These disturbances, together with a warming rate of about twice the global mean, have induced serious Tibetan pasture degradation. To date, around 30-70% of Tibetan pastures have been being degraded to different degrees (Li et al., 2013; Holzner and Kriechbaum, 2000; Wang et al., 2016). These degraded grasslands have caused considerable economic losses due to unexpected losses of organic C, N and species diversity (Wen et al., 2013), while simultaneously threatening human well-being.

1.1.3 Classification and Definition of degradation in the Tibetan Plateau

Degradation of Tibetan pastures in this particularly harsh environment have drawn considerable research interest to investigate the mechanisms of pasture degradation and its consequences for ecosystem services, water dynamics and plant and soil variations. For instance, Wen et al. (2013) reported that until 2008, economic losses resulting from C emissions and N loss on extremely degraded pastures reached around \$8000 ha⁻¹ and \$13000 ha⁻¹, respectively. Babel et al. (2014) concluded that increasing Tibetan pasture degradation significantly decreased the C uptake, as well as the function of pastures as a C sink, by classifying the pasture degradation into three stages. Similarly, Ma et al (2002) classified the pasture degradation into five degradation stages

using several vegetation characteristics (Fig. 1). They found that plant biomass strongly decreased and plant community composition also shifted from gramineae and sedges to weeds along the degradation continuum. Besides vegetation characteristics, various indicators, such as soil properties (Kimetu *et al.*, 2008; Alados *et al.*, 2007), plant species composition (Van der Westhuizen *et al.*, 2005; Jordaan *et al.*, 1997), species abundance of wildlife, and death rate of domestic livestock (Behnke & Scoones, 1993; White *et al.*, 2000), have been proposed to assess and classify pasture degradation. Though several indicators have been recommended, it is challenging to make a general and globally accepted definition for pasture degradation due to differences in which pasture conditions are emphasized (e.g. pastoral productivity, vegetation composition, biological diversity, soil fertility, C and nutrient stocks) (White *et al.*, 2000). Considering the importance of soil fertility and plant productivity for pasture quality, we define “pasture degradation” as the retrogressive succession of a pasture ecosystem affected by interference of rational and irrational anthropogenic (e.g. overgrazing, deforestation, and infrastructure construction) and/or environmental (e.g. permafrost melting and climate change) factors, leading to decreases in plant productivity, soil quality etc.

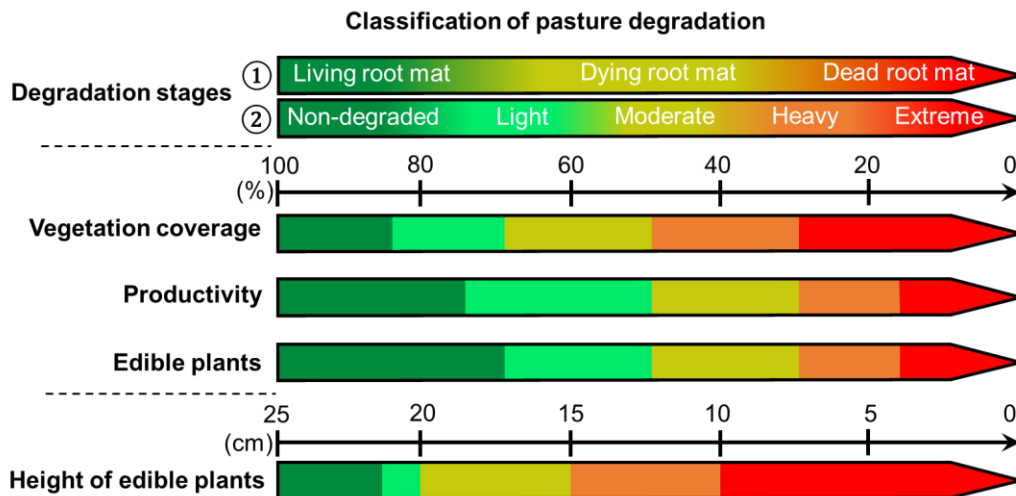


Figure 1 Classification of Tibetan pasture degradation. The two classifications of degradation stages (① & ②) were determined based on vegetation coverage, plant productivity, portion of edible plants and height of edible plants (Babel *et al.*, 2014; Ma *et al.*, 2002). The first classification was used in Studies 3 & 4, while the second classification was used in Study 1.

1.1.4 Unknown or unclear questions related to pasture degradation

Many local studies have investigated the impact of pasture degradation on soil properties and plant characteristics by classifying the degradation (Zeng *et al.*, 2013; Li

et al., 2014) and varied conclusions have been reached. Meanwhile, strategies to recover soil fertility have also been proposed and examined (Dong et al., 2012; Feng et al., 2010). However, regional-scale analyses offering a better understanding of the relationship between SOC and nutrient status and degradation remain unexplored. Furthermore, the pathways and mechanisms of degradation-induced SOC and nutrient losses were also still unclear.

1.2 Objectives

As the introduction has shown a clear lack of knowledge on the mechanisms of pasture degradation, its effect on C and nutrient cycles and the strategies for Tibetan pasture recovery, this thesis focuses on the following objectives:

1.2.1 Identification of the mechanisms of pasture degradation to

- determine the drivers of accelerated pasture degradation (Study 1)
- summarize the socio-economic factors inducing pasture degradation (Study 1)
- investigate the environmental factors which result in pasture degradation, providing an overview (study 1) but a detailed understanding of the effect of warming on biochemical functions (study 2) and the effect of increased precipitation on soil CO₂ emission.

1.2.2 Elucidation of the effect of degradation on C and nutrient cycles to

- identify the processes of C losses with pasture degradation (Study 3)
- identify the processes of N losses with pasture degradation (Study 4)
- synthesize and generalize the consequences of pasture degradation for SOC and nutrient cycles (Study 1).

1.2.3 Assessment of the recovery strategies of degraded Tibetan pastures to

- summarize the effect of reseeded and grazing exclusion on pasture recovery (Study 1)
- summarize the effect of N and P fertilization on pasture recovery (Study 1)
- investigate the effect of yak manure strategies on plant growth (Study 5)

1.3 Material and Methods

To achieve these objectives, we took samples from several sites on the Tibetan Plateau, conducted relevant incubation experiments and compiled related datasets.

1.3.1 Sampling sites

1.3.1.1 Site 1-KEMA research station

The first sampling for studies 3, 4 and 5 was carried out on field sites located at the research station of the Tibet University and the Institute of Tibetan Plateau Research-“*Kobresia* Ecosystem Monitoring Area” (KEMA) (31°16'45"N, 92°59'37"E, 4410 m a.s.l.) in Nagqu, Tibet. The station is located in the core area of the *Kobresia pygmaea* distribution. Mean annual temperature and precipitation are -1.2 °C and 430 mm, respectively. From June to September, the mean summer precipitation reaches 272 mm, whereas snowfall is low (climate station in Nagqu, Miehe *et al.*, 2011). The growing season ranges from May to October.

1.3.1.2 Site 2-Reting

The second sampling site for study 2 is located in the upper Kyi Chu catchment north of Lhasa in Pando County, Tibet, above the Reting Monastery of Qinghai-Tibetan Plateau (south west of China, 4330 m a.s.l.). The mean precipitation during the growing season (from May to October) is 330 mm. The temperature during the growing season ranges from -4 to +17.7 °C. This site has the largest and most sacred *Juniperus* forest in Tibet, diffusely growing in a carpet-like felty turf of *Kobresia pygmaea* C.B. Clarke (Miehe *et al.*, 2008).

1.3.2 Incubation experiments

1.3.2.1 Climate chamber incubation (Studies 3 and 4)

Six samples from each root mat were selected to conduct the experiment. These samples were put in incubation boxes (Fig. 2, left) allowing for simultaneous analyses of CO₂ efflux and leaching. A constant temperature of 20°C was maintained throughout the experiment. Samples were illuminated diurnally for 14 h with a photosynthetic photon flux density of 80 $\mu\text{m}^{-2} \text{s}^{-1}$ and kept in the darkness for 10 h.

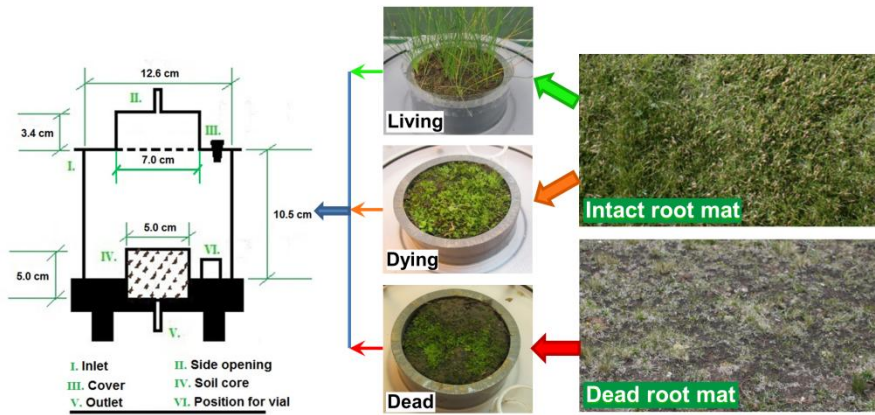


Figure 2 Longitudinal section of chamber (left) and origin of three *Kobresia* root mat types (right). “Living” = living root mat; “Dying” = dying root mat; “Dead” = dead root mat.

1.3.2.2 Temperature gradient incubation (Study 2)

Thirty grams of soil was placed in air-tight vials (125 ml) equipped with rubber seals. Six enzymes targeting C-, N- and P-containing substrates were investigated after progressively incubating the soil at 0, 5, 10, 15, 20, 25, 30, 35 and 40 °C for one month. During the incubation, soil moisture was maintained gravimetrically at 60 % of WHC. Nine temperature-regulating climate chambers (SBS C120) were used for the incubations ($< \pm 0.5$ °C).

1.3.2.3 Manure application incubation (Study 5)

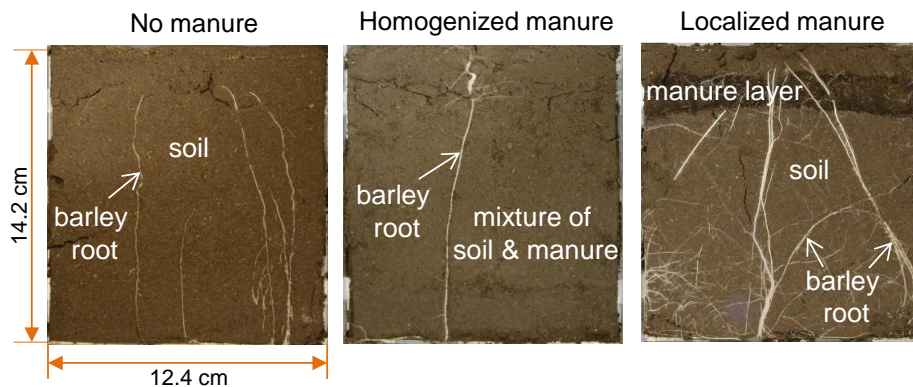


Figure 3 Rhizoboxes with barley growing under three manure application strategies: No manure (left), manure homogenized with the whole soil (middle), and manure localized in the soil layer between 1.0 and 2.5 cm below the soil surface (right).

Experimental samples were prepared to simulate the following manure applications (Fig. 3): 1) Localized manure: manure applied as a layer buried in the upper soil; 2) Homogenized manure: manure mixed into the soil. Homogenized manure application was comparable to fertilizer broadcasting and plowing; and 3) No manure: a control without manure application. For the localized manure application, 110 g fresh soil was first added to a rhizobox and then 5 g of composted yak dung was evenly spread across

the soil surface in a 1.5 cm layer. For the homogenized manure strategy, 110 g fresh soil and 5 g composted yak dung were mixed homogeneously and placed in rhizoboxes. The third treatment only included 110 g soil and was the control (“No manure”). Each application strategy had three replicates. Tibetan barley seeds (*Hordeum vulgare L.*) were germinated on filter paper for 72 h. One seedling was then planted in each rhizobox at a depth of 5 mm. The rhizoboxes were placed in an incubation chamber set to 20 °C, with a photosynthetically active radiation intensity of 300 $\mu\text{mol m}^{-2} \text{s}^{-1}$ and a 14/10 hour light/dark cycle.

1.3.3 Data collection for review (Study 1)

Literature about the effects of pasture degradation on SOC and nutrient content was assembled mainly through four channels: 1) Web of Science V.5.22.1 (available online), 2) ScienceDirect (Elsevier B.V.), 3) Google Scholar and 4) Chinese-language literature using the China Knowledge Resource Integrated Database (CNKI). The search terms were “degradation gradient/stages”, “alpine meadow”, “Tibetan Plateau” and “soil”.

The criteria for inclusion in the review were: (1) the classification of degradation stages is clearly stated; (2) the literature includes analysis of SOC (or soil organic matter), total nitrogen (TN), total phosphorus (TP), vegetation characteristics or soil properties; (3) the non-degradation stage (stage 1 according to Fig. 1) is included as the “reference”, to enable the “effect size” analysis. At least one of the degradation stages (light degradation, moderate degradation, heavy degradation and extreme degradation) is also presented in relation to the “reference”; and (4) the sampling depth and study location are clearly presented.

1.4 Main results and discussion

1.4.1 Mechanisms of pasture degradation

— Harsh environmental conditions on the Tibetan Plateau, for example, low mean annual temperature, low CO₂ pressure, short vegetation period and shallow soil depth, accelerates the pasture degradation (Table 1). The harsh conditions on the Tibetan Plateau make the region very sensitive to changes in environmental and socio-economic factors and accelerate pasture degradation.

Table 1 Factors and drivers of pastures degradation on Tibetan Plateau

Factors inducing degradation	
○ <i>Environmental</i>	<ul style="list-style-type: none"> • Glacial retreat; snow melting • Permafrost degradation • Drying of wetlands • Shrinkage of lakes • Destruction of root mats by rodents
○ <i>Socio-economic</i>	<ul style="list-style-type: none"> ○ <i>Socio</i> <ul style="list-style-type: none"> • Overgrazing • Population growth • Sedentarization of nomads • Privatization of pastures • Removal and burning of yak dung ○ <i>Economic</i> <ul style="list-style-type: none"> • Deforestation • Land use change • Mining • Road construction • Dam construction • Booming tourist industry
Drivers accelerating degradation	
○ <i>Soil</i>	<ul style="list-style-type: none"> • Shallow soil depth (~30-50 cm) • Nutrient (N, P) limitation • Nutrient-poor parent materials • Slow weathering (because of climate)
○ <i>Climate</i>	<ul style="list-style-type: none"> • Very strong solar radiation (21 MJ m⁻² day⁻¹) • Low mean annual temperature (< 0 °C) • High variation of spatial and temporal precipitation • Low mean annual precipitation (~440 mm) • Low CO₂ pressure
○ <i>Vegetation</i>	<ul style="list-style-type: none"> • Very short vegetation period (< 3.5 months) • Poor plant germination
○ <i>Topography</i>	<ul style="list-style-type: none"> • Steep slopes • Slope exposition

- Socio-economic and environmental factors which may induce pasture degradation were summarized (Table 1). The interferences of all these environmental and socio-economic factors in recent decades, and their interactions, have intensified Tibetan pasture degradation and accelerated SOC and nutrient losses. In contrast to environmental factors, socio-economic factors (e.g. overgrazing) have stronger, progressive and more rapid negative impacts on Tibetan pastures.
- Simulated warming accelerated activities of enzymes relating to C, N and P cycles (Fig. 4). Continuous warming in the region will increase C and nutrient release and may contribute to C and nutrient losses.

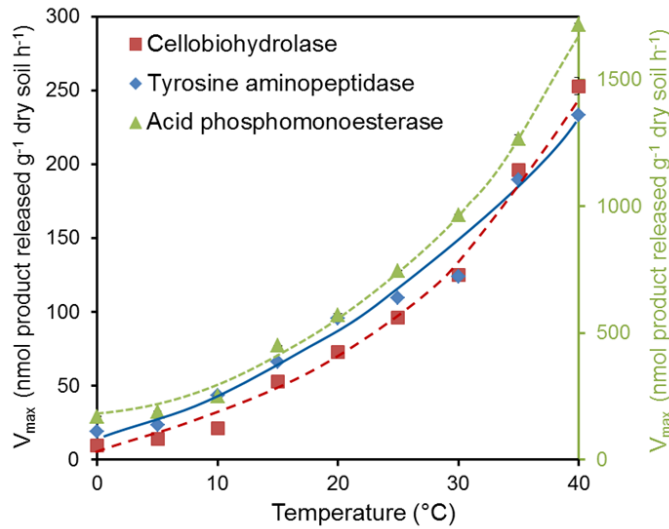


Figure 4 Enzyme activity as a function of temperature demonstrates a gradual increase for cellobiohydrolase (top), tyrosine aminopeptidase (middle) and acid phosphomonoesterase (bottom) within the range of nine temperatures.

- Soil respiration was positively related to simulated increasing precipitation, indicating an enhancement of SOC decomposition with increasing moisture in Tibetan pastures (Fig. 5). This implies that increasing precipitation will accelerate C loss from Tibetan pastures.

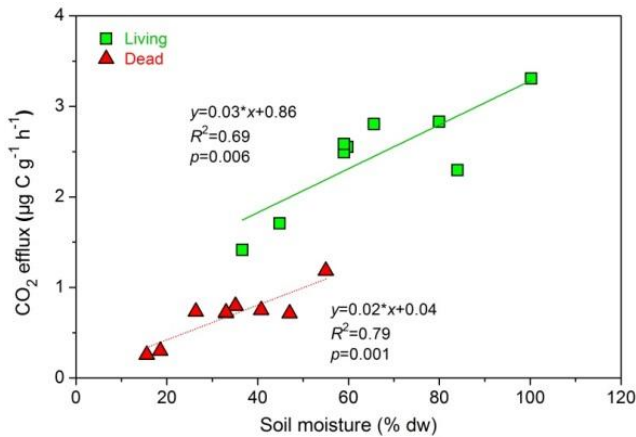


Figure 5 Correlation between soil moisture content (% dw) and nighttime CO₂ efflux during the second experiment. 'Living' = living root mat; 'Dead' = dead root mat.

1.4.2 Effect of pasture degradation on C and nutrient cycles

- Carbon loss as CO₂ emissions and DOC leaching was highest in dying root mat (Fig. 6). The initial dying of plants will rapidly convert pastures to a C source. However, photosynthesis of plant shoots in living root mat mitigated the respiratory C losses and consequently prevented Tibetan pastures from becoming a C source. The low C losses from dead root mat suggest that the stimulation of SOC mineralization by the high root litter inputs may disappear, and CO₂ release subsequently decline, when labile OC stocks are not sufficient to support microbial activity.

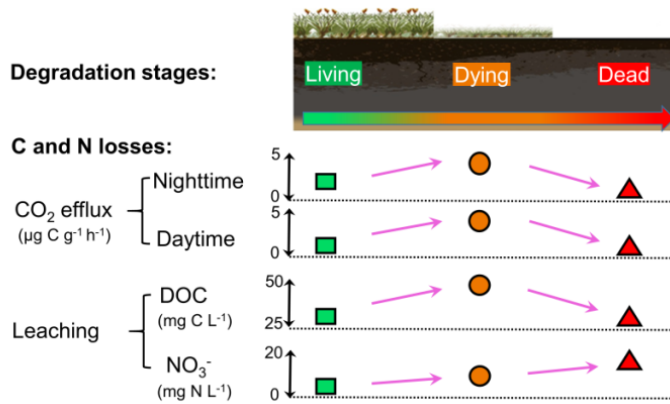


Figure 6 Conceptual diagram of C and N losses from *K. pygmaea* pastures depending on degradation stages. “Living”, “Dying” and “Dead” correspond to the degradation stages of “Living root mat”, “Dying root mat” and “Dead root mat,” respectively, in Fig. 1.

- Nitrogen loss from the leaching was highest in dead root mat compared with other root mats (Fig. 6). Leaching was the primary cause of high N losses (mainly as NO₃⁻) from dying and dead root mats, while the lower N loss from living root mats can be attributed to N uptake by living plants (Fig. 7). The large NO₃⁻ losses from dead root mats were mainly caused by long-term NO₃⁻ accumulation during SOC decomposition in the field, which were subsequently flushed by leaching. These losses reduce the potential of Tibetan pastures to recover from degradation, as N is often a limited nutrient in alpine grasslands.

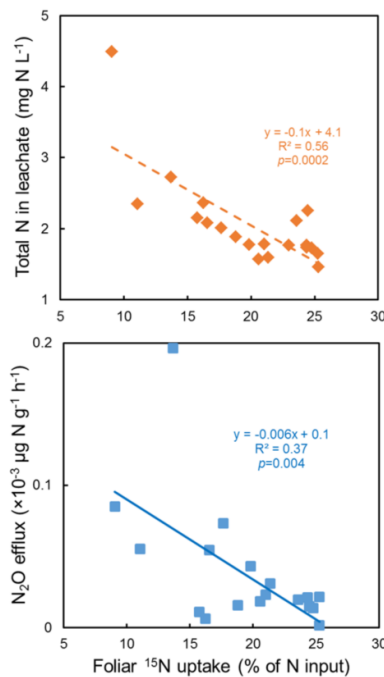


Figure 7 Relations between foliar ¹⁵N uptake and total N in the leachate (top) and N₂O efflux (bottom). *p* values less than 0.05 represent the significance of the correlation.

- In total, 20-60% of SOC stocks were lost from degraded pastures, relative to their non-degraded counterparts (Fig. 1 & 8). These SOC losses are very close to the

decreases in N stocks ($-33 \pm 6\%$), as well as aboveground ($-42 \pm 3\%$) and belowground ($-45 \pm 6\%$) plant biomass. Phosphorus losses were lower ($-17 \pm 4\%$), likely due to the reduced bioavailability of P when precipitated as $\text{Ca}_3(\text{PO}_4)_2$. SOC and nutrient stocks in the upper 10 cm are especially sensitive to pasture degradation.

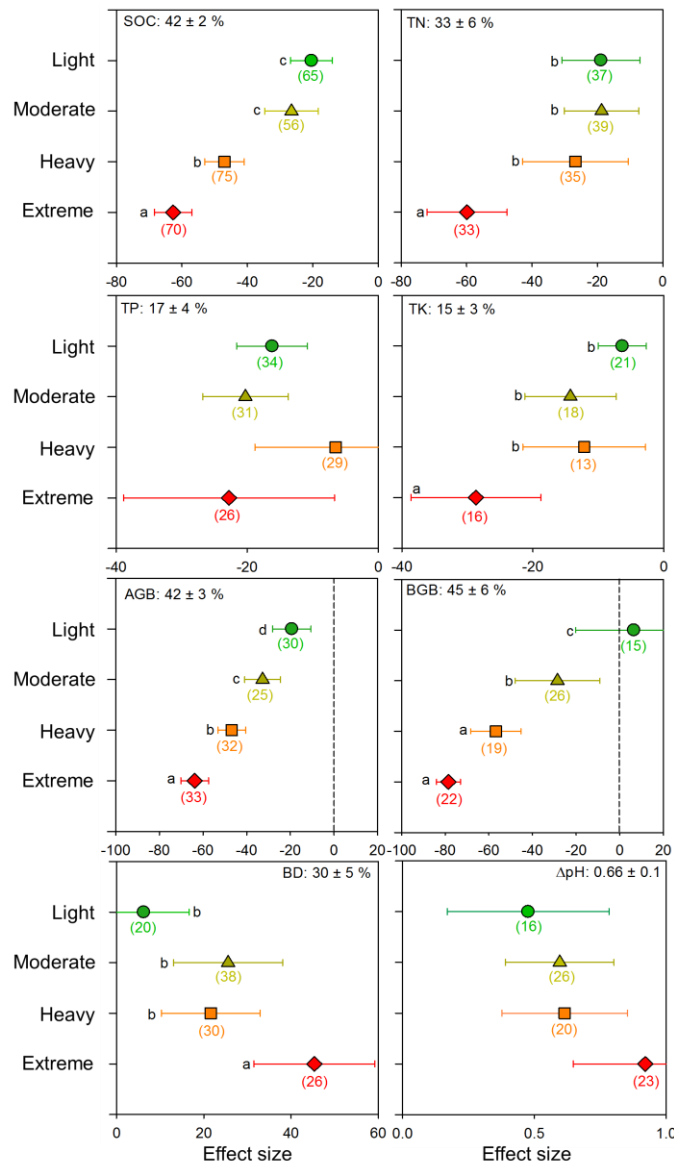


Figure 8 Effect sizes of SOC content, nutrient content, plant biomass, soil bulk density (BD) and soil pH for four degradation stages compared to non-degraded pastures. Colors represent degradation stages “②” in Fig. 1. The percentage value at the top shows the average effect size of the four degradation stages. The number in the parenthesis is the number of sampling points. Lower-case letters indicate significant differences between the degradation stages.

1.4.3 Recovery strategies of degraded Tibetan pastures

— Reseeding strategy has no significant effect on soil organic carbon; Grazing exclusion showed inconsistent results among different studies. Inconsistent results of reseeded and grazing exclusion strategies suggest that recovery strategies must be implemented over a long period of time to realize improvements in soil fertility.

This reflects the time necessary for soil formation, restoration of the eroded soil and accumulation of nutrients – by weathering and N₂ fixation. Therefore, to improve soil fertility, a complex of various strategies is necessary.

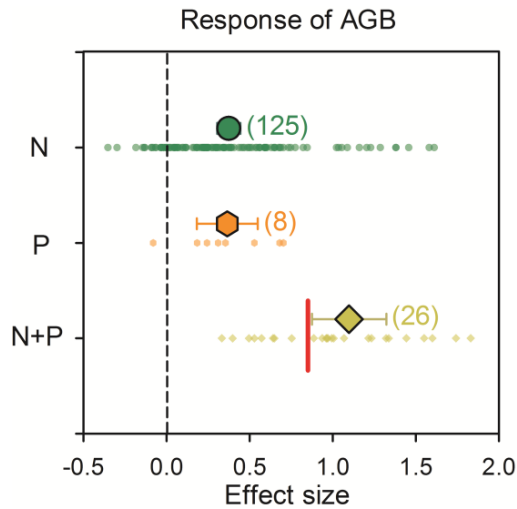


Figure 9 Response of aboveground biomass (AGB) to single and combined additions of N and P. The short red line represents the calculated N+P effect without N+P interactions. The numbers in parenthesis show the number of experiments. This figure was generated based on the database from Miede et al.'s (unpublished) literature. Error bars show standard errors (SE).

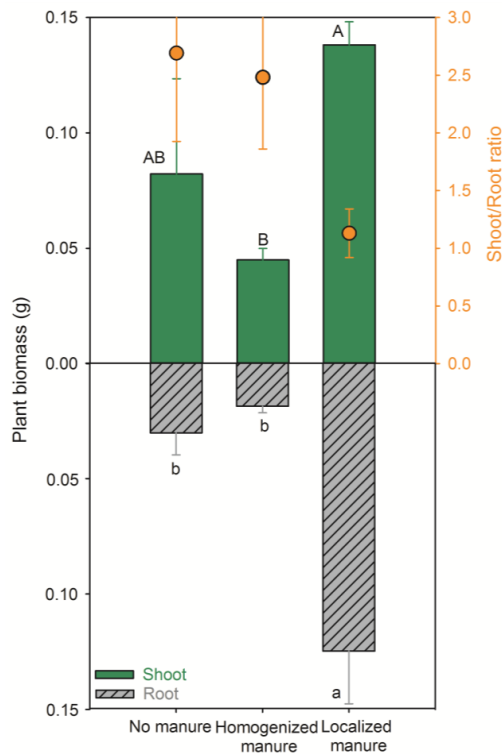


Figure 10 Plant biomass and shoot/root ratio under three manure application strategies: 1) No manure, 2) Homogenized manure and 3) Localized manure. The capital and lower-case letters show significant differences between application strategies ($p < 0.05$). Error bars represent standard deviations (\pm SD).

- Mineral fertilization (N and P) significantly increased aboveground biomass (Fig. 9); N addition directly increased the N losses from leaching in degraded Tibetan pastures. Nitrogen addition can facilitate plant growth in intact Tibetan pastures. In

the degraded stages of Tibetan pastures, N addition directly increased the N losses from leaching. Thus, degradation together with N addition intensifies N losses in Tibetan pastures, hampering pasture restoration, increasing the NO_3^- loading of adjacent lower landscapes and exasperating headwater pollution.

- Shoot and root biomass was 3.1 and 6.7 times higher, respectively, with localized manure application (Fig. 10), but homogenized manure led to 3-29% higher enzyme activities than localized manure. Localized manure application decreases competition for nutrients between microorganisms and roots and simultaneously increases plant performance. This may represent a potential strategy to recover degraded Tibetan pastures using yak manure.

1.5 Conclusions

Highly intensive anthropogenic activities (e.g. overgrazing) have occurred for decades across the entire Tibetan Plateau to meet the demands of fast socio-economic development. These, in addition to a warming rate of about twice the global mean, have exerted extreme pressure on the vulnerable alpine pastoral ecosystems sensitive to disturbances, which induced widespread pasture degradation. This thesis summarized the mechanisms of Tibetan pasture degradation and investigated the impact of simulated warming on enzyme activities and the effect of simulated increasing precipitation on CO_2 emission of pasture soils. Both simulated environmental factors prompted nutrient release and CO_2 emission, indicating more losses of C and nutrients from Tibetan pastures. Investigation of the effect of pasture degradation on C and N cycles showed that Tibetan pastures at the intermediate degradation stage have the highest C losses as CO_2 emission and DOC leaching, while the highest N losses occur in the extreme degradation stage of Tibetan pastures. These are primarily explained by the gradual disappearance of living plants and decrease of C stocks, along with the more serious Tibetan pasture degradation. The literature review revealed that degradation on the Tibetan Plateau has triggered significant losses of SOC ($-42 \pm 2 \%$), N ($-33 \pm 6 \%$) and P ($-17 \pm 4 \%$) contents compared to the non-degraded pastures. While losses of TN and plant biomass are found to be accompanied by SOC losses, TP loss is resistant to decreasing SOC content because of its precipitation as $\text{Ca}_3(\text{PO}_4)_2$. While various strategies have been implemented to cease and even reverse the

degradation processes, their effects on soil quality are still unclear, and restoration is impossible without strong support and cooperation at regional, local and household scales. If pasture degradation in the Tibetan Plateau continues, the natural *Kobresia* root mats will disappear in the coming decades. This will dramatically destabilize these unique alpine ecosystems and have lasting negative impacts on global environmental changes.

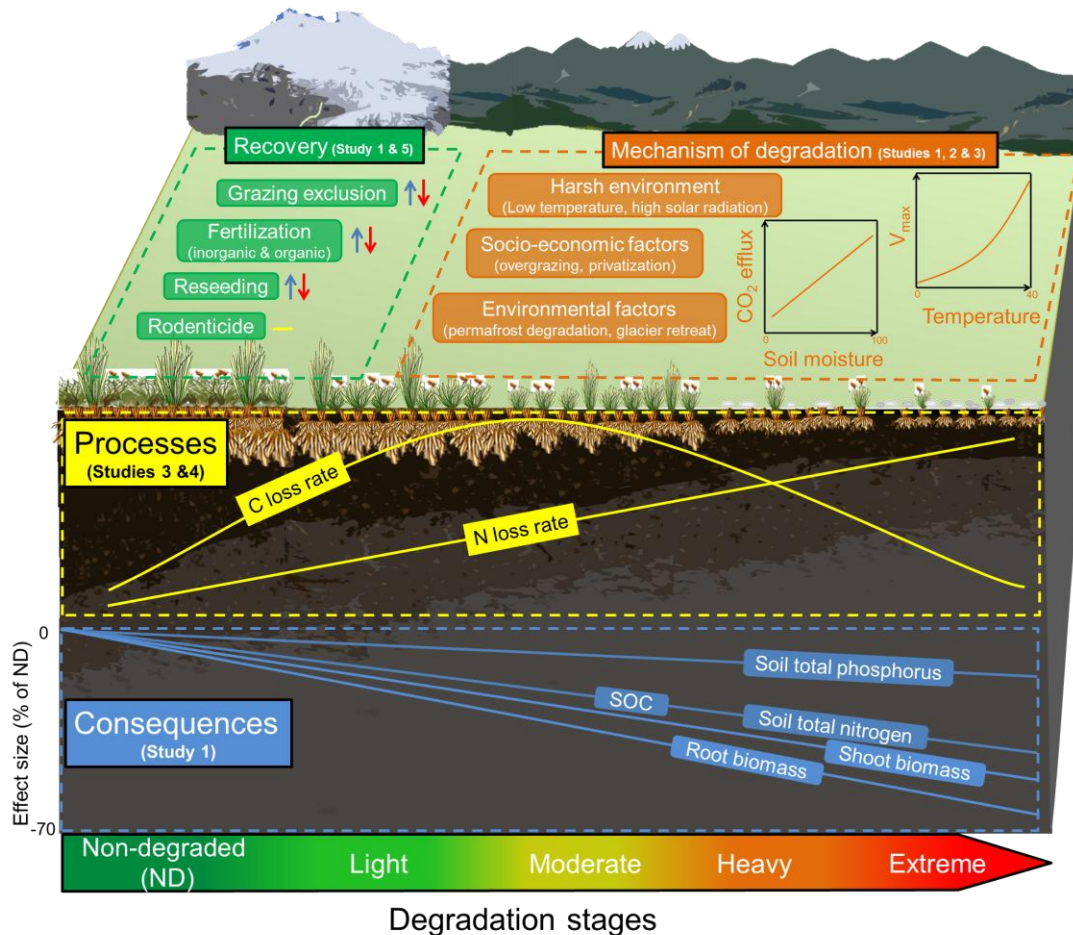


Figure 11 Synthesis of the main results of the studies. Carbon loss rate refers to losses as CO₂ emission and DOC leaching. Nitrogen loss refers to losses from leaching processes.

1.6 References

- Alados CL, Aich AE, Komac B *et al.* 2007. Self-organized spatial patterns of vegetation in alpine grasslands. *Ecological Modelling*, 201: 233-242. doi: 10.1016/j.ecolmodel.2006.09.014.
- Babel W, Biermann T, Coners H, Falge E, Seeber E, Ingrisch J, Schleuß P.M, Gerken T, Leonbacher J, Leipold T, Willinghöfer S, Schützenmeister K, Shibistova O, Becker L, Hafner S, Spielvogel S, Li X, Xu X, Sun Y, Zhang L, Yang Y, Ma Y, Wesche K, Graf H.F, Leuschner C, Guggenberger G, Kuzyakov Y, Miede G, Foken T. 2014. Pasture degradation modifies the water and carbon cycles of the Tibetan highlands. *Biogeosciences*, 11: 6633-6656.
- Bai, Z.G., Dent, D.L., Olsson, L., Schaepman, M.E., 2008. Global assessment of land degradation and improvement. 1. Identification by Remote Sensing. Report 2008/01. ISRIC—World Soil Information, Wageningen.

- Behnke R, Scoones I. 1993. Rethinking range ecology: Implications for rangeland management in Africa. In: Range Ecology at Disequilibrium (eds Behnke R, Scoones I, Kerven C). pp. 24, Overseas Development Institute, London, UK.
- Dlamini P., Chivenge P., Chaplot V. 2016. Overgrazing decreases soil organic carbon stocks the most under dry climates and low soil pH: A meta-analysis shows. *Agriculture, Ecosystems and Environment*, 221: 258-269.
- Dong SK, Wen L, Li YY et al. (2012) Soil-quality effects of grassland degradation and restoration on the Qinghai-Tibetan Plateau. *Soil Science Society of America Journal*, 76, 2256-2264. doi: 10.2136/sssaj2012.0092.
- Fan YJ, Hou XY. 2016. Relationship between vegetation degeneration and water-tower function on alpine meadow in the three-headwater-river-source region. *Journal of Southwest University for Nationalities (Natural Science Edition)*, 42: 9-13. (in Chinese with English abstract)
- FAO (Food and Agriculture Organization of the United Nations). 2010. Challenges and opportunities for carbon sequestration in grassland systems. A technical report on grassland management and climate change mitigation. *Integrated Crop Management*, Vol. 9.
- Feng R, Long R, Shang Z et al. 2010. Establishment of *Elymus natans* improves soil quality of a heavily degraded alpine meadow in Qinghai-Tibetan Plateau, China. *Plant and Soil*, 327, 403-411. doi: 10.1007/s11104-009-0065-3.
- Harris RB. 2010. Rangeland degradation on the Qinghai-Tibetan plateau: A review of the evidence of its magnitude and causes. *Journal of Arid Environments*, 74: 1-12.
- Holzner W, Kriechbaum M. 2000. Pastures in south and central Tibet (China) I. Methods for a rapid assessment of pasture conditions. *Die Bodenkultur*, 51(4): 259-266.
- Jordaan FP, Biel LC, du Plessis PIM. 1997. A comparison of five range condition assessment techniques used in the semi-arid western grassland biome of southern Africa. *Journal of Arid Environments*, 35: 665-671. doi: 10.1006/jare.1996.0166.
- Kimetu JM, Lehmann J, Ngoze SO et al. 2008. Reversibility of soil productivity decline with organic matter of differing quality along a degradation gradient. *Ecosystems*, 11: 726-739. doi: 10.1007/s10021-008-9154-z.
- Kwon HY., Nkonya E., Johnson T., Graw V., Kato E., Kihui E. 2015. Global estimates of the impacts of grassland degradation on livestock productivity from 2001 to 2011. In: *Economics of Land Degradation and Improvement – A Global Assessment for Sustainable Development* (Eds. Nkonya E., Mirzabaev A., Braun J.), pp. 197-214, Springer International Publishing, Switzerland.
- Li XL, Gao J, Brierley G, Qiao YM, Zhang J, Yang YW. 2013. Rangeland degradation on the Qinghai-Tibet Plateau: Implications for rehabilitation. *Land Degradation and Development*, 24: 72-80.
- Li Y, Dong S, Liu S et al. 2015. Seasonal changes of CO₂, CH₄ and N₂O fluxes in different types of alpine grassland in the Qinghai-Tibetan Plateau of China. *Soil Biology and Biochemistry*, 80, 306-314. doi: 10.1016/j.soilbio.2014.10.026.
- Li YY, Dong SK, Wen L et al. 2014. Soil carbon and nitrogen pools and their relationship to plant and soil dynamics of degraded and artificially restored grasslands of the Qinghai-Tibetan Plateau. *Geoderma*, 213: 178-184. doi: 10.1016/j.geoderma.2013.08.02.
- Liu S, Schleuss P-M, Kuzyakov Y., 2016. Carbon and nitrogen losses from soil depend on degradation of Tibetan *Kobresia* pastures. *Land Degradation and Development*. doi: 10.1002/ldr.2522.
- Ma Y, Lang B, Li Q et al. 2002. Study on rehabilitating and rebuilding technologies for degenerated alpine meadow in the Changjiang and Yellow river source region. *Pratacultural Science*, 19: 1-5. (in Chinese with English abstract)
- Miehe G, Miehe S, Bach K, Nölling J, Hanspach J, Reudenbach C, Kaiser K, Wesche K, Mosbrugger V, Yang YP, Ma YM. 2011. Plant communities of central Tibetan pastures in the Alpine Steppe/*Kobresia pygmaea* ecotone. *Journal of Arid Environments*, 75: 711–723. doi:10.1016/j.jaridenv.2011.03.001.
- Miehe G, Miehe S, Kaiser K, Liu JQ, Zhao X. 2008. Status and dynamics of the *Kobresia pygmaea* ecosystem on the Tibetan Plateau. *Ambio A Journal of the Human Environment* 37:272–279. Available from: <http://www.jstor.org/stable/25547897>.
- Ni J. 2002. Carbon storage in grasslands of China. *Journal of Arid Environments*, 50: 205-218.
- Squires VR, Lu XS, Lu Q, Wang T, Yang Y. 2009. Rangeland degradation and recovery in China's pastoral lands. pp. 188, MPG Books Group, UK.
- Qiao Y, Duan Z. 2016. Understanding alpine meadow ecosystems. In: *Landscape and Ecosystem Diversity, Dynamics and Management in the Yellow River Source Zone* (eds Brierley GJ, Li X, Cullum C, Gao J). pp. 117-135, Springer International Publishing, Switzerland.
- Sun HL, Zheng D, Yao TD, Zhang YL. 2012. Protection and construction of the national ecological security shelter zone on Tibetan Plateau. *Acta Geographica Sinica*, 67: 3-12. (in Chinese with English abstract)
- Suttie, J.M., Reynolds, S.G., Batello, C., 2005. *Grasslands of the World*. Food and Agricultural Organization of the United Nations, Rome, Italy.
- Tennigkeit, T. & Wilkies, A. 2008. An assessment of the potential for carbon finance in rangelands. ICRAF. Available at: http://www.fao.org/fileadmin/templates/agphome/scpi/cgwg/carbon_finance.pdf.
- Tian HQ, Wang SQ, Liu JY, Pan SF, Chen H, Zhang C, Shi XZ. 2006. Patterns of soil nitrogen storage in China. *Global Biogeochemical Cycles*, 20: GB1001.

- Van der Westhuizen HC, Snyman HA, Fouché HJ. 2005. A degradation gradient for the assessment of rangeland condition of a semi-arid sourveld in Southern Africa. *African Journal of Range and Forage Science*, 22: 47–59. doi: 10.2989/10220110509485861.
- Wang Z. Zhang Y. Yang Y. Zhou W. Gang C. Zhang Y. Li J. An R. Wang K. Odeh I. Qi J. 2016. Quantitative assess the driving forces on the grassland degradation in the Qinghai-Tibet Plateau, in China. *Ecological Informatics*, 33: 32-44.
- Wen L., Dong S., Li Y., Li XY., Shi JJ., Wang YL., Liu DM., Ma YS. 2013. Effect of degradation intensity on grassland ecosystem services in the alpine region of Qinghai-Tibetan Plateau, China. *PLoS ONE*, 8: e58432.
- White PR, Murray S, Rohweder M. 2000. Pilot analysis of global ecosystems-Grassland ecosystems. World Resources Institute, Washington DC, USA.
- Xie GD. Lu CX. Xiao Y. Zheng D. 2003. The economic evaluation of grassland ecosystem services in Qinghai-Tibet Plateau. *Journal of Mountain Science*, 21: 50-55.
- Zeng C, Zhang F, Wang Q *et al.* 2013. Impact of alpine meadow degradation on soil hydraulic properties over the Qinghai-Tibetan Plateau. *Journal of Hydrology*, 478: 148-156. doi: 10.1016/j.jhydrol.2012.11.058.
- Zhong XH. Liu SZ. Wang XD. Zhu WZ. Li XM. Yang L. 2006. A research on the protection and construction of the state ecological safe shelter zone on the Tibetan Plateau. *Journal of Mountain Science*, 24: 129-136.

1.7 Contributions to the included manuscripts

This PhD thesis consists of five studies which were finished in cooperation with several coauthors. The contributions of these coauthors are as follows:

Study 1: Degradation of Tibetan grasslands: Consequences for carbon and nutrient cycles

Status: Submitted in *Agriculture, Ecosystems & Environment*

Shibin Liu: 50% (data collection, analysis and interpretation; manuscript preparation)

Kazem Zamanian: 15% (discussion of manuscript structure; comments to improve the manuscript)

Per-Marten Schleuss: 12% (comments to improve the manuscript)

Mohsen Zarebanadkouki: 3% (preparation of data)

Yakov Kuzyakov: 20% (discussion of manuscript structure; comments to improve the manuscript)

Study 2: Hot experience for cold-adapted microorganisms: Temperature sensitivity of soil enzymes

Status: published in *Soil Biology & Biochemistry*

Bahar S. Razavi: 60% (experimental design, accomplishment of experiment, laboratory analyses, data preparation and interpretation, manuscript preparation)

Shibin Liu: 30% (data preparation and interpretation, discussion of experimental design and results, comments to improve the manuscript)

Yakov Kuzyakov: 10% (comments to improve the manuscript)

Study 3: Carbon and nitrogen losses from soil depend on degradation of Tibetan *Kobresia* pastures

Status: published online in *Land Degradation & Development*

Shibin Liu: 50% (data collection, analysis and interpretation; manuscript preparation)

Per-Marten Schleuss: 35% (comments to improve the manuscript)

Yakov Kuzyakov: 15% (discussion of manuscript structure; comments to improve the manuscript)

Study 4: Responses of degraded Tibetan *Kobresia* pastures to N addition

Status: published online in *Land Degradation & Development*

Shibin Liu: 50% (data collection, analysis and interpretation; manuscript preparation)

Per-Marten Schleuss: 35% (comments to improve the manuscript)

Yakov Kuzyakov: 15% (discussion of manuscript structure; comments to improve the manuscript)

Study 5: Spatio-temporal patterns of enzyme activities after manure application reflect mechanisms of niche differentiation between plants and microorganisms

Status: published in *Soil Biology & Biochemistry*

Shibin Liu: 50% (accomplishment of experiment, laboratory analyses, data preparation and interpretation, manuscript preparation)

Bahar S. Razavi: 25% (experimental design, accomplishment of experiment, data interpretation, comments to improve the manuscript)

Xu Su: 3% (experimental design, comments to improve the manuscript)

Menuka Maharjan: 3% (laboratory analyses, comments to improve the manuscript)

Mohsen Zarebanadkouki: 3% (data analysis, comments to improve the manuscript)

Evgenia Blagodatskaya: 12% (comments to improve the manuscript)

Yakov Kuzyakov: 4% (discussion of experimental design and results; comments to improve the manuscript)

2 Publications and Manuscripts

2.1 Study 1: Degradation of Tibetan grasslands: Consequences for carbon and nutrient cycles

Shibin Liu^{a*}, Kazem Zamanian^b, Per-Marten Schleuss^a, Mohsen Zarebanadkouki^c, Yakov Kuzyakov^{a,b,d}

Status: Submitted to *Agriculture, Ecosystems and Environment*

^a Department of Soil Science of Temperate Ecosystems, University of Göttingen, Göttingen, Germany

^b Department of Agricultural Soil Science, University of Göttingen, Göttingen, Germany

^c Division of Soil Hydrology, University of Göttingen, Göttingen, Germany

^d Institute of Environmental Sciences, Kazan Federal University, 420049 Kazan, Russia

2.1.1 Abstract

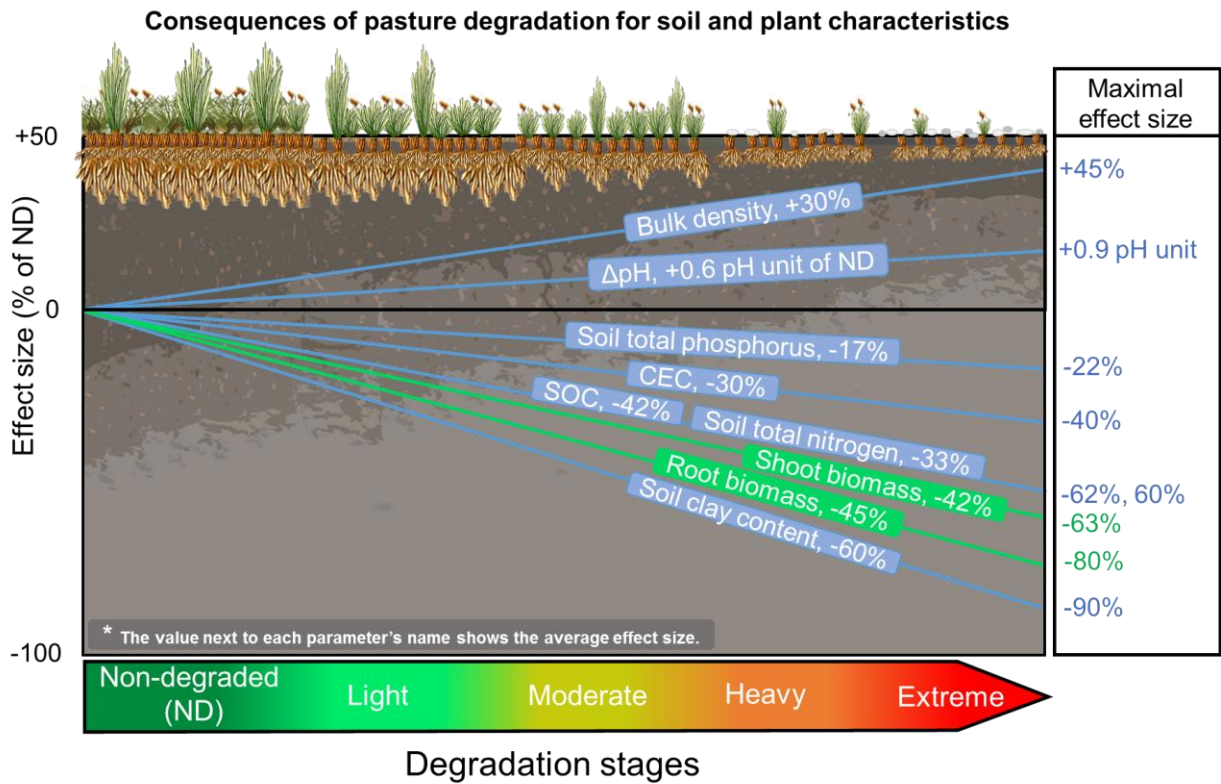
The Tibetan Plateau hosts the world's largest alpine pastoral ecosystems, dominated by the endemic sedge *Kobresia pygmaea*. Owing to the very harsh environment and also to soil nitrogen (N) and phosphorus (P) limitations, these pastoral ecosystems are very sensitive to disturbances (e.g. anthropogenic activities and climate change) and recover extremely slowly. Overgrazing on the Tibetan Plateau has caused severe degradation of vegetation and soils in the last 30-50 years. For the first time, for the whole Tibetan Plateau, we have summarized and generalized the consequences of pasture degradation for soil organic carbon (SOC) and nutrient stocks, and evaluated the main biotic and abiotic mechanisms of their loss. Based on 44 literature studies as well as own data, we demonstrated that 42 % of SOC stocks were lost, relative to non-degraded pastures. These SOC losses are similar to the decreases in N stocks (-33 %), and aboveground (-42 %) and belowground (-45 %) plant biomass. Although P losses are lower (-17 ± 4%), its precipitation as $\text{Ca}_3(\text{PO}_4)_2$ makes it unavailable for plants. These losses are in fact underestimates, since undisturbed natural sites no longer exist on the Tibetan Plateau. The losses are much higher in the upper 10 cm and in some areas extend to complete removal of soil cover. This has dramatic repercussions for local livestock, human populations and river pollution. While some rehabilitation projects have shown positive outcomes, the complete recovery of degraded pastures (e.g. soil fertility, ecosystem stability) is infeasible, because of very slow pedogenic processes, slow vegetation restoration, as well as continuously increasing anthropogenic pressure and climate change. Considering the rapid losses of SOC

and nutrients, and the very slow recovery potential, Tibetan pastures may disappear in the next few decades.

Key words: Tibetan Plateau, Soil organic matter, Pasture degradation, Soil nutrients, Carbon sequestration

Corresponding Author: *Shibin Liu, sliu3@gwdg.de*

Graphical Abstract



2.1.2 Introduction

The *Kobresia* pastures, commonly known as “alpine meadow”, cover the southeastern quarter of the Tibetan Highlands (~450,000 km²) and form the world’s largest alpine pastoral ecosystem (Babel *et al.*, 2015). Several major Asian rivers, such as the Huang He, Salween River, Yangtze River, Mekong River etc., originate on the Tibetan Plateau and flow through *Kobresia* pastures (Fig. 1). These rivers collectively constitute the main water resource for billions of people in the adjacent regions of southeastern Asia (Pomeranz, 2013). The *Kobresia* pastures provide important grazing grounds for livestock (i.e. yaks, sheep and goats) and thus ensure the livelihood of the Tibetan herders (Harris, 2010). More than 4.0% of the world’s grassland soil carbon (C) is stored in soils under Tibetan pastures (ca. 10.7 Pg C; Ni, 2002). Around 920 Tg nitrogen (N) is preserved in the Tibetan pasture soils, which represents 0.7-1.0 % of total global N storage (Tian *et al.*, 2006) and is required for sufficient forage production. Consequently, Tibetan pastures are of considerable importance to livestock productivity, Tibetan herders (ca. 5 million), nutrient cycling and ecosystem stability.

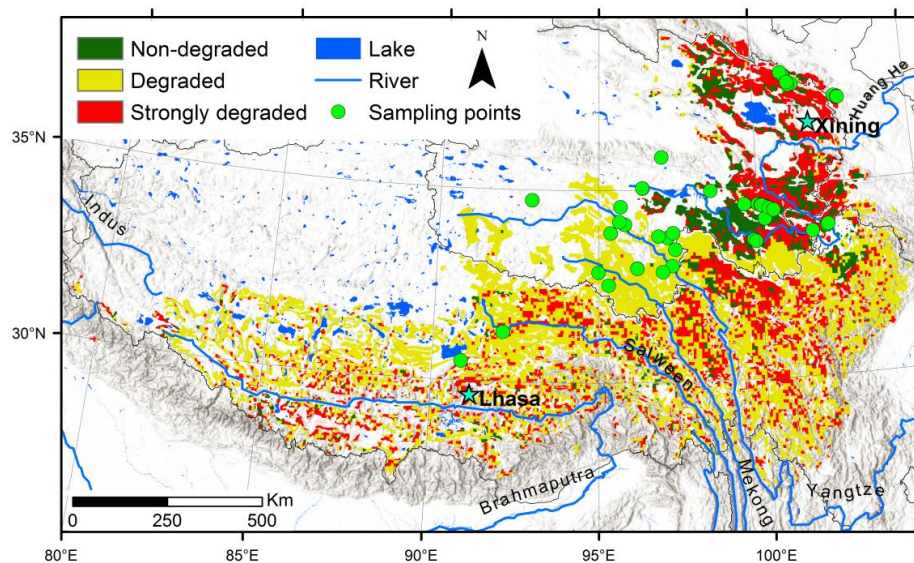


Figure 1 Degradation of pastures on the Tibetan Plateau. The circular green points are the locations of the study sites included in the literature review. The extent of Tibetan pastures is taken from Lehnert *et al.*, (2015). The three degradation stages were classified by integrating the current status (low or high degradation) and future trend (degrading or improving) of four aggregated biophysical ecosystem factors (plant biomass, soil, water and plant biodiversity) (Nachtergaele *et al.*, 2011). This map was created in ArcGIS based on distribution and degradation information for Tibetan pastures. The degradation information was derived from: http://www.fao.org/nr/lada/gladis/glad_ind/.

The Tibetan pastures are developed over centuries in extreme environments: low mean

annual temperatures (below 0°C, Frauenfeld *et al.*, 2005), high temperature and precipitation variation (Kuang & Jiao, 2016), low annual mean precipitation (~437 mm, Xu *et al.*, 2008), very high solar radiation (Liu *et al.*, 2012), very short plant growing season (~3.5 months, Leonard & Crawford, 2002), strong erosion by wind and water (48 t ha⁻¹ yr⁻¹, Yan *et al.*, 2000), very limited nutrients (e.g. N and phosphorus (P); Li *et al.*, 2014a), very shallow soil profiles (~30-50 cm, Chang *et al.*, 2014) and low air pressure and CO₂ concentration. These harsh conditions make the region very sensitive to changes in environmental and socio-economic factors (Wang *et al.*, 2008b). For instance, warming across the whole plateau is greater and faster than the global mean (Kuang & Jiao, 2016). In response to this, glaciers retreat dramatically and permafrost thaws rapidly. The water table subsequently drops, erosion is exacerbated, and soil fertility declines (Chen *et al.*, 2013). This directly contributes to the removal of the shallow soil profile and soil organic carbon (SOC) and nutrient losses, i.e. the degradation of vulnerable Tibetan pastures.

The Tibetan pastures have suffered from serious degradation for several decades, due to frequent and very strong anthropogenic pressure (e.g. overgrazing) and large-scale environmental changes (e.g. climate change). This has had a variety of ecological consequences, including decreased plant species richness (Wang *et al.*, 2009a), accelerated soil erosion (Wu & Tiessen, 2002) and shrinking grazing ground (Wu & Du, 2007). To characterize the degradation problems and compare the situation in various pastures, the term “pasture degradation” needs to be defined. Considering differences in which pasture conditions are emphasized (e.g. pastoral productivity, vegetation composition, biological diversity, soil fertility, C and nutrient stocks), making a general and globally accepted definition is challenging (White *et al.*, 2000). Instead, various indicators, for instance soil properties (Kimetu *et al.*, 2008; Alados *et al.*, 2007), plant species composition (Van der Westhuizen *et al.*, 2005; Jordaan *et al.*, 1997), species abundance of wildlife, and death rate of domestic livestock (Behnke & Scoones, 1993; White *et al.*, 2000), have been recommended to assess pasture degradation. Among them, vegetation characteristics (i.e. vegetation coverage, productivity and proportion of edible plants) are most frequently proposed (Zeng *et al.*, 2013), as vegetation status not only relates to animal productivity but also reflects soil quality. For instance, Ma *et al.*

(2002) divided the degradation of Tibetan pastures into five stages: non-degradation, light degradation, moderate degradation, heavy degradation and extreme degradation (Table S1, Fig. 2). This is the most frequently used degradation classification for pastures of the Tibetan Plateau. Similar classification systems have also been applied in other studies, but with variable percentage ranges (Zeng *et al.*, 2013). In this review, we use the classification of degradation stages proposed by Ma *et al.* (2002). We define “pasture degradation” as the retrogressive succession of a pasture ecosystem affected by interference of rational and irrational anthropogenic (e.g. overgrazing, deforestation, and infrastructure construction) and/or environmental factors (e.g. permafrost melting and climate change) leading to decreases in plant productivity, soil quality etc.

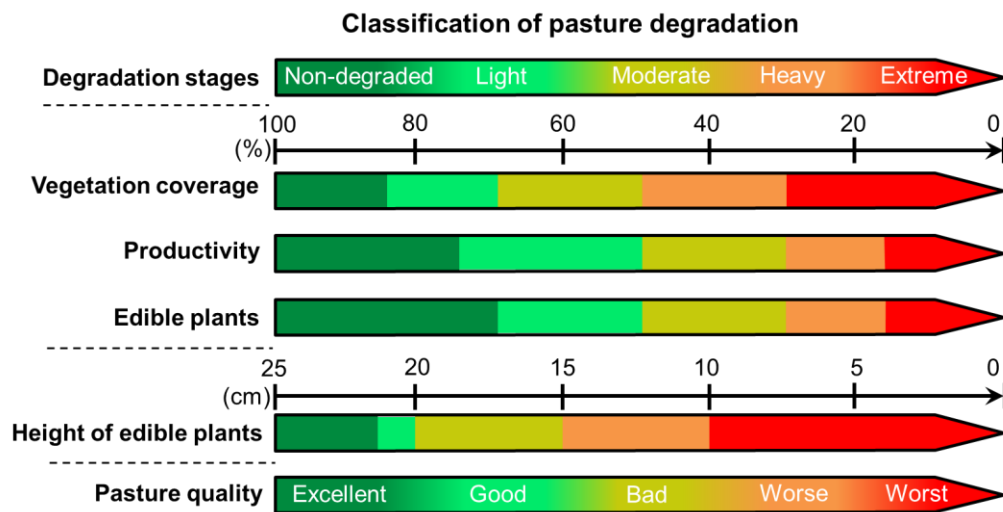


Figure 2 Classification of Tibetan pasture degradation. The degradation stages were determined based on vegetation coverage, plant productivity, portion of edible plants and height of edible plants.

When applying this classification to pasture degradation, the primary concern is the assessment of SOC and nutrient status, due to their fundamental roles in biogeochemical cycles, plant productivity and ecosystem stability. By far, many studies have been implemented at the local scale and reached varied conclusions. Meanwhile, mechanisms for SOC and nutrient losses and the consequences have also been investigated (Babel *et al.*, 2015; Liu *et al.*, 2016; Li *et al.*, 2015) and strategies to restore soil quality have been proposed and examined (Dong *et al.*, 2012; Feng *et al.*, 2010). However, regional-scale generalization with a better understanding of SOC and nutrient status in Tibetan pastures and the current degradation situation remains unknown.

To clarify these points and provide generalizations, the literature that has classified the pastures' degradation using vegetation characteristics was assembled and the data concerning SOC, N and P content or stocks were extracted. We focused this review on degradation-related losses of two nutrients (N and P) because these are the most limiting nutrients worldwide (Vitousek *et al.*, 2010) and especially on Tibetan Plateau.

Our objectives were to: 1) quantify SOC and nutrient losses under five degradation stages of Tibetan pasture ecosystems; 2) relate vegetation characteristics and a broad range of soil properties to SOC and nutrient losses; 3) comprehensively understand how socio-economic and environmental factors contribute to pasture degradation and 4) identify the negative feedbacks of degradation to ecosystem services and functions.

2.1.3 Materials and Methods

2.1.3.1 Data collection

Literature about the effects of pasture degradation on SOC and nutrient content was assembled mainly through four channels: 1) Web of Science V.5.22.1 (available online), 2) ScienceDirect (Elsevier B.V.), 3) Google Scholar and 4) Chinese-language literature using the China Knowledge Resource Integrated Database (CNKI). The search terms were “degradation gradient/stages”, “alpine meadow”, “Tibetan Plateau” and “soil”.

The criteria for inclusion in this review were: (1) the classification of degradation stages is clearly stated; (2) the literature includes analysis of SOC (or soil organic matter), total nitrogen (TN), total phosphorus (TP), vegetation characteristics or soil properties; (3) the non-degradation stage (stage 1 according to Table S1) is necessarily included as the “reference”, to enable the “effect size” analysis. At least one of the degradation stages (light degradation, moderate degradation, heavy degradation and extreme degradation) is also presented in relation to the “reference”; and (4) the sampling depth and study location are clearly presented. Totally, 44 literature studies were found (Fig. 1).

2.1.3.2 Data analysis

Data examination and standardization was performed to standardize the units of each parameter. Data illustrated in original publications as graphs were extracted using

g3data (v.1.5.1) software (<http://www.frantz.fi/software/g3data.php>). When soil organic matter content was presented, this was converted to soil organic carbon content using a conversion factor of 2.0 (Pribyl, 2010). Soil organic C and nutrient stocks were calculated using the following equation:

$$\text{Stock} = 100 \times \text{Cont} \times \text{BD} \times \text{Depth} \quad (1)$$

Where Stock is C or nutrient (N, P) stock [kg ha^{-1}]; Cont is soil C or nutrient (N, P) content, [g kg^{-1}]; BD is soil bulk density, [g cm^{-3}]; and Depth is the soil sampling depth, [cm]. To continue this conversion, only studies were considered which took samples in 10 cm intervals because of the relatively large database size compared to other depth intervals. In some studies, bulk density was not presented. To calculate stocks for these studies, significant relationships between SOC or nutrient content and their stocks were established using existing data (Fig. S1). Based on these relationships, SOC or nutrient stocks were calculated.

Power regressions between vegetation coverage and SOC or nutrients for the five degradation stages (N, P) were performed. When studies presented ranges for vegetation coverage, we took the median value. The effect sizes of individual variables (i.e. SOC, nutrients, bulk density and plant biomass) were quantified to illustrate differences between the non-degraded and the degraded stages. The following equation was used:

$$ES = (D - R) / R \times 100\% \quad (2)$$

Where *ES* is the effect size, in %; *D* is the value of the corresponding variable in the relevant degradation stage (light degradation, moderate degradation, heavy degradation and extreme degradation); and *R* is the value of each variable in the non-degradation stage (reference site). When *ES* is positive, zero or negative, this indicates an increase, no change or a decrease, respectively, of the parameter compared to the non-degradation stage. 95% confidence intervals were also calculated and illustrated in the figures. Because pH is the negative of the base 10 logarithm of the H^+ concentration, the effect size of degradation on soil pH cannot be quantified by Eq. (2). Therefore, we used the difference: *D* - *R*, which was expressed as ΔpH . For instance, when *D*=8 and

$R=7$, $\Delta\text{pH}=1$, meaning that pH increases by one pH unit with degradation to the relevant extent, i.e. $-\log 10^{-8}-(-\log 10^{-7}) = -\log 10^{-1}$ or 1. Significant differences of effect size among the degradation stages were tested using one-way analysis of variance (ANOVA). Before ANOVA was applied, data were checked for normality (Shapiro–Wilk test, $p > 0.05$) and homogeneity of variance (Levene test, $p > 0.05$). After a significant omnibus test result was obtained, a post hoc test (Tukey's honestly significant difference test) was conducted for multiple comparisons.

Sensitivity of 1) soil fertility (e.g. TN, TP) and 2) vegetation (e.g. aboveground plant biomass (AGB), belowground plant biomass (BGB)) indicators to SOC losses were evaluated for each degradation stage. All parameters were standardized to the non-degraded stage as reference (every indicator of the non-degraded stage equals to 1.0). Consequently, all the values range from 1.0 to 0. The standardized SOC contents were then plotted against the standardized soil fertility and vegetation indicators.

2.1.4 Results and discussion

2.1.4.1 Degradation-induced losses of soil carbon, nitrogen and phosphorus

Degraded Tibetan grasslands have lost on average $42 \pm 2\%$ of their SOC content relative to the non-degraded pastures (Fig. 3). Soil total N contents had declined by $33 \pm 6\%$ (Fig. 3) and total P and K content were reduced by $17 \pm 4\%$ and $15 \pm 3\%$, respectively (Fig. 3). Furthermore, SOC, N and K losses significantly increase from light to extreme degradation, while P loss is consistent among degradation stages. Because the non-degraded stage is defined by wide ranges for several indicators (Table S1; Fig. 2), the reference sites may also have experienced some degradation compared to completely intact sites. Therefore, the SOC and nutrient losses reviewed here are actually underestimations and should be considered as minimum values.

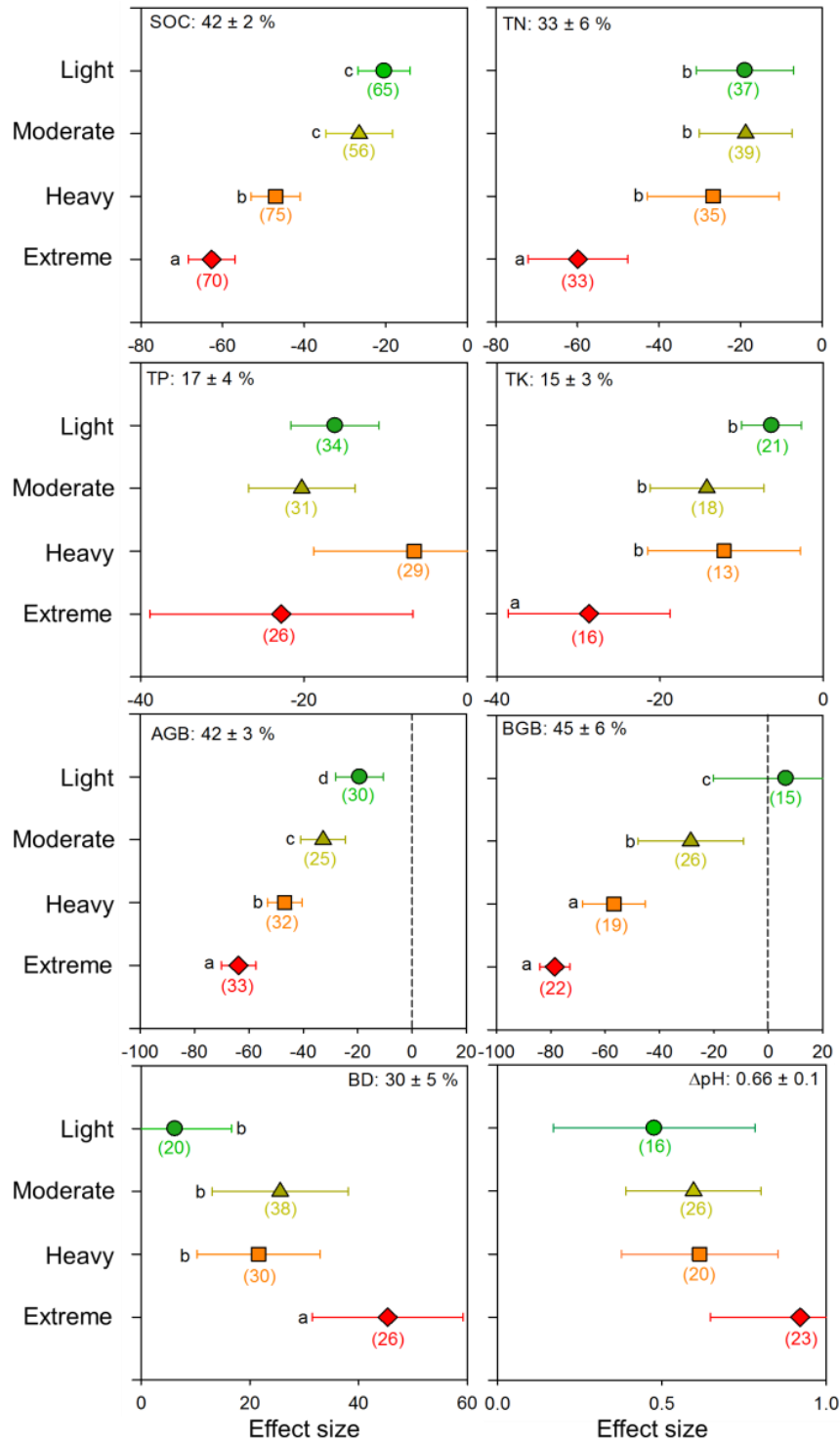


Figure 3 Effect sizes of SOC content, nutrient content, plant biomass, soil bulk density (BD) and soil pH for four degradation stages compared to non-degraded pastures. The effect size is calculated by Equation 2 and presented as percent (except for pH, which is expressed as $\Delta pH = pH_{\text{Degraded}} - pH_{\text{Non-Degraded}}$). Colors represent degradation stages. The percentage value at the top shows the average effect size of four degradation stages. The number in the parenthesis is the number of sampling points. Low-case letters show the significant differences between the degradation stages.

SOC and nutrients are inherently related to vegetation characteristics and soil properties. Therefore, these parameters directly contribute to variations in SOC and nutrient composition. In the following, we present the responses of vegetation characteristics and soil properties to pasture degradation and discuss how they can be related to SOC and nutrient losses.

(1) Degradation effects on vegetation

Plants assimilate CO₂ and allocate part of this C belowground. The amount of C incorporated into the SOC pool from this newly assimilated C largely depends on plant biomass and vegetation coverage (Phillips *et al.*, 2011). Pasture degradation leads to strong decreases in plant coverage, aboveground biomass (AGB, $\sim 42 \pm 3$ %) and belowground biomass (BGB, $\sim 45 \pm 6$ %) (Fig. 3) and consequently decreases C input into soil, with negative feedbacks on SOC storage. Further, plants take up nutrients, recycle them within the ecosystem, and thus protect them from being leached. Following degradation, however, there is less nutrient preservation in vegetation and they are more prone to leaching. Furthermore, pasture degradation decreases plant species richness and diversity and changes functional groups from graminoids and legumes in favour of forbs (Wang *et al.*, 2009a; Li *et al.*, 2014b; Wang *et al.*, 2014). In sum, a decrease in vegetation cover and changes in species composition reduce C assimilation and nutrient uptake (i.e. less complementarity and facilitation) and so have negative effects on the total productivity of plant communities (Vicca *et al.*, 2007), and ultimately on SOC storage and nutrient retention.

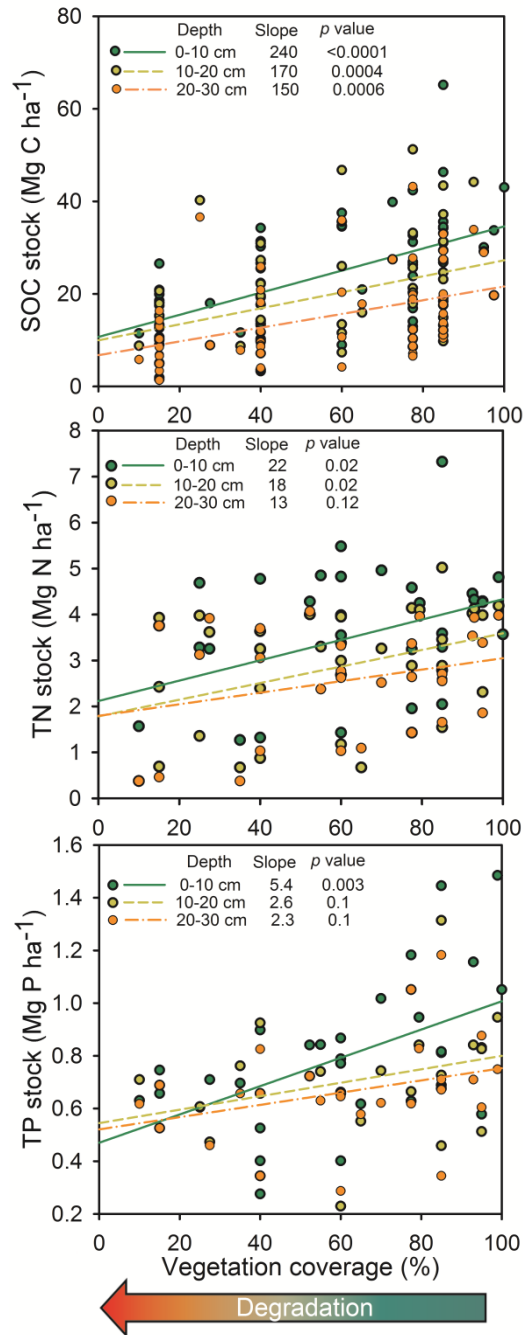


Figure 4 Relationships between vegetation coverage (in % of area) and stocks of soil organic carbon: SOC (top), total nitrogen: TN (middle) and total phosphorus: TP (bottom) for three depth intervals (0-10, 10-20 and 20-30 cm). 'Slope' shows the slopes of the regression lines. p values represent the significance of the regressions. The Y axis for C, N, and P are presented at ratios: 50:5:1. All regressions show clear decreases of the closeness (slope) and significance (p) of the degradation (here as vegetation coverage) with depth, confirming that degradation starts from the vegetation and topsoil.

High vegetation coverage significantly increases SOC and nutrient stocks (Fig. 4) by: i) facilitating photosynthesis (McAllister *et al.*, 1998), which induces more belowground C input, including roots and the organic compounds released through roots; ii) protecting

SOC and nutrients from being lost directly (decreasing water and wind erosion rates) and indirectly (storing nutrients in the living biomass) (Mchunu & Chaplot, 2012; Chaplot *et al.*, 2005; Wu & Tiessen, 2002); and iii) preventing soil heating by absorbing strong solar radiation, which subsequently decreases soil temperature and slows down SOC decomposition and CO₂ release (Schrott, 1991; Liu *et al.*, 2012).

Though pasture degradation leads to lower C input from plants, it does not necessarily mean microbial decomposition of SOC will be limited and C losses via respiration will decrease after degradation. Two mechanisms support this statement: First, additional C supply from root litter (i.e. dying and dead roots) is available for microbes following degradation. Second, the decrease of root biomass eliminates the competition between plants and microbes for limited nutrients (especially nitrogen, Kuzyakov, 2002; Xu *et al.*, 2006). In fact, a significant increase in soil CO₂ emission from degraded pastures has been confirmed (Li *et al.*, 2015; Wang *et al.*, 2010), indicating stimulated microbial activities that lead to more C loss via SOC and root litter decomposition. This demonstrates that degraded grassland ecosystems release more CO₂ and lose more C than will be sequestered from plant input into the soil (i.e. net CO₂ loss).

Decreased plant biomass and vegetation coverage are also accompanied by intensified soil erosion, leading to removal of nutrient-enriched topsoil and exposure of the underlying soil layer (FAO, 1990; Tan, 2000). In consequence, soil structure becomes weaker, bulk density increases and pH may also increase due to higher CaCO₃ content in the subsoil. These changes in soil physical and chemical properties may further affect microbial activity and contribute to the modification of SOC and nutrient status and cycles.

(2) Degradation effects on soil chemical properties

Soil pH increased by 0.66 units on average over the full range of degradation ($\Delta\text{pH}=0.66 \pm 0.1$; Fig. 3). The common sources of acidity in soil are either H⁺ released via roots to take up basic cations or dissociated H⁺ from functional groups of organic matter. Intensified degradation will decrease both acidity sources, and so soil pH will be mostly controlled by CaCO₃ from parent materials (including continuous loess

deposition) and/or hydrolysis of basic cations. This causes increased soil pH following intensified degradation. Soil erosion can also elevate the pH by exposing the subsoil, which generally has higher pH than the removed surface soil. Increased soil pH facilitates microbial activity, which stimulates SOM mineralization and may thus further increase nutrient release into the soil solution (Pietri & Brookes, 2008; McLaren & Cameron, 1996).

Soil with high cation exchange capacity (CEC), like *Kobresia* root mats, can protect the nutrients from being leached. However, Tibetan pasture degradation substantially decreased CEC (effect size: -19 to -40 %, Wang *et al.*, 2007; Wu & Tiessen, 2002), because of the decrease in clay and SOM content and increase in soil pH, reducing both the soil permanent and pH-dependent charges (Zeng *et al.*, 2013; McLaren & Cameron, 1996). Consequently, the released nutrients will be more easily leached following pasture degradation.

Soil inorganic carbon (SIC) content showed inconsistent responses to pasture degradation, with its effect size ranging from -60 to +80% (Wen *et al.*, 2013; Liu *et al.*, 2015; Li *et al.*, 2014b). SIC density (on average 11.9 kg C m⁻² down to 1 m depth) in Tibetan pastures has very high spatial heterogeneity across the whole plateau (Yang *et al.*, 2010b). This largely depends on underlying parent materials: In sites with non-calcareous parent materials, SIC content decreases with depth and degradation stage (Liu *et al.*, 2015). The higher SIC in the topsoil derives from CaCO₃-containing dusts. In soils developed from calcareous parent materials (e.g. loess, limestone, marl), SIC content increases with depth and degradation stage (Wen *et al.*, 2013; Li *et al.*, 2014b). Because of these two contrasting scenarios - parent materials with or without CaCO₃ - soil pH responds to pasture degradation in different directions, and therefore the overall effect of pasture degradation on pH has the strongest variability (Fig. 3).

(3) Degradation effects on soil physical properties

Clay content decreases (effect size: -29 to -91%; Zeng *et al.*, 2013; Lu *et al.*, 2014; Li *et al.*, 2015; Li *et al.*, 2016) and BD increases by 30 ± 5 % (Fig. 3) with pasture degradation. This is the result of soil erosion that preferentially removes the fine

particles (Lal, 2003) and simultaneously exposes the deeper, often clay-depleted subsoil. Decreased clay content results in less formation of organic-clay complexes and less protection of incorporated SOC against microbial and enzymatic attacks. This additionally facilitates SOC decomposition and CO₂ emission rates in degraded pastures. CO₂ emission has already been shown to be higher in degraded pasture than in non-degraded pasture (Li *et al.*, 2015; Liu *et al.*, 2016). However, this stimulation of SOC mineralization may disappear and CO₂ release decline, when the labile OC stock is not sufficient to support microbial activity (Vinton & Burke, 1995; Kuzyakov *et al.*, 2009). This may occur at extreme degradation stages, where plant coverage is generally around 15% and belowground C stocks are even less than ~13 Mg C ha⁻¹ for 0-10 cm (Fig. 4).

2.1.4.2 Depth profiles of SOC and nutrient contents

SOC and nutrient contents decrease with depth for all degradation stages (Fig. 5). In Tibetan pastures, 60~80 % of roots are concentrated at 0-10 cm (Fig. 5, Wang *et al.*, 2009a; Li *et al.*, 2011). Therefore, C and nutrient inputs through root litter decomposition and rhizodeposition are the highest in the topsoil. Furthermore, other sources of C and nutrients (e.g. animal excretion, atmospheric deposition) are also readily incorporated into the topsoil.

The differences in SOC and nutrient contents between degradation stages is most marked in the top 10 cm of soil, and gradually decreases for 10-20 and 20-30 cm depths. This suggests that 1) the degradation starts from the topsoil, and 2) SOC and nutrients in the topsoil are the most sensitive to losses. This sensitivity is also revealed by the significant relationships between vegetation coverage and SOC or nutrient stocks (Fig. 4): All regression lines show the highest slope for the 0-10 cm depth, meaning that with one unit decrease in vegetation coverage, SOC and nutrient contents in the top 10 cm show the highest decrease. Consequently the degradation, which initiates from and is more intensive in the topsoil, has especially strong relevance for nutrient losses.

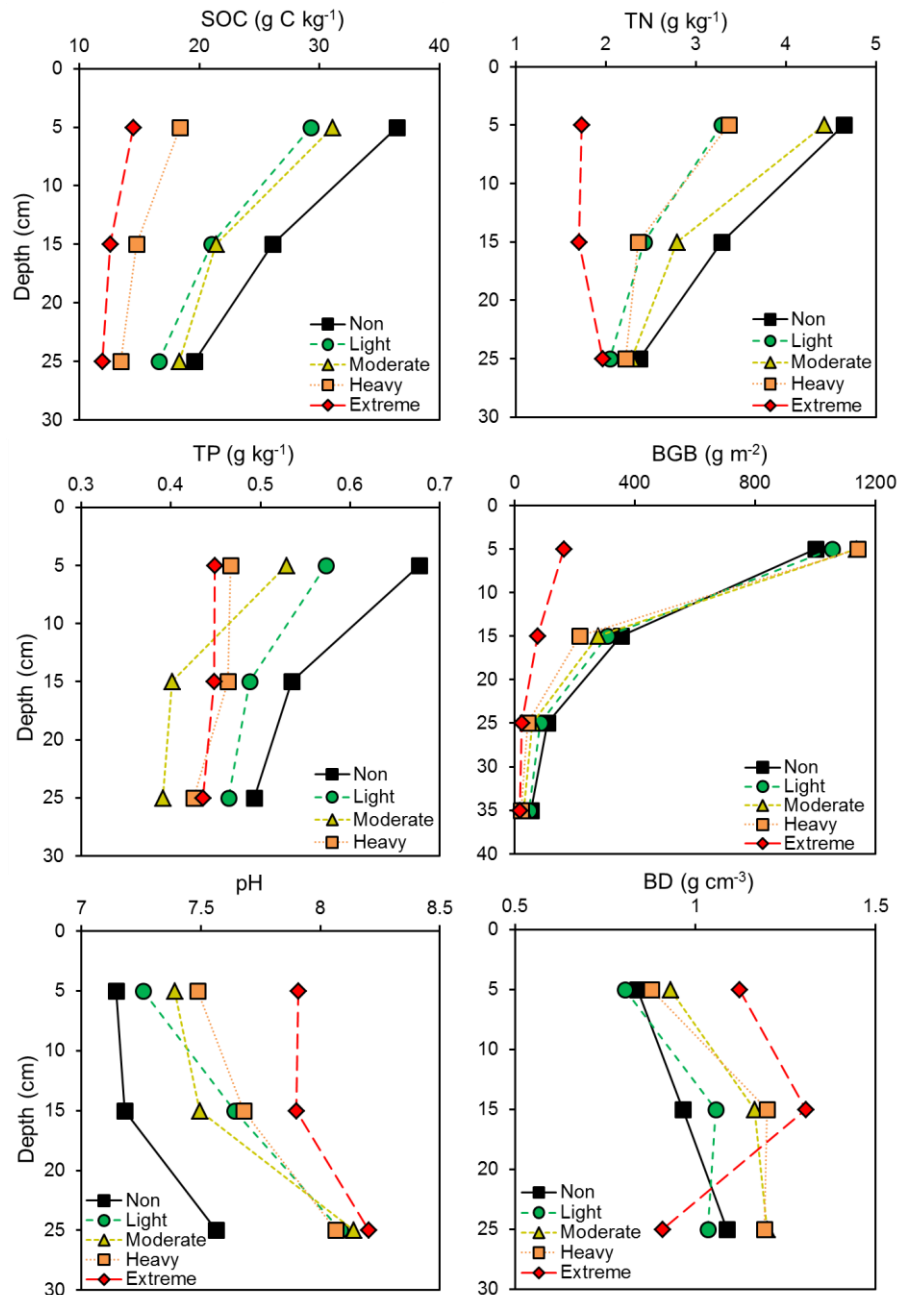


Figure 5 Soil organic carbon (SOC) and nutrient contents, belowground biomass (BGB) and soil properties depending on depths. “Non”, “Light”, “Moderate”, “Heavy” and “Extreme” represent non-degraded, light degradation, moderate degradation, heavy degradation and extreme degradation stages, respectively. For a better overview, the standard errors (SE) are deleted here.

2.1.4.3 Sensitivity of soil nutrients and plant biomass losses to the decreasing SOC due to pasture degradation

According to the trend lines (Fig. S2), high consistency of TN and some resistance of TP to SOC losses are evident. The trend line between the decreasing SOC and

decreasing TN fits well with a 1:1 line, indicating that TN losses are accompanied by SOC decrease. Even though the loss rate of TN is similar to that of SOC, the pathways of losses are different. Pathways of SOC losses include 1) SOC mineralization to CO₂; 2) leaching of DOM and 3) wind and water erosion of particulate organics. In contrast, soil N is lost by 1) gas emissions (e.g. N₂O, ~0.1 Tg N yr⁻¹ for Tibetan pastures; Du *et al.*, 2008) through nitrification and denitrification; 2) leaching of N, mainly in inorganic form (i.e. NO₃⁻, Liu *et al.*, 2016); 3) surface soil erosion; and 4) removal of N by grazing animals.

In contrast, P losses are generally less than SOC and N losses, as indicated by the trend line for decreasing TP and SOC, which is above the 1:1 line (Fig. S2). Available P in soils of Tibetan pastures accounts for only 0.3-2.2% of the TP (Shang *et al.*, 2016; Li *et al.*, 2016), indicating that most P is insoluble, and would thus be lost mainly by erosion. Even though SOM decomposition releases soluble P, in soils with pH ≥ 7.0 (Fig. 5) this P leaching from surface SOM-rich horizons to the deeper horizons rich in CaCO₃ will finally be precipitated as insoluble tricalcium phosphate (McLaren & Cameron, 1996). This precipitation reduces P losses by leaching, but causes less P availability for plant growth.

The trend between decreasing plant biomass (AGB and BGB) and decreasing SOC content almost overlaps with the 1:1 line (Fig. S2), suggesting that most of the SOC stocks are closely related to degradation of vegetation cover. As plant biomass decreases due to pasture degradation, the labile C input and subsequently total SOC stocks decrease. This means that the SOC stock is quite fragile and very sensitive to pasture degradation, and emphasizes the importance of pasture preservation.

2.1.5 Synthesis

2.1.5.1 Factors inducing pasture degradation

Multiple factors are responsible for degradation of Tibetan grasslands and consequently for the SOC and nutrient losses. These can be classified into two groups: (1) environmental factors and (2) socio-economic factors (Wang *et al.*, 2015b; Harris, 2010).

(1) Environmental factors: Very harsh conditions of climate, soils, relief etc. (Table 1) have existed on the Tibetan Plateau for millennia. The natural Tibetan pastures were adapted to this harsh environment and a dynamic equilibrium existed between vegetation, grazing livestock and burrowing animals as well as local nomads. However, this equilibrium has been disturbed because of fast climate change, which induced widespread permafrost degradation and glacial retreat. Permafrost degradation, for instance, increases the thickness of the active layer and lowers the groundwater table. Deeper groundwater decreases water availability for plants during dry seasons, and hence reduces total plant biomass and coverage and also SOC content (Fig. S3; Yang *et al.*, 2010a; Wang *et al.*, 2012; Wang *et al.*, 2006). Burrowing activity by pika (*Ochotona curzoniae*; a small diurnal and non-hibernating mammal) and plateau zokors (*Myospalax baileyi*, a small blind subterranean rodent) causes an additional ~8-23 % loss of SOC stock in the topsoil by improving soil aeration, decreasing plant C input and transferring underlying nutrient-poor soil to the surface (Qin *et al.*, 2015; Li *et al.*, 2009). These and other environmental factors (Table 1) make the Tibetan pastures very fragile and very slow-recovering ecosystems.

(2) Socio-economic factors: For thousands of years, domestic yaks, sheep and goats on the eastern Tibetan Highlands have grazed on the pastures (Miehe *et al.*, 2014; Guo *et al.*, 2006), and the ecosystem has remained stable. This has changed markedly since the 1960s because of a rapid increase in population and food and energy demand (Chen *et al.*, 2013). Increasing population led to land-use change from pastures to cropland, as well as higher livestock density (particularly of yak) causing severe overgrazing. Large pressures on Tibetan pastures also arise from two widely-implemented policies based on two misleading assumptions: 1) Sedentarization of Tibetan nomads with the hope that this would benefit the herdsman and their families (Lu *et al.*, 2009); 2) Privatization of pastures, assuming that open access to common pastures for privately owned livestock was the underlying cause of degradation (Yan *et al.*, 2005). Both raising of yaks and removal of yak dung for heating and cooking also cause large SOC and nutrient losses and regional redistribution. For instance, of the ca. 40 million tons of dung produced by livestock in 2006, about 60% was removed. Carbon, N and P contents in yak dung comprise about 40, 2 and 0.4 % of dung dry weight,

respectively (Cai *et al.*, 2013). This implies that a total of 16 million tons C, 0.8 million tons N and 0.2 million tons P are removed annually from the pasture ecosystems. This equates to 0.1, 0.1 and 0.3% per year of the total C, N and P (ca. 77 Tg P) stocks, respectively, in Tibetan pastures (Ni, 2002; Tian *et al.*, 2006; Lu *et al.*, 2015a).

In addition to the direct effects of higher population and grazing intensity, economic growth led to a rapid increase in infrastructure construction (Table 1, Fig. S4), which further intensified soil and land disturbance (Cui & Graf, 2009; Harris, 2010; Wang *et al.*, 2015b). From 2000 to 2014, the length of highways increased 3.6 times (Fig. S4). Such construction directly fragmented the pastures and destroyed the soil cover. The terrestrial ecosystems adjacent to this construction were also severely affected by excavation, road dust, blockage of natural water fluxes and heavy metal and gasoline contamination.

Overall, the interferences of all these environmental and socio-economic factors in recent decades, and their interactions, have intensified Tibetan pasture degradation and accelerated SOC and nutrient losses (Qiao & Duan, 2016). In contrast to environmental factors, socio-economic factors have stronger, continuously increasing and more rapid negative impacts on Tibetan pastures. This is because 1) socio-economic activities are more intensive at local scales, compared to regional environmental effects; and 2) socio-economic activities, such as fossil-fuel burning, fertilization and pollutant release, subsequently accelerate environmental changes.

Table 1 Factors, drivers and consequences of pastures degradation on Tibetan Plateau*

Factors inducing degradation		Consequences	References**
○ <i>Environmental</i>	• Glacial retreat; snow melting	- Irregular water fluxes → Accelerated vegetation drying;	Wang et al. 2015b
	• Permafrost degradation (Figure S2)	- Deeper groundwater table; Less plant water availability; Soil shrinking	Yang et al. 2010a
	• Drying of wetlands		Cheng et al. 2007
	• Shrinking of lakes		Wang et al. 2012
	• Destruction of root mats by rodents	- Plant dying; Root-mat destruction; Increased erosion	Qin et al. 2015
○ <i>Socio-economic</i>	• Overgrazing (Figure S3)	- Soil compaction; Plant dying; Removal of nutrients	Wu et al. 2009
	• Population growth	- High resource demand from pastures; Pasture deterioration	Harris, 2010
	• Sedentarization of nomads	- Habitat fragmentation; Very strong local overgrazing	Lu et al. 2009
	○ <i>Socio</i> • Privatization of pastures	- Intensive pasture use; Strong local overgrazing	Yan et al. 2005
	• Removal and burning of yak dung	- Nutrient losses; Increased GHG (CH ₄ , N ₂ O) emissions	Wang, 2009b
	• Deforestation	- Stronger soil erosion; Nutrient leaching; GHG emissions	Cui & Graf, 2009
	• Land use change		
	• Mining	- Water contamination by heavy metals; Reduced vegetation coverage; Complete soil destruction	Huang et al. 2009
	○ <i>Economic</i> • Road construction (Figure S3)	- Habitat fragmentation; Root-mat destruction	Zheng & Cao, 2015
	• Dam construction	- High evaporation from the reservoir → Changing microclimate	Zheng & Cao, 2015
	• Booming tourist industry (Figure S3)	- Trampling; Contamination; Increase of all kinds of anthropogenic pressure	Foggin, 2012
Drivers accelerating degradation		Consequences	References**
○ <i>Soil</i>	• Shallow soil depth (~30-50 cm)	- High soil erosion; Slow recovery; Low nutrient stocks	Harris, 2010
	• Nutrient (N, P) limitation (Figure S4)	- Limited plant growth; Slow recovery	Zong et al. 2014
	• Nutrient-poor parent materials	- Low compensation of nutrient losses by weathering	
	• Slow weathering (because of climate)	- Slow recovery; Slow compensation of lost nutrients	
	• Very strong solar radiation (21 MJ m ⁻² day ⁻¹)	- Higher bare soil temperature; Plant damage; Decreased plant productivity and species richness	Liu et al. 2012
○ <i>Climate</i>	• Low mean annual temperature (< 0 °C)	- Slow plant growth; Slow SOM decomposition and nutrient release	Xu et al. 2008
	• High variation of spatial and temporal precipitation	- Uneven plant water availability	Chen et al. 2013
	• Low mean annual precipitation (~440 mm)	- Low plant water availability; Slow litter and SOM decomposition	
	• Low CO ₂ pressure	- Low photosynthetic rate	Fan et al. 2011
○ <i>Vegetation</i>	• Very short vegetation period (< 3.5 months)	- Very low primary production; Poor recovery potential	FAO, 2005
	• Poor plant germination	- Slow and poor recovery potential	
○ <i>Topography</i>	• Steep slopes	- Strong erosion; Water redistribution	
	• Slope exposition	- Contrasting solar radiation on different slopes → Diverse plant community composition	

* Please note that in some cases the consequences of degradation are also the drivers.

** Only some of the references are mentioned to the respective topic; they do not cover all the literature sources.

2.1.5.2 Socio-economic and environmental consequences of pasture degradation

Besides SOC and nutrient losses, pasture degradation has substantial negative impacts on the ecosystem services and functions of Tibetan pastures (Table 1). Pasture degradation directly exacerbates N and P limitation (Vitousek *et al.*, 2010) by inducing greater losses of both these nutrients. This impacts plant establishment and survival, and forage production rapidly declines. The reduction of forage production directly impedes development of animal husbandry, which decreases the economic income of the local population (Wen *et al.*, 2013).

Degradation-induced leaching of nutrients also pollutes surface and groundwater (Zhang *et al.*, 2013). Therefore, the local and regional degradation of Tibetan pastures has large-scale consequences for large rivers (Huang He, Salween River, Yangtze River, Mekong River and etc.) and threatens the livelihood of human beings living downstream in the whole of southern and eastern Asia. Increasing frequency of strong wind and dust storms was also evident after pasture degradation (Wang *et al.*, 2008a). Each year, 90×10^9 kg of soil and sand are carried into the rivers by erosion (Dong *et al.*, 2013). About 20% of all settlements in the central-west part of Nagqu Prefecture are at risk of being covered with transported sand (Squires & Zhang, 2009).

2.1.5.3 Strategies for pasture recovery and restoration

The high SOC and nutrient (N, P) losses and their far-reaching consequences require urgent intervention to slow pasture degradation or even improve the grassland's status.

Direct recovery strategies: Considering overgrazing as the major driver of degradation, grazing exclosure has been most frequently undertaken for pasture recovery. Weeding, fertilization and rodenticide applications are considered appropriate countermeasures, which are generally applied to light and moderate degradation stages (Dong *et al.*, 2013). For heavy and extreme degradation stages, reseedling is also proposed in addition to the above-mentioned strategies. Nevertheless, these recovery strategies have produced inconsistent outcomes (Harris, 2010): (1) grazing exclosure decreased soil C sequestration and C input as assessed by plant $^{13}\text{CO}_2$ pulse labelling, because

high C allocation belowground requires moderate grazing (Hafner *et al.*, 2012). Positive (Wu *et al.*, 2009; Sun *et al.*, 2014) or insignificant (Zhang *et al.*, 2015; Lu *et al.*, 2015b) effects of grazing exclosure on soil fertility were also reported. (2) Nitrogen and P fertilization or combined applications of both fertilizers on Tibetan pastures showed a significant promotion of AGB production by 37-110% (Fig. 6). However, the fertilizer applications also contribute to nutrients leaching in degraded pastures, which may hamper pasture recovery and exasperate headwater pollution (Liu *et al.*, 2017). (3) Reseeding was ineffective (Dong *et al.*, 2012) or had positive effects (Feng *et al.*, 2010) on ameliorating soil fertility. In fact, recovery strategies must be implemented over a long period of time to realize improvements in soil fertility (Cao *et al.*, 2014). To return SOC and nutrient contents to the status before degradation, at least hundreds of years are required (Preger *et al.*, 2010). This reflects the time necessary for soil formation, restoration of the eroded soil and accumulation of nutrients – by weathering and N₂ fixation. Therefore, to improve soil fertility, a complex of various strategies is necessary.

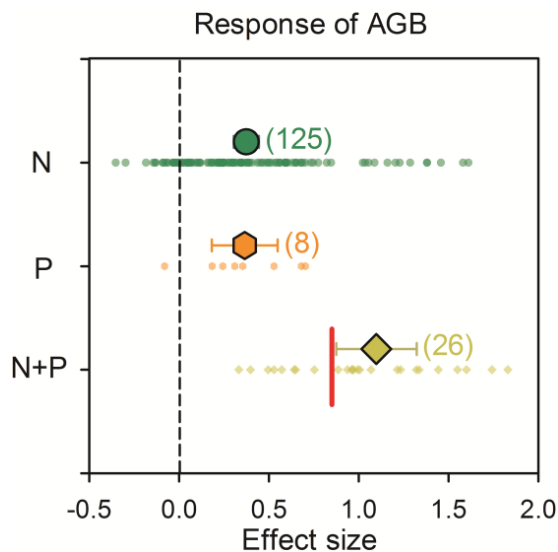


Figure 6 Response of aboveground biomass (AGB) to single and combined additions of N and P. The short red line represents the calculated N+P effect without N+P interactions. The higher response of AGB to simultaneous N and P addition reflects the positive effect of interactions between the nutrients for higher AGB. The numbers in parenthesis show the number of experiments. This figure was generated based on the database from Miede *et al.*'s (unpublished) literature. Error bars show standard errors (SE).

Indirect recovery strategies: Improving stove efficiency, use of solar energy and construction of household or communal biogas plants have been proposed as effective strategies to reduce yak dung collection for energy (Wang, 2009b). This is because yak dung collection (ca. 53% of Tibet's total rural energy consumption) prevents the return of nutrients from dung to the soil, and so continuously decreases soil fertility. All these strategies, however, require large investments at the regional, local and household

scales and are impossible without strong governmental support.

2.1.5.4 Current degradation status and expected patterns of future change

Tibetan pasture degradation status is estimated at various spatial and temporal scales and is conducted by remote sensing techniques coupled with spatial modelling. These estimations mostly focus on vegetation state (i.e. vegetation coverage and net primary production) and disregard soil degradation. From 1987 to 2004, 34% of the total grassland area has been degraded in the source region of the Three Rivers, which caused an annual decrease of aboveground biomass by 4-16 kg ha⁻¹ yr⁻¹ (Li *et al.*, 2013). A similar rate of decrease in aboveground biomass (22 kg ha⁻¹ yr⁻¹, Wang *et al.*, 2008c) from 2001 to 2004 was also observed on the northeastern Tibetan Plateau. We speculate that the degradation rates in the last decade have been even faster. Even if the decrease in grassland productivity remains the same (~4-22 kg ha⁻¹ yr⁻¹) for the whole plateau, the grassland will disappear over the next 30-170 years, given the estimated total AGB for Tibetan grasslands in 2001-2004 (688 kg ha⁻¹, Yang *et al.*, 2009).

Since the beginning of the century, a series of ecological projects and special policies were implemented, mostly in the source regions of the Three Rivers, to restore the Tibetan grasslands and save their ecosystem functions. Countermeasures in these projects include various combinations of the above-mentioned recovery strategies. Some positive results, at least for vegetation characteristics, have been achieved. For instance, positive trends in NDVI residues and net primary production have been seen since the implementation of these projects, indicating significantly restored vegetation (Cai *et al.*, 2015; Wang *et al.*, 2016). Nevertheless, it is still challenging (and may be impossible) to completely recover the degraded Tibetan pastures because of very strong and continuously ongoing SOC and nutrient losses and much slower pedogenetic processes and vegetation recovery, compared to rapid and increasing anthropogenic pressures and climate change.

2.1.6 Conclusions

Highly intensive anthropogenic activities (e.g. overgrazing) have occurred for decades across the whole Tibetan Plateau at the demand of fast socio-economic development.

These, in addition to a warming rate of about twice the global mean, have exerted extreme pressure on the vulnerable alpine pastoral ecosystems and induced widespread pasture degradation. The literature review elucidated that degradation on the Tibetan Plateau has triggered significant losses of SOC ($42 \pm 2 \%$), N ($33 \pm 6 \%$) and P ($17 \pm 4 \%$) contents compared to the non-degraded pastures. Because of the absence of natural, undisturbed pastures, all these values are underestimations of the real losses. Various vegetation characteristics and soil properties are closely related to SOC and nutrient losses. While losses of TN and plant biomass are found to be accompanied by SOC losses, TP loss is resistant to the decreasing SOC content because of its precipitation as $\text{Ca}_3(\text{PO}_4)_2$. Though various strategies have been implemented to cease and even reverse the degradation processes, their effects on soil quality are still ambiguous, and restoration is impossible without strong support and cooperation at regional, local and household scales. If pasture degradation in the Tibetan Plateau continues, the natural *Kobresia* root mats will disappear in the coming decades. This will dramatically destabilize these unique alpine ecosystems and have strong negative impacts on global environmental changes.

2.1.7 Acknowledgements

This work was funded by the China Scholarship Council (CSC) within the fellowship for S. L., the German Research Foundation (DFG) within the Priority Programme 1372: Tibetan Plateau: Formation-Climate-Ecosystems (Project KU 1184/14-2) and the National Key Research and Development Program of China (2016YFC0501802).

2.1.8 References

- Alados CL, Aich AE, Komac B *et al.* (2007) Self-organized spatial patterns of vegetation in alpine grasslands. *Ecological Modelling*, **201**, 233-242. doi: 10.1016/j.ecolmodel.2006.09.014.
- Babel W, Biermann T, Coners H *et al.* (2014) Pasture degradation modifies the water and carbon cycles of the Tibetan highlands. *Biogeosciences*, **11**, 6633-6656. doi: 10.5194/bg-11-6633-2014.
- Behnke R, Scoones I (1993) Rethinking range ecology: Implications for rangeland management in Africa. In: *Range Ecology at Disequilibrium* (eds Behnke R, Scoones I, Kerven C). pp. 24, Overseas Development Institute, London, UK.
- Cai H, Yang X, Xu X (2015) Human-induced grassland degradation/restoration in the central Tibetan Plateau: The effects of ecological protection and restoration projects. *Ecological Engineering*, **83**, 112-119. doi: 10.1016/j.ecoleng.2015.06.031.
- Cai YJ, Wang XD, Ding WX *et al.* (2013) Potential short-term effects of yak and Tibetan sheep dung on greenhouse gas emissions in two alpine grassland soils under laboratory conditions. *Biology and Fertility of Soils*, **49**, 1215-1226. doi: 10.1007/s00374-013-0821-7.
- Cao SX, Ma H, Yuan WP *et al.* (2014) Interaction of ecological and social factors affects vegetation recovery in China. *Biological Conservation*, **180**, 270-277. doi: 10.1016/j.biocon.2014.10.009.
- Chang XF, Zhu XX, Wang SP *et al.* (2014) Impacts of management practices on soil organic carbon in degraded

- alpine meadows on the Tibetan Plateau. *Biogeosciences*, **11**, 3495-3503. doi: 10.5194/bg-11-3495-2014.
- Chaplot VAM, Rumpel C, Valentin C (2005) Water erosion impact on soil and carbon redistributions within uplands of Mekong River. *Global Biogeochemical Cycles*, **19**, GB4004. doi: 10.1029/2005GB002493.
- Chen H, Zhu Q, Peng C *et al.* (2013) The impacts of climate change and human activities on biogeochemical cycles on the Qinghai-Tibetan Plateau. *Global Change Biology*, **19**, 2940-2955. doi: 10.1111/gcb.12277.
- Cheng GD, Wu TH (2007) Responses of permafrost to climate change and their environmental significance, Qinghai-Tibet Plateau. *Journal of Geophysical Research-Earth Surface*, **112**, F02S03. doi:10.1029/2006JF000631.
- Cui X, Graf HF (2009) Recent land cover changes on the Tibetan Plateau: a review. *Climatic Change*, **94**, 47-61. doi: 10.1007/s10584-009-9556-8.
- Dong QM, Zhao XQ, Wu GL *et al.* (2013) A review of formation mechanism and restoration measures of "black-soil-type" degraded grassland in the Qinghai-Tibetan Plateau. *Environmental Earth Sciences*, **70**, 2359-2370. doi: 10.1007/s12665-013-2338-7.
- Dong SK, Wen L, Li YY *et al.* (2012) Soil-quality effects of grassland degradation and restoration on the Qinghai-Tibetan Plateau. *Soil Science Society of America Journal*, **76**, 2256-2264. doi: 10.2136/sssaj2012.0092.
- Du Y, Cui Y, Xu X *et al.* (2008) Nitrous oxide emissions from two alpine meadows in the Qinghai-Tibetan Plateau. *Plant and Soil*, **311**, 245-254. doi: 10.1007/s11104-008-9727-9.
- Fan YZ, Zhong ZM, Zhang XZ (2011) Determination of photosynthetic parameters $V_{C_{max}}$ and J_{max} for a C_3 plant (spring hulless barley) at two altitudes on the Tibetan Plateau. *Agricultural and Forest Meteorology*, **151**, 1481-1487. doi: 10.1016/j.agrformet.2011.06.004.
- FAO (1990) Keeping the land alive: Soil erosion-its causes and cures. Available from: <http://www.fao.org/docrep/t0389e/T0389E00.htm#Contents>.
- FAO (2005) Livestock sector brief, China. Available from: http://www.fao.org/ag/againfo/resources/en/publications/sector_briefs/lbs_CHN.pdf.
- Feng R, Long R, Shang Z *et al.* (2010) Establishment of *Elymus natans* improves soil quality of a heavily degraded alpine meadow in Qinghai-Tibetan Plateau, China. *Plant and Soil*, **327**, 403-411. doi: 10.1007/s11104-009-0065-3.
- Foggin M (2012) Pastoralists and wildlife conservation in western China: collaborative management within protected areas on the Tibetan Plateau. *Pastoralism: Research, Policy and Practice*, **2**, 17. doi: 10.1186/2041-7136-2-17.
- Frauenfeld OW, Zhang TJ, Serreze MC (2005) Climate change and variability using European Centre for Medium-Range Weather Forecasts reanalysis (ERA-40) temperatures on the Tibetan Plateau. *Journal of Geophysical Research*, **110**, D02101. doi: 10.1029/2004JD005230.
- Gao Y, Yang S, Xie GD *et al.* (2015). *Qinghai Statistical Yearbook*. Qinghai Statistical Press, Xining, Qinghai. (in Chinese)
- Guo SC, Savolainen P, Su JP *et al.* (2006) Origin of mitochondrial DNA diversity of domestic yaks. *BMC Evolutionary Biology*, **6**, 73. doi: 10.1186/1471-2148-6-73.
- Harris RB (2010) Rangeland degradation on the Qinghai-Tibetan plateau: A review of the evidence of its magnitude and causes. *Journal of Arid Environments*, **74**, 1-12. doi: 10.1016/j.jaridenv.2009.06.014.
- Hafner S, Unteregelsbacher S, Seeber E *et al.* (2012) Effect of grazing on carbon stocks and assimilate partitioning in a Tibetan montane pasture revealed by ^{13}C CO₂ pulse labeling. *Global Change Biology*, **18**, 528-538. doi: 10.1111/j.1365-2486.2011.02557.x.
- Huang X, Sillanpää M, Gjessing ET *et al.* (2009) Water quality in the Tibetan Plateau: Major ions and trace elements in the headwaters of four major Asian rivers. *Science of the Total Environment*, **407**, 6242-6254. doi: 10.1016/j.scitotenv.2009.09.001.
- Jordaan FP, Biel LC, du Plessis PIM (1997) A comparison of five range condition assessment techniques used in the semi-arid western grassland biome of southern Africa. *Journal of Arid Environments*, **35**, 665-671. doi: 10.1006/jare.1996.0166.
- Kimetu JM, Lehmann J, Ngoze SO *et al.* (2008) Reversibility of soil productivity decline with organic matter of differing quality along a degradation gradient. *Ecosystems*, **11**, 726-739. doi: 10.1007/s10021-008-9154-z.
- Kuang XX, Jiao JJ (2016) Review on climate change on the Tibetan Plateau during the last half century. *Journal of Geophysical Research: Atmospheres*, **121**, 3979-4007. doi: 10.1002/2015JD024728.
- Kuzyakov Y (2002) Review: Factors affecting rhizosphere priming effects. *Journal of Plant Nutrition and Soil Science*, **165**, 382-396. doi: 10.1002/1522-2624(200208)165:4<382::AID-JPLN382>3.0.CO;2-#.
- Kuzyakov Y, Blagodatskaya E, Blagodatsky S (2009) The Biology of the Regulatory Gate: Comments on the paper by Kemmitt *et al.* (2008) 'Mineralization of native soil organic matter is not regulated by the size, activity or composition of the soil microbial biomass – a new perspective' [Soil Biology & Biochemistry 40, 61-73]. *Soil Biology & Biochemistry*, **41**, 435-439. doi: 10.1016/j.soilbio.2008.07.023.
- Lal R (2003) Soil erosion and the global carbon budget. *Environment International*, **29**, 437-450. doi: 10.1016/S0160-4120(02)00192-7.
- Lehnert LW, Meyer H, Wang Y *et al.* (2015) Retrieval of grassland plant coverage on the Tibetan Plateau based on a multi-scale, multi-sensor and multi-method approach. *Remote Sensing of Environment*, **164**, 197-207. doi: 10.1016/j.rse.2015.04.020.

- Leonard WR, Crawford MH (2002) The human biology of pastoral populations. pp. 133. Cambridge University Press, Cambridge, UK.
- Li JH, Yang YJ, Li BW, Li WJ, Wang G, Knops JMH (2014a) Effects of nitrogen and phosphorus fertilization on soil carbon fractions in alpine meadows on the Qinghai-Tibetan Plateau. *PLoS ONE*, **9**: e103266. DOI: 10.1371/journal.pone.0103266.
- Li XG, Zhang ML, Li ZT *et al.* (2009) Dynamics of soil properties and organic carbon pool in topsoil of zokor-made mounds at an alpine site of the Qinghai-Tibetan Plateau. *Biology and Fertility of Soils*, **45**, 865-872. doi: 10.1007/s00374-009-0398-3.
- Li XL, Gao J, Brierley G *et al.* (2013) Rangeland degradation on the Qinghai-Tibet Plateau: Implications for rehabilitation. *Land Degradation and Development*, **24**, 72-80. doi: 10.1002/ldr.1108.
- Li X, Zhang X, Wu J *et al.* (2011) Root biomass distribution in alpine ecosystems of the northern Tibetan Plateau. *Environmental Earth Sciences*, **64**, 1911-1919. doi: 10.1007/s12665-011-1004-1.
- Li Y, Dong S, Liu S *et al.* (2015) Seasonal changes of CO₂, CH₄ and N₂O fluxes in different types of alpine grassland in the Qinghai-Tibetan Plateau of China. *Soil Biology and Biochemistry*, **80**, 306-314. doi: 10.1016/j.soilbio.2014.10.026.
- Li YY, Dong SK, Wen L *et al.* (2014b) Soil carbon and nitrogen pools and their relationship to plant and soil dynamics of degraded and artificially restored grasslands of the Qinghai-Tibetan Plateau. *Geoderma*, **213**, 178-184. doi: 10.1016/j.geoderma.2013.08.02.
- Li Y, Wang S, Jiang L *et al.* (2016) Changes of soil microbial community under different degraded gradients of alpine meadow. *Agriculture, Ecosystems and Environment*, **222**, 213-222. doi: 10.1016/j.agee.2016.02.020.
- Liu JD, Liu JM, Linderholm HW *et al.* (2012) Observation and calculation of the solar radiation on the Tibetan Plateau. *Energy Conversion and Management*, **57**, 23-32. doi: 10.1016/j.enconman.2011.12.007.
- Liu S, Schleuss P-M, Kuzyakov Y (2016) Carbon and nitrogen losses from soil depend on degradation of Tibetan *Kobresia* pastures. *Land Degradation and Development*. doi: 10.1002/ldr.2522.
- Liu Y, Wei W, Wen X, Li J (2015) Distribution characteristics of soil carbon on different degraded degree alpine meadow in the source area of Three Major Rivers in China. *Hubei Agricultural Sciences*, **54**, 308-312. (in Chinese with English abstract)
- Lu T, Wu N, Luo P (2009) Sedentarization of Tibetan Nomads. *Conservation Biology*, **23**, 1074. doi:10.1111/j.1523-1739.2009.01312.x.
- Lu X, Yan Y, Sun J *et al.* (2015a) Carbon, nitrogen, and phosphorus storage in alpine grassland ecosystems of Tibet: effects of grazing exclusion. *Ecology and Evolution*, **5**, 4492-4504. doi: 10.1002/ece3.1732.
- Lu X, Yan Y, Sun J *et al.* (2015b) Short-term grazing exclusion has no impact on soil properties and nutrients of degraded alpine grassland in Tibet, China. *Solid Earth*, **6**, 1195-1205. doi: 10.5194/se-6-1195-2015.
- Lu JF, Dong ZB, Li WJ *et al.* (2014) The effect of desertification on carbon and nitrogen status in the northeastern margin of the Qinghai-Tibetan Plateau. *Environmental Earth Sciences*, **71**: 807-815. doi: 10.1007/s12665-013-2482-0.
- Ma Y, Lang B, Li Q *et al.* (2002) Study on rehabilitating and rebuilding technologies for degenerated alpine meadow in the Changjiang and Yellow river source region. *Pratacultural Science*, **19**, 1-5. (in Chinese with English abstract)
- McAllister CA, Knapp AK, Maragni LA (1998) Is leaf-level photosynthesis related to plant success in a highly productive grassland? *Oecologia*, **117**, 40-46. doi: 10.1007/s004420050629.
- Mchunu C, Chaplot V (2012) Land degradation impact on soil carbon losses through water erosion and CO₂ emissions. *Geoderma*, **177-178**, 72-79. doi: 10.1016/j.geoderma.2012.01.038.
- McLaren RG, Cameron KC (1996) *Soil Science: Sustainable production and environment protection*. Oxford University Press, Auckland, New Zealand.
- Miehe G, Miehe S, Böhrner J *et al.* (2014) How old is the human footprint in the world's largest alpine ecosystem? A review of multiproxy records from the Tibetan Plateau from the ecologists' viewpoint. *Quaternary Science Reviews*, **86**, 190-209. doi: 10.1016/j.quascirev.2013.12.004.
- Nachtergaele FO, Petri M, Biancalani R *et al.* (2011) An information database for land degradation assessment at global level. pp. 48. Available from: http://www.fao.org/nr/lada/index.php?option=com_docman&task=doc_download&gid=773&lang=en.
- Ni J (2002) Carbon storage in grasslands of China. *Journal of Arid Environments*, **50**, 205-218. doi: 10.1006/jare.2001.0902.
- Phillips RP, Finzi AC, Bernhardt ES (2011) Enhanced root exudation induces microbial feedbacks to N cycling in a pine forest under long-term CO₂ fumigation. *Ecology Letters*, **14**, 187-194. doi: 10.1111/j.1461-0248.2010.01570.x.
- Pietri JCA, Brookes PC (2008) Relationships between soil pH and microbial properties in a UK arable soil. *Soil Biology and Biochemistry*, **40**, 1856-1861. doi: 10.1016/j.soilbio.2008.03.020.
- Pomeranz K, Turner JL, Shifflett SC *et al.* (2013) Himalayan water security: The challenges for south and southeast Asia. *Asia Policy*, **16**, 1-50. doi: 10.1353/asp.2013.0023.
- Preger AC, Kösters R, Preez CCD *et al.* (2010) Carbon sequestration in secondary pasture soils: a chronosequence study in the South African Highveld. *European Journal of Soil Science*, **61**, 551-562. doi: 10.1111/j.1365-

- 2389.2010.01248.x.
- Pribyl DW (2010) A critical review of the conventional SOC to SOM conversion factor. *Geoderma*, **156**, 75-83. doi: 10.1016/j.geoderma.2010.02.003.
- Qiao Y, Duan Z (2016) Understanding alpine meadow ecosystems. In: *Landscape and Ecosystem Diversity, Dynamics and Management in the Yellow River Source Zone* (eds Brierley GJ, Li X, Cullum C, Gao J). pp. 117-135, Springer International Publishing, Switzerland.
- Qin Y, Chen JJ, Yi SH (2015) Plateau pikas burrowing activity accelerates ecosystem carbon emission from alpine grassland on the Qinghai-Tibetan Plateau. *Ecological Engineering*, **84**: 287-291. doi: 10.1016/j.ecoleng.2015.09.012.
- Schrott L (1991) Global solar radiation, soil temperature and permafrost in the central Andes, Argentina: a progress report. *Permafrost and Periglacial Processes*, **2**, 59-66. doi: 10.1002/ppp.3430020110.
- Shang Z, Yang S, Wang Y *et al.* (2016) Soil seed bank and its relation with above-ground vegetation along the degraded gradients of alpine meadow. *Ecological Engineering*, **90**, 268-277. doi: 10.1016/j.ecoleng.2016.01.067.
- Squires VR, Zhang K (2009) The context for the study of rangeland degradation and recovery in China's pastoral lands. In: *Rangeland degradation and recovery in China's pastoral lands* (eds Squires VR, Lu XS, Lu Q, Wang T, Yang Y). pp. 12, MPG Books Group, UK. doi: 10.1079/9781845934965.0000.
- Sun J, Wang X, Cheng G *et al.* (2014) Effects of grazing regimes on plant traits and soil nutrients in an alpine steppe, northern Tibetan Plateau. *PLoS ONE*, **9**, e108821. doi:10.1371/journal.pone.0108821.
- Tan HK (2000) *Environmental soil science* (2nd edn). pp. 290-294. Marcel Dekker, New York, USA.
- Tian HQ, Wang SQ, Liu JY *et al.* (2006) Patterns of soil nitrogen storage in China. *Global Biogeochemical Cycles*, **20**, GB1001. doi: 10.1029/2005GB002464.
- Van der Westhuizen HC, Snyman HA, Fouché HJ (2005) A degradation gradient for the assessment of rangeland condition of a semi-arid sourveld in Southern Africa. *African Journal of Range and Forage Science*, **22**, 47-59. doi: 10.2989/10220110509485861.
- Vicca S, Serrano-Ortiz P, De Boeck HJ *et al.* (2007) Effects of climate warming and declining species richness in grassland model ecosystems: acclimation of CO₂ fluxes. *Biogeosciences*, **4**, 27-36. doi: 10.5194/bg-4-27-2007.
- Vinton MA, Burke IC (1995) Interactions between individual plant species and soil nutrient status in shortgrass steppe. *Ecology*, **76**, 1116-1133. doi: 10.2307/1940920.
- Vitousek PM, Porder S, Houlton BZ *et al.* (2010) Terrestrial phosphorus limitation: mechanisms, implications, and nitrogen-phosphorus interactions. *Ecological Applications*, **20**, 5-15. doi: 10.1890/08-0127.1.
- Wang CT, Cao GM, Wang QL *et al.* (2008c) Changes in plant biomass and species composition of alpine *Kobresia* meadows along altitudinal gradient on the Qinghai-Tibetan Plateau. *Science in China Series C: Life Sciences*, **51**, 86-94. doi: 10.1007/s11427-008-0011-2.
- Wang CT, Long RJ, Wang QL *et al.* (2009a) Changes in plant diversity, biomass and soil C, in alpine meadows at different degradation stages in the headwater region of three rivers, China. *Land Degradation and Development*, **20**, 187-198. doi: 10.1002/ldr.879.
- Wang G, Wang Y, Li Y *et al.* (2007) Influences of alpine ecosystem responses to climatic change on soil properties on the Qinghai-Tibet Plateau, China. *Catena*, **70**, 506-514. doi: 10.1016/j.catena.2007.01.001.
- Wang GX, Li YS, Wu QB *et al.* (2006) Impacts of permafrost changes on alpine ecosystem in Qinghai-Tibet Plateau. *Science in China Series D: Earth Sciences*, **49**, 1156-1169. doi: 10.1007/s11430-006-1156-0.
- Wang H, Zhou X, Wan C *et al.* (2008a) Eco-environmental degradation in the northeastern margin of the Qinghai-Tibetan Plateau and comprehensive ecological protection planning. *Environmental Geology*, **55**, 1135-1147. doi: 10.1007/s00254-007-1061-7.
- Wang JF, Wang GX, Hu HC *et al.* (2010) The influence of degradation of the swamp and alpine meadows on CH₄ and CO₂ fluxes on the Qinghai-Tibetan Plateau. *Environmental Earth Sciences*, **60**, 537-548. doi: 10.1007/s12665-009-0193-3.
- Wang DJ, Feng ZD, Wang J *et al.* (2015a) *Tibet Statistical Yearbook*. Tibet Renmin Press, Lhasa, Tibet. (in Chinese)
- Wang P, Lassoie JP, Morreale SJ *et al.* (2015b) A critical review of socioeconomic and natural factors in ecological degradation on the Qinghai-Tibetan Plateau, China. *The Rangeland Journal*, **37**, 1-9. doi: 10.1071/RJ14094.
- Wang Q (2009b) Prevention of Tibetan eco-environmental degradation caused by traditional use of biomass. *Renewable and Sustainable Energy Reviews*, **13**, 2562-2570. doi: 10.1016/j.rser.2009.06.013.
- Wang XD, Zhong XH, Liu SZ *et al.* (2008b) Regional assessment of environmental vulnerability in the Tibetan Plateau: Development and application of a new method. *Journal of Arid Environments*, **72**, 1929-1939. doi: 10.1016/j.jaridenv.2008.06.005.
- Wang XX, Dong SK, Yang B *et al.* (2014) The effects of grassland degradation on plant diversity primary productivity, and soil fertility in the alpine region of Asia's headwaters. *Environmental Monitoring and Assessment*, **186**, 6903-6917. doi: 10.1007/s10661-014-3898-z.
- Wang Z, Zhang Y, Yang Y *et al.* (2016) Quantitative assess the driving forces on the grassland degradation in the Qinghai-Tibet Plateau, in China. *Ecological Informatics*, **33**, 32-44. doi: 10.1016/j.ecoinf.2016.03.006.
- Wang ZR, Yang GJ, Yi SH *et al.* (2012) Different response of vegetation to permafrost change in semi-arid and semi-

- humid regions in Qinghai-Tibetan Plateau. *Environmental Earth Sciences*, **66**, 985-991. doi: 10.1007/s12665-011-1405-1.
- Wen L, Dong S, Li Y *et al.* (2013) Effect of Degradation Intensity on Grassland Ecosystem Services in the Alpine Region of Qinghai-Tibetan Plateau, China. *PLoS ONE*, **8**, e58432. doi:10.1371/journal.pone.0058432.
- White PR, Murray S, Rohweder M (2000) *Pilot analysis of global ecosystems-Grassland ecosystems*. World Resources Institute, Washington DC, USA.
- Wu GL, Du GZ (2007) Discussion ecological construction and sustainable development of degraded alpine grassland ecosystem of the Qinghai-Tibetan Plateau. *Chinese Journal of Nature*, **29**, 159-164. (in Chinese with English abstract)
- Wu GL, Du GZ, Liu ZH *et al.* (2009) Effect of fencing and grazing on a *Kobresia*-dominated meadow in the Qinghai-Tibetan Plateau. *Plant and Soil*, **319**, 115-126. doi: 10.1007/s11104-008-9854-3.
- Wu R, Tiessen H (2002) Effect of land use on soil degradation in alpine grassland soil, China. *Soil Science Society of America Journal*, **66**, 1648-1655. doi:10.2136/sssaj2002.1648.
- Xu XD, Lu CG, Shi XH (2008) World water tower: An atmospheric perspective. *Geophysical Research Letters*, **35**, L20815. doi: 10.1029/2008GL035867.
- Xu XL, Ouyang H, Kuzyakov Y *et al.* (2006) Significance of organic nitrogen acquisition for dominant plant species in an alpine meadow on the Tibet plateau, China. *Plant and Soil*, **285**, 221-231. doi: 10.1007/s11104-006-9007-5.
- Yan P, Dong GR, Zhang XB *et al.* (2000) Preliminary results of the study on wind erosion in the Qinghai-Tibetan Plateau using ¹³⁷Cs technique. *Chinese Science Bulletin*, **45**, 1019-1025. doi: 10.1007/BF02884984.
- Yan ZL, Wu N, Yeshe D *et al.* (2005) A review of rangeland privatization and its implications in the Tibetan Plateau, China. *Nomadic Peoples*, **9**, 31-51. doi: 10.3167/082279405781826155.
- Yang MX, Nelson FE, Shiklomanov NI *et al.* (2010a) Permafrost degradation and its environmental effects on the Tibetan Plateau: A review of recent research. *Earth-Science Reviews*, **103**, 31-44. doi: 10.1016/j.earscirev.2010.07.002.
- Yang YH, Fang JY, Ji CJ *et al.* (2010b) Soil inorganic carbon stock in the Tibetan alpine grasslands. *Global Biogeochemical Cycles*, **24**, GB4022. doi: 10.1029/2010GB003804.
- Yang YH, Fang JY, Pan YD *et al.* (2009) Aboveground biomass in Tibetan grasslands. *Journal of Arid Environments*, **73**, 91-95. doi: 10.1016/j.jaridenv.2008.09.027.
- Zeng C, Zhang F, Wang Q *et al.* (2013) Impact of alpine meadow degradation on soil hydraulic properties over the Qinghai-Tibetan Plateau. *Journal of Hydrology*, **478**, 148-156. doi: 10.1016/j.jhydrol.2012.11.058.
- Zhang F, Zhu B, Zheng J *et al.* (2013) Soil properties as indicators of desertification in an alpine meadow ecosystem of the Qinghai-Tibet Plateau, China. *Environmental Earth Sciences*, **70**, 249-258. doi: 10.1007/s12665-012-2120-2.
- Zhang WN, Ganjurjav H, Liang Y *et al.* (2015) Effect of a grazing ban on restoring the degraded alpine meadow of Northern Tibet, China. *The Rangeland Journal*, **37**, 89-95. doi: 10.1071/RJ14092.
- Zheng HR, Cao SX (2015) Threats to China's biodiversity by contradictions policy. *AMBIO*, **44**, 23-33. doi: 10.1007/s13280-014-0526-7.
- Zong N, Song MH, Shi PL *et al.* (2014) Timing patterns of nitrogen application alter plant production and CO₂ efflux in an alpine meadow on the Tibetan Plateau, China. *Pedobiologia-Journal of Soil Ecology*, **57**, 263-269. doi: 10.1016/j.pedobi.2014.08.001.

2.1.9 Supporting information

Table S1 Classification of pasture degradation (adapted from Ma *et al.*, 2002)

Degradation stages	Vegetation coverage (%)	Productivity (%)	Portion of edible plants (%)	Height of edible plants (cm)	Pasture quality
1. Non-degraded	80-90	100	> 70	> 25	Excellent
2. Light degradation	70-85	50-75	50-70	20-25	Good
3. Moderate degradation	50-70	30-50	30-50	15-20	Bad
4. Heavy degradation	30-50	15-30	15-30	10-15	Worse
5. Extreme degradation	< 30	< 15	0	—	Worst

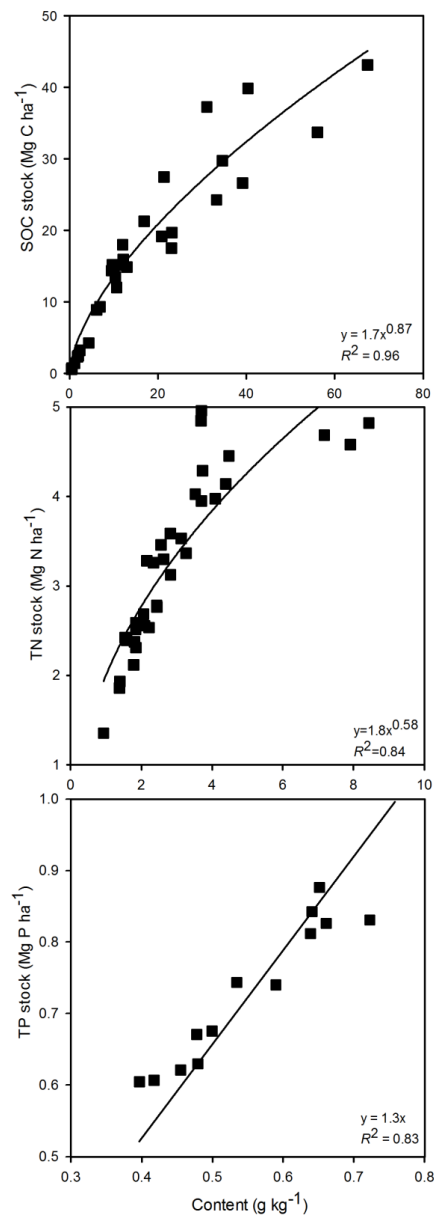


Figure S1 Relationships between content and stocks of soil organic carbon: SOC (top), total nitrogen: TN (middle) and total phosphorus: TP (bottom) in a 10 cm depth intervals. The calculation of stocks based on Equation 1 involves 10 cm sampling depth intervals: 0-10 cm, 10-20 cm, 20-30 cm. R^2 values show the strength of the correlation. All correlations are significant at $p < 0.0001$. The Y axis for C, N, and P are presented at ratios: 50:5:1.

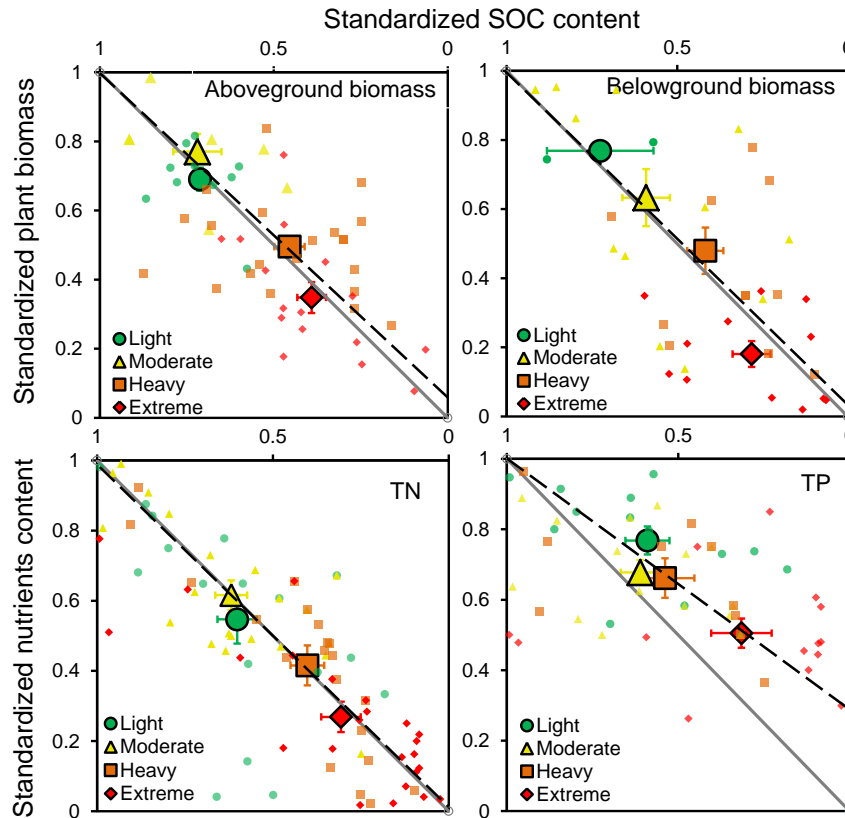


Figure S2 Indicators of degradation of vegetation and soil fertility: Sensitivity of nutrient losses in plant biomass (top row) and soil (bottom row) to SOC losses. The (1.0, 1.0) point represents the status of SOC and nutrients/plant biomass in non-degraded Tibetan pastures. The centroids (\pm SE) show the average values for each degradation stage. The grey solid line is the 1:1 ($Y = X$) line. The dashed lines are the correlation lines for all data points. The closer the dashed line is to the 1:1 line, the stronger is the dependence between SOC losses and the related parameter. The positive deviation from 1:1 line (e.g. for P) shows that the losses are less sensitive to SOC losses and are dependent from other factors.

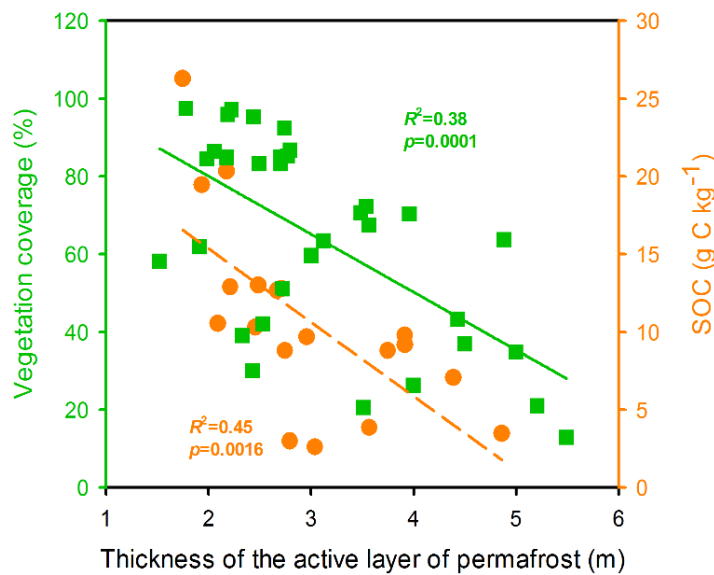


Figure S3 Response of vegetation coverage (%) and SOC content (g C kg^{-1}) to thickness of the active layer of permafrost (m). Data are collected from Yang *et al.* (2010), Wang *et al.* (2012) and Wang *et al.* (2006).

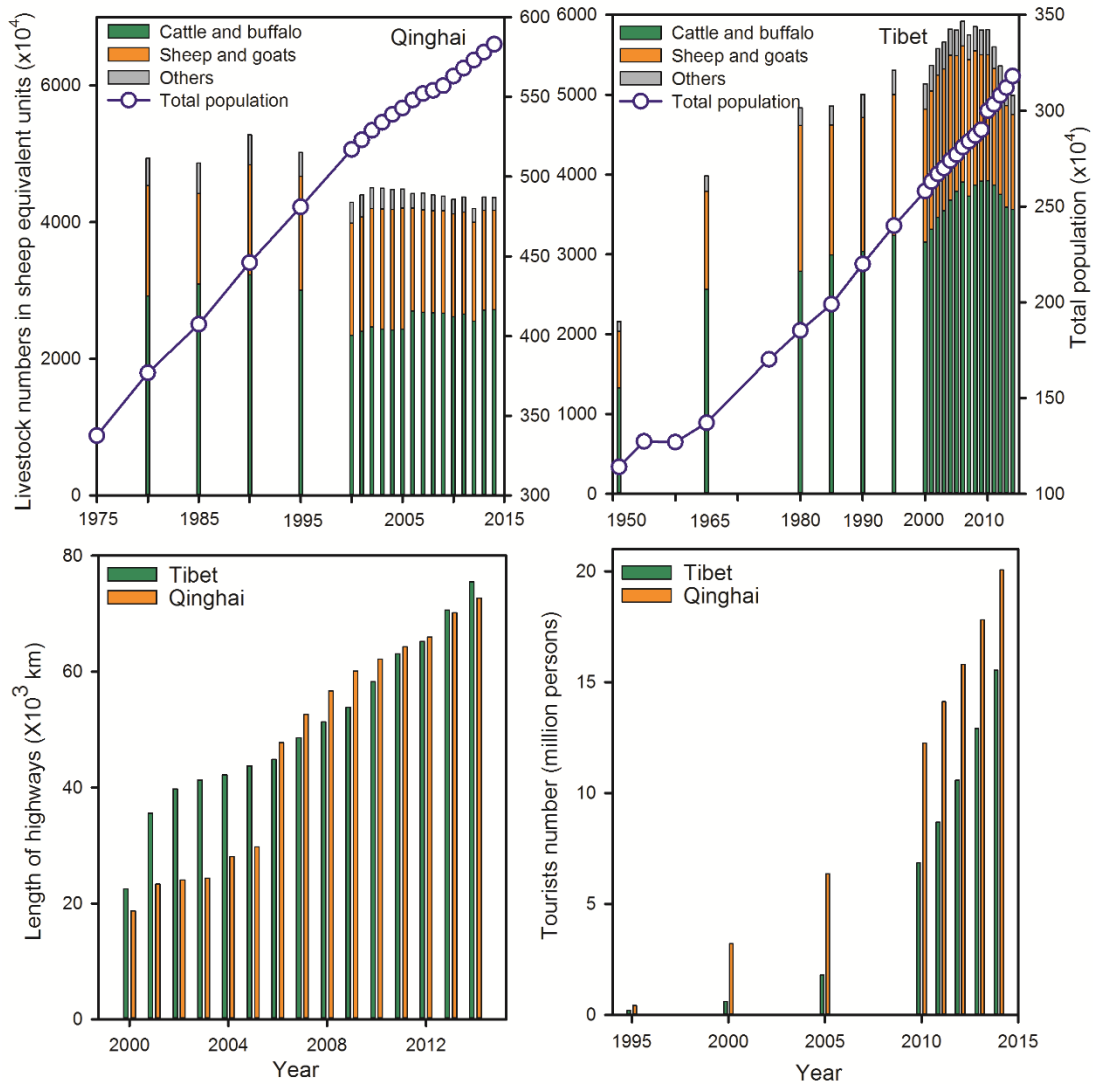


Figure S4 Decadal development of socio-economic factors affecting pasture degradation: livestock numbers in Qinghai (top left) and Tibet (top right), length of highways (bottom left) and tourists (bottom right) in Qinghai and Tibet. All the numbers for the provinces Qinghai and Tibet were taken from the official statistical surveys (Gao *et al.*, 2015; Wang *et al.*, 2015a). The absolute numbers of different animals were converted to sheep equivalents (FAO, 2005).

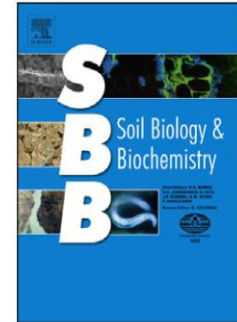
2.2 Study 2: Hot experience for cold-adapted microorganisms: Temperature sensitivity of soil enzymes

Bahar S. Razavi^{a*}, **Shibin Liu**^{b*}, Yakov Kuzyakov^{a,b}

Status: Published in *Soil Biology & Biochemistry*

^a Department of Agricultural Soil Science, University of Göttingen, Göttingen, Germany

^b Department of Soil Science of Temperate Ecosystems, University of Göttingen, Göttingen, Germany



2.2.1 Abstract

High latitude and cold ecosystems, which constitute the major environment on Earth, are particularly threatened by global warming. Consequently, huge amounts of SOC stored in these ecosystems may be released to the atmosphere by accelerated enzymatic decomposition. Effects of intensive warming on temperature sensitivity and catalytic properties of soil enzymes were tested in cold-adapted alpine grassland of the Tibetan Plateau. We hypothesized that 1) maximal reaction rate will be insensitive to intensive warming at high temperature range ($V_{max} \cdot Q_{10}=1$); 2) substrate affinity (K_m) remains constant at elevated temperatures due to expression of enzymes with less flexibility. These hypotheses were tested by examining the kinetics of six enzymes involved in carbon (cellobiohydrolase, β -glucosidase, xylanase), nitrogen (tyrosine-aminopeptidase, leucine-aminopeptidase) and phosphorus (acid phosphomonoesterase) cycles after soil incubation at temperatures from 0 to 40°C.

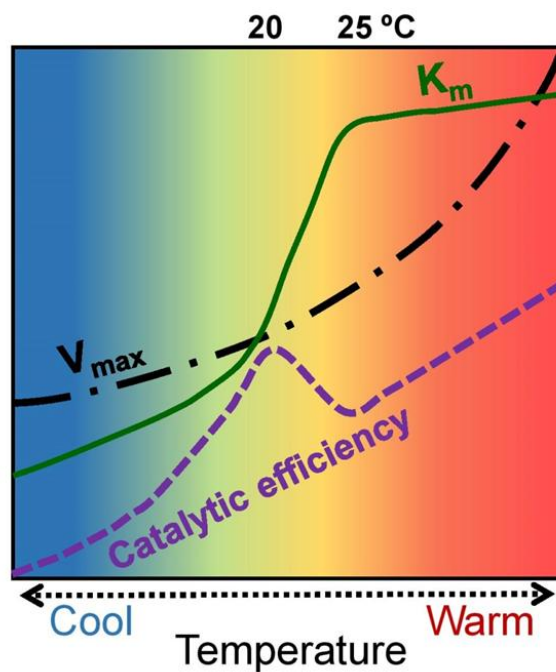
Q_{10} and E_a decreased at high temperature (25–40°C). However, enzymes that degrade low quality polymers remained temperature-sensitive even above 25°C ($V_{max} \cdot Q_{10}=2$), which explains the faster decomposition of recalcitrant C compounds under warming. Substrate affinity of all enzymes gradually increased up to 20°C. At 25°C, however, K_m increased rapidly, leading to an extreme decrease in catalytic efficiency. Above 25°C, K_m of C and N cycles remained nearly constant, while V_{max} gradually increased from 0–40°C. These results reveal two important implications of warming: 1) there are some temperature thresholds (here 20–25°C) that lead to sudden reductions in substrate affinity, decreasing temperature sensitivity and catalytic efficiency, 2) decoupled temperature sensitivity of V_{max} and K_m and the resulting maintenance of stable enzyme systems at high temperatures ensured efficient enzymatic functioning and

persistent decomposition of SOM at temperatures much higher than the common adaptation range of the ecosystem. Thus, the temperature thresholds of strong changes in enzyme-based processes should be considered and included in the next generation of models in order to improve the prediction of SOM feedbacks to warming.

Key words: cold-adapted enzymes, soil enzymes, Michaelis-Menten kinetics, catalytic efficiency, activation energy

Corresponding Authors: Bahar S. Razavi, brazavi@gwdg.de; Shibin Liu, sliu3@gwdg.de

Graphical Abstract



2.2.2 Introduction

Microorganisms in the natural environment cope with changing conditions that demand a wide range of metabolic adaptations (Neidhart et al., 1990). Among the most challenging environments are high latitude and cold ecosystems, which are threatened by global warming (Davidson and Janssens, 2006). Warming has a fundamental impact on microbial activity, metabolism and enzyme activities (Allison et al., 2010; Van Gestel et al., 2013; Zimmermann and Bird, 2012). Enzymes are essential to microbial metabolism and soil functioning, as they depolymerize large organic compounds and generate soluble oligomers and monomers that can be transported into the cells (Blagodatskaya et al., 2016; Wallenstein et al., 2010). Three mechanisms have been proposed to explain thermal adaptation of enzyme catalyzed processes: 1) change in the enzyme systems 2) the alterations in soil microbial biomass and enzyme expression at higher temperatures and 3) changes in quantity and quality of substrate, affecting reaction rates (Blagodatskaya et al., 2016).

Enzyme activity is a saturating function of substrate concentration and is described by the Michaelis-Menten relationship (Michaelis and Menten, 1913). Enzyme saturation occurs when all the enzyme active sites are already occupied by substrate. In this case adding more substrate will not increase the overall rate of the reaction. Both parameters of the Michaelis-Menten equation – the maximal catalytic reaction rate at a given temperature (V_{max}) and the half-saturation constant (K_m), are temperature-sensitive (Davidson et al., 2006; Davidson and Janssens, 2006) and usually increase with temperature (Stone et al., 2012). Various enzymes have different temperature sensitivities and changes in soil temperature may also alter the relative rates of decomposition of different components of organic matter (Koch et al., 2007; Wallenstein et al., 2010; Stone et al., 2012; Razavi et al., 2015). This may affect nutrient availability, for instance it has been observed that N availability may be decoupled from C and P cycling under warming conditions (Allison and Treseder, 2008). Therefore, the temperature sensitivity of enzymes responsible for organic matter decomposition is the most crucial parameter for predicting the effects of global warming on the nutrient and C cycles (Davidson et al., 2006; Davidson and Janssens, 2006).

The temperature sensitivity of V_{max} is directly related to the activation energy for enzyme reaction (Davidson and Janssens, 2006). Activation energies are parameters that mechanistically link enzyme kinetics and temperature response through the Arrhenius equation (Wallenstein et al., 2010). Based on the Arrhenius law, when activation energy is low, the exponential term will tend to 1 and consequently the reaction will become temperature independent (Marx et al., 2007). In the other words, the lower the activation energy, the lower the temperature sensitivity of the reaction rate. Enzymes catalyze biochemical reactions by lowering their activation energy (Gerlt and Gassman, 1993). Thus, a super-efficient enzyme will bring the activation energy to zero (Marx et al., 2007). This is important because, in the context of cold-adapted microorganisms, one way to maintain decomposition processes at low temperatures would be to develop enzymes that are temperature-independent (Marx et al., 2007).

Microbial physiology is evolutionarily selected for the most efficient enzyme systems (Allison et al., 2010; Hochachka and Somero, 2002). Moreover, the activities of hydrolytic enzymes could be adapted to different temperature regimes (Baldwin and Hochachka, 1969; German et al., 2012) with the goal of maintaining critical enzymatic functions. There is evidence for biogeographical patterns in enzyme temperature sensitivity (Huston et al., 2000; Feller, 2003; German et al., 2012). Many studies have observed that cold-adapted microorganisms can produce cold-adapted enzymes that catalyze reactions at lower temperatures with lower activation energy and with higher binding affinity (i.e. low K_m) (Fields, 2001; Bradford, 2013) than their mesophilic counterparts (Gerday et al., 1997). Importantly, microbial adaptation and acclimation strategies have physiological costs (Schimel et al., 2007) and can reduce enzyme catalytic efficiency – determined as V_{max}/K_m (Stone et al., 2012; Tischer et al., 2015).

The parameters of enzyme kinetics – specifically K_m , which determines the binding affinity of the enzyme to substrate – are indicative of enzyme flexibility (the capacity for quick conformation change) (Somero, 1975). The increased flexibility would cause the cold-adapted enzyme to spend more time maintaining conformations that are not optimal for substrate binding (Siddiqui and Cavicchioli, 2006). This can be measured as a gradual increase of K_m with temperature (Fields, 2001). Key to effective enzymatic

function is the trade-off between functional capacity and enzyme flexibility, which co-vary with habitat temperature (Somero, 1995; Fields, 2001; Tokuriki et al., 2012). Conformational flexibility and enzyme function are closely related, and organisms have evolved to produce enzymes with thermal optima at their habitat temperature. For example, more flexible enzyme systems are expected under cold conditions, while strongly reduced enzyme flexibility (i.e. low temperature sensitivity of K_m) is predicted in warmer climates (Johns and Somero, 2004; Dong and Somero, 2009; Bradford, 2013).

Furthermore, as enzyme systems are altered by climate warming, different sets of isoenzymes (i.e., enzymes with the same function but different conformations and structures) are expected to be expressed at cold and warm temperatures (Sommer, 1978; Bradford, 2013; Razavi et al., 2016). Isoenzymes with higher temperature optima can be produced by the same microbial species adapted to warming (Hochachka and Somero, 2002). Alternatively, isoenzymes can be expressed as a result of changes in microbial community structure caused by warming (Baldwin and Hochachka, 1970; Vanhala et al., 2011). In both cases, temperature sensitivity of catalytic reactions is dependent on enzyme isoforms. Nonetheless, all these mechanisms suggest that microbes prefer to produce enzymes that maintain optimal activity under native soil conditions.

Despite intensive discussion on the mechanisms of enzyme temperature sensitivity, it remains unclear how the functional characteristics of enzymes in cold-adapted soil will be altered by temperature increases. This is extremely important because it provides evidence of the response of cold-adapted soil microbes and the fate of huge amounts of SOC stored in these ecosystems by acceleration of enzymatic decomposition in a warmer world. In addition, there is a lack of studies on the catalytic efficiency of soil enzymes in cold ecosystems as affected by warming.

This study was designed to test the effects of intensive warming on the catalytic properties of soil enzymes in a cold-adapted environment. We hypothesized that maximal reaction rate will be insensitive to intensive warming at high temperature range (H1); and that the substrate affinity (K_m) will remain constant at elevated temperature

(H2). To test our hypothesis we collected soil from the Tibetan Plateau and incubated the samples for one month over a temperature range of 0–40 °C (with 5 °C steps) and determined the kinetics, temperature sensitivities and activation energy of six enzymes involved in decomposition of soil organics: cellobiohydrolase and β -glucosidase, which are commonly measured as enzymes responsible for consecutive stages of cellulose degradation (German et al., 2011); xylanase, which degrades xylooligosaccharides into xylose and is thus responsible for breaking down hemicelluloses (Chen et al., 2012); acid phosphomonoesterase, which hydrolyzes (mono) ester bonds of organic P to phosphate under acidic conditions (Eivazi and Tabatabai, 1977; Malcolm, 1983; German et al., 2011). Activities of tyrosine aminopeptidase and leucine aminopeptidase were analyzed to assess the hydrolysis of peptide bonds (Koch et al., 2007; Chen et al., 2012).

2.2.3 Material and methods

2.2.3.1 Site description and soil collection

The sampling site is located in the upper Kyi Chu catchment north of Lhasa in Pando County, above the Reting Monastery in Qinghai-Tibetan Plateau (south west of China, 4330 m a.s.l.) (Table 1). The mean precipitation during the growing season (from May to October) is 330 mm. The temperature during the growing season ranges between –4 to +17.7 °C. This site has the largest and most sacred *Juniperus* forest in Tibet, diffusely growing in a carpet-like felty turf of *Kobresia pygmaea* C.B. Clarke (Miehe et al., 2008) which is the dominant and eponymous species (covering up to 98% of the root-mat surface).

Table 1 Basic information of the sampling site

Site	Location	MAP (mm yr ⁻¹)	MAT (°C)	Dominant soil types	Horizon	Dominant species
Reting, Lahsa	30°18'50"N 91°30'47"E	549	2.4	Cambisols	A	<i>Juniperus tibetica</i> , <i>Kobresia pygmaea</i> C.B. Clarke

Four composites of six soil samples each were collected using soil cores (18.5 cm long 4.5 cm diameter). Each composite sample was collected over a 30 m² area. A variable-depth sampling scheme was used to obtain the entire A-horizon. This sampling scheme increases our confidence for minimizing random variation in soil properties. Samples

were collected in August 2015 when the mean monthly air temperatures were around 2.4 °C.

Once collected, samples were hand-mixed, roots and stones were separated and composite samples were placed in ziplock bags, and kept cold (~4 °C) for transport back to the laboratory (Göttingen University). Thereafter, samples were passed through a 2 mm screen and prepared for incubation.

Extra soil samples were oven-dried under 60°C for 48 hours and used for measurement of soil properties. Soil pH, at the ratio of 1 to 2.5 (soil to water), was measured using a pH-meter (Metrohm, Herisau, Switzerland). Soils were analyzed for total C and N using an elemental analyzer (Vario Max CN, Hanau, Germany). Soil properties are shown in Table 2.

Table 2 Description of soil properties

Site	Soil bulk density (g cm ⁻³)	C (%)	N (%)	C/N	Soil pH
Reting	1.1	4.4±0.2	0.3±0.01	14±0.3	5.5

2.2.3.2. Soil incubation and enzyme assays

Enzyme assays were prepared by placing 30 g of soil in air-tight vials (125 ml) equipped with rubber seals. Six enzymes targeting C-, N- and P-containing substrates were investigated after progressively incubating the soil at 0, 5, 10, 15, 20, 25, 30, 35 and 40 °C for one month. During the incubation, soil moisture was checked by weighing and was immediately adjusted to equal 60 % of WHC. In order to avoid anaerobiosis, all the samples were regularly aerated by opening the vials for 1 minute. Nine climate chambers (SBS C120) were used to regulate the temperature (< ± 0.5 °C).

The kinetics of hydrolytic enzymes involved in C, N and P cycles were measured by fluorimetric microplate assays of 4-methylumbelliferone (MUF) and 7-amino-4-methylcoumarin (AMC) (Marx et al., 2005). Four types of fluorogenic substrates based on MUF and two types based on AMC were used to assess enzymatic activities: 4-methylumbelliferyl-β-D-cellobioside (MUF-C) to detect cellobiohydrolase activity; 4-methylumbelliferyl-β-D-glucoside (MUF-G) to detect β-glucosidase activity; and 4-methylumbelliferyl-β-D-xylopyranoside (MUF-X) to detect xylanase activity. The

activities of tyrosine aminopeptidase and leucine aminopeptidase were measured using L-tyrosine-7-amido-4-methyl-coumarin (AMC-T) and L-leucine-7-amino-4-methyl coumarin (AMC-L). 4-methylumbelliferyl-phosphate (MUF-P) was used to detect acid phosphomonoesterase activity. All substrates and chemicals were purchased from Sigma (Germany).

We determined enzyme activities over a range of substrate concentrations from low to high (0, 10, 20, 30, 40, 50, 100, 200 $\mu\text{mol g}^{-1}$ soil). At each temperature four replicates were incubated. In addition, for all four incubation replicates, the assay of each enzyme at each substrate concentration was performed using three analytical replicates (12 wells in the microplate). To ensure the saturation concentrations of fluorogenic substrates preliminary experiments were performed. Besides, linear increase of fluorescence over time during the assay was properly checked and data, which was obtained after 2 h, was used for further calculation (German et al., 2011).

Suspensions of 0.5 g soil (dry weight equivalent) with 50 ml water were prepared using low-energy sonication (40 J s^{-1} output energy) for 2 min (Stemmer et al., 1998). Then 50 μl of soil suspension was added to 100 μl substrate solution and 50 μl of buffer [MES (pH:6.8) buffer for MUF substrate and TRIZMA (pH:7.2) buffer for AMC substrate] in a 96-well microplate (Koch et al., 2007). During pipetting, the soil suspension was kept agitation. Later each well was homogenized with 2 or 3 aspirations/ejections using a multi-channel micropipette. Fluorescence was measured in microplates at an excitation wavelength of 355 nm and an emission wavelength of 460 nm, slit width of 25 nm, with a Victor 3 1420-050 Multi Label Counter (Perkin Elmer, USA). Right before each measurement each plate was shaken for 1 min. All enzymes were determined and incubated at exact temperature over 2 hours. After each fluorescence measurement (i.e. after 30 min, 1 h and 2 h) the microplates were promptly returned to the climate chambers, so that the measurement time did not exceed 2–2.5 min. During assay-incubation, microplates, at all different temperatures, were covered tight to prevent evaporation of solutions within the microplates.

Enzyme activities were expressed as MUF or AMC release in nmol per g dry soil per hour (nmol product released $\text{h}^{-1} \text{g}^{-1}$ dry soil). Enzyme activity (nmol product released $\text{h}^{-1} \text{g}^{-1}$ dry soil) was calculated from the MUF or AMC standard curve following German et al. (2011). We checked possible temperature effects on the chemical decomposition and thermal hydrolysis of the four MUF-substrates and two AMC-substrates, but no significant effects were detected over the range 0–40 °C (Razavi et al., 2015).

The Michaelis-Menten equation was used to determine parameters of the enzyme activity (V):

$$V = \frac{V_{\max} [S]}{K_m + [S]} \quad (1)$$

where V_{\max} is the maximum enzyme activity; K_m represents the half-saturation constant, or the substrate concentration at which the reaction rate equals $V_{\max}/2$; and S is the substrate concentration at active site of the enzyme (Michaelis and Menten, 1913; Segel, 1975; Von Lützow and Kögel-Knabner, 2009). Both V_{\max} and K_m parameters were approximated by the Michaelis-Menten equation (1) with the non-linear regression routine of STATISTICA. Fitting was performed for the mean of 12 replicates. Analysis of variance (ANOVA) followed by the Tukey HSD at a probability level of $p < 0.05$ was used to define the ranges of temperatures with significantly different K_m ($p < 0.05$). This means that pairwise differences were applied to distinguish the significant differences for each neighboring pair of independent variables (mean values of K_m at 0, 5, 10, 15, 20, 25, 30, 35, 40 °C) (Razavi et al., 2015; Razavi et al., 2016). Homogeneity of variance and normality of the values was tested by Levene's test and the Shapiro-Wilk test. We used the routine Q_{10} function (2) to examine temperature sensitivity and to express temperature responses of each enzyme kinetic parameter (i.e., K_m or V_{\max} separately).

$$Q_{10} = \left(\frac{R_{(T+10^\circ\text{C})}}{R_{(T)}} \right) \quad (2)$$

where R is the rate of a process or a value of a kinetic parameter and T is temperature (Kirschbaum, 1995).

The activation energy was calculated according to the classical Arrhenius equation (Eq. 3):

$$k = A \exp(-E_a / RT) \quad (3)$$

where k is the reaction rate constant; A is the frequency of molecular collisions; E_a is the required activation energy in Joules per mole; R is the gas constant ($8.314 \text{ J mol}^{-1} \text{ K}^{-1}$) and T is the temperature in Kelvin. The activation energy was calculated in two steps: once for the low temperature range from 0–20 °C and once for the elevated range from 25–40 °C. These two steps were selected on the basis of the absolute maximum temperature of the studied area: 24.1 °C (Miehe et al., 2008).

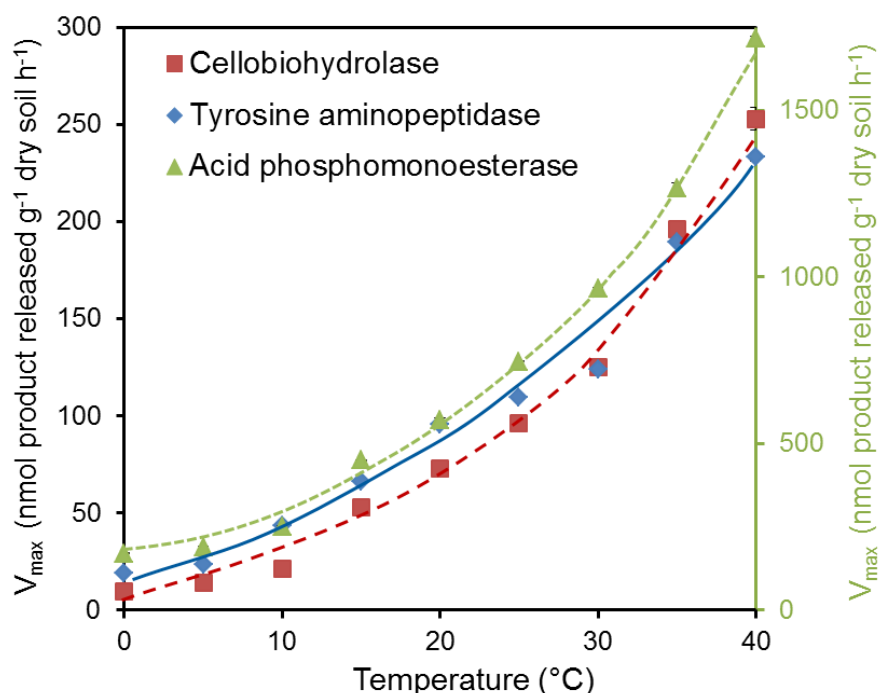


Figure 1 Enzyme activity as a function of temperature demonstrates a gradual increase for cellobiohydrolase (top), tyrosine aminopeptidase (middle) and acid phosphomonoesterase (bottom) within the range of nine temperatures. Each enzyme was assayed at a range of substrate concentrations (8 concentrations) at each of 9 temperatures. Values are means of 4 replications (\pm SE). (Activities of the other three enzymes are presented in Table S1).

2.2.4 Results

2.2.4.1 Temperature sensitivity of enzyme activity

The V_{max} values increased with temperature for all enzymes (Fig. 1 and Fig. S1).

Changes in $V_{max}\text{-}Q_{10}$ were not gradual over the whole range of temperatures tested, and were clearly pronounced between 0 and 15 °C (Fig. 2). The magnitude of the temperature response varied between enzymes, ranging from 1.3 to 3.8, which corresponds to E_a values of 19 to 53 kcal mol⁻¹ (Fig. 3). For all enzymes, E_a was higher in the low temperature range (0-20 °C) and decreased strongly from 25 to 40 °C (Fig. 3). The fitting of V_{max} to the Arrhenius model demonstrated higher E_a values for cellobiohydrolase and xylanase compared to proteases, acid phosphomonoesterase and β -glucosidase.

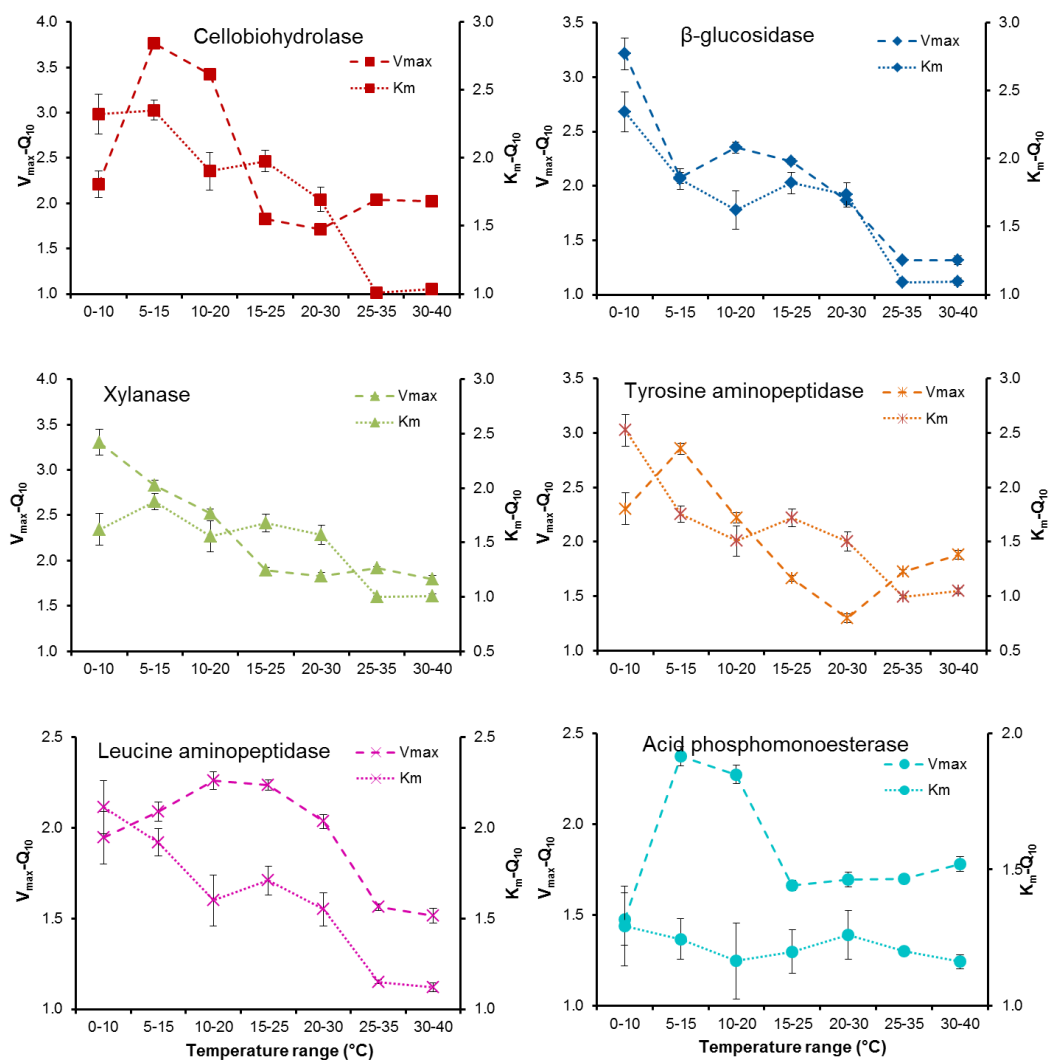


Figure 2 Temperature sensitivity of maximal reaction rate ($V_{max}\text{-}Q_{10}$) and substrate affinity ($K_m\text{-}Q_{10}$) of six enzymes as a function of temperature with 5 °C increments.

2.2.4.2 Response of substrate affinity to temperature

The changes in K_m - Q_{10} were not gradual over the range of temperatures tested, and were maximal between 0 and 15 °C (Fig. 2, Table S1). The Q_{10} values for K_m varied over a more narrow range of 1.0 to 2.5 that was 1.5 times lower compared to V_{max} - Q_{10} . The K_m - Q_{10} demonstrated two enzyme-specific patterns: 1. Decrease of K_m - Q_{10} for the whole temperature ranges; this pattern corresponded to enzymes of the C and N cycles. 2. The pattern observed for acid phosphomonoesterase K_m - Q_{10} was nearly constant over the whole temperature range.

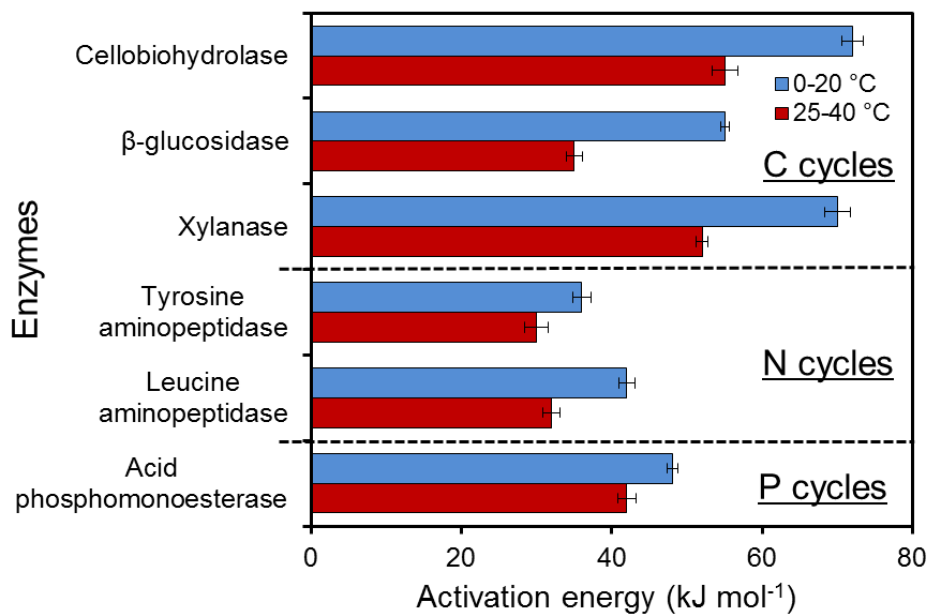


Figure 3 The activation energy (E_a) of all tested enzymes at two temperature ranges: low (0-20 °C) and high (25-40 °C).

The temperature effect on K_m revealed a distinct threshold with a significant decrease in the affinity of all enzymes to substrate at temperatures above 25 °C (Fig. 4). Cellobiohydrolase, β-glucosidase and xylanase demonstrated stepwise increases of K_m values at low to moderate temperatures (0-20 °C). The K_m values of these enzymes strongly increased (by around 40%) between 20 and 25 °C (Fig. 4). After such an extreme increase, the K_m values did not change significantly up to 40 °C (Fig. 4). The changes of acid phosphomonoesterase's K_m followed a pattern different to that of the enzymes involved in carbohydrate decomposition and proteases. Acid phosphomonoesterase demonstrated slightly increased K_m values across the whole temperature range (0-40 °C), (Fig. 4).

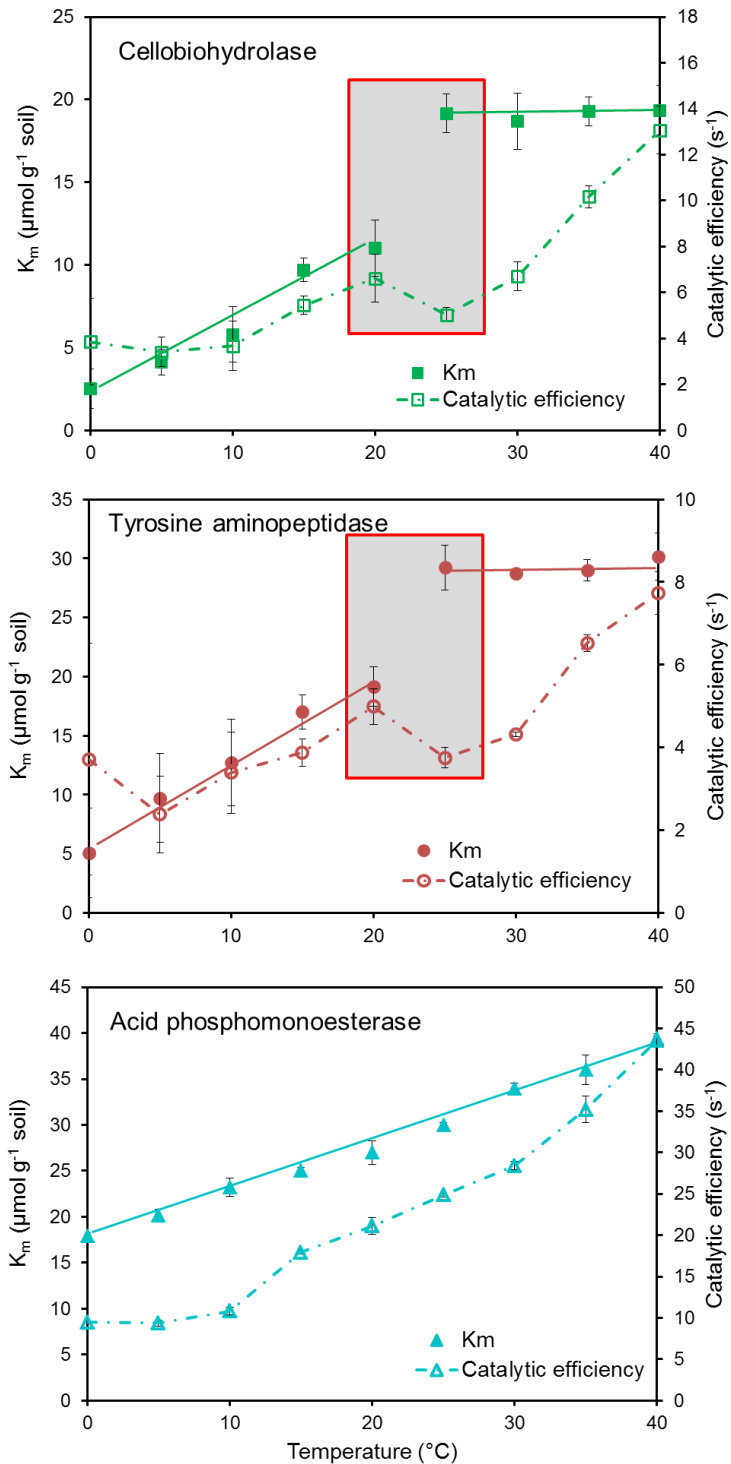


Figure 4 K_m and catalytic efficiency (V_{max}/K_m) of cellobiohydrolase (top), tyrosine aminopeptidase (middle) and acid phosphomonoesterase (bottom). Shading indicates temperature ranges with extreme K_m increases accompanied by decreases in catalytic efficiency. (K_m and catalytic efficiency of the other three enzymes are presented in Table S1).

Thus, the K_m of all C and N cycle enzymes changed significantly within psychrophilic and mesophilic temperatures, while substrate affinity was relatively constant within the elevated range (25–40 °C).

2.2.4.3 Catalytic efficiency of enzymes as affected by temperature

The catalytic efficiency of the enzymes (V_{max}/K_m) increased from cold to moderate temperatures (0–20 °C). Further extreme increases in K_m at the 25 °C threshold were always accompanied with a sharp decrease in the catalytic efficiency of enzymes of the C and N cycles (Fig. 4), and leveled off above 25 °C. In contrast, the catalytic efficiency of acid phosphomonoesterase increased gradually from 0 to 40 °C (Fig. 4).

2.2.5 Discussion

Most soil studies and models tacitly accept the gradual (according to Q_{10}) increase of reaction rates (and consequently process intensities) with temperature. Both V_{max} and K_m increased with temperature for all tested enzymes, although the increase was not linear and indicated different temperature sensitivities of V_{max} and K_m (Fig. 1, 4). The Q_{10} values of reaction rates varied from 1.9 to 3.8 within the low temperature range and decreased to 1.3 at higher temperature. Similarly, the activation energy of all tested enzymes was higher at low and moderate temperatures (0–20 °C) compared to elevated levels (25–40 °C). This general reduction of temperature sensitivity confirms theoretical predictions (Davidson and Janssens, 2006) and experimental observations on reduced reaction rate Q_{10} values at elevated temperature (Tjoelker et al., 2001; Razavi et al., 2015). In line with previous studies, activation energy and temperature sensitivity of enzymes responsible for complex C-compound degradation (i.e. xylanase and cellobiohydrolase) were higher compared to β -glucosidase (Craine et al., 2010; Conant et al., 2011). However, contrary to our hypothesis (H1), reaction rates of enzymes that degrade low quality polymers remained temperature sensitive (i.e. $V_{max}-Q_{10}=2$) even in warm temperature ranges. According to Arrhenius law the higher activation energy associated with the breakdown of recalcitrant substrates could result in a greater temperature sensitivity of decomposition (Knorr et al., 2005; Hartley and Ineson, 2008). This logic appears to be supported by measurements of the temperature sensitivity of leaf litter decomposition (Fierer et al., 2005).

We found a gradual increase of K_m from 0–40 °C (acid phosphomonoesterase) and for all other tested enzymes from 0–20 °C. This could be a consequence of increased

enzyme flexibility, i.e. the capacity for quick conformation changes ensuring a fast rate of catalytic reaction by changing temperature. We also assume that the gradual increase of K_m with increasing temperature may reflect stepwise expression of isoenzymes. Proteases and cellulolytic enzymes demonstrated constant K_m from 25 to 40 °C which is in line with the previous findings of Fields and Somero (1998) and the theoretical prediction of Bradford (2013) regarding the stability of enzyme systems at high temperatures. A strong increase in K_m by 40–50% at high temperatures (25 versus 20°C) reflected a two-fold reduction of the enzyme-substrate affinities. However, such temperature thresholds seem to be higher in temperate climates (30 °C), (Razavi et al., 2016) compared to highland areas like Tibet (25 °C).

Following the strong increase at 20 °C, the K_m remained nearly constant from 25 to 40 °C, while the maximal enzyme activity (V_{max}) gradually increased with temperature. The accelerated enzymatic activity (V_{max}) by temperature could indicate the increase in enzyme production due to an increase in microbial biomass. Alternatively, constant K_m – accordance with our hypothesis (H2) – can be explained by an expression of multiple isoenzymes each with a different temperature optimum (Somero, 1995; Bradford, 2013). Such isoenzyme expression leads to an optimal balance between the static character of the enzyme (responsible for high efficiency at constant optimal temperature) and functional capacity, under their respective optimal working conditions (Zavodsky et al., 1998; Conant et al., 2011; Razavi et al., 2016).

Sudden and strong changes in K_m at 25 °C indicated a switch from cold- and moderate- to warm-adapted enzyme systems with decreased substrate affinity. In fact, such an increase was responsible for the reduced temperature sensitivity and catalytic efficiency of overall enzyme function. A constant K_m value from 25 to 40 °C was accompanied by a gradual increase of catalytic efficiency with temperature. From another point of view, production of enzymes with similar substrate affinity and higher efficiency might be a preferred microbial strategy (Stone et al., 2012; Hoang et al., 2016) in the studied soil. Catalytic efficiency demonstrated a general trend of gradually increasing with temperature at both cold and warm temperatures (Fig. 4, 5). The only remarkable exception occurred at 25 °C, where a strong increase in K_m was accompanied by a

significant decrease in catalytic efficiency (Fig. 5). Thus, decoupled responses of V_{max} and K_m to temperature resulted in irregular increases of catalytic efficiency with temperature. Quite simply, if catalytic properties are to be maintained under a particular thermal regime, the "goal" that must be met would be expression of isoenzymes with similar K_m values (Somero, 1978). Thus, maintaining the high binding affinity to substrate (constant K_m) ensured efficient enzyme conformation within the unaccustomed temperate range.

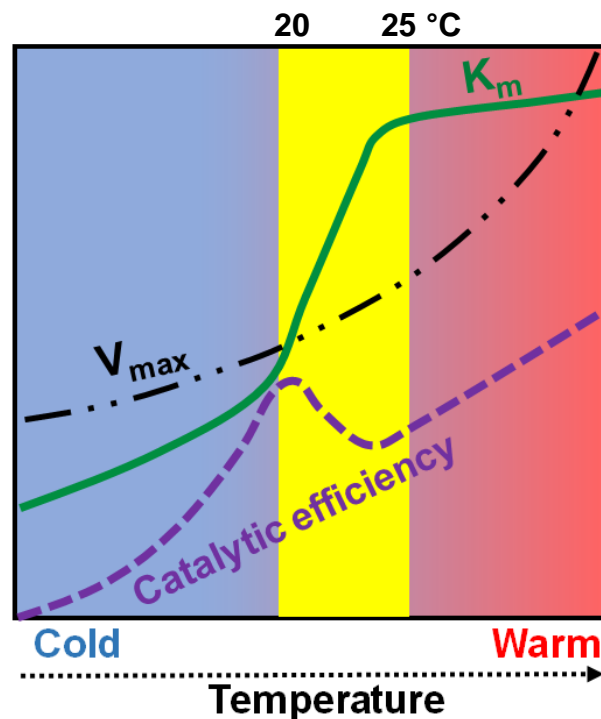


Figure 5 Generalized thermal responses of enzyme catalytic properties to a temperature increase. The scheme explains that catalytic efficiency gradually increases with temperature at both cold and warm temperatures except at 25 °C, where a strong increase in K_m occurs.

However, to generalize the conclusions based on one soil type from alpine climate, more soils from various zones need to be tested. Therefore, we need more mechanistic work, *in situ* studies along with the studies of pure and isolated enzymes from a range of habitats to verify assumptions regarding temperature responses of specific proteins. Previous studies on pure cultures demonstrated a decline in catalytic efficiency between 20-30 °C (Siddiqui and Cavicchioli, 2006). However, the pattern observed here was different which might be due to the complex composition of microbial communities in

soil. In addition, as these temperatures are extremely unusual for the original microbial community under the natural climate, with an annual temperature of 2.4 °C (Bárcenas-Moreno et al., 2009), such sharp changes in K_m could be an indicator of isoenzyme expression (Baldwin and Hochchka, 1970) due to a major shift in species dominance above 25 °C or an alteration in enzyme systems (Khalili et al., 2011; Bradford, 2013). However, while such a conclusion has been done for the one soil studied here, the relevance of the observed patterns needs to be proven for soils with contrasting properties (e.g., texture, structure, pH, C content, etc.) in a range of climate zones, e.g., in boreal and tropical environments. Furthermore, thermal denaturation – usually occurring at temperatures much higher than 40°C (dos Santos et al., 2004; Goyal et al., 2014) – affects the kinetic constants of enzymes and also increases K_m (Dick and Tabatabai, 1987). These indirect mechanisms of K_m increase with temperature due to interactions of enzymes with soil particles.

Overall, i) enzymes that degrade low quality polymers are temperature-sensitive over the whole range of temperatures (0 – 40 °C); ii) soil microorganisms are able to maintain stable or flexible enzyme systems with low or high substrate affinity within wide temperature ranges to ensure efficient enzymatic functioning under diurnally and annually varying temperatures. This ensures the easier adaptation of microbially driven decomposition to changing climate. Thus, acclimation may involve the expression of enzymes at a warmer temperature, potentially with the same K_m but not necessarily. We conclude that consideration must be given to the temperature thresholds of strong changes in enzyme-based processes and that this is crucial to modeling the consequences of warming for C, N and P cycles and predicting the fate of soil carbon stocks in a warmer world.

2.2.6 Acknowledgements

The authors thank Per Schleuß for his fruitful help in the soil sampling and transportation. We acknowledge the DAAD for supporting BSR and China Scholarship Council for supporting SL. Thanks to Anita Kriegel, Karin Schmidt and Susanne Grube for laboratory assistant and Kyle Mason-Jones for linguistic help. This study was supported by DFG within the framework of SPP 1372. Tibetan Plateau: Formation-

Climate-Ecosystem (subproject KU 1184/14-2). The support of the steering committee of SPP 1372 is especially acknowledged.

2.2.7 References

- Allison, S.D., Treseder, K.K., 2008. Warming and drying suppress microbial activity and carbon cycling in boreal forest soils. *Global Change Biology*, 14, 2898-2909.
- Allison, S.D., Wallenstein, M.D., Bradford, M.A., 2010. Soil-carbon response to warming dependent on microbial physiology. *Nature Geoscience* 3, 336–340. DOI: 10.1038/ngeo846.
- Baldwin, J., Hochachka, P.W., 1970. Functional significance of isoenzymes in thermal acclimatization: acetylcholinesterases from trout brain. *Biochemical Journal* 116, 883–887.
- Bárcenas-Moreno, G., Gómez-Brandón, M., Rousk, J., Bååth, E., 2009. Adaptation of soil microbial communities to temperature: comparison of fungi and bacteria in a laboratory experiment. *Global Change Biology* 15, 2950–2957. DOI: 10.1111/j.1365-2486.2009.01882.x.
- Blagodatskaya, E., Blagodatsky, S., Khomyakov, N., Myachina, O., Kuzyakov, Y., 2016. Temperature sensitivity and enzymatic mechanisms of soil organic matter decomposition along an altitudinal gradient on Mount Kilimanjaro. *Scientific Reports* 6, 22240. DOI: 10.1038/srep22240.
- Bradford, M.A., 2013. Thermal adaptation of decomposer communities in warming soils. *Frontiers in Microbiology* 4. DOI: 10.3389/fmicb.2013.00333.
- Buyer, J.S., Drinkwater, L.E., 1997. Comparison of substrate utilization assay and fatty acid analysis of soil microbial communities. *Journal of Microbiological Methods* 30, 3–11. DOI: 10.1016/S0167-7012(97)00038-9.
- Chen, R., Blagodatskaya, E., Senbayram, M., Blagodatsky, S., Myachina, O., Dittert, K., Kuzyakov, Y., 2012. Decomposition of biogas residues in soil and their effects on microbial growth kinetics and enzyme activities. *Biomass and Bioenergy* 45, 221–229. DOI: 10.1016/j.biombioe.2012.06.014.
- Conant, R.T., Ryan, M.G., Ågren, G.I., Birge, H.E., Davidson, E.A., Eliasson, P.E., Evans, S.E., Frey, S.D., Giardina, C.P., Hopkins, F.M., Hyvönen, R., Kirschbaum, M. U.F., Lavelle, J.M., Leifeld, J., Parton, W.J., Megan Steinweg, J., Wallenstein, M.D., Martin Wetterstedt, J.Å., Bradford, M.A., 2011. Temperature and soil organic matter decomposition rates - synthesis of current knowledge and a way forward. *Global Change Biology* 17, 3392–3404. DOI: 10.1111/j.1365-2486.2011.02496.x.
- Craine, J.M., Fierer, N., Mclauchlan, K.K., 2010. Widespread coupling between the rate and temperature sensitivity of organic matter decay. *Nature Geoscience* 3, 854–857. DOI: 10.1038/ngeo1009.
- Davidson, E.A., Janssens, I.A., 2006. Temperature sensitivity of soil carbon decomposition and feedbacks to climate change. *Nature* 440, 165–173. DOI: 10.1038/nature04514.
- Davidson, E.A., Janssens, I.A., Luo, Y., 2006. On the variability of respiration in terrestrial ecosystems: moving beyond Q_{10} . *Global Change Biology* 12, 154–164. DOI: 10.1111/j.1365-2486.2005.01065.x.
- Dick, W. A., Tabatabai, M. A., 1978. Inorganic pyrophosphatase activity of soils. *Soil Biology and Biochemistry* 10, 58-65.
- Dong, Y., Somero, G.N., 2009. Temperature adaptation of cytosolic malate dehydrogenases of limpets (genus *Lottia*): differences in stability and function due to minor changes in sequence correlate with biogeographic and vertical distributions. *Journal of Experimental Biology* 212, 169-177. DOI: 10.1242/jeb.024505.
- dos Santos, M. M., da Rosa, A. S., Dal'Boit, S., Mitchell, D. A., Krieger, N., 2004. Thermal denaturation: is solid-state fermentation really a good technology for the production of enzymes?. *Bioresource Technology* 93, 261-268.
- Eivazi, F., Tabatabai, M.A., 1977. Phosphatases in soils. *Soil Biology and Biochemistry* 9, 167–172. DOI: 10.1016/0038-0717(77)90070-0.
- Feller, G., 2003. Molecular adaptations to cold in psychrophilic enzymes. *Cellular and Molecular Life Sciences* 60, 648-662. DOI: 10.1007/s00018-003-2155-3.
- Fields, P.A., 2001. Review: Protein function at thermal extremes: balancing stability and flexibility. *Comparative Biochemistry and Physiology Part A: Molecular & Integrative Physiology* 129, 417–431. DOI: 10.1016/S1095-6433(00)00359-7.
- Fields, P.A., Somero, G.N., 1998. Hot spots in cold adaptation: localized increases in conformational flexibility in lactate dehydrogenase A4 orthologs of Antarctic notothenoid fishes. *Proceedings of the National Academy of Sciences of the United States of America* 95, 11476–11481.
- Gerday, C., Aittaleb, M., Arpigny, J.L., Baise, E., Chessa, J.P., 1997. Psychrophilic enzymes: a thermodynamic challenge. *Biochimica et Biophysica Acta* 1342, 119-131.
- Gerlt, J.A., Gassman, P.G., 1993. An explanation for rapid enzyme-catalyzed proton abstraction from carbon acids: importance of late transition states in concerted mechanisms. *Journal of the American Chemical Society* 115, 11552-11568.
- German, D.P., Marcelo, K.R.B., Stone, M.M., Allison, S.D., 2012. The Michaelis–Menten kinetics of soil extracellular enzymes in response to temperature: a cross-latitudinal study. *Global Change Biology* 18, 1468–1479. DOI: 10.1111/j.1365-2486.2011.02615.x.

- German, D.P., Weintraub, M.N., Grandy, A.S., Lauber, C.L., Rinkes, Z.L., Allison, S.D., 2011. Optimization of hydrolytic and oxidative enzyme methods for ecosystem studies. *Soil Biology and Biochemistry* 43, 1387–1397. DOI: 10.1016/j.soilbio.2011.03.017.
- Goyal, M., Chaudhuri, T. K., Kuwajima, K., 2014. Irreversible Denaturation of Maltodextrin Glucosidase Studied by Differential Scanning Calorimetry, Circular Dichroism, and Turbidity Measurements. *PloS one* 9, e115877.
- Hartley, Iain P., Ineson P., 2008. Substrate quality and the temperature sensitivity of soil organic matter decomposition. *Soil Biology and Biochemistry* 40, 1567-1574.
- Hochachka, P.W., Somero, G.N., 2002. *Biochemical Adaptation*. Oxford University Press, New York, NY, USA.
- Huston, A.L., Krieger-Brockett, B.B., Deming, J.W., 2000. Remarkably low temperature optima for extracellular enzyme activity from Arctic bacteria and sea ice. *Environmental Microbiology* 2, 383-388. DOI: 10.1046/j.1462-2920.2000.00118.x.
- Johns, G.C., Somero, G.N., 2004. Evolutionary convergence in adaptation of proteins to temperature: A4-lactate dehydrogenases of Pacific damselfishes (*Chromis* spp.). *Molecular Biology and Evolution* 21, 314 – 320. DOI: 10.1093/molbev/msh021.
- Khalili, B., Nourbakhsh, F., Nili, N., Khademi, H., Sharifnabi, B., 2011. Diversity of soil cellulase isoenzymes is associated with soil cellulase kinetic and thermodynamic parameters. *Soil Biology and Biochemistry* 43, 1639–1648. DOI: 10.1016/j.soilbio.2011.03.019.
- Kirschbaum, M.U.F., 1995. The temperature-dependence of soil organic-matter decomposition, and the effect of global warming on soil organic-C storage. *Soil Biology and Biochemistry* 27, 753-760. DOI: 10.1016/0038-0717(94)00242-S.
- Knorr, W., Prentice, I.C., House, J.I., Holland, E.A., 2005. Long-term sensitivity of soil carbon turnover to warming. *Nature* 433, 298-301. DOI: 10.1038/nature03226.
- Koch, O., Tscherko, D., Kandeler, E., 2007. Temperature sensitivity of microbial respiration, nitrogen mineralization, and potential soil enzyme activities in organic alpine soils. *Global Biogeochemical Cycles* 21, 1-11. DOI: 10.1029/2007GB002983.
- Lipson, D.A., Schadt, C.W., Schmidt, S.K., 2002. Changes in soil microbial community structure and function in an alpine dry meadow following spring snow melt. *Microbial Ecology* 43, 307-314. DOI: 10.1007/s00248-001-1057-x.
- Malcolm, R.E., 1983. Assessment of phosphatase activity in soils. *Soil Biology and Biochemistry* 15, 403–408. DOI: 10.1016/0038-0717(83)90003-2.
- Marx, J.C., Collins, T., D'Amico, S., Feller, G., Gerday, C., 2007. Cold-adapted enzymes from marine Antarctic microorganisms. *Marine Biotechnology* 9, 293-304.
- Marx, M.C., Kandeler, E., Wood, M., Wermbter, N., Jarvis, S.C., 2005. Exploring the enzymatic landscape: distribution and kinetics of hydrolytic enzymes in soil particle size fractions. *Soil Biology and Biochemistry* 37, 35–48. DOI: 10.1016/j.soilbio.2004.05.024.
- Michaelis, L., Menten, M.L., 1913. Die kinetik der invertinwirkung. *BiochemischesZeitschrift* 49, 334–336.
- Miehe, G., Miehe, S., Will, M., Opgenoorth, L., Duo, L., Dorgeh, T., Liu, J.Q., 2008. An inventory of forest relicts in the pastures of Southern Tibet (Xizang A.R., China). *Plant Ecology* 194: 157-177. DOI: 10.1007/s11258-007-9282-0.
- Nannipieri, P., Gianfreda, L., 1998. Kinetics of enzyme reactions in soil environments. In: Huang, P.M., Senesi, N., Buffle, J. (Eds.), *Structure and Surface Reactions of Soil Particles*. John Wiley & Sons, pp. 449-479.
- Neidhardt, F.C., Ingraham, J.L., Schaechter, M., 1990. *Physiology of the bacterial cell: a molecular approach*, Sinauer Associates, Sunderland, MA, USA.
- Razavi, B.S., Blagodatskaya, E., Kuzyakov, Y., 2015. Nonlinear temperature sensitivity of enzyme kinetics explains canceling effect - a case study on loamy haplic Luvisol. *Frontiers in Microbiology* 6, 1126. DOI: 10.3389/fmicb.2015.01126.
- Razavi, B.S., Blagodatskaya, E., Kuzyakov, Y., 2016. Temperature selects for static soil enzyme systems to maintain high catalytic efficiency. *Soil Biology and Biochemistry* 97: 15-22. DOI: 10.1016/j.soilbio.2016.02.018.
- Schimel, J., Balsler, T.C., Wallenstein, M., 2007. Microbial stress-response physiology and its implications for ecosystem function. *Ecology* 88, 1386–1394. DOI: 10.1890/06-0219.
- Segel, I.H., 1975. *Enzyme Kinetics: Behavior and Analysis of Rapid Equilibrium and Steady-State Enzyme Systems*, Willey-Interscience, New York, USA.
- Siddiqui, K.S., Cavicchioli, R., 2006. Cold-adapted enzymes. *The Annual Review of Biochemistry* 75, 403-33. DOI: 10.1146/annurev.biochem.75.103004.142723.
- Somero, G.N., 1975. The role of isozymes in adaptation to varying temperatures. In: Markert, C.L., (Eds.), *Isozymes II: Physiological Function*. Academic, New York, USA, pp. 221-234.
- Somero, G.N., 1978. Temperature adaptation of enzymes- biological optimization through structure function compromises. *Annual Review of Ecology and Systematics* 9, 1-29. DOI: 10.1146/annurev.es.09.110178.000245.
- Somero, G.N., 1995. Proteins and temperature. *Annual Review Physiology* 57, 43-68. DOI: 10.1146/annurev.ph.57.030195.000355.

- Stemmer, M., Gerzabek, M.H., Kandeler, E., 1998. Organic matter and enzyme activity in particle-size fractions of soils obtained after low energy sonication. *Soil Biology and Biochemistry* 30, 9–17. DOI: 10.1016/S0038-0717(97)00093-X.
- Stone, M.M., Weiss, M.S., Goodale, C.L., Adams, M.B., Fernandez, I.J., German, D.P., Allison, S.D., 2012. Temperature sensitivity of soil enzyme kinetics under N-fertilization in two temperate forests. *Global Change Biology* 18, 1173–1184. DOI: 10.1111/j.1365-2486.2011.02545.x.
- Stotzky, G., 1986. Influence of soil mineral colloids and metabolic processes, growth adhesion, and ecology of microbes and viruses. In: Huang, M., Schnitzer, M. (Eds.), *Interactions of soil minerals with natural organics and microbes*. Soil Science Society of America, Madison, USA, pp. 305-428.
- Tischer, A., Blagodatskaya, E., Hamer, U., 2015. Microbial community structure and resource availability drive the catalytic efficiency of soil enzymes under land-use change conditions. *Soil Biology and Biochemistry* 89, 226–237. DOI: 10.1016/j.soilbio.2015.07.011.
- Tjoelker, M.G., Oleksyn, J., Reich, P.B., 2001. Modelling respiration of vegetation: evidence for a general temperature-dependent Q_{10} . *Global Change Biology* 7, 223–230. DOI: 10.1046/j.1365-2486.2001.00397.x.
- Tokuriki, N., Jackson, C.J., Afriat-Jurnou, L., Wyganowski, K.T., Tang, R., Tawfik, D.S., 2012. Diminishing returns and tradeoffs constrain the laboratory optimization of an enzyme. *Nature Communications* 3, 1257. DOI: 10.1038/ncomms2246.
- Van Gestel, N.C., Reischke, S., Bååth, E., 2013. Temperature sensitivity of bacterial growth in a hot desert soil with large temperature fluctuations. *Soil Biology and Biochemistry* 65, 180–185. DOI: 10.1016/j.soilbio.2013.05.016.
- Vanhala, P., Karhu, K., Tuomi, M., Björklöf, K., Fritze, H., Hyvärinen, H., Liski, J., 2011. Transplantation of organic surface horizons of boreal soils into warmer regions alters microbiology but not the temperature sensitivity of decomposition: Warming, soil biology and decomposition. *Global Change Biology* 17, 538–550. DOI: 10.1111/j.1365-2486.2009.02154.x.
- Von Lütow, M., Kögel-Knabner, I., 2009. Temperature sensitivity of soil organic matter decomposition—what do we know? *Biology and Fertility of Soils* 46, 1–15. DOI: 10.1007/s00374-009-0413-8.
- Wallenstein, M., Allison, S.D., Ernakovich, J., Steinweg, J.M., Sinsabaugh, R., 2010. Controls on the temperature sensitivity of soil enzymes: a key driver of in situ enzyme activity rates. In: Shukla, G., Varma, A. (Eds.), *Soil Enzymology*. Springer Berlin Heidelberg, Germany, pp. 245-258.
- Zavodsky, P., Kardos, J., Svingor, A., Petsko, G.A., 1998. Adjustment of conformational flexibility is a key event in the thermal adaptation of proteins. *Proceedings of the National Academy of Sciences of the United States of America* 95, 7406–7411.
- Zimmermann, M., Bird, M.I., 2012. Temperature sensitivity of tropical forest soil respiration increase along an altitudinal gradient with ongoing decomposition. *Geoderma* 187-188, 8–15. DOI: 10.1016/j.geoderma.2012.04.015.

2.2.8 Supporting information

Table S1 K_m and catalytic efficiency (V_{max}/K_m) of β -glucosidase, xylanase and leucine aminopeptidase

Enzymes	Temperature (°C)	V_{max} (nmol MUF/AMC g ⁻¹ soil h ⁻¹)	K_m (μ mol g ⁻¹ soil)	V_{max}/K_m
β -glucosidase	0	30 \pm 1.3	6 \pm 0.3	4.9 \pm 0.3
	5	80 \pm 1.8	12 \pm 0.4	6.8 \pm 0.3
	10	98 \pm 1.7	14 \pm 0.4	6.8 \pm 0.2
	15	166 \pm 1.8	22 \pm 0.3	7.6 \pm 0.1
	20	230 \pm 2.7	23 \pm 0.3	9.8 \pm 0.2
	25	369 \pm 2.6	40 \pm 0.3	9.3 \pm 0.1
	30	429 \pm 7.7	41 \pm 0.7	10.6 \pm 0.3
	35	487 \pm 6.3	43 \pm 0.3	11.3 \pm 0.2
	40	564 \pm 14	44 \pm 0.8	12.7 \pm 0.4
Xylanase	0	5 \pm 0.1	5.3 \pm 0.9	1.0 \pm 0.2
	5	11 \pm 0.3	6.5 \pm 1.4	1.7 \pm 0.4
	10	17 \pm 0.3	8.6 \pm 1.4	2.0 \pm 0.3
	15	31 \pm 0.3	12 \pm 1.1	2.6 \pm 0.2
	20	42 \pm 0.6	13 \pm 1.9	3.2 \pm 0.4
	25	59 \pm 0.3	20 \pm 0.9	2.9 \pm 0.1
	30	77 \pm 0.4	21 \pm 1.3	3.7 \pm 0.2
	35	113 \pm 0.4	20 \pm 1.5	5.6 \pm 0.4
	40	138 \pm 0.5	21 \pm 1.7	6.6 \pm 0.5
Leucine aminopeptidase	0	33 \pm 0.4	5 \pm 1.3	6.3 \pm 1.5
	5	50 \pm 0.6	7.8 \pm 1.0	6.4 \pm 0.8
	10	64 \pm 0.5	11 \pm 0.9	5.8 \pm 0.5
	15	105 \pm 0.4	15 \pm 0.6	7.0 \pm 0.3
	20	145 \pm 0.6	18 \pm 0.7	8.3 \pm 0.3
	25	204 \pm 0.7	25 \pm 1.5	8.0 \pm 0.5
	30	295 \pm 1	27 \pm 1.1	10.8 \pm 0.4
	35	365 \pm 1	29 \pm 0.7	12.5 \pm 0.3
	40	448 \pm 2	31 \pm 1.1	14.7 \pm 0.5

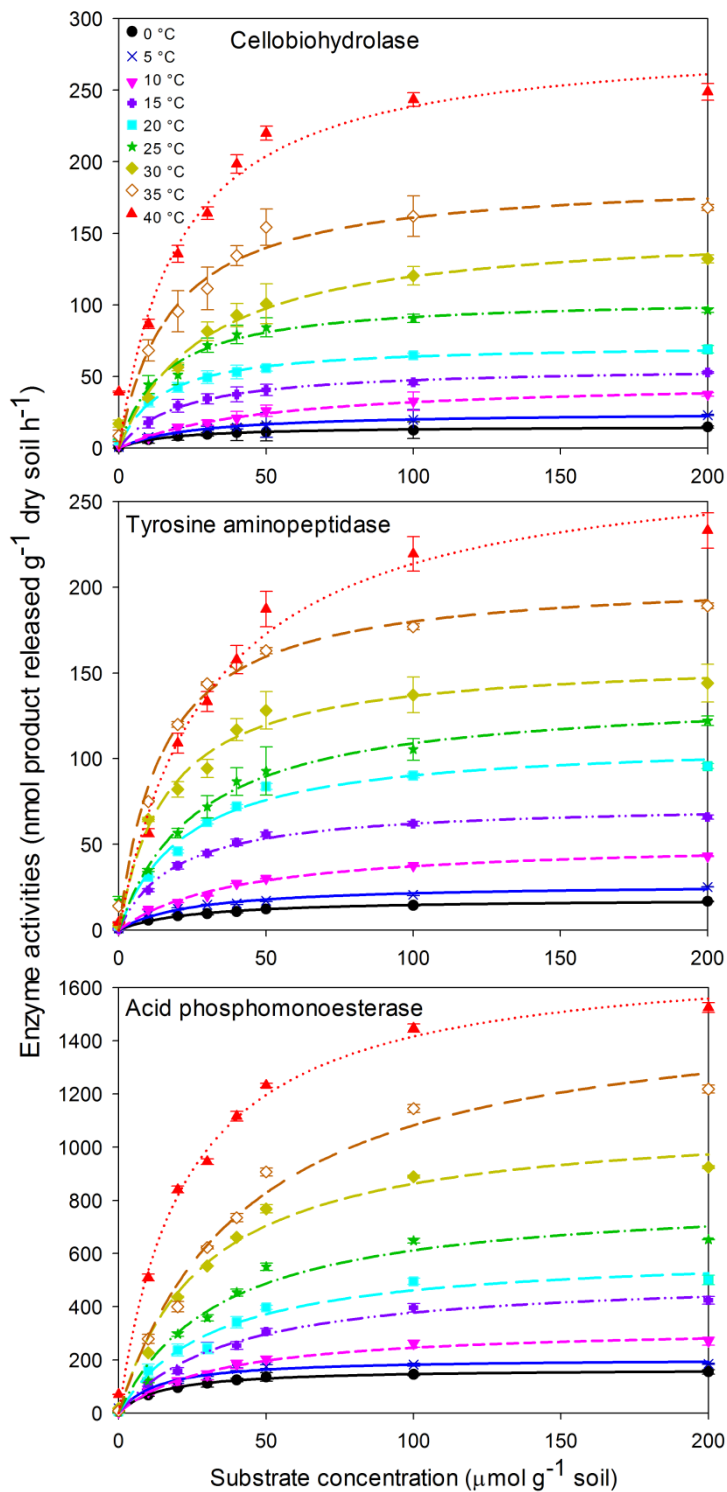


Figure S1 Examples of Michaelise Menten kinetics (enzyme activity as a function of substrate concentration) in response to increasing temperature for cellobiohydrolase (top), tyrosine aminopeptidase (middle), acid phosphomonoesterase (bottom) measured at nine temperatures. Each enzyme was assayed at a range of substrate concentrations (8 concentrations) at each of 9 temperatures. Error bars stand for standard error.

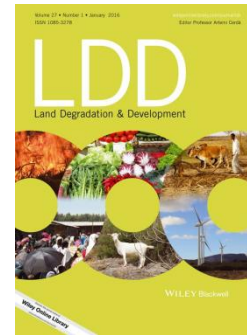
2.3 Study 3: Carbon and nitrogen losses from soil depend on degradation of Tibetan *Kobresia* pastures

Shibin Liu^{a*}, Per-Marten Schleuss^a, Yakov Kuzyakov^{a,b}

Status: Published online on *Land Degradation & Development*

^a Department of Soil Science of Temperate Ecosystem, University of Göttingen, Büsgenweg 2, 37077 Göttingen, Germany

^b Department of Agricultural Soil Science, University of Göttingen, Büsgenweg 2, 37077 Göttingen, Germany



2.3.1 Abstract

Degradation of *Kobresia pygmaea* pastures has strongly increased on the Tibetan Plateau over the last few decades and contributed to a high loss of soil organic carbon (SOC) and nutrients. Nonetheless, the pathways of carbon (C) and nitrogen (N) losses from degraded *K. pygmaea* pastures are still unclear but is a prerequisite to assess the recovery of Tibetan grasslands. We investigated the response of day- and nighttime CO₂ efflux and leaching of DOC, DON, NH₄⁺ and NO₃⁻ from *K. pygmaea* root mats in three degradation stages: living root mat, dying root mat and dead root mat. Dying root mat had the highest C loss as CO₂ and DOC from leaching. This indicates *K. pygmaea* pastures shift from a C sink to a C source following plant death. In contrast, living root mat had the lowest daytime CO₂ efflux ($0.38 \pm 0.1 \mu\text{g C g}^{-1} \text{h}^{-1}$) because CO₂ was assimilated via photosynthesis. Nighttime CO₂ efflux positively correlated with soil moisture for living and dead root mats. It indicates that increasing precipitation might accelerate C losses due to enhanced SOC decomposition. Furthermore, dead root mat had the highest average NO₃⁻ loss ($23 \pm 2.6 \text{ mg N L}^{-1}$) from leaching compared to other root mats. It reflects that leaching increases the negative impacts of pasture degradation on N availability in these often N limited ecosystems and thus impedes the recovery of *K.* pastures following degradation.

Key words: *Kobresia pygmaea* pasture, CO₂ efflux, Nitrate leaching, Grassland degradation, Dissolved organic carbon.

Corresponding Author: Shibin Liu, sliu3@gwdg.de

2.3.2 Introduction

Globally, grasslands occupy an area of about 24 million km² (Scurlock & Hall, 1998) and play an important role because they provide large grazing ground and store huge amounts of carbon (C) in soil (ca. 343 Gt C; FAO, 2010). However, about 20-35 % of the world's grasslands are degraded with the consequence of declining vegetation cover, decreasing soil organic carbon (SOC) storage and soil fertility (FAO, 2010). The drivers for grassland degradation are numerous including biotic and abiotic impacts and are mostly amplified by human activities. For instance, overgrazing is expected to trigger grassland degradation by reducing the vegetation cover, changing vegetation composition and causing direct damages via trampling (Hiernaux, 1998). Fire, permafrost and drought were also considered as factors which may influence soil structure and C storage (Pereira *et al.*, 2014; Liu & Diamond, 2005; Novara *et al.*, 2013; Yang *et al.*, 2010). A reversal of grassland degradation, however, can be induced by changing management options i.e. by planting legumes or shifting to organic farming (Parras-Alcántara *et al.*, 2015; Hu *et al.*, 2015).

The Tibetan Plateau (TP) covers up to 2.5 million square kilometers and hosts the largest montane and alpine grasslands of the world. As the only dominant *Cyperaceae* mats in southeastern humid TP (450,000 km²), the pastures of *Kobresia pygmaea* C.B. Clarke (*K. pygmaea*) are often characterized by very dense root mats, which developed as a consequence of the long-term grazing history (Miehe *et al.*, 2008). This selected plants with very high belowground investments (Hafner *et al.*, 2012). Accordingly, *K. pygmaea* is very competitive compared to other plant species because its belowground reserves ensure a rapid regrowth following grazing and the recapture of nutrients such as N is very efficient (Schleuss *et al.*, 2015).

Due to the high altitude of about 4500 m a.s.l. (Thompson *et al.*, 1997) and the harsh environment (i.e. strong solar radiation, high diurnal and annual temperature variations, low CO₂ partial pressure, strong temporal and spatial precipitation variations and steep slopes) (Fan *et al.*, 2011; Liu-Zeng *et al.*, 2008; Ren *et al.*, 1997; Zhang *et al.*, 2015), *K. pygmaea* pastures are considered to be very vulnerable ecosystems (Wang *et al.*, 2002; Schleuss *et al.*, 2015). The *Kobresia* pastures are intensively affected by grassland

degradation (Wang *et al.*, 2015). Almost all *K. pygmaea* pastures are degraded in Nagqu, 90% of which is under medium degradation stage (Wei *et al.*, 2004). According to Babel *et al.* (2014) roughly 20% of the *Kobresia* root mats on the Kema study sites were dead, whereas still 65% were in intact conditions or showed only light degradation. For the remaining part, the topsoil was removed (bare soil) by SOC decomposition or soil erosion.

Most researchers attribute the *Kobresia* pasture degradation to overgrazing (Shao & Cai, 2008). Climate change, i.e. increasing temperature or precipitation, can also stimulate SOC turnover and plant species richness and thus amplify degradation (Du *et al.*, 2004; Klein *et al.*, 2004). Soil pools of C and nitrogen (N) and plant biomass decreased along grassland degradation from healthy to severe status (Wang *et al.*, 2015; Yao *et al.*, 2016). Seedling density in the soil seed bank also significantly decreased with grassland degradation (Kassahun *et al.*, 2009). However, knowledge about C and N losses via SOC decomposition and leaching is limited for *Kobresia* root mats in different degradation stages.

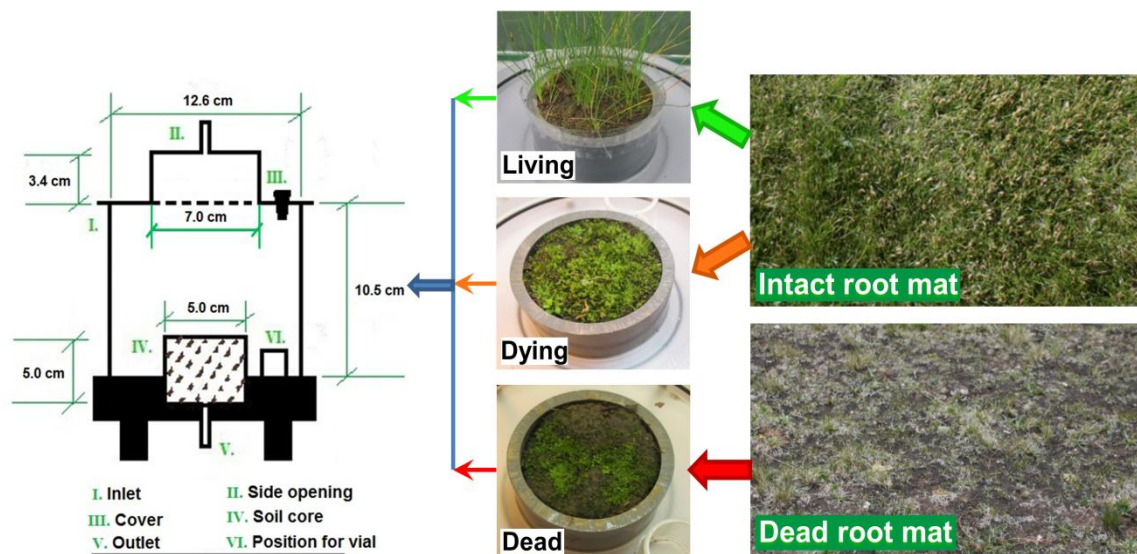


Figure 1 Longitudinal section of chamber (left) and origin of three *Kobresia* root mat types (right). “Living” = living root mat; “Dying” = dying root mat; “Dead” = dead root mat.

Therefore, root mats of different degradation stages were investigated in this study (Fig.1): (a) living root mat (Living), (b) dying root mat (Dying) and (c) dead root mat (Dead). The dying stage represents the transition between living and dead root mats. It

was in living condition during sampling but died during transport reflecting the initial stage of root mat degradation. We hypothesized that the dying root mat shows the highest C losses (mineralized as CO₂ and leached as DOM) and N losses (leached as organic and mineral N) because of rapid decomposition of SOC and fresh root litter (Hansson *et al.*, 2010). Considering the presence of living plants, we also hypothesized that living root mat assimilates CO₂ and counterbalances C losses (Ingrisch *et al.*, 2015). We also investigated the effect of soil moisture on nighttime CO₂ efflux and hypothesized that CO₂ efflux from living and dead *K. pygmaea* root mats will strongly increase with higher soil moisture because it stimulates SOC mineralization (Mukhopadhyay & Maiti, 2014).

2.3.3 Materials and Methods

2.3.3.1 Site description

Sampling was carried out on sites at the research station of the Tibet University and the Institute of Tibetan Plateau Research-“*Kobresia* Ecosystem Monitoring Area” (KEMA) (31°16'45"N 92°59'37"E, 4410 m a.s.l.) in Nagqu, Tibet. The station is located in the core area of the *Kobresia pygmaea* distribution (Babel *et al.*, 2014) and lies in the “Plateau Frigid Monsoon Region with semi-moist climate” (Leber *et al.*, 1995). Mean annual temperature and precipitation are -1.2 °C and 430 mm, respectively. From June to September, the mean summer precipitation reaches 272 mm, whereas snowfall is low (climate station in Nagqu, Miede *et al.*, 2011). The growing season ranges from May to October and mainly depends on the on- and off-set of the summer monsoon (Miede *et al.*, 1988).

The soils are classified as *Stagnic Eutric Cambisol (Humic)* (WRB, 2014) with a texture of 50% sand, 33% silt, and 17% clay. The mean pH value (H₂O) is 6.9 ± 0.03, and the topsoil is free of carbonates. Large amounts of living and dead roots are present in the topsoil, developing very dense root mats (Schleuss *et al.*, 2015). The root mats are mainly covered by *K. pygmaea* and have an average shoot height of not more than 2 cm (Miede *et al.*, 2008).

Kobresia pygmaea is the dominant vegetation type across the whole catchment of the Nagqu River (He & Richards, 2015). Average shoot biomass was 0.3 ± 0.02 kg dry

mass m^{-2} . Besides *Kobresia pygmaea* (covering up to 98%), other monocotyledons occur, such as *Carex spp.*, *Festuca spp.*, *K.humilis*, *Poa spp.*, *Stipa purpurea* and *Trisetum spp.* (Babel *et al.*, 2014).

Large areas on the study sites are affected by grassland degradation. Around 65% of the area is covered by living *Kobresia* root mats, while the remaining parts are occupied by dead root mats (16%) and bare soil patches (19%) (Babel *et al.*, 2014). The sites are grazed by livestock (yaks and sheep) from January to April and also by ground-dwelling Plateau pika (*Ochotona curzoniae*) (He & Richards, 2015).

2.3.3.2 Soil sampling and preparation

Samples were randomly selected within an area of about 25,000 m^2 to maintain equal environmental conditions. We used soil cores (diameter: 5 cm; height: 5 cm) to take undisturbed samples from living and dead root mats at a depth of 5 cm (Fig. 1, right). Before transportation, the shoot biomass was removed and samples were put into PVC collars, which had the same size as the sampling cores. In the laboratory, samples were pre-incubated for 28 days but some samples of living stage did not recover. These recently died samples were used as an additional treatment (dying root mat). In total, we had three treatments: living root mat, dying root mat and dead root mat (Fig. 1, middle). Since the dying stage was still living before sampling but died during transport or storage, they had the same initial soil characteristics compared to the intact stage i.e. C and N contents, microbial biomass and root biomass. The only difference between both root mats (Living vs Dying) is the presence of *Kobresia* shoots, which assimilate $\text{CO}_2\text{-C}$. Consequently, the dying stage was disabled from C assimilation and began to degrade. In contrast, the soil characteristics of the dead root mat totally differed compared to the living and dying stages because of long-term degradation in the field: i.e. lower C and N contents, microbial biomass and root biomass. Therefore, the three treatments reflect a gradual degradation sequence (Living < Dying < Dead).

Three samples were selected from living and dead root mats to determine water holding capacity (WHC). Another three samples were used to separate root from soil. Roots were washed carefully with distilled water to remove soil particles. Afterwards, roots were oven-dried (60 °C) and subsequently milled. Soil was oven-dried under 105 °C,

sieved (2 mm) and grounded respectively. Then soil and root were analyzed for total C and N using an elemental analyzer (Vario Max CN, Hanau, Germany). The dying root mat stage was considered to have the same initial C and N content and bulk density as living root mat.

2.3.3.3 Experimental set-up

Six samples from each root mat were selected to conduct the experiment. These samples were put in incubation boxes (Fig. 1, left) allowing simultaneous analyses of CO₂ efflux and leaching. According to Geng *et al.* (2012), diurnal soil temperature variation in Nagqu had no strong effect on soil respiration. Moreover, the average daily soil temperature during growing season was in the range of 9.3-21.3°C. Within the experiments, we used a constant temperature of 20°C during day and night. Samples were illuminated diurnally for 14 h with a photosynthetic photon flux density of 80 $\mu\text{m}^{-2} \text{s}^{-1}$ and kept in the darkness for 10 h.

The first experiment was conducted to assess CO₂-C loss and leaching of dissolved C and N. Living, dying and dead root mats were included. Daytime and nighttime CO₂ efflux was measured separately. To measure the CO₂ efflux, soil moisture was firstly adjusted to 70% of WHC (i.e. 59% of dry weight for living and dying root mats; 33% of dry weight for dead root mat) for all soil cores at the beginning of the photosynthetic period. Distilled water was added homogeneously on the surface using a syringe. Vials with 3 ml 1.0 M NaOH solution were placed into the incubation box to trap CO₂. NaOH solution was exchanged before the start of the night period. Net ecosystem production (difference between gross primary production and ecosystem respiration) was measured with simulated solar radiation during daytime. Only ecosystem respiration was investigated during nighttime. The leaching was examined on the day following CO₂ measurement. Soil moisture of each sample was slowly adjusted to 100% of WHC (i.e. 84% of dry weight for living and dying root mats; 47% of dry weight for dead root mat). Distilled water (11 ml) was then added to each incubation box with a syringe to simulate increasing precipitation. The amount corresponded to 5 mm precipitation and reflected strong rainfall events, which occurred several times on the study sites (Ingrisch *et al.*, 2015). The leachates were collected at the outlet of the incubation box (Fig. 1,

left). After taking the leachate samples, the cover of the incubation box was opened again for ensuring photosynthesis. This two-day collection of CO₂ efflux and leachate was repeated weekly and lasted in total nine weeks.

The second experiment focused on the effect of soil moisture on nighttime CO₂ efflux. Soil moisture was regulated to two levels of WHC: 100% (at Day 11) and 70% of WHC (at Day 15 and 17) as above. Nighttime CO₂ efflux was measured every two days. Vials with 3 ml 1.0 M NaOH solution were placed into the incubation box to trap CO₂. This second experiment included living and dead root mats and lasted for 17 days.

To measure CO₂ efflux, 1 ml of the NaOH trap solution was titrated against 0.1 M HCl solution. Leachate was passed through filter paper (0.45 µm) and analyzed for total carbon (TC), total nitrogen (TN) and dissolved inorganic carbon (DIC) using a multi N/C 2100s analyzer (Analytik Jena Inc, Germany). Dissolved inorganic nitrogen (DIN: NH₄⁺ and NO₃⁻) was measured using Cenco (Dual Tubingpump, Instrumenten B.V., Breda the Netherlands). Dissolved organic carbon (DOC) and organic nitrogen (DON) were calculated by subtracting DIC and DIN from TC and TN. Microbial biomass carbon (MBC) and nitrogen (MBN) were determined by the fumigation-extraction method (Brookes *et al.*, 1985; Vance *et al.*, 1987). SOC contents in soils were also separately determined after the incubation using the elemental analyzer (Vario Max CN, Hanau, Germany).

2.3.3.4 Statistical analyses

Soil and plant properties were analyzed and expressed as means with standard errors (mean ± SE). Normality (Shapiro-Wilk-test, $p > 0.05$) and homogeneity of variance (Levene-test, $p > 0.05$) were examined. The significance was tested at $p < 0.05$ using one-way ANOVA following Tukey's HSD test for multiple comparisons. Relationship between soil moisture content and nighttime CO₂ efflux was analyzed using linear regression. The cumulative CO₂-C for all replicates during this experiment was correlated to their final SOC contents. All analyses were conducted using STATISTICA 10.0 (StatSoft Inc.).

Table 1 Distribution of carbon and nitrogen in pools of soil, root and microbial biomass

Root mats	Soil		Root		MBC (mg C g ⁻¹ dry soil)	MBN (mg N g ⁻¹ dry soil)
	N (%)	C (%)	C/N Ratio	C (%)		
Living	0.52 ± 0.01 a	6.2 ± 0.3 a	11 ± 0.3 a	0.74 ± 0.0 a	1.2 ± 0.1 b	0.12 ± 0.02 a
Dying	0.37 ± 0.03 b	3.4 ± 0.4 b	9.1 ± 0.1 b	0.83 ± 0.1 a	1.6 ± 0.1 a	0.23 ± 0.03 a
Dead	0.37 ± 0.03 b	3.4 ± 0.4 b	9.1 ± 0.1 b	0.83 ± 0.1 a	0.86 ± 0.1 b	0.18 ± 0.03 a

Values with the same letters among root mats are not significantly different at the $p < 0.05$ level (determined by a Tukey's HSD test). "Living", "Dying" and "Dead" represent living, dying and dead *Kobresia* root mats, respectively. As living and dying root mats were taken from the same plot, initial C and N composition was considered to be similar.

2.3.4 Results

2.3.4.1 Plant and soil characteristics

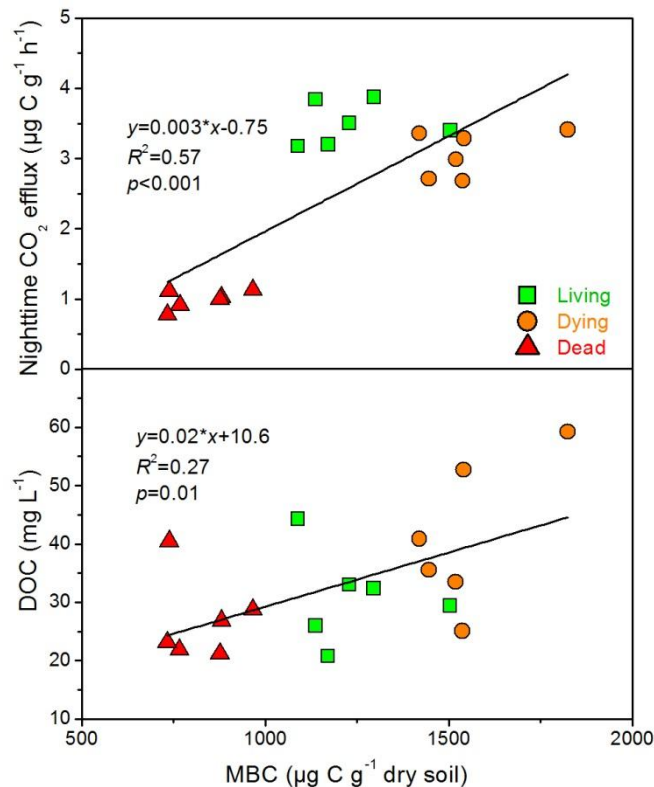


Figure 2 Relations between microbial biomass carbon (MBC) and nighttime CO₂ efflux (top) and DOC concentration in the leachate (bottom) at Day 114. "Living" = living root mat; "Dying" = dying root mat; "Dead" = dead root mat.

Carbon and N contents in soils of living and dying root mats were approximately 1.8 and 1.4 times higher than those of dead root mat, while the C and N content of the root biomass did not differ significantly from each other (Table 1). After the incubation, the MBC content of dying root mat was roughly twice that of dead root mat. MBC was positively correlated with nighttime CO₂ efflux and DOC concentration in the leachate (Fig. 2). Living root mat had an average aboveground biomass of $215 \pm 2.2 \text{ g m}^{-2}$.

2.3.4.2 CO₂ efflux related to degradation stages of *Kobresia* pastures

The hypothesis of the highest C loss from dead root mats was confirmed considering the nighttime CO₂ efflux. It was roughly 1.2 and 3.1 times higher compared to living and dead root mats,

respectively (Fig. 3, top). Nighttime CO₂ efflux of dying root mat was stable over time, whereas it increased for living root mat until the fifth week and then remained stable. After the fifth week the nighttime CO₂ efflux did not differ significantly from that of dying root mat. The cumulative CO₂-C for all replicates during this experiment was positively related to their final SOC contents (Fig. 4, $p < 0.05$).

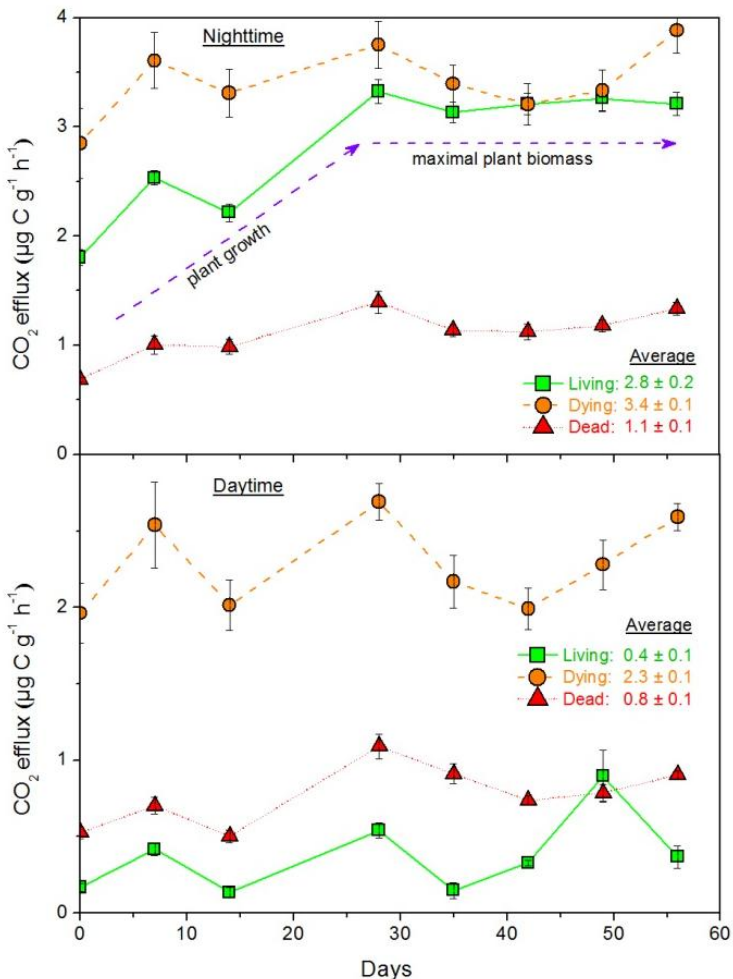


Figure 3 Nighttime (top) and daytime (bottom) CO₂ efflux of three *Kobresia* root mat types. "Living" = living root mat; "Dying" = dying root mat; "Dead" = dead root mat. Error bars represent standard error (n=6).

Daytime CO₂ efflux of living root mat was the lowest (Fig. 3, bottom), confirming our second hypothesis about the strong CO₂ assimilation by living *Kobresia*. The average daytime CO₂ efflux of living root mat was even 6 and 2 times lower than dying and dead root mats, respectively. The trend of daytime CO₂ efflux for the three root mat types was stable during the two months.

Overall, the dying of *K. pygmaea* induced the significantly highest CO₂-C losses, whereas the presence of living *K. pygmaea*, in reverse, showed a strong CO₂-C uptake by photosynthesis.

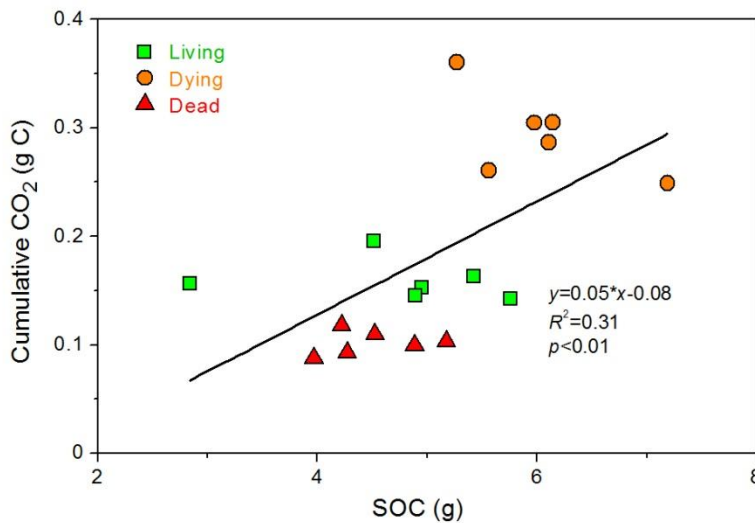


Figure 4 Correlation between cumulative CO₂-C for all replicates and their final soil organic carbon (SOC) contents. “Living” = living root mat; “Dying” = dying root mat; “Dead” = dead root mat.

2.1.4.3 Effects of soil moisture on nighttime CO₂ efflux

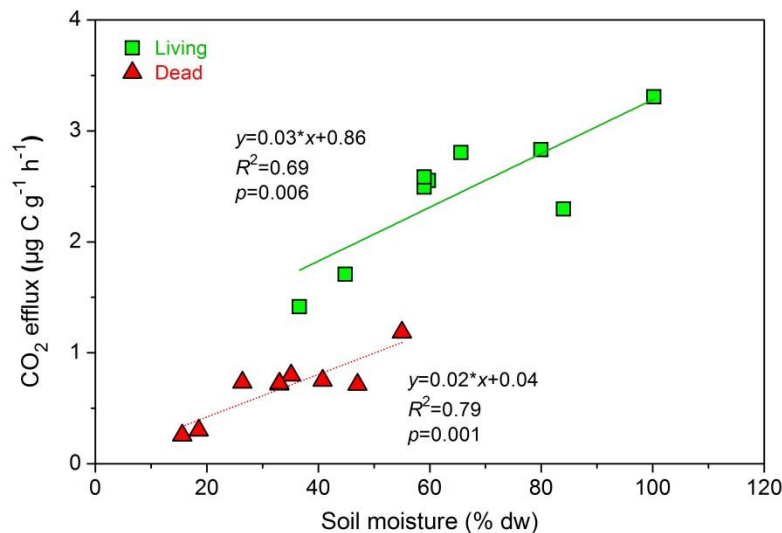


Figure 5 Correlation between soil moisture content (% dw) and nighttime CO₂ efflux during the second experiment. “Living” = living root mat; “Dead” = dead root mat.

A strong positive relation between nighttime CO₂ efflux and soil moisture was obtained for living and dead root mats considering the total duration of the second experiment (Fig. 5, $p=0.001$). This confirmed our third hypothesis. Moreover, nighttime CO₂ efflux was the higher under the increased soil moisture level (70% vs 100% WHC) for living and dead root mats (Fig. 6). Soil moisture of living root mat was also higher than dead

root mat. After the first rewetting at Day 11, CO₂ efflux of living and dead root mats increased. The CO₂ efflux of living root mat continued to increase from Day 11 to Day 13 ($p=0.04$), although soil moisture decreased.

2.3.4.4 Leaching of C and N related to degradation stages of *Kobresia pastures*

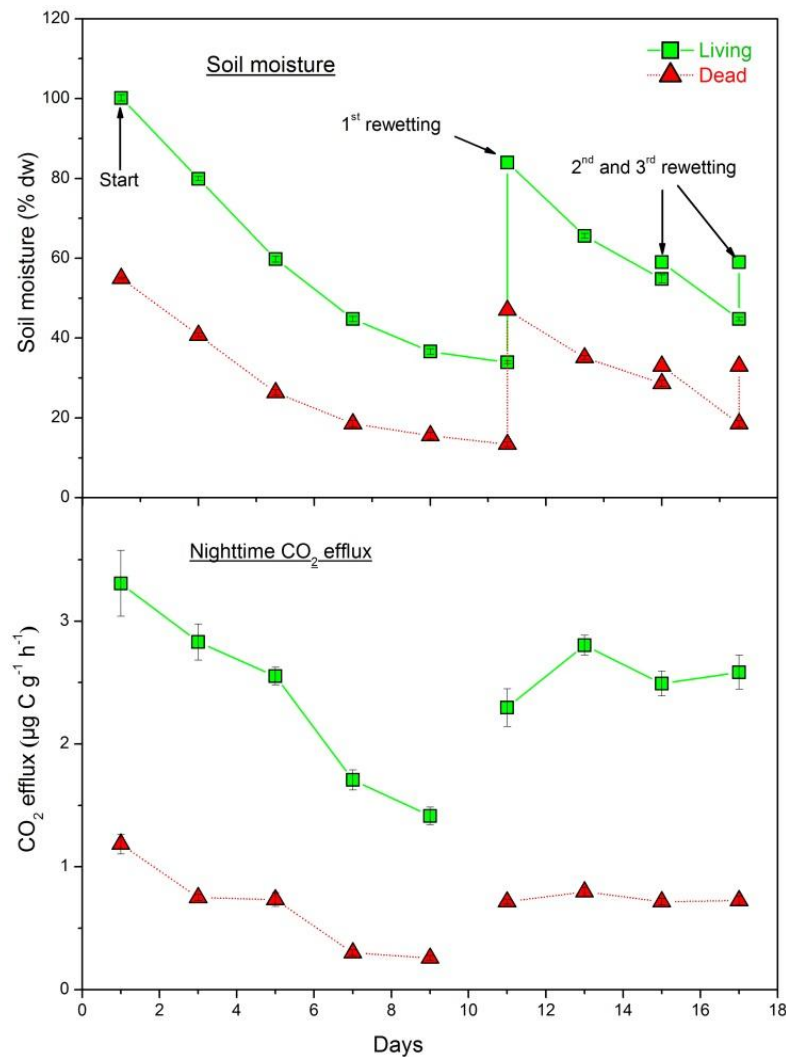


Figure 6 Change of soil moisture content (top) and response of nighttime CO₂ efflux (bottom) in living and dead root mats to increased moisture. “Living” = living root mat; “Dying” = dying root mat; “Dead” = dead root mat. Soil moisture content is expressed as percent of dry weight (% dw). When the experiment started, samples were over-saturated. For the 1st rewetting, samples from living and dead root mats were rewetted to 84 and 47 % dw, which correspond to 100% of WHC. For the 2nd and 3rd rewetting, their moisture were adjusted to 59 and 33 % dw, which correspond to 70% of WHC. Error bars represent standard error (n=6).

The dying root mat had the highest DOC and DON concentrations in leachates compared to living and dead root mats (Fig. 7, top and middle). This was consistent with our first hypothesis. However, the NO₃⁻ concentration was highest from the dead root mat compared to the living and dying stages (Fig. 7, bottom). It strongly decreased over time but was significant higher throughout the experiment. The nitrate concentration from the dying root mat was slightly higher than that of the living stage at the beginning

and decreased to zero within the first 14 days. In contrast, no nitrate was leached from the living stage (Fig. 7, bottom). The ammonium concentrations in leachates were very low (below the detection limit) for all three root mats. As we hypothesized, dying of *K. pygmaea* resulted in the highest DOM losses from the leaching; unexpectedly, dead root mat showed the highest nitrate loss from leaching.

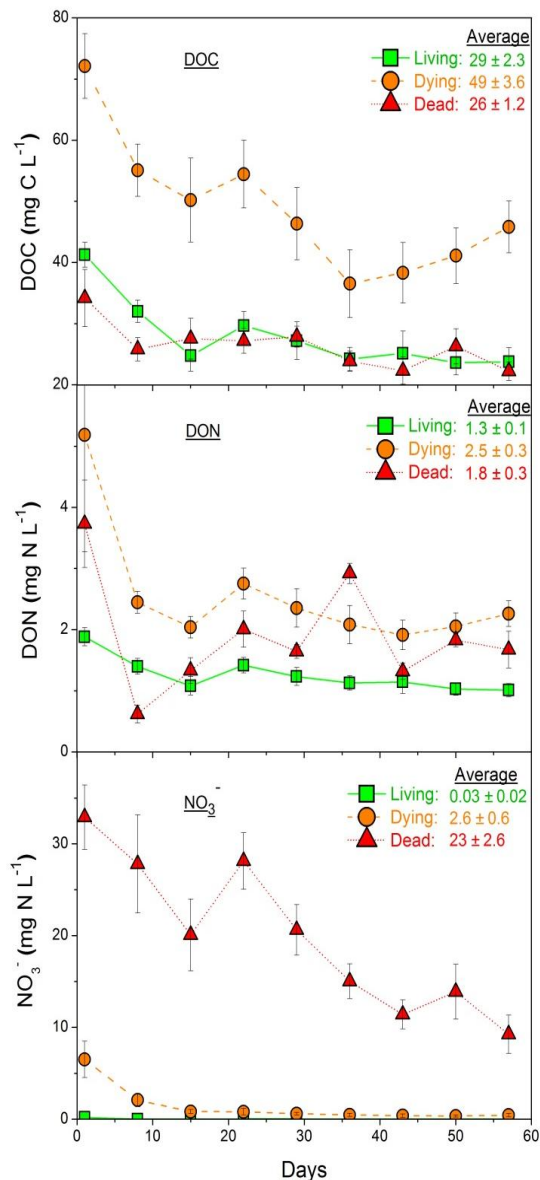


Figure 7 Concentrations of DOC (top), DON (middle) and NO₃⁻ (bottom) in the leachate of three *Kobresia* root mat types during the leaching experiment. “Living” = living root mat; “Dying” = dying root mat; “Dead” = dead root mat. Error bars represent standard error (n=6).

2.3.5 Discussion

2.3.5.1 C loss from soil respiration

The nighttime CO₂ efflux was highest from the dying, slightly lower from living and lowest from dead *Kobresia* root mat throughout the incubation period. In fact, the dead root mat had the lowest SOC content and consequently a lower C availability explaining the lower soil respiration rates. In contrast, the SOC contents were up to 1.8 times higher for living and dying root mats (Table 1), indicating that the higher C-availability stimulated microbial respiration (Cleveland *et al.*, 2007). This finding was supported by a positive correlation of cumulative CO₂-C for all degradation stages and their SOC contents (Fig. 4). The positive relation between MBC and nighttime CO₂ efflux also supported this finding (Fig. 2, top).

The CO₂ efflux was slightly higher for the dying versus living root mat. This was especially pronounced in the first four weeks. We suggest that an additional supply of root litter following plant death was respired and slightly increased the CO₂ efflux to a constantly high level. However, the absence of living root biomass in the dying stage may have eliminated the competition between uptake by *K. pygmaea* and microbes for limited nutrients (i.e. nitrogen, Kuzyakov, 2002; Xu *et al.*, 2006). Therefore, the higher SOC and nutrient availability in dying root mat stimulated microbial growth and then increased heterotrophic respiration. In agreement with this, the highest microbial biomass C was detected for dying stage (Table 1).

Nighttime CO₂ efflux from living root mat increased within the first four weeks due to the gradual growth of plant biomass. Respiration by living roots and shoots as well as microbial decomposition of root exudates contributed to a higher CO₂ efflux (Lehmeier *et al.*, 2008; Wild *et al.*, 2014). We argue that the release of exudates from living root biomass stimulated the microorganisms to decompose additional SOC (“priming effect”, de Graaff *et al.*, 2014). However, after reaching the maximal shoot biomass the root respiration and the input of rhizodeposition remained stable (ca. 30 days, Peng *et al.*, 2010). This is because root exudation strongly depends on the photosynthetic assimilation during net primary production (Aulakh *et al.*, 2001). Thus a constant input of root exudates explains the stable CO₂ efflux after Day 28.

2.3.5.2 Effects of photosynthesis on CO₂ losses

To consider for the photosynthetic C input with regard to SOC loss, we included daytime CO₂ efflux measurements and hypothesized that living root mat strongly mitigated C loss from *Kobresia* pastures. Daytime CO₂ efflux of living root mat was 6 times lower than that of dying stage due to CO₂ assimilation via photosynthesis. It mitigated the C loss from soil respiration compared to the dying and dead stages but didn't totally prevented the switch from being a C sink to becoming C source. This is inconsistent with several other studies, demonstrating that alpine grasslands are considered to be C sinks due to the photosynthetic CO₂ fixation during the growing season (Ingrisch *et al.*, 2015; Peng *et al.*, 2014). We suggest that the increased soil moisture and the constant high temperature (20°C in this study) stimulated soil respiration. In fact we found that

the nighttime CO₂ efflux increased during plant growth within the first four weeks, whereas the daytime CO₂ efflux remained on a constant low level for the living stage (Fig. 3). It demonstrates that the increasing CO₂ uptake during plant growth was offset by a higher CO₂ release from soil respiration (Suter *et al.*, 2002).

2.3.5.3 Soil respiration as influenced by soil moisture

The effect of changing soil moisture on soil respiration (nighttime CO₂ efflux) for living and dead root mats was tested in the second experiment. Soil moisture was positively correlated with nighttime CO₂ efflux for living and dead root mats, indicating that increasing moisture enhanced SOC decomposition. Therefore, the expected increase of precipitation on the Tibetan Plateau (Xu *et al.*, 2008) is assumed to trigger additionally C and N losses from *Kobresia* pastures. This implies that the intact *Kobresia* pastures are at risk to become a C source by increasing precipitation rates, which accelerates the pasture degradation (Babel *et al.*, 2014).

Degradation from living to dead root mat is accompanied with a decrease of the plant biomass (especially the root biomass: 4.2 kg m⁻² for living and 2.5 g m⁻² for dead root mat). Consequently it enhances the soil bulk density in this root-dominated soil after root turnover, which thereby decreased the WHC (Wang *et al.*, 2003). Therefore, lower soil moisture was observed for the dead root mat when we adjusted soil moisture to 100% of WHC (Fig. 6, top).

Surprisingly, nighttime CO₂ efflux from living root mat continued to increase between Day 11 and Day 13, although soil moisture already decreased. This can be explained by the time lag for transporting photosynthetic assimilates from shoots to roots (Hill *et al.*, 2007). This time lag delayed the stimulation of root exudates to soil respiration and ultimately caused a delayed response of nighttime CO₂ efflux. This lag was longer than that for most other grassland ecosystems (Kuzyakov & Gavrichkova, 2010).

When soil moisture was kept at around 100% dw on the first day, nighttime CO₂ efflux remained at a relatively high level for living and dead root mats (Fig. 6). This contrasted to some studies showing that SOC decomposition and CO₂ production decreased under a high soil moisture level because oxygen diffusion into the soil was inhibited (Ganjurjav

et al., 2014; Tang *et al.*, 2006). The *Kobresia* root mats, however, have very low bulk density (around 0.8 g cm^{-3} for living and dead root mats, 1.1 g cm^{-3} for dead root mat) and with a large pore system so that O_2 diffusion was not hindered in our study.

2.3.5.4 C and N loss from leaching

DOM leaching was highest from dying root mats compared to living and dead root mats. This confirmed our hypothesis regarding highest C and N losses from dying root mat via leaching. We suggest that the strong decomposition of insoluble organic matter, especially of dying root mat, resulted in an enrichment of low and high weight molecular substances. Low molecular weight components of DOM will be very rapidly taken up or respired by microorganisms (Fischer *et al.*, 2010), whereas the high molecular weight pool with much lower turnover rates becomes the major source for DOM (Jones *et al.*, 2004). This explained why the dying stage showed far higher DOC losses (Fig. 2, bottom).

The highest NO_3^- losses were observed from dead root mat. This partly contradicted our first hypothesis about the highest N loss from dying root mat. We suggest that nitrate accumulated in the dead root mat during long-term decomposition in the field and later was leached by water amendments. To a minor contribution, it is also possible that N_2 fixation by lichen-dominated crusts increased the N transfer into soil (Neff *et al.*, 2005). The leaching of NO_3^- from living root mat was always close to zero and only slightly higher for dying root mat in the first few days. It indicated that active N uptake by living plants significantly decreased the NO_3^- concentration in the soil during plant growth (Wirén *et al.*, 1997; Xu *et al.*, 2011). We argue that the NO_3^- released from mineralization of organic carbon was rapidly immobilized by microorganisms before and after transformation to nitrate or ammonium. The decreasing C/N ratio in the microbial biomass from the living ($\text{C/N}_{\text{Living}}$: 9.4), dying ($\text{C/N}_{\text{Dying}}$: 7.3) and dead stage (C/N_{Dead} : 4.9) also supported this finding. The C/N ratio of the microbial biomass in the living stage was 1.3 and 1.9 than that of the dying and dead stage, respectively. It clearly reflects that N gets limited for microorganisms in the presence of living plants.

There was no ammonium leaching for any root mat type during the two months. The growing plants in the living stage took up NH_4^+ and thus prevented ammonium from

being leached. Since the *Kobresia* root mats are well aerated and nitrifying bacteria are abundant in the upper soil compared with that in subsoil (Guan *et al.*, 2013), NH_4^+ will be immediately converted to NO_3^- and then NO_3^- will be taken up by plants or will be leached.

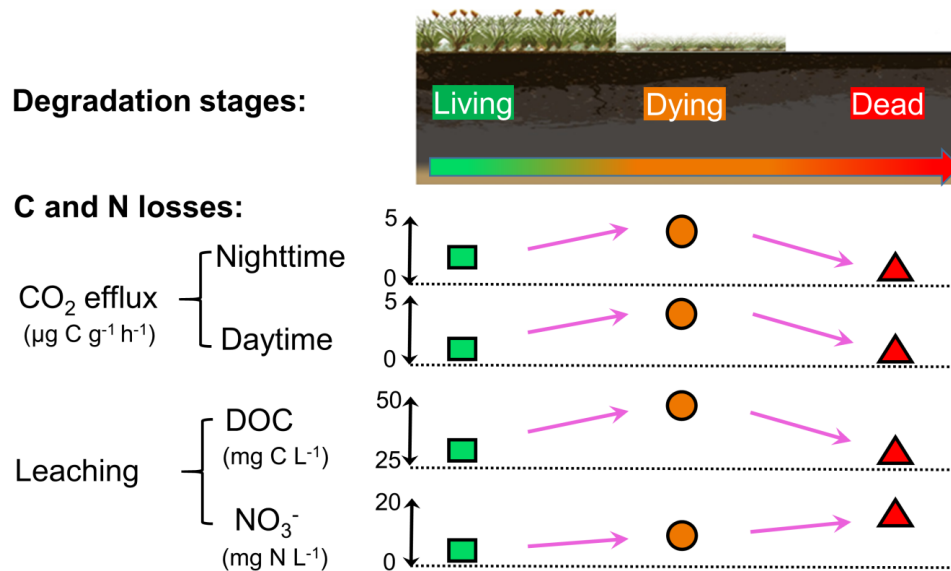


Figure 8 Conceptual diagram of C and N loss from *K. pygmaea* pastures depending on degradation stages. C loss as CO₂ emission and leaching was highest in dying root mat. This is mainly caused by the high initial root litter inputs after plant dying and the elimination of competition between plant and microbes for nutrient acquisition. N loss from the leaching of dead root mat was the highest compared with other root mats. We argued that nitrate accumulated in the dead root mat during long-term decomposition in the field and later was leached by water amendments. “Living” = living root mat; “Dying” = dying root mat; “Dead” = dead root mat.

2.3.6 Conclusions

The dying root mat showed the highest C losses (Fig. 8) from: (a) decomposition of SOC and roots (CO₂ efflux) and (b) leaching of DOM. The dying of *K. pygmaea* provided more labile organic matter to microorganisms due to the high initial root litter inputs after plant dying. It indicated that the initial dying of *K. pygmaea* will rapidly convert pastures into a C source. However, photosynthesis in living root mat mitigated the respiratory C losses and consequently prevents *Kobresia* pastures from becoming a C-source. Highest nitrate loss from dead root mat was mainly caused by long-term nitrate accumulation during SOC decomposition in the field and then initiated by the leaching. It demonstrates that the increasing precipitation on the TP, as predicted with climate change, will enhance N losses. Probably this induces a negative feedback

mechanism because N is often a limited nutrient in alpine grasslands. Thus any N loss reduces the potential of *Kobresia* pastures to recover from degradation.

2.3.7 Acknowledgements

This work was funded by the China Scholarship Council (CSC) and the German Research Foundation (DFG) within the Priority Programme 1372 (Project KU 1184/14-2). We are very thankful to the Volkswagen Foundation for establishing the KEMA research station and to Georg Miede for selecting the study sites. The authors disclose any potential conflict of interests.

2.3.8 References

- Aulakh MS, Wassmann R, Bueno C, Kreuzwieser J, Rennenberg H. 2001. Characterization of root exudates at different growth stages of ten rice (*Oryza sativa* L.) Cultivars. *Plant Biology* 3: 139-148. DOI:10.1055/s-2001-12905.
- Babel W, Biermann T, Coners H, Falge E. 2014. Pasture degradation modifies the water and carbon cycles of the Tibetan highlands. *Biogeosciences* 11: 8861-8923. DOI:10.5194/bg-11-6633-2014.
- Brookes PC, Landman A, Pruden G, Jenkinson DS. 1985. Chloroform fumigation and the release of soil nitrogen: A rapid direct extraction method to measure microbial biomass nitrogen in soil. *Soil Biology & Biochemistry* 17:837-842. DOI:10.1016/0038-0717(85)90144-0.
- Cleveland CC, Nemergut DR, Schmidt SK, Townsend AR. 2007. Increases in soil respiration following labile carbon additions linked to rapid shifts in soil microbial community composition. *Biogeochemistry* 82:229-240. DOI:10.1007/s10533-006-9065-z.
- De Graaff M, Jastrow JD, Gillette S, Johns A, Wulfschleger SD. 2014. Differential priming of soil carbon driven by soil depth and root impacts on carbon availability. *Soil Biology & Biochemistry* 69:147-156. DOI:10.1016/j.soilbio.2013.10.047.
- Du MY, Kawashima S, Yonemura S, Zhang XZ, Chen SB. 2004. Mutual influence between human activities and climate change in the Tibetan Plateau during recent years. *Global and Planetary Change* 41:241-249. DOI:10.1016/j.gloplacha.2004.01.010.
- Fan YZ, Zhong ZM, Zhang XZ. 2011. Determination of photosynthetic parameters $V_{C_{max}}$ and J_{max} for a C_3 plant (spring hulless barley) at two altitudes on the Tibetan Plateau. *Agricultural and Forest Meteorology* 151:1481-1487. DOI: 10.1016/j.agrformet.2011.06.004.
- FAO (Food and Agriculture Organization of the United Nations). 2010. Challenges and opportunities for carbon sequestration in grassland systems. A technical report on grassland management and climate change mitigation. *Integrated Crop Management*, Vol. 9.
- Fischer H, Ingwersen J, Kuzyakov Y. 2010. Microbial uptake of low-molecular-weight organic substances out-competes sorption in soil. *European Journal of Soil Science* 61:504-513.
- Ganjurjav H, Gao QZ, Borjigidai A, Guo YQ, Wan YF, Li Y, Jiangcun WZ, Danjiu LB. 2014. Alpine grassland ecosystem respiration variation under irrigation in Northern Tibet. *Acta Ecologica Sinica* 34:271-276. DOI:10.1016/j.chnaes.2014.07.004.
- Geng Y, Wang YH, Yang K, Wang SP, Zeng H, Baumann F, Kuehn P, Scholten T, He JS. 2012. Soil respiration in Tibetan alpine grasslands: Belowground biomass and soil moisture, but not soil temperature, best explain the large-scale patterns. *PLoS ONE* 7:e34968.
- Guan XY, Wang JF, Zhao H, Wang JJ, Luo XM, Liu F, Zhao FQ. 2013. Soil bacterial communities shaped by geochemical factors and land use in a less-explored area, Tibetan Plateau. *BMC Genomics* 14:820. DOI:10.1186/1471-2164-14-820.
- Hafner S, Unteregelsbacher S, Seeber E, Lena B, Xu XL, Li XG, Guggenberger G, Miede G, Kuzyakov Y. 2012. Effect of grazing on carbon stocks and assimilate partitioning in a Tibetan montane pasture revealed by ^{13}C pulse labeling. *Global Change Biology* 18:528-538. DOI:10.1111/j.1365-2486.2011.02557.x.
- Hansson K, Kleja DB, Kalbitz K, Larsson H. 2010. Amounts of carbon mineralized and leached as DOC during decomposition of Norway spruce needles and fine roots. *Soil Biology & Biochemistry* 42:178-185. DOI: 10.1016/j.soilbio.2009.10.013.
- He SY, Richards K. 2015. Impact of meadow degradation on soil water status and pasture management-A case study in Tibet. *Land Degradation & Development* 26:468-479. DOI:10.1002/ldr.2358.

- Hiernaux P. 1998. Effects of grazing on plant species composition and spatial distribution in rangelands of the Sahel. *Plant Ecology* 138:191–202. DOI:10.1023/A:1009752606688.
- Hill PW, Kuzyakov Y, Jones DL, Farrar J. 2007. Response of root respiration and root exudation to alterations in root C supply and demand in wheat. *Plant and Soil* 291:131–141. DOI:10.1007/s11104-006-9180-6.
- Hu GZ, Liu HY, Yin Y. 2015. The role of legumes in plant community succession of degraded grasslands in northern China. *Land Degradation & Development*, DOI: 10.1002/ldr.2382.
- Ingrisch J, Biermann T, Seeber E, Leopold T, Li MS, Ma YM, Xu XL, Miehe G, Guggenberger G, Foken T, Kuzyakov Y. 2015. Carbon pools and fluxes in a Tibetan alpine *Kobresia pygmaea* pasture partitioned by coupled eddy-covariance measurements and ¹³CO₂ pulse labeling. *Science of the Total Environment* 505:1213–1224. DOI: 10.1016/j.scitotenv.2014.10.082.
- Jones DL, Shannon D, Murphy DV, Farrar J. 2004. Role of dissolved organic nitrogen (DON) in soil N cycling in grassland soils. *Soil Biology & Biochemistry* 36:749–756. DOI:10.1016/j.soilbio.2004.01.003.
- Kassahun A, Snyman HA, Smit GN. 2009. Soil seed bank evaluation along a degradation gradient in arid rangelands of the Somali region, eastern Ethiopia. *Agriculture, Ecosystems and Environment* 129: 428–436. DOI: 10.1016/j.agee.2008.10.016.
- Klein JA, Harte J, Zhao XQ. 2004. Experimental warming causes large and rapid species loss, dampened by simulated grazing, on the Tibetan Plateau. *Ecology Letters* 7 (12): 1170–1179. DOI: 10.1111/j.1461-0248.2004.00677.x.
- Kuzyakov Y. 2002. Review: Factors affecting rhizosphere priming effects. *Journal of Plant Nutrition and Soil Science* 165:382–396. DOI:10.1002/1522-2624(200208)165:4<382::AID-JPLN382>3.0.CO;2-#.
- Kuzyakov Y, Gavrichkova O. 2010. Time lag between photosynthesis and carbon dioxide efflux from soil: a review of mechanisms and controls. *Global Change Biology* 16:3386–3406. DOI:10.1111/j.1365-2486.2010.02179.x.
- Leber D, Holawe F, Häusler H. 1995. Climatic classification of the Tibet Autonomous Region using multivariate statistical methods. *GeoJournal* 37:451–472. DOI:10.1007/BF00806934.
- Lehmeier CA, Lattanzi FA, Schäufole R, Wild M, Schnyder H. 2008. Root and shoot respiration of perennial ryegrass are supplied by the same substrate pools: assessment by dynamic ¹³C labeling and compartmental analysis of tracer kinetics. *Plant Physiology* 148:1148–1158. DOI:10.1104/pp.108.127324.
- Liu-Zeng J, Taponnier P, Gaudemer Y, Ding L. 2008. Quantifying landscape differences across the Tibetan plateau: Implications for topographic relief evolution. *Journal of Geographical Research* 113:F04018. DOI:10.1029/2007JF000897.
- Liu JG, Diamond J. 2005. China's environment in a globalizing world. *Nature* 435, 1179–1186. DOI: 10.1038/4351179a.
- Miehe G. 1988. Vegetation patterns on Mount Everest as influenced by monsoon and föhn. *Vegetatio* 79:21–32. DOI:10.1007/BF00044845.
- Miehe G, Miehe S, Bach K, Nölling J, Hanspach J, Reudenbach C, Kaiser K, Wesche K, Mosbrugger V, Yang YP, Ma YM. 2011. Plant communities of central Tibetan pastures in the Alpine Steppe/*Kobresia pygmaea* ecotone. *Journal of Arid Environments* 75:711–723. DOI:10.1016/j.jaridenv.2011.03.001.
- Miehe G, Miehe S, Kaiser K, Liu JQ, Zhao X. 2008. Status and dynamics of the *Kobresia pygmaea* ecosystem on the Tibetan Plateau. *Ambio* 37:272–279. Retrieved from: <http://www.jstor.org/stable/25547897>.
- Mukhopadhyay S, Maiti SK. 2014. Soil CO₂ flux in grassland, afforested land and reclaimed coalmine overburden dumps: A case study. *Land Degradation & Development* 25:216–227. DOI:10.1002/ldr.1161.
- Neff JC, Reynolds RL, Belnap J, Lamothe P. 2005. Multi-decadal impacts of grazing on soil physical and biogeochemical properties in southeast Utah. *Ecological Applications* 15:87–95. DOI:10.1890/04-0268.
- Novara A, Gristina L, Rühl J, Pasta S, D'Angelo G, La Mantia T, Pereira P. 2013. Grassland fire effect on soil organic carbon reservoirs in a semiarid environment. *Solid Earth* 4: 381–385. DOI: 10.5194/se-4-381-2013.
- Parras-Alcántara L, Díaz-Jaimes L, Lozano-García B. 2015. Management effects on soil organic carbon stock in Mediterranean open rangelands-treeless grasslands. *Land Degradation & Development* 26: 22–34. DOI: 10.1002/ldr.2269.
- Peng F, You QG, Xu MH, Guo J, Wang T, Xue X. 2014. Effects of warming and clipping on ecosystem carbon fluxes across two hydrologically contrasting years in an alpine meadow of the Qinghai-Tibet Plateau. *PLoS ONE* 9:e109319. DOI:10.1371/journal.pone.0109319.
- Peng HC, Han F, Wang H, Shi SB, Shen JW, Zhou DW. 2010. Characteristics of seasonal and altitude variation of UV-absorbing compounds content in three alpine plants on Qinghai-Tibet Plateau. *Acta Botanica Boreali-Occidentalia Sinica* 30:1197–1203. (in Chinese with English abstract).
- Pereira P, Ūbeda X, Mataix-Solera J, Oliva M, Novara A. 2014. Short-term changes in soil Munsell colour value, organic matter content and soil water repellency after a spring grassland fire in Lithuania. *Solid Earth* 5: 209–225. DOI: 10.5194/se-5-209-2014.
- Ren PBC, Sigernes F, Gjessing Y. 1997. Ground-based measurements of solar ultraviolet radiation in Tibet: Preliminary results. *Geophysical Research Letters* 24:1359–1362. DOI:10.1029/97GL01319.
- Schleuss PM, Heitkamp F, Sun Y, Miehe G, Xu X, Kuzyakov Y. 2015. Nitrogen uptake in an alpine *Kobresia* pasture on the Tibetan Plateau: localization by ¹⁵N labeling and implications for a vulnerable ecosystem. *Ecosystems* 18: 946–957. DOI:10.1007/s10021-015-9874-9.

- Scurlock JMO, Hall DO. 1998. The global carbon sink: a grassland perspective. *Global Change Biology* 4:229–233. DOI:10.1046/j.1365-2486.1998.00151.x.
- Shao W, Cai XB. 2008. Grassland degradation and its formation causes analysis in Tibetan plateau. *Science of Soil and Water Conservation* 1, 021.
- Suter D, Frehner M, Fischer BU, Nösberger J, Lüscher A. 2002. Elevated CO₂ increases carbon allocation to the roots of *Lolium perenne* under free-air CO₂ enrichment but not in a controlled environment. *New Phytologist* 154:65–75. Retrieved from: <http://www.jstor.org/stable/1513933>.
- Tang XL, Zhou GY, Liu SG, Zhang DQ, Liu SZ, Li J, Zhou CY. 2006. Dependence of soil respiration on soil temperature and soil moisture in successional forests in southern China. *Journal of Integrative Plant Biology* 48:654–663. DOI:10.1111/j.1744-7909.2006.00263.x.
- Thompson LG, Yao T, Davis ME, Henderson KA, Mosley-Thompson E, Lin PN, Beer J, Synal HA, Cole-Dai J, Bolzan JF. 1997. Tropical climate instability: The last glacial cycle from a Qinghai-Tibetan ice core. *Science* 276:1821–1825. DOI:10.1126/science.276.5320.1821.
- Vance ED, Brookes PC, Jenkinson DS. 1987. An extraction method for measuring soil microbial biomass C. *Soil Biology & Biochemistry* 19:703–707. DOI:10.1016/0038-0717(87)90052-6.
- Wang GX, Cheng GD, Shen YP, Qian J. 2003. Influence of land cover changes on the physical and chemical properties of alpine meadow soil. *Chinese Science Bulletin* 48:118–124. DOI:10.1007/BF03037014.
- Wang GX, Qian J, Cheng GD, Lai YM. 2002. Soil organic carbon pool of grassland soils on the Qinghai-Tibetan Plateau and its global implication. *Science of The Total Environment* 291:207–217. DOI:10.1016/S0048-9697(01)01100-7.
- Wang J, Wang Z, Zhang X, Zhang Y, Ran C, Zhang J, Chen B, Zhang B. 2015. Response of *Kobresia pygmaea* and *Stipa purpurea* grassland communities in northern Tibet to nitrogen and phosphate addition. *Mountain Research and Development* 35:78–86. DOI:10.1659/MRD-JOURNAL-D-11-00104.1.
- Wang XX, Dong SK, Sherman R, Liu QR, Liu SL, Li YY, Wu Y. 2015. A comparison of biodiversity-ecosystem function relationships in alpine grasslands across a degradation gradient on the Qinghai-Tibetan Plateau. *The Rangeland Journal* 37: 45-55. DOI: 10.1071/RJ14081.
- Wei XH, Yang P, Li S, Chen HS. 2004. Effects of over-grazing on vegetation degradation of the *Kobresia pygmaea* meadow and determination of degenerative index in the Naqu Prefecture of Tibet. *Acta Prataculturae Sinica* 14:41–49.
- Wild B, Schnecker J, Alves RJE, Barsukov P, Bárta J, Čapek P, Gentsch N, Gittel A, Guggenberger G, Lashchinskiy N, Mikutta R, Rusalimova O, Santrůčková H, Shibistova O, Urich T, Watzka M, Zrazhevskaya G, Richter A. 2014. Input of easily available organic C and N stimulates microbial decomposition of soil organic matter in arctic permafrost soil. *Soil Biology & Biochemistry* 75:143–151. DOI:10.1016/j.soilbio.2014.04.014.
- Wirén N, von Gazzarrini S, Frommer WB. 1997. Regulation of mineral nitrogen uptake in plants. *Plant and Soil* 196:191–199. DOI:10.1023/A:1004241722172.
- WRB. 2014. World Reference Base for Soil Resources. FAO, World Soil Resources Reports 106, Rome.
- Xu XL, Ouyang H, Kuzyakov Y, Richter A, Wanek W. 2006. Significance of organic nitrogen acquisition for dominant plant species in an alpine meadow on the Tibet plateau, China. *Plant Soil* 285: 221-231. DOI: 10.1007/s11104-006-9007-5.
- Xu XL, Ouyang H, Richter A, Wanek W, Cao GM, Kuzyakov Y. 2011. Spatio-temporal variations determine plant-microbe competition for inorganic nitrogen in an alpine meadow. *Journal of Ecology* 99: 563-571. DOI: 10.1111/j.1365-2745.2010.01789.x.
- Xu ZX, Gong TL, Li JY. 2008. Decadal trend of climate in the Tibetan Plateau-regional temperature and precipitation. *Hydrological Processes* 22:3056–3065. DOI:10.1002/hyp.6892.
- Yang MX, Nelson FE, Shiklomanov NI, Guo DL, Wang GN. 2010. Permafrost degradation and its environmental effects on the Tibetan Plateau: A review of recent research. *Earth-Science Reviews* 103(1-2): 31-44. DOI: 10.1016/j.earscirev.2010.07.002.
- Yao ZY, Zhao CY, Yang KS, Liu WC, Li Y, You JD, Xiao JH. 2016. Alpine grassland degradation in the Qilian Mountains, China-A case study in Damaying Grassland. *Catena* 137: 494-500. DOI: 10.1016/j.catena.2015.09.021.
- Zhang XL, Wang SJ, Zhang JM, Wang G, Tang XY. 2015. Temporal and spatial variability in precipitation trends in the Southeast Tibetan Plateau during 1961–2012. *Climate of the Past Discussions* 11:447–487. DOI: 10.5194/cpd-11-447-2015.

2.4 Study 4: Responses of degraded Tibetan *Kobresia* pastures to N addition

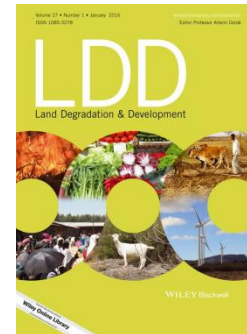
Shibin Liu^{a*}, Per-Marten Schleuss^a, Yakov Kuzyakov^{a,b,c}

Status: Published online on *Land Degradation & Development*

^a Department of Soil Science of Temperate Ecosystem, University of Göttingen, Büsgenweg 2, 37077 Göttingen, Germany

^b Department of Agricultural Soil Science, University of Göttingen, Büsgenweg 2, 37077 Göttingen, Germany

^c Institute of Environmental Sciences, Kazan Federal University, 420049 Kazan, Russia



2.4.1 Abstract

Kobresia pastures on Tibetan Plateau are the largest alpine pastoral ecosystems. *K.* pastures have experienced severe degradation in recent decades, inducing large nitrogen (N) losses from these ecosystems. This is particularly problematic, as it intensifies prevailing N limitation in these regions. Simultaneously, anthropogenic N deposition has increased across these ecosystems, but the fate of added N on variously-degraded *K.* pastures remains unclear. *K.* pastures of three degradation stages were investigated: living-, dying- and dead root mats. High and very low (as a tracer) amounts of ¹⁵N-labelled ammonium nitrate (NH₄NO₃) were applied to root mats under controlled conditions. Leaching was simulated over 3 months and ¹⁵N recovery was measured in the plant-soil system. N addition promoted aboveground biomass and foliar N content of *Kobresia* during the early growth period, indicating a short-term offset of N limitation. After 7-8 weeks, plant growth and ¹⁵N uptake were reduced in plants with initial N-addition, reflecting a transition to N limitation induced by N uptake and leaching from soil. This limitation was also indicated by the strong decline of NO₃⁻ in leachates from living root mats compared to degraded root mats. Leaching N losses from dying and dead root mats increased 2.2 and 6.3 times, respectively, compared to those of living root mats. We conclude that N addition can facilitate plant growth in living root mats, but contributes to N leaching in degraded pastures. This contribution to N leaching may weaken ecosystem recovery, increase NO₃⁻ loading of adjacent lower landscape parts and eutrophicate aquatic ecosystems.

Key words: Pasture degradation, N loss, Tibetan Plateau, ¹⁵N labeling, NO₃⁻ leaching

Corresponding Author: Shibin Liu, sliu3@gwdg.de

2.4.2 Introduction

The *Kobresia* pastures of the Tibetan Plateau cover approximately 45 million ha and are the world's largest alpine pastoral ecosystems. These ecosystems are the source region for the largest rivers in southeastern Asia and are mainly dominated by *Kobresia pygmaea* C.B. Clarke (*K. pygmaea*) (Miehe *et al.*, 2008a; Zhou *et al.*, 2005). *K.* pastures store vast amounts of soil organic carbon (SOC) and nutrients (nitrogen (N), phosphorus), while providing important grazing grounds for native fauna and cattle (Unteregelsbacher *et al.*, 2012; Yang *et al.*, 2009).

However, *K.* pastures have experienced severe degradation in recent decades. In this study, degradation is defined as a deterioration of plant and soil characteristics (including decreasing vegetation cover, variations in species composition, as well as changes in physical and chemical soil characteristics) due to harsh environmental conditions and improper management. The primary drivers of degradation can be summarized as anthropogenic factors (e.g. deforestation, overgrazing and infrastructure construction) and/or environmental factors (e.g. permafrost degradation and climate change) (Harris, 2010; Wang *et al.*, 2015a). Ongoing pasture degradation has initiated high losses of carbon (C) and N via erosion, soil organic matter mineralization and leaching (Wang *et al.*, 2009b; Feng *et al.*, 2009; He & Richards, 2015). Degradation also causes plant death (i.e. reduces vegetation cover and above- and belowground biomass) and impairs grassland recovery (Wang *et al.*, 2013; Zhang *et al.*, 1998; Wang *et al.*, 2009a). This has put the large human population of the Tibetan Plateau at risk regarding their livelihoods and food security (O'Mara, 2012).

Nitrogen is a limited nutrient in most terrestrial ecosystems (Lebauer & Treseder, 2008; Menge *et al.*, 2012). This is particularly true for the degraded *Kobresia* grasslands, where low temperature and precipitation hamper N fixation as well as mineralization of soil organic matter and therefore nutrient release (Shi *et al.*, 2012; Vitousek & Howarth, 1991). Nitrogen fertilization has been proposed to improve degraded *K.* pastures by mitigating N limitation (Dong *et al.*, 2013). The suggested fertilization rates range from 10-150 kg N ha⁻¹ yr⁻¹ and have been observed to facilitate plant growth (Li *et al.*, 2014;

Zong *et al.*, 2014; Jiang *et al.*, 2015). Atmospheric N deposition on the Tibetan Plateau has also increased since the mid-20th century (Thompson *et al.*, 2000; Kang *et al.*, 2002), with total N deposition rates recently reaching 3.43 kg N ha⁻¹ yr⁻¹ in rural areas of the Qinghai-Tibetan plateau (Xu *et al.*, 2015b). Lü & Tian (2007) estimated that the total N deposition rate ranges from 7.0 to 7.5 kg N ha⁻¹ yr⁻¹ across the whole Tibetan Plateau. These alterations in atmospheric N deposition likely result from changes in annual mean ambient N₂O concentrations, which increased 79%-124% in southern Tibet from 1994 to 2003 (Lü & Tian, 2007) and will continue to increase in the near future (Kanakidou *et al.*, 2016). However, the impact of increasing N addition (from either N deposition or fertilization) on degraded pastures remains unknown. In contrast to the aforementioned benefits, higher N additions may pose environmental risks by enhancing N leaching, which could pollute these ecosystems and the surrounding headwaters of the Tibetan Plateau that supply billions of people with clean water in southeastern Asia (Pomeranz *et al.*, 2013).

To clarify the impact of increasing N addition, previous studies focused on various aspects of *K. pygmaea* pastures (e.g. plant biomass, plant species richness, plant community stability and soil microbial activities etc.) (Wang *et al.*, 2015b; Fang *et al.*, 2014; Song *et al.*, 2012; Song *et al.*, 2015). The fate of added N in *K.* pasture ecosystems was also investigated using a ¹⁵N-labelling technique (Xu *et al.*, 2003 & 2004). A recent study determined the ¹⁵N recovery in soil and plant of non-crust and crust patches of *K.* pastures, in which the crust patches were considered to be degraded (Zhang *et al.*, 2016). They observed lower total recovery from inorganic N but higher from organic N in crust patches, concluding that crusts changed the fate of added N. However, these ¹⁵N-labelling studies only added very low levels of N as a tracer and did not consider the impact of increasing N addition (from increasing N deposition or fertilizer inputs to reverse degradation) on the fate of N in intact and degraded *K.* pastures.

We investigated the effects of increasing N addition using three types of *Kobresia pygmaea* root mats with increasing degradation: (a) living root mats, (b) dying root mats and (c) dead root mats. Living root mats were sampled from intact *K.* pastures (covering

approximately 65% of the study site, Babel *et al.*, 2014). Dying root mats—from plants which were alive during sampling but died during transport—represent the transition between living and dead root mats. Consequently, they reflect the initial stage of root mat degradation. Dead root mats were sampled from degraded *K. pastures* in the field, covering approximately 16 % of the study area (Babel *et al.*, 2014). For the dead root mats the exact time of initial degradation is unknown, but presumably it is in the range of years to decades. Consequently, soil characteristics of dead root mats were substantially different compared with the living and dying root mats. NH_4NO_3 was added to evaluate the effects of increasing N addition on *K. pygmaea* growth as well as on N cycling. The ^{15}N labelling technique was utilized to quantify N partitioning among different pools (soil, microbial biomass, above- and belowground biomass, and root litter). Leaching was simulated to determine losses of dissolved N (organic N, NH_4^+ and NO_3^-) and organic C from soil. We hypothesize that N addition increases *Kobresia* biomass (above- and belowground) and its foliar N stock in the living root mats because the *Kobresia* pastures are N limited and extra N promotes plant growth (H1). Furthermore, we hypothesize that degraded root mats (dying and dead root mats) are less capable of retaining N due to the absence of the N uptake by living plants, indicating that N addition of degraded pastures will result in higher levels of N leaching rather than ecosystem improvement (H2). Finally, total N stocks were hypothesized to be significantly lower in the degraded stages compared to the intact stage, due to higher N losses from leaching and N_2O emissions with degradation (H3).

2.4.3 Materials and Methods

2.4.3.1 Sampling site and soils

The sampling site was located at the research station “*Kobresia* Ecosystem Monitoring Area” (KEMA) (31°16'45"N 92°59'37"E, 4410 m a.s.l.) close to the village Kema, near Nagqu, Tibetan Autonomous Region (TAR). The region is described as “Plateau Frigid Monsoon Region with semi-moist climate” (Leber *et al.*, 1995). Mean annual precipitation and temperature are 430 mm and -1.2 °C, respectively. The site is located in the core area of *K. pygmaea* distribution, and *K. pygmaea* is the dominant plant species with an average height of no more than 2 cm (Miehe *et al.*, 2008a). The other

species are *Carex* spp., *Festuca* spp., *Kobresia humilis*, *Poa* spp., *Stipa purpurea* and *Trisetum* spp. (Seeber *et al.*, 2015). The growing season of *K. pygmaea* pastures mainly depends on the summer monsoon and ranges from May to October (Miehe *et al.*, 1989). Soils contain 50% sand, 33% silt and 17% clay and are categorized as *Stagnic Eutric Cambisol (Humic)* (WRB, 2014). No carbonates were found in the soils and their pH (H₂O) was 6.85. The topsoil (0-5 cm) contains large amount of living and dead roots which form a very dense root mat (Miehe *et al.*, 2008b; Schleuss *et al.*, 2015). Intact living *Kobresia* root mats cover 65% of the area, while dead *Kobresia* root mats occupy 16% of the area. The remaining part is covered by completely degraded bare soil patches (19%), which are entirely devoid of the dense *Kobresia pygmaea* turf (Babel *et al.*, 2014). Bare soil degradation was not considered during this experiment.

2.4.3.2 Sampling, preparation and experimental set-up

Undisturbed soil cores (height: 5.0 cm, diameter: 5.0 cm) were collected in August, 2012 from intact living and dead *Kobresia pygmaea* root mats. Shoot biomass was removed from the surface prior to transport. Sub-samples from each root mat (n=6) were collected to measure the water holding capacity (WHC). All samples were put in PVC collars (height: 5.0 cm, diameter: 5.0 cm) and transferred to the laboratory.

Before beginning the experiment, samples of living and dead root mats were pre-incubated for two months to enable *K. pygmaea* to recover and reach maximum biomass. In some samples of the living root mats, however, the *K. pygmaea* did not recover. These samples were considered as an additional treatment “dying root mats.” A total of three root mats were considered: living root mats, dying root mats and dead root mats. Since the dying root mats were still living before sampling but died during transport or storage, they had the same initial soil properties compared to the living root mats (i.e. C and N contents, microbial biomass and root biomass). The main difference between the living and dying root mats is: (a) the presence of living *Kobresia* plants in the “living stage,” in contrast to (b) recently deceased plants in the “dying stage.” Consequently, the *Kobresia* plants assimilate and reallocate C, take up nutrients and, with this, preserve leaching losses in the living root mats. In contrast, the dying root mats were unable to assimilate C and began the initial stages of degradation. The

primary causes of death in *Kobresia* root mats are overgrazing and natural mortality of single *Kobresia* clones (Unteregelsbacher *et al.*, 2012; Zhang *et al.*, 2016). Over time, intensified root and SOC decomposition as well as increasing leaching losses result in altered soil properties. These long-term degradation processes gradually shift the *Kobresia* pastures to dead root mats with lower C and N contents, microbial biomass and root biomass. Thus, the three root mats varieties sampled in our study represent the degradation continuum of *Kobresia* pastures (Living < Dying < Dead, Liu *et al.*, 2016).

Six samples were randomly picked out from each root mat type and transferred to incubation boxes (Liu *et al.*, 2016). The experiment was conducted at a constant temperature (20 °C), which is in the range of daily mean temperatures during the growing season in Nagqu (9.3-21.3°C, Geng *et al.*, 2012). Samples were illuminated diurnally for 14 h with a photosynthetic photon flux density of 80 $\mu\text{m}^{-2} \text{s}^{-1}$ and were kept in darkness for 10 h.

^{15}N labelling and addition were conducted when the incubation started. ^{15}N -labelled NH_4NO_3 solution (95% ^{15}N enrichment in total) with a total N amount of 0.5 mg was homogeneously injected as a tracer (very low N addition level) into each soil core (multi-needle injection technique, Murphy *et al.*, 1997). Three replicates from each type of ^{15}N labelled root mat were then randomly selected and added with unlabeled NH_4NO_3 solution (9.5 mg N per soil core). This consequently changed the ^{15}N tracer enrichment from 95 atom% to 4.75 atom% in the N-added treatment and was considered for the calculation of the ^{15}N recovery (see equation 2). In total, a two-factor design included the three root mats (living, dying and dead) and two N-addition levels (high N addition: 50.9 kg N ha^{-1} and low N addition: 2.5 kg N ha^{-1}). The low N addition (as a tracer) will henceforth be referred to as “no N” and the high N addition as “with N”.

One week after labelling and addition (Day 7), all shoots from living root mats were harvested (termed “1st generation”) and the ^{15}N recovery in shoots determined. A small proportion of the “new” upcoming shoot biomass in living stage (termed “2nd generation”) was harvested on days 21, 28, 35, 42, 49, 56, 63, 70, 77 and 98. The total dry weight of

the upcoming shoot biomass at each sampling event was estimated and ^{15}N recovery was measured.

N_2O emission was measured weekly starting at Day 1. Before measuring the N_2O efflux, soil moisture was first adjusted to 70% of WHC (i.e. 59% of dry weight for living and dying root mats; 33% of dry weight for dead root mats) for all soil cores. Briefly, the chamber was sealed and an aliquot of 15 ml gas was extracted from the chamber using an evacuated tube. After one day, another aliquot of 15 ml gas was extracted from the chamber.

The leaching experiment was conducted from Day 10 to assess the effect of N addition on dissolved C and N concentration in the leachate. Soil moisture was initially adjusted to 100% WHC (i.e. 84% of dry weight for living and dying root mats; 47% of dry weight for dead root mats). Then, 11 ml distilled water was added onto each sample from the inlet of the incubation box to simulate precipitation events (5 mm week^{-1}). Later, a glass tube was connected to the outlet of the incubation box to collect leachate. Leaching was repeated weekly during the experiment, i.e. on Days 10, 17, 24, 31, 38, 45, 52, 59, 66, 73, 80, 87, 94 and 101. The leachate was analyzed for dissolved organic carbon (DOC), dissolved organic nitrogen (DON), NH_4^+ and NO_3^- concentration.

Total aboveground biomass (AGB) and belowground biomass (BGB; including living and dead roots) was determined at the end of the incubation by separating roots from soil cores, washing with distilled water and drying at 60°C for 24 h. Carbon and N contents in soil and roots of each sample were analyzed using an elemental analyzer (Vario Max CN, Hanau, Germany). DOC, DON, NH_4^+ and NO_3^- concentration in the leachate were determined with a multi N/C 2100s analyzer (Analytik Jena Inc., Germany) and Cenco (Dual Tubingpump, Instrumenten B.V., Breda, The Netherlands). Soil microbial biomass C and N were determined using the chloroform fumigation extraction method (Brookes *et al.*, 1985; Vance *et al.*, 1987). The N_2O concentration was measured using a gas chromatograph (GC 6000 Vega series 2, Carlo Erba Instruments, Milan, Italy) equipped with an electron capture detector and an auto-sampler.

For microbial biomass ^{15}N analysis, fumigated and non-fumigated soil extracts were

freeze-dried. Samples of oven-dried soil, shoots (1st and 2nd generations) and roots were ground. All samples were analyzed using an isotope ratio mass spectrometer (Delta plus, Conflo III, Thermo Electron Cooperation, Bremen, Germany) coupled to an elemental analyzer (NA1500, Fisons instruments, Milano, Italy) to obtain the stable isotope signatures of N. Nitrogen stable isotope values were reported as atom% ¹⁵N via the following equation:

$$\text{atom\% } ^{15}\text{N} = (100 \times R_{\text{standard}} \times (\delta^{15}\text{N}/1000 + 1)) / (1 + R_{\text{standard}} \times (\delta^{15}\text{N}/1000 + 1)) \quad (1)$$

Where R_{standard} is the absolute ratio of ¹⁵N/¹⁴N in the standard (i.e. air). N recovery was calculated from atom% ¹⁵N according to the equation presented by Cabrera & Kissel (1989):

$$\text{Recovered N (\%)} = \frac{N_{\text{stock}} \times \frac{\text{atom\% } ^{15}\text{N}_{\text{labeled}} - \text{atom\% } ^{15}\text{N}_{\text{NA}}}{\text{atom\% } ^{15}\text{N}_{\text{added}} - \text{atom\% } ^{15}\text{N}_{\text{NA}}}}{N_{\text{added}}} \quad (2)$$

Where N_{stock} is the total N (mg) in soil, shoot, root and microbial biomass (non-fumigated and fumigated), respectively; N_{added} is the added N (mg); atom% ¹⁵N_{labeled} is the content of ¹⁵N atoms in the sample; atom% ¹⁵N_{NA} is the content of ¹⁵N atoms in the sample (i.e. soil, shoot and root) before labeling; atom% ¹⁵N_{added} is the content of ¹⁵N atoms in the added N pool, which is 4.75% for N-added samples and 95% for non-added samples. ¹⁵N recovery in microbial biomass was calculated as the difference in ¹⁵N mass between fumigated and non-fumigated soil extracts. Atom% ¹⁵N_{NA} for microbial biomass was assumed to be the same as that of the soil.

2.4.3.3 Statistical analysis

Soil and plant characteristics were analyzed and expressed as means with standard errors (mean ± SE). Significance differences of ¹⁵N among the three root mats were also tested using two-way ANOVA. Before applying ANOVA, data were checked for normality (Shapiro-Wilk-test, $p > 0.05$) and homogeneity of variance (Levene-test, $p > 0.05$). After obtaining a significant omnibus test result, a post-hoc test (Tukey's HSD test) was conducted for multiple comparisons. Repeated measures ANOVA was conducted to evaluate the impact of N addition on AGB and its foliar N content. All analyses were conducted using STATISTICA 10.0 (StatSoft Inc.).

2.4.4 Results

2.4.4.1 Plant and soil characteristics

The AGB of the 1st generation was similar in N-added and non-added root mats, whereas in the 2nd generation, N addition increased AGB and its foliar N stock (Fig. 1, top and bottom left; $p=0.008$). Some moss was found growing in dying root mats (ca. 0.04 kg m^{-2}), whereas the dead root mats were free of any vegetation. After the 2nd generation, total BGB of the living stage significantly increased to $4.2 \pm 0.02 \text{ kg m}^{-2}$, which was nearly double that of the dying and dead root mats (Table 1, $p<0.05$). Soil C content decreased from $70 \pm 7 \text{ g kg}^{-1}$ to $48 \pm 2 \text{ g kg}^{-1}$ along the degradation stages (Table 1). Soil bulk density increased from $0.66 \pm 0.07 \text{ g cm}^{-3}$ to $0.92 \pm 0.01 \text{ g cm}^{-3}$ with intensified degradation. Microbial biomass C in dying root mats was 1.4 times higher than in living root mats and 1.9 times than in dead root mats ($p<0.05$). The microbial biomass C/N ratio decreased from living to dead root mats.

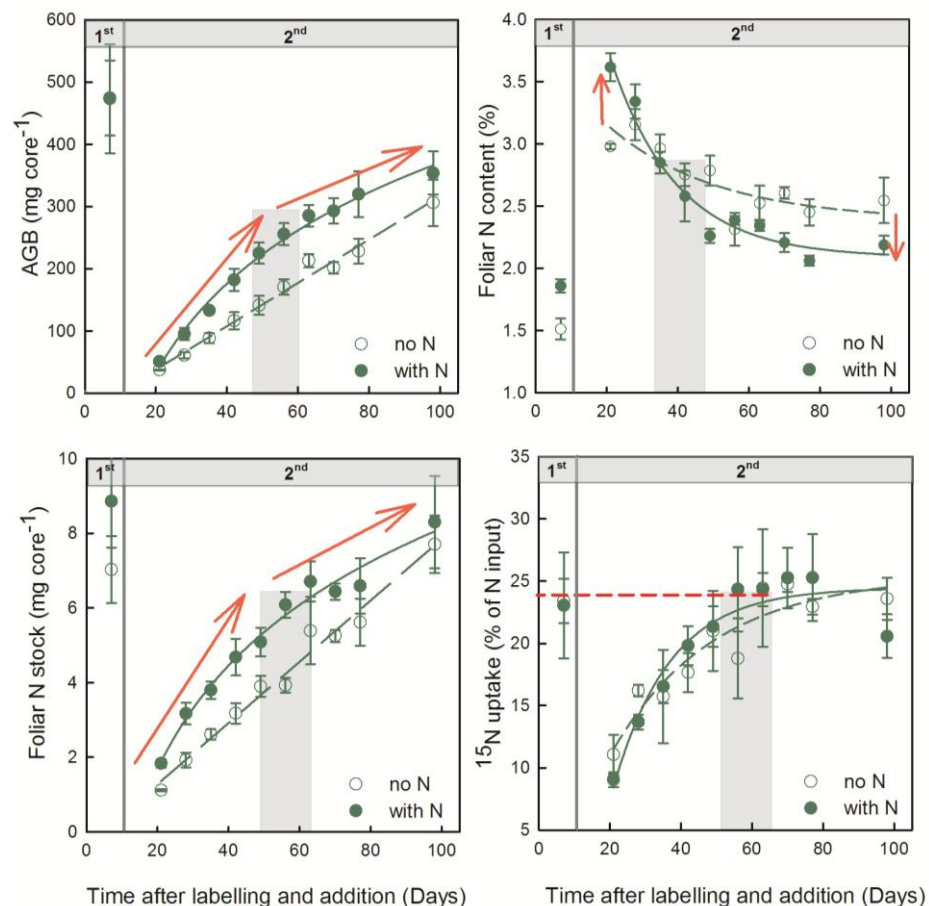


Figure 1 Aboveground biomass (AGB, top left), foliar N content (top right), foliar N stock (bottom left) and ^{15}N uptake (bottom right) by *K. pygmaea*. The shading area corresponds to a period during which the factors showed a gradual switch in their trends. “no N”: samples with low N addition (as a tracer); “with N”: samples with high N addition. “1st” and “2nd”: first and second generations of *K. pygmaea*. Error bars are standard error (SE).

Table 1 Characteristics of soil, root and microbial biomass

Root mat	pH	Bulk density (g cm ⁻³)	BGB (kg m ⁻²)	MBC (mg C g ⁻¹ dry soil)	MBN (mg N g ⁻¹ dry soil)	MBC/MBN	Root C (%)	Root N (%)	Root C/N	Soil C (%)	Soil N (%)
Living	6.7 ± 0.04 b	0.66 ± 7.1 b	4.2 ± 0.02 a	1.17 ± 0.1 b	0.12 ± 0.02 b	10 ± 2.3 a	46 ± 0.5 a	0.6 ± 0.02 c	79 ± 3.9 a	7 ± 0.7 a	0.5 ± 0.04 a
Dying	6.3 ± 0.06 c	0.68 ± 2.6 b	2.3 ± 0.02 b	1.63 ± 0.1 a	0.22 ± 0.03 a	7.5 ± 1.1 ab	44 ± 1.3 ab	0.7 ± 0.03 b	63 ± 3.8 b	8.5 ± 0.4 a	0.6 ± 0.02 a
Dead	7.2 ± 0.03 a	0.92 ± 1.1 a	2.5 ± 0.03 b	0.86 ± 0.1 c	0.18 ± 0.03 a	5.0 ± 0.5 b	41 ± 0.9 b	0.9 ± 0.04 a	45 ± 2.7 c	4.8 ± 0.2 b	0.4 ± 0.01 b

Values with the same letters among root mats are not significantly different at the $p < 0.05$ level (determined by a Tukey's HSD test). BGBB represents "below-ground biomass". "Living", "Dying" and "Dead" represent living, dying and dead *Kobresia* root mats, respectively. MBC and MBN represent microbial biomass C and N.

Foliar N contents in N-added living root mats were higher than those in the non-added root mats but then decreased and were lower after 6 weeks (Fig. 1, top right). The foliar N stock increased strongly from Day 21 to Day 49, but the magnitude of this increase slowed after 7-8 weeks. The ¹⁵N recovery of the AGB in the N-added root mats gradually increased and became stable after 7 weeks, whereas in the non-added root mats this response was delayed (after ca. 10-11 weeks) (Fig. 1, bottom right).

2.4.4.2 Effects of N addition on C and N leaching

Nitrogen addition increased the NO₃⁻ concentration in the leachate of all degradation stages (living, dying and dead stages), but had a minor effect on NH₄⁺ and DON concentrations. Overall, N addition resulted in higher total N losses from all N-added root mats compared to non-added root mats (Fig. 2). After 38 days, NO₃⁻ leaching from the living root mats dropped to zero, whereas DON and NH₄⁺ leaching remained the same (Fig. 2, top left). In contrast, NO₃⁻ was still present in the leachate of dying root mats after 45 days when the total N concentration stabilized (Fig. 2, top right). The total N concentration in the leachate of N-added dead root mats was higher in comparison to non-added throughout the experiment (Fig. 2, bottom left). This increment was mainly caused by high NO₃⁻ concentrations in dead root mats.

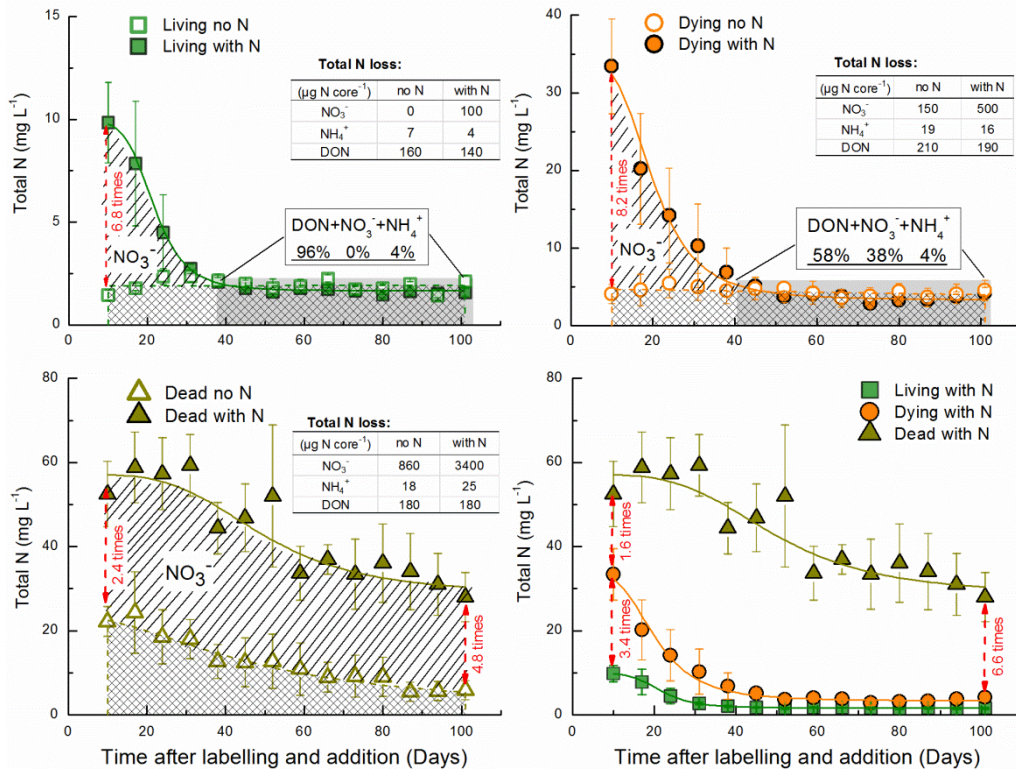


Figure 2 Total N concentration in the leachate of living (top left), dying (top right) and dead (bottom left) root mats and comparison among three N-added root mats (bottom right). The data in the inserted table showed the cumulative N loss during the whole incubation period. The shading area means that during this period the non-added samples show the similar N concentration with the N-added samples. The data above the shading area demonstrated the percentage of each form of N (DON, NH_4^+ , NO_3^-) in the cumulative N during this period. “Living”: living root mats; “Dying”: dying root mats; “Dead”: dead root mats; “no N”: samples with low N addition (as a tracer); “with N”: samples with high N addition. Error bars are standard error (SE).

The DOC concentration in the leachate of N-added root mats was similar to that of non-added root mats (Fig. 3). Living and dying root mats had an average DOC concentration of 29 ± 2.5 and $34 \pm 6.9 \text{ mg L}^{-1}$, respectively. However, dead root mats always demonstrated lower DOC concentrations ($24 \pm 2.7 \text{ mg L}^{-1}$) regardless of N addition.

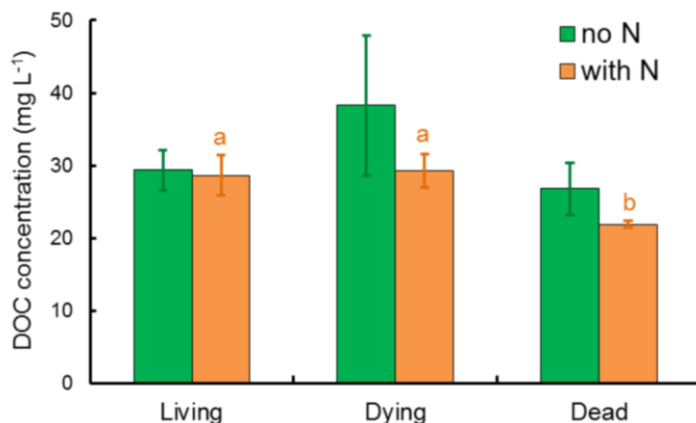


Figure 3 DOC concentrations averaged over 101 days in the leachate of three root mats. Abbreviations are as in Fig. 2. Different lowercase letters represent significant difference among the three root mats. Error bars are standard error (SE).

2.4.4.3 N recovery in plant, soil and microbial biomass

Total recovered ^{15}N (% of total ^{15}N input) of N-added root mats was similar to non-added root mats for all three degradation stages 91 days after labelling (Fig. 4). ^{15}N recovery in living root mats was the highest (93 ± 2.2 % for non-added, 81 ± 2.4 % for N-added; $p < 0.05$) among the three root mats. In non-added and N-added dying root mats, 69 ± 9.4 % and 57 ± 4.0 % of ^{15}N was recovered, respectively. Surprisingly, 75 ± 4.5 % and 61 ± 7.7 % of ^{15}N was allocated into root litter, soil and microbes in non-added and N-added dead root mats, respectively.

In the living shoots, 45 ± 2.1 % of ^{15}N was recovered, of which 23 ± 1.9 % and 22 ± 1.2 % were contributed by the 1st generation and the 2nd generation, respectively (Fig. 4). Moss in dying root mats recovered approximately 9.4 ± 1.2 % of ^{15}N .

^{15}N recovery in total BGB of N-added living root mats (21 ± 2.4 %) was similar to that of non-added mats (24 ± 3.4 %). Non-added dying root mats allocated 19 ± 5.9 % of ^{15}N in their root litter, which was twice that of N-added dying root mats (9.0 ± 1.7 %). Similarly, ^{15}N allocated by the root litter of non-added dead root mats (34 ± 0.6 %) was also twice that of N-added dead root mats (17 ± 1.5 %) (Fig. 4, $p < 0.001$).

Soil of dying and dead root mats retained 37 ± 2.6 % and 35 ± 3.4 % of ^{15}N , respectively, while only 17 ± 2.0 % was retained in soil of living root mats. Microbial biomass in dead root mats immobilized 6.1 ± 0.9 % of ^{15}N , which was more than twice that of dying root mats (2.8 ± 0.2 %, $p < 0.01$). In comparison, microbes in living root mats immobilized only 1.5 ± 0.3 % of ^{15}N .

2.4.5 Discussions

2.4.5.1 Sensitivity of plants to N addition

Nitrogen addition increased the AGB of *K. pygmaea* during the second generation, confirming our first hypothesis (H1) of a sensitive response of the AGB to N addition. This is in agreement with data from field experiments, where addition with NO_3^- or NH_4^+ increased the shoot biomass of *K. pygmaea* (Seeber, 2016; Xu *et al.*, 2004). This is because N addition offset the prevailing N limitation at least over the short-term (Xu *et*

al., 2015a). The shoot biomass of the first generation did not increase after N addition because shoots were already full-grown at the time of N-addition (Fig. 1, top left).

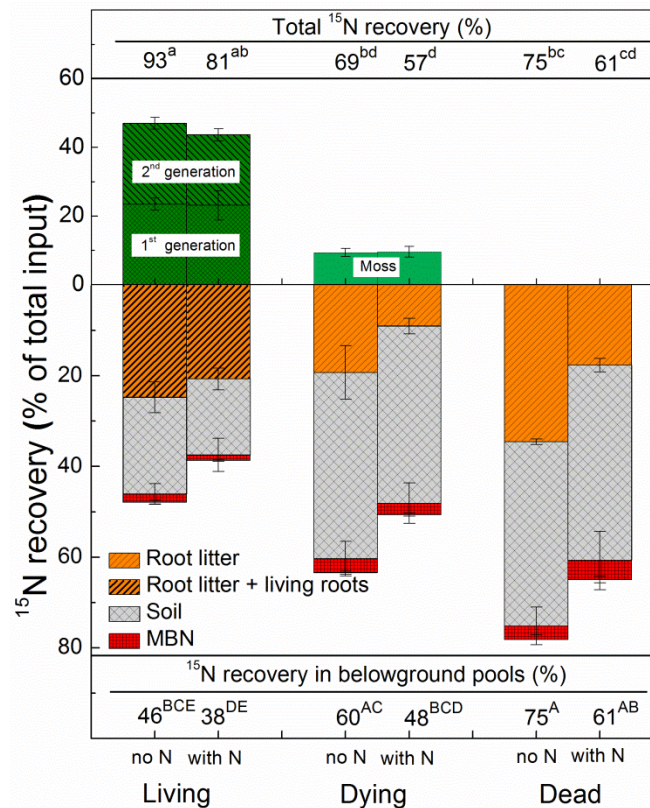


Figure 4 ^{15}N recovery in plant and soil pools of three non-added and N-added root mats 91 days after labelling. Data above/below the zero line is for AGB/BGB. AGB represents “aboveground biomass” and BGB “belowground biomass”. Because living and dead roots were not differentiated, ^{15}N recovery in the roots of living root mats included the total recovery in “living root and root litter”. For dying and dead root mats, only root litter existed and thus ^{15}N recovered in the “root litter” for both root mats. Other abbreviations are as in Fig. 2. Lowercase and capital letters represent significant difference among the three root mats. Error bars are standard error (SE).

The increase of AGB (2nd generation) after N addition was stronger than in the non-added living root mats during the first 7-8 weeks (Fig. 1, top left). N addition offset N limitation in living *K. pygmaea* but shifted to a N-limited state again after 7-8 weeks. This is because most of the added N was already incorporated in AGB and BGB (Fig. 4), immobilized by microorganisms, fixed by soil organic matter or lost via leaching and gas emissions (i.e. N_2O).

The transition from an N-unlimited to N-limited state (after 7-8 weeks) was also supported by foliar N content, aboveground N stock and ^{15}N uptake dynamics (Fig. 1), which also shifted their trend after 5-10 weeks. The constant ^{15}N recovery for both N-

added and non-added root mats after 10-11 weeks demonstrated that no ^{15}N was taken up by plants after this period. We suggest that aboveground N demands were almost saturated at a recovery rate of about 20-23% of total input, because aboveground biomass approximated to its maximum. The strategy of *K. pygmaea* to develop dense root mats indicates that the plants mainly invested resources belowground rather than in AGB (Wang *et al.*, 2015b; Ingrisch *et al.*, 2015). Wen *et al.* (2013) also observed that 98% of plant biomass was allocated to belowground biomass in *K.* pastures. The fact that the plants grew to no more than 2-3 cm high during their flowering time also supported this finding (Miehe *et al.*, 2009). This recovery rate precisely matches results from the field, where *K. pygmaea* shoots took up 18% of the total added ^{15}N 45 days after labeling (Schleuss *et al.*, 2015).

Nitrogen addition did not stimulate belowground root production, which partly contradicted our first hypothesis (H1). This non-significant response of BGB to N addition was also observed by other studies with *K. pygmaea* (i.e. Seeber, 2016; Yang *et al.*, 2014). We suggest that living *K. pygmaea* initially allocated more resources (e.g. N) to shoots, as indicated by the increase of AGB. This is presumably because *K. pygmaea* needs to cover the high belowground C costs to maintain the root biomass (root to shoot ratio: 90, Ingrisch *et al.*, 2015) by producing photosynthetically-active shoot biomass for CO_2 assimilation (Zong *et al.*, 2012; Schleuss *et al.*, 2015). High belowground investments of C and N in upper root mats (0-5 cm) were also indicated by field ^{15}N and ^{13}C pulse labelling studies, where approximately 50 % of labelled ^{15}N and ^{13}C were incorporated into topsoil root biomass 45 and 15 days after labeling, respectively (Schleuss *et al.*, 2015; Ingrisch *et al.*, 2015).

2.4.5.2 Sensitivity of microbes to N addition

Microbial biomass was not sensitive to N addition in any of the three root mats, but changed with intensifying degradation stages (Dying > Living > Dead, Table 1). The ratio of microbial biomass C to N decreased with degradation, suggesting that microbes shift from an N-limited to N-unlimited state with increased degradation. In N-limited living root mats, microbes compete with plants for N (Kuzyakov & Xu, 2013). Xu *et al.* (2011) concluded that the amount of root biomass strongly controls the competition between

plants and microbes: a high root biomass ($> 4.2 \text{ kg m}^{-2}$) enables plants to outcompete microbes for N uptake. This was also supported by the low ratio of ^{15}N recovered by microbial biomass to ^{15}N recovered in living plants (ca. $0.03 < 1.0$), with ratios lower than 1.0 indicating that plants recover more ^{15}N and thus, outcompete microbes. Dying root mats provided a favorable environment for microbial growth because of the abundance of easily decomposable organic residues. Furthermore, there was no competition with living roots for N. These conditions lead to a weak effect of N addition on microbial growth in dying root mats. Microbial growth in dead root mats was not N limited. Dead root mats possessed the lowest root C/N as well as DOC concentrations, suggesting that availability of labile organic C was the limiting factor for microbial growth in dead root mats.

2.4.5.3 Fate of N in the belowground pools

Total ^{15}N recovery was higher in living root mats compared with dying and dead root mats (Fig. 4), confirming our second hypothesis (H2). However, the belowground pools (root litter, soil, and microbial biomass) in dying and dead root mats retained more ^{15}N than that in the living root mats (Fig. 4).

The higher ^{15}N recovery in the belowground pools of dying and dead root mats was mainly induced by the stronger N affinity of soil and root litter (Fig. 4). ^{15}N recovery in soil of dying and dead root mats was about twice that of living root mats irrespective of N addition. Once released to the soil, ^{15}N can adhere to soil particles or be fixed in soil organic matter as NH_4^+ (Drury & Beauchamp, 1991; Burge & Broadbent, 1960). ^{15}N can also be released by microbes. The higher turnover rate of microbes in dying and dead root mats induced the release of immobilized ^{15}N in the form of organic N (Schmidt *et al.*, 2007), which was then incorporated into the ^{15}N pool in soil.

Roots in dying and dead root mats did not take up ^{15}N as living roots did. Nonetheless, a certain amount of ^{15}N was still retained in their root litter due to microbial N immobilization (Fig. 4). Thus, the magnitude of root litter ^{15}N was controlled by the size and activity of the root-associated microorganisms (Gallardo *et al.*, 1992). As it is challenging for microorganisms to maintain metabolic homeostasis when utilizing

substrates with high C/N ratios such as root litter (Table 1), microorganisms living under these conditions must take up all available forms of N to meet their N demands (Mooshammer *et al.*, 2014; Cleveland & Liptzin, 2007). Since reactive N forms (i.e. NO_3^- and NH_4^+) were added with the ^{15}N tracer, it is likely that they were immobilized by root-associated microorganisms. This interpretation is also partly supported by Downs *et al.* (1996), who found that several litter types retained a substantial proportion of added $^{15}\text{NO}_3^-$ -N, indicating that NO_3^- was a viable source of N for microbial immobilization in litter decomposition.

2.4.5.4 Nitrogen loss via leaching and N_2O emission

Nitrogen loss via leaching increased with degradation stage (Living < Dying < Dead, Fig. 2). Cumulative DON loss was similar in the three root mats and the loss of NH_4^+ was negligible compared with that of DON and NO_3^- . Therefore, the N loss pattern – increasing from the living to the dead root mats – was mainly explained by intensified NO_3^- leaching. The much lower N loss (especially as NO_3^-) from living root mats indicates that the plants efficiently recapture N, reducing N leaching. This was also reflected by the correlations between N uptake and N loss due to leaching (Fig. 5 top). This agrees with Xu *et al.* (2004), who showed that *K. pygmaea* preferentially took up NO_3^- . In contrast, the root litter in dying root mats provided abundant labile organic matter for microbial decomposition and mineralization. In the absence of living plants, less NO_3^- released from mineralization processes will be taken up by plants or immobilized by microorganisms and will accumulate in soil. The subsequent leaching of unbound N explains the increase in NO_3^- losses from dying root mats as compared to living root mats.

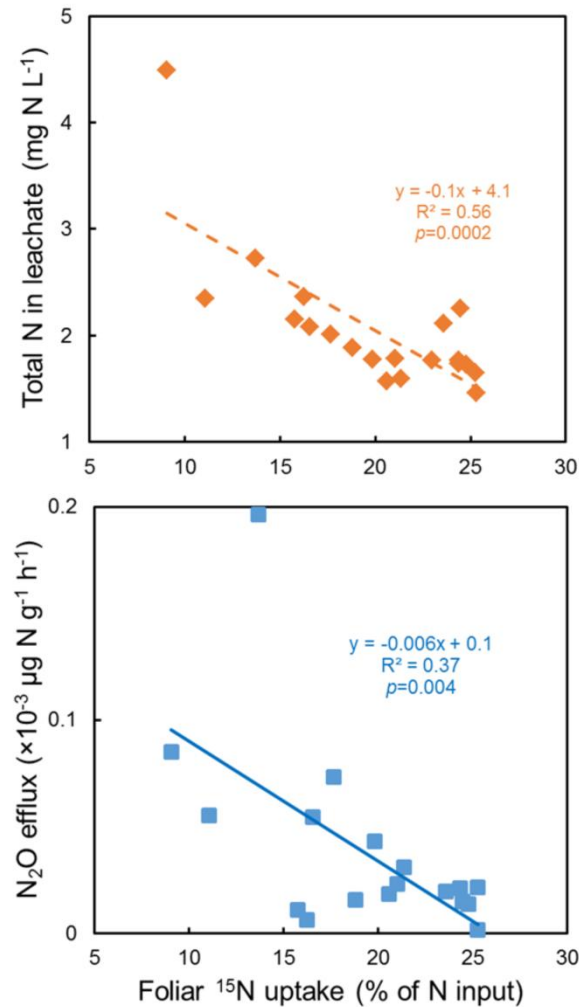


Figure 5 Relations between foliar ¹⁵N uptake and total N in the leachate (top) and N₂O efflux (bottom). *p* values less than 0.05 represent the significance of the correlation.

The N loss by N₂O emission was relatively low compared with that from leaching, and increased with the degree of degradation (Dying > Dead > Living, Fig. S1). Our interpretation is that increasing amounts of labile organic matter from root litter in the dying stage stimulated heterotrophic microbial activity and promoted denitrification (Killham, 1994; Senbayram *et al.*, 2012). By contrast, the lowest N₂O emission from living root mats may be attributed to relatively lower microbial activity and higher N uptake by living plants (Fig. 5 bottom).

2.4.5.5 Net N losses and N stocks along degradation stages

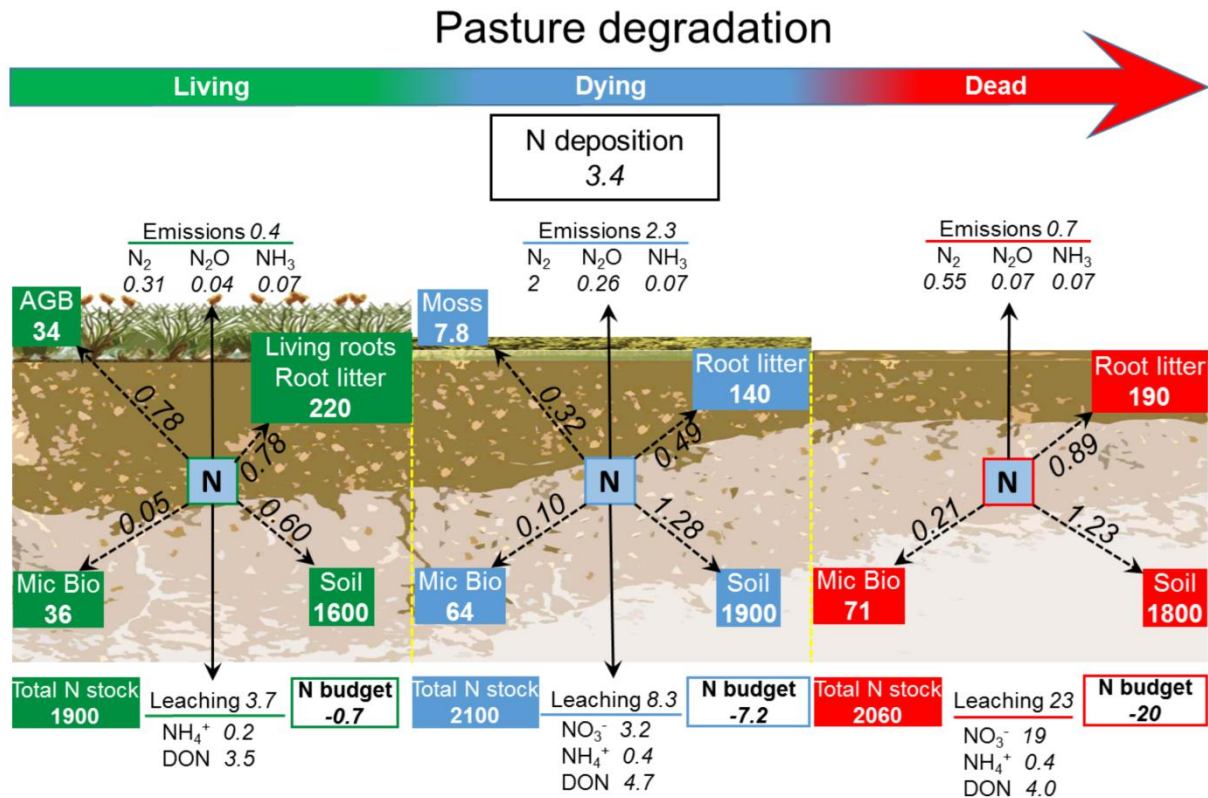


Figure 6 Total N stock and N fluxes in the three root mats during the growing season. “Mic Bio” means microbial biomass. Values in **bold**: N stock (kg N ha⁻¹ in the upper 5 cm); values in *italics*: N flux (kg N ha⁻¹ yr⁻¹). The data along the dash line show the partitioning of deposited N into various pools. We used 3.4 kg N ha⁻¹ as total atmospheric N deposition (Xu et al., 2015b). N₂ emission from denitrification was calculated using an average N₂/N₂O ratio of 7.8 for sandy loam soil (Maag and Vinther, 1996). Ammonia emission from volatilization was calculated as 2% of the deposited mineral N (van der Hoek, 1998). Total N loss from leaching during the growing season was predicted based on mean precipitation in growing season in Nagqu (356 mm, Hua et al., 2015). Negative values of N budget represents net N losses from the three root mats. By extrapolation for the field, the N fluxes and intensities of processes might be different, but the mechanisms remain the same.

Net N losses and N stocks along degradation stages were illustrated based on our observations and those of previous studies (Fig. 6). Despite the fact that it is unrealistic to extrapolate observed data from the laboratory to those from field conditions because of environmental variations (i.e. light density, diurnal temperature variation), the pathways of N losses (i.e. gas emission, leaching) and N recovery were similar between lab and field experiments. Thus, while the N transformation rates and intensities of processes might be different under field conditions, the overall mechanisms remain the same. Knowledge of these mechanisms may give us a better understanding of the N cycling components along different degraded stages.

Net N losses from dead root mats were slightly higher than those of dying root mats, and much higher than those of the living root mats (Fig. 6). Leaching was the primary cause of high N losses (mainly as NO_3^-) from dying and dead root mats, while the lower N loss from living root mats can be attributed to N uptake by *K. pygmaea*. The negative relationships between foliar ^{15}N recovery and N_2O flux or TN leachate also confirmed the importance of living *K. pygmaea* for N preservation (Fig. 5).

Total N stocks in the three root mats were similar ($p>0.05$). This contradicted our third hypothesis for declining N stocks with degradation stages (H3). Most N was stored in soil, but the soil N content decreased with degradation stages (Table 1), indicating that the similarity in total N stocks resulted from the increase in soil bulk density (Table 1). As pasture degrades, roots decompose and their biomass decreases, which tends to weaken their reinforcement of the soil (Trückmann *et al.*, 2009). The concurrent livestock trampling on *Kobresia* pasture as well as the higher relative portion of mineral particles then increases soil bulk density (Hiltbrunner *et al.*, 2012).

2.4.6 Conclusions

Aboveground biomass and the foliar N content of *K. pygmaea* increased with N addition during the early growth period. This indicates that the N limitation common in *Kobresia* pastures on the Tibetan Plateau was alleviated. Nonetheless, plant growth and ^{15}N uptake were not further promoted after around 7-8 weeks. This suggests that living root mats reverted to an N limited state due to N uptake by plants and N leaching. NO_3^- leaching in living root mats strongly decreased and became undetectable after 38 days. In contrast, NO_3^- leaching markedly increased in dying and dead root mats and accounted for most of the N losses from leaching ($\text{NO}_3^- > \text{DON} > \text{NH}_4^+$). Leaching N losses from dying and dead mats increased remarkably compared to living root mats. N losses from leaching were also considerably higher than N losses from N_2O emissions for dying and dead root mats. We conclude that N addition can facilitate plant growth in intact *K. pygmaea* pastures at least over the short term, and that continuous N addition in the field conditions may prolong this facilitation based on the permanent supply of N from dust deposition and rainfall. In the degraded stages of *K. pygmaea* pastures, N addition directly increased the N losses from leaching. Thus, degradation together with

N addition intensifies N losses in *K. pygmaea* pastures, hampering pasture restoration, increasing the NO₃⁻ loading of adjacent lower landscapes and exasperating headwater pollution.

2.4.7 Acknowledgements

This work was funded by the China Scholarship Council (CSC) within the fellowship for SL and the German Research Foundation (DFG) within the Priority Programme 1372: Tibetan Plateau: Formation-Climate-Ecosystems (Project KU 1184/14-2). We are very thankful to the Volkswagen Foundation for establishing the KEMA research station and to Georg Miehe for selecting the study sites. The authors thank Kazem Zamanian and Amit Kumar for their helpful suggestions on this manuscript and Anita Kriegel for the experimental assistance. Special thanks to the staff at Kompetenzzentrum Stabile Isotope (KOSI), University of Göttingen for measuring ¹⁵N. The authors disclose any potential conflict of interests.

2.4.8 References

- Babel W, Biermann T, Coners H, Falge E, Seeber E, Ingrisch J, Schleuß P-M, Gerken T, Leonbacher J, Leipold T, Willinghöfer S, Spielvogel S, Li X, Xu X, Sun Y, Zhang L, Yang Y, Ma Y, Wesche K, Graf H-F, Leuschner C, Guggenberger G, Kuzyakov Y, Miehe G, Foken T. 2014. Pasture degradation modifies the water and carbon cycles of the Tibetan highlands. *Biogeosciences* **11**:6633-6656. DOI: 10.5194/bg-11-6633-2014.
- Brookes PC, Landman A, Pruden G, Jenkinson DS. 1985. Chloroform fumigation and the release of soil nitrogen: A rapid direct extraction method to measure microbial biomass nitrogen in soil. *Soil Biology & Biochemistry* **17**: 837-842. DOI: 10.1016/0038-0717(85)90144-0.
- Burge WD, Broadbent FE. 1960. Fixation of ammonia by organic soils. *Soil Science Society of America Journal* **25**: 199-204. DOI: 10.2136/sssaj1961.03615995002500030018x.
- Cabrera ML, Kissel DE. 1989. Review and simplification of calculations in ¹⁵N tracer studies. *Fertilizer Research* **20**: 11-15. DOI: 10.1007/BF01055396.
- Cleveland CC, Liptzin D. 2007. C: N: P stoichiometry in soil: is there a "Redfield ratio" for the microbial biomass? *Biogeochemistry*, **85**, 235–252. DOI: 10.1007/s10533-007-9132-0.
- Dong QM, Zhao XQ, Wu GL, Shi JJ, Ren GH. 2013. A review of formation mechanism and restoration measures of "black-soil-type" degraded grassland in the Qinghai-Tibetan Plateau. *Environmental Earth Sciences*, **70**: 2359-2370. DOI: 10.1007/s12665-013-2338-7.
- Downs MR, Nadelhoffer KJ, Melillo JM, Aber JD. 1996. Immobilization of a ¹⁵N-labeled nitrate addition by decomposing forest litter. *Oecologia* **105**: 141-150. DOI: 10.1007/BF00328539.
- Drury CF, Beauchamp EG. 1991. Ammonium fixation, release, nitrification, and immobilization in high- and low-fixing soils. *Soil Science Society of America Journal* **55**: 125-129. DOI: 10.2136/sssaj1991.03615995005500010022x.
- Fang HJ, Cheng SL, Yu GR, Xu MJ, Wang YS, Li LS, Dang XS, Wang L, Li YN. 2014. Experimental nitrogen deposition alters the quantity and quality of soil dissolved organic carbon in an alpine meadow on the Qinghai-Tibetan Plateau. *Applied Soil Ecology* **81**: 1-11. DOI: 10.1016/j.apsoil.2014.04.007.
- Feng Y, Lu Q, Tokola T, Liu H, Wang X. 2009. Assessment of grassland degradation in Guinan county, Qinghai Province, China, in the past 30 years. *Land Degradation & Development* **20** (1): 55-68. DOI: 10.1002/ldr.877.
- Gallardo A, Merino J. 1992. Nitrogen immobilization in leaf litter at two Mediterranean ecosystems of SW Spain. *Biogeochemistry* **15**: 213-228. DOI: 10.1007/BF00002937
- Geng Y, Wang YH, Yang K, Wang SP, Zeng H, Baumann F, Kuehn P, Scholten T, He JS. 2012. Soil respiration in Tibetan alpine grasslands: belowground biomass and soil moisture, but not soil temperature, best explain the large-scale patterns. *PLoS ONE* **7**: e34968. DOI: 10.1371/journal.pone.0034968.

- Harris RB. 2010. Rangeland degradation on the Qinghai-Tibetan plateau: A review of the evidence of its magnitude and causes. *Journal of Arid Environments* **74**: 1-12. DOI: 10.1016/j.jaridenv.2009.06.014.
- He SY, Richards K. 2015. Impact of meadow degradation on soil water status and pasture management-A case study in Tibet. *Land Degradation & Development* **26** (5): 468-479. DOI: 10.1002/ldr.2358.
- Hiltbrunner D, Schulze S, Hagedorn F, Schmidt MWI, Zimmermann S. 2012. Cattle trampling alters soil properties and changes soil microbial communities in a Swiss sub-alpine pasture. *Geoderma* **170**: 369-377. DOI: 10.1016/j.geoderma.2011.11.026.
- Hua T, Wang XM, Ci Z, Lang LL, Zhang CX. 2015. Response of vegetation activity to climate variation on the Qinghai-Tibetan Plateau (China) from 1992 to 2011. *Climate Research* **66**: 65-73. DOI: 10.3354/cr01333.
- Ingrisch J, Biermann T, Seeber E, Leopold T, Li M, Ma Y, Xu X, Miede G, Guggenberger G, Foken T, Kuzyakov Y. 2015. Carbon pools and fluxes in a Tibetan alpine *Kobresia pygmaea* pasture partitioned by coupled eddy-covariance measurements and ¹³CO₂ pulse labeling. *Science of the Total Environment* **505**: 1213-1224. DOI: 10.1016/j.scitotenv.2014.10.082.
- Jiang J, Shi PL, Zong N, Fu G, Shen ZX, Zhang XZ, Song MH. 2015. Climatic patterns modulate ecosystem and soil respiration responses to fertilization in an alpine meadow on the Tibetan Plateau, China. *Ecological Research* **30**: 3-13. DOI: 10.1007/s11284-014-1199-1.
- Kanakidou M., Myriokefalitakis S., Daskalakis N., Fanourgakis G., Nenes A., Baker A.R., Tsigaridis K., Mihalopoulos N. 2016. Past, present, and future atmospheric nitrogen deposition. *Journal of the Atmospheric Sciences* **73**: 2039-2047. DOI: 10.1175/JAS-D-15-0278.1.
- Kang SC, Mayewski PA, Qin DH, Yan YP, Zhang DQ, Hou SG, Ren JW. 2002. Twentieth century increase of atmospheric ammonia recorded in Mount Everest ice core. *Journal of Geophysical Research: Atmospheres* **107** (D21). DOI: 10.1029/2001JD001413.
- Killham K. 1994. The ecology of soil nutrient cycling. In: *Soil Ecology*. Cambridge University Press, London, pp: 89-149.
- Kuzyakov Y, Xu XL. 2013. Competition between roots and microorganisms for nitrogen: mechanisms and ecological relevance. *New Phytologist* **198**: 656-669. DOI: 10.1111/nph.12235.
- Lebauer DS, Treseder KK. 2008. Nitrogen limitation of net primary productivity in terrestrial ecosystems is globally distributed. *Ecology* **89** (2): 371-379. DOI: 10.1890/06-2057.1.
- Leber D, Holawe F, Häusler H. 1995. Climatic classification of the Tibet Autonomous Region using multivariate statistical methods. *GeoJournal* **37**:451-472. DOI: 10.1007/BF00806934.
- Li JH, Yang YJ, Li BW, Li WJ, Wang G, Knops JMH. 2014. Effects of nitrogen and phosphorus fertilization on soil carbon fractions in alpine meadows on the Qinghai-Tibetan Plateau. *PLoS ONE* **9** (7): e103266. DOI: 10.1371/journal.pone.0103266.
- Liu SB, Schleuss PM, Kuzyakov Y. 2016. Carbon and nitrogen losses from soil depend on degradation of Tibetan *Kobresia* pastures. *Land Degradation & Development* DOI: 10.1002/ldr.2522.
- Lü CQ, Tian HQ. 2007. Spatial and temporal patterns of nitrogen deposition in China: Synthesis of observational data. *Journal of Geophysical Research: Atmospheres* **112**: D22S05. DOI: 10.1029/2006JD007990.
- Maag M, Vinther FP. 1996. Nitrous oxide emission by nitrification and denitrification in different soil types and at different soil moisture contents and temperatures. *Applied Soil Ecology* **4** (1): 5-14. DOI: 10.1016/0929-1393(96)00106-0.
- Menge DNL, Hedin LO, Pacala SW. 2012. Nitrogen and phosphorus limitation over long-term ecosystem development in terrestrial ecosystems. *PLoS ONE* **7**(8): e42045. DOI: 10.1371/journal.pone.0042045.
- Miede G. 1989. Vegetation patterns on Mount Everest as influenced by monsoon and föhn. *Vegetatio* **79**:21-32. DOI: 10.1007/BF00044845.
- Miede G, Miede S, Kaiser K, Liu JQ, Zhao XQ. 2008a. Status and dynamics of the *Kobresia pygmaea* ecosystem on the Tibetan Plateau. *AMBIO: A Journal of the Human Environment* **37** (4): 272-279. DOI: 10.1579/0044-7447(2008)37[272:SADOTK]2.0.CO;2.
- Miede G, Miede S, Kaiser K, Reudenbach C, Behrendes L, Duo L, Schlütz F. 2009. How old is pastoralism in Tibet? An ecological approach to the making of a Tibetan landscape. *Palaeogeography Palaeoclimatology Palaeoecology* **276**: 130-147. DOI: 10.1016/j.palaeo.2009.03.005.
- Miede G, Miede S, Will M, Opgenoorth L, Duo L, Dorgeh T, Liu JQ. 2008b. An inventory of forest relicts in the pastures of Southern Tibet (Xizang A.R., China). *Plant Ecology* **194**: 157-177. DOI: 10.1007/s11258-007-9282-0.
- Mooshammer M, Wanek W, Hämmerle I, Fuchslueger L, Hofhansl F, Knoltsch A, Schneckner J, Takriti M, Watzka M, Wild B, Keiblinger KM, Zechmeister-Boltenstern S, Richter A. 2014. Adjustment of microbial nitrogen use efficiency to carbon : nitrogen imbalances regulates soil nitrogen cycling. *Nature Communications* **5**: 3694. DOI: 10.1038/ncomms4694.
- Murphy DV, Fillery IRP, Sparling GP. 1997. Method to label soil cores with ¹⁵NH₃ gas as a prerequisite for ¹⁵N isotopic dilution and measurement of gross N mineralization. *Soil Biology & Biochemistry* **29**: 1731-1741. DOI: 10.1016/S0038-0717(97)00067-9.
- O'Mara FP. 2012. The role of grasslands in food security and climate change. *Annals of Botany* mcs209. DOI: 10.1093/aob/mcs209.

- Pomeranz K, Turner JL, Shifflett SC, Batten R, Shah T, Giordano M, Cronin RP, Matthew R, Bandyopadhyay J. 2013. Himalayan water security: The challenges for south and southeast Asia. *Asia Policy* **16**: 1-50. DOI: 10.1353/asp.2013.0023.
- Schleuss P-M, Heitkamp F, Sun Y, Miede G, Xu XL, Kuzyakov Y. 2015. Nitrogen uptake in an alpine *Kobresia* pasture on the Tibetan plateau: Localization by ¹⁵N labeling and implications for a vulnerable ecosystem. *Ecosystems* **18**(6): 946-957. DOI: 10.1007/s10021-015-9874-9.
- Schmidt SK, Costello EK, Nemergut DR, Cleveland CC, Reed SC, Weintraub MN, Meyer AF, Martin AM. 2007. Biogeochemical consequences of rapid microbial turnover and seasonal succession in soil. *Ecology* **88** (6): 1379-1385. DOI: 10.1890/06-0164.
- Seeber E. 2016. An investigation into the *Kobresia pygmaea* ecotone of the Tibetan Plateau-From species to community ecology. Dissertation, Martin Luther University of Halle-Wittenberg.
- Seeber E, Miede G, Hensen I, Yang YP, Wesche K. 2015. Mixed reproduction strategy and polyploidy facilitate dominance of *Kobresia pygmaea* on the Tibetan Plateau. *Journal of Plant Ecology* **9**(1). DOI: 10.1093/jpe/rtv035.
- Senbayram M, Chen R, Budai A, Bakken L, Dittert K. 2012. N₂O emission and the N₂O/(N₂O+N₂) product ratio of denitrification as controlled by available carbon substrates and nitrate concentrations. *Agriculture, Ecosystems & Environment* **147**: 4-12. DOI: 10.1016/j.agee.2011.06.022.
- Shi Y, Baumann F, Ma Y, Song C, Kühn P, Scholten T, He JS. 2012. Organic and inorganic carbon in the topsoil of the Mongolian and Tibetan grasslands: pattern, control and implications. *Biogeosciences* **9**: 2287-2299. DOI: 10.5194/bg-9-2287-2012.
- Song MH, Yu FH. 2015. Reduced compensatory effects explain the nitrogen-mediated reduction in stability of an alpine meadow on the Tibetan Plateau. *New Phytologist* **207**: 70-77. DOI: 10.1111/nph.13329.
- Song MH, Yu FH, Ouyang H, Cao GM, Xu XL, Cornelissen JHC. 2012. Different inter-annual responses to availability and form of nitrogen explain species coexistence in an alpine meadow community after release from grazing. *Global Change Biology* **18**: 3100-3111. DOI: 10.1111/j.1365-2486.2012.02738.x.
- Thompson LG, Yao T, Mosley-Thompson E, Davis ME, Henderson KA, Lin PN. 2000. A high-resolution millennial record of the south Asian monsoon from Himalayan ice cores. *Science* **289**: 1916-1919. DOI: 10.1126/science.289.5486.1916.
- Trückmann K, Horn R, Reintam E. 2009. Impact of roots on soil stabilization in grassland. ISTRO 18th Triennial Conference Proceedings T4-022, pp. 1-7
- Unteregelsbacher S, Hafner S, Guggenberger G, Miede G, Xu X, Liu J, Kuzyakov Y. 2012. Response of long-, medium- and short-term turnover processes of the carbon budget to overgrazing on the Tibetan Plateau. *Biogeochemistry* **111**: 187-201. DOI: 10.1007/s10533-011-9632-9.
- van der Hoek KW. 1998. Estimating ammonia emission factors in Europe: summary of the work of the UNECE ammonia expert panel. *Atmospheric Environment* **32**: 315-316. DOI: 10.1016/S1352-2310(97)00168-4.
- Vance ED, Brookes PC, Jenkinson DS. 1987. An extraction method for measuring soil microbial biomass C. *Soil Biology & Biochemistry* **19**: 703-707. DOI: 10.1016/0038-0717(87)90052-6.
- Vitousek PM, Howarth RW. 1991. Nitrogen limitation on land and in the sea: How can it occur? *Biogeochemistry* **13**: 87-115. DOI: 10.1007/BF00002772.
- Wang CT, Long RJ, Wang QL, Ling ZC, Shi JJ. 2009a. Changes in plant diversity, biomass and soil C, in alpine meadows at different degradation stages in the headwater region of three rivers, China. *Land Degradation & Development* **20**: 187-198. DOI: 10.1002/ldr.879.
- Wang JS, Wang ZK, Zhang XZ, Zhang YL, Ran CQ, Zhang JL, Chen BX, Zhang BS. 2015b. Response of *Kobresia pygmaea* and *Stipa purpurea* grassland communities in northern Tibet to nitrogen and phosphate addition. *Mountain Research and Development* **35** (1): 78-86. DOI: 10.1659/MRD-JOURNAL-D-11-00104.1.
- Wang P., Lassoie JP., Morreale SJ., Dong S. 2015a. A critical review of socioeconomic and natural factors in ecological degradation on the Qinghai-Tibetan Plateau, China. *The Rangeland Journal* **37**: 1-9. DOI: 10.1071/RJ14094.
- Wang JS, Zhang XZ, Chen BX, Shi PL, Zhang JL, Shen ZX, Tao J, Wu JS. 2013. Causes and restoration of degraded alpine grassland in northern Tibet. *Journal of Resources and Ecology* **4**(1): 43-49. DOI: 10.5814/j.issn.1674-764x.2013.01.006.
- Wang WY, Wang QJ, Lu ZY. 2009b. Soil organic carbon and nitrogen content of density fractions and effect of meadow degradation to soil carbon and nitrogen of fractions in alpine *Kobresia* meadow. *Science in China Series D: Earth Sciences* **52**(5): 660-668. DOI: 10.1007/s11430-009-0056-5.
- Wen L, Dong SK, Li YY, Wang XX, Li XY, Shi JJ, Dong QM. 2013. The impact of land degradation on the C pools in alpine grasslands of the Qinghai-Tibet Plateau. *Plant Soil* **368**: 329-340. DOI: 10.1007/s11104-012-1500-4.
- WRB. 2014. World Reference Base for Soil Resources. FAO, World Soil Resources Reports 106, Rome.
- Xu W, Luo XS, Pan YP, Zhang L, Tang AH, Shen JL, Zhang Y, Li KH, Wu QH, Yang DW, Zhang YY, Xue J, Li WQ, Li QQ, Tang L, Lu SH, Liang T, Tong YA, Liu P, Zhang Q, Xiong ZQ, Shi XJ, Wu LH, Shi WQ, Tian K, Zhong XH, Shi K, Tang QY, Zhang LJ, Huang JL, He CE, Kuang FH, Zhu B, Liu H, Jin X, Xin YJ, Shi XK, Du EZ, Dore AJ, Tang S, Collett Jr JL, Goulding K, Sun YX, Ren J, Zhang FS, Liu XJ. 2015b. Quantifying atmospheric nitrogen deposition through a nationwide monitoring network across China. *Atmospheric Chemistry and*

- Physics* **15**: 12345-12360. DOI: 10.5194/acp-15-12345-2015.
- Xu XL, Ouyang H, Pei ZY, Zhou CP. 2003. Fate of ¹⁵N labeled nitrate and ammonium salts added to an alpine meadow in the Qinghai-Xizang Plateau, China. *Acta Botanica Sinica* **45** (3): 276-281. Retrieved from: <http://sourcedb.igsnr.cas.cn/zw/stxtsys/sysslw/200906/P020090625725014523943.PDF>.
- Xu XL, Ouyang H, Pei ZY, Zhou CP. 2004. Long-term partitioning of ammonium and nitrate among different components in an alpine meadow ecosystem. *Acta Botanica Sinica* **46** (3): 279-283. Retrieved from: <http://ir.igsnr.ac.cn/handle/311030/4399>.
- Xu XL, Ouyang H, Richter A, Wanek W, Cao GM, Kuzyakov Y. 2011. Spatial-temporal variations determine plant-microbe competition for inorganic nitrogen in an alpine meadow. *Journal of Ecology* **99**: 563-571. DOI: 10.1111/j.1365-2745.2010.01789.x.
- Xu XT, Liu HY, Song ZL, Wei W, Hu GZ, Qi ZH. 2015a. Response of aboveground biomass and diversity to nitrogen addition along a degradation gradient in the Inner Mongolian steppe, China. *Scientific Reports* **5**: 10284. DOI: 10.1038/srep10284.
- Yang XX, Ren F, Zhou HK, He JS. 2014. Responses of plant community biomass to nitrogen and phosphorus additions in an alpine meadow on the Qinghai-Xizang Plateau. *Chinese Journal of Plant Ecology* **38** (2): 159-166. DOI: 10.3724/SP.J.1258.2014.00014.
- Yang YH, Fang JY, Smith P, Tang YH, Chen AP, Ji CJ, Hu HF, Rao S, Tan K, He JS. 2009. Changes in topsoil carbon stock in the Tibetan grasslands between the 1980s and 2004. *Global Change Biology* **15**: 2723-2729. DOI: 10.1111/j.1365-2486.2009.01924.x.
- Zhang JP, Liu SZ, Zhou L. 1998. Soil degradation of main grassland in Naqu area of Tibet. *Journal of Soil Erosion and Soil Water Conservation* **4**(3): 6-11 (in Chinese).
- Zhang L, Unteregelsbacher S, Hafner S, Xu XL, Schleuss PM, Miede G, Kuzyakov Y. 2016. Fate of organic and inorganic nitrogen in crusted and non-crusted *Kobresia* grasslands. *Land Degradation & Development* **28**: 166-174. DOI: 10.1002/ldr.2582.
- Zhou HK, Zhao XQ, Tang YH, Gu S, Zhou L. 2005. Alpine grassland degradation and its control in the source region of the Yangtze and Yellow Rivers, China. *Grassland Science* **51**: 191-203. DOI: 10.1111/j.1744-697x.2005.00028.x.
- Zong N, Shi PL, Song MH, Lin L, Ma WM, Jiang J, Fu G, He YT, Zhang XZ. 2012. Clipping alters the response of biomass allocation pattern under nitrogen addition in an alpine meadow on the Tibetan Plateau. *Journal of Natural Resources* (10): 1696-1707. DOI: 10.11849/zrzyxb.2012.10.008.
- Zong N, Song MH, Shi PL, Jiang J, Zhang XZ, Shen ZX. 2014. Timing patterns of nitrogen application alter plant production and CO₂ efflux in an alpine meadow on the Tibetan Plateau, China. *Pedobiologia - Journal of Soil Ecology* **57**: 263-269. DOI: 10.1016/j.pedobi.2014.08.001.

2.4.9 Supporting information

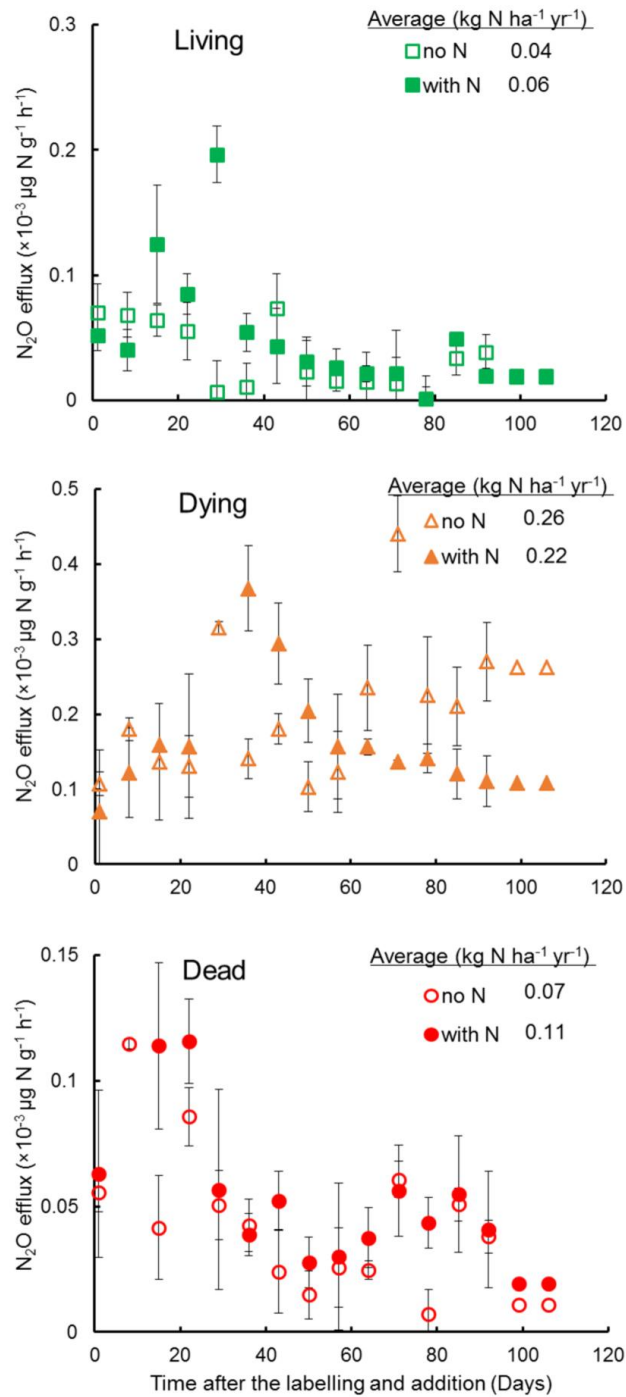
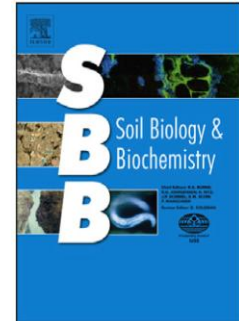


Figure S1 N_2O efflux from living (top), dying (middle) and dead (bottom) root mats during the incubation. “Living”: living root mats; “Dying”: dying root mats; “Dead”: dead root mats. “no N”: samples with low N addition (as a tracer); “with N”: samples with high N addition. Error bars are standard error (SE).

2.5 Study 5: Spatio-temporal patterns of enzyme activities after manure application reflect mechanisms of niche differentiation between plants and microorganisms

Shibin Liu^{a*}, Bahar S. Razavi^b, Xu Su^c, Menuka Maharjan^b, Mohsen Zarebanadkouki^d, Evgenia Blagodatskaya^a, Yakov Kuzyakov^{a,b,e}

Status: published in *Soil Biology & Biochemistry*



^a Department of Soil Science of Temperate Ecosystems, University of Göttingen, Göttingen, Germany

^b Department of Agricultural Soil Science, University of Göttingen, Göttingen, Germany

^c Key Laboratory of Education Ministry on Environments and Resources in Tibetan Plateau, Xining, China

^d Division of Soil Hydrology, University of Göttingen, Göttingen, Germany

^e Huazhong Agricultural University, Wuhan, China

2.5.1 Abstract

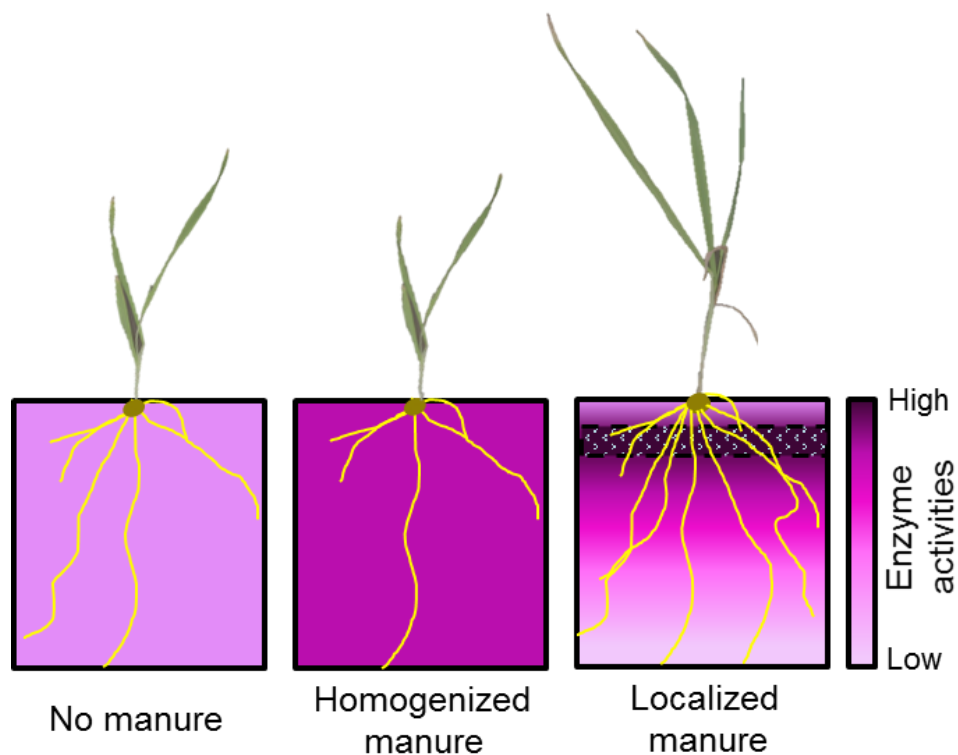
Manure is an important source of nutrients for plants and stimulates a wide range of enzyme-mediated microbial processes. Such stimulation, however, depends on manure distribution and the duration of its decomposition in soil. For the first time, we investigated the spatio-temporal patterns of enzyme activities as affected by manure application strategies: 1) Localized manure: manure application as a layer in the upper soil; 2) Homogenized manure: mixing manure throughout the soil; and 3) Control without manure. Tibetan barley was planted on soil managed with yak manure from the Tibetan Plateau. Soil zymography was used to visualize the two-dimensional distribution and dynamics of the activities of three enzymes responsible for cycling of carbon (β -glucosidase), nitrogen (N-acetylglucosaminidase) and phosphorus (phosphomonoesterase) over 45 days. The manure detritusphere increased enzyme activities relative to the control (which had only the rhizosphere effect of barley) and this stimulation lasted less than 45 days. Enzyme activities in the manure-induced hotspots were higher than on the barley rhizoplane, indicating that the detritusphere stimulated microbial activities more strongly than roots. Homogenized manure led to 3-29% higher enzyme activities than localized manure, but shoot and root biomass was respectively 3.1 and 6.7 times higher with localized manure application. Nutrients released by high enzyme activities within the whole soil volume will be efficiently trapped by microorganisms. In contrast, nutrients released from manure locally are in excess for microbial uptake and remain available for roots. Consequently,

microorganisms were successful competitors for nutrients from homogeneous manure application, while plants benefited more from localized manure application. We conclude that localized manure application decreases competition for nutrients between the microbial community of manure and the roots, and thereby increases plant performance.

Keywords: Manure application strategies, Direct zymography, Tibetan Plateau, Enzyme activity visualization, Barley roots, *Hordeum vulgare*.

Corresponding Author: *Shibin Liu, sliu3@gwdg.de*

Graphical Abstract



2.5.2 Introduction

Livestock manure application has been widely accepted as a sustainable management practice in agriculture, providing environmentally and agronomically sound outcomes (Risse et al., 2006; Brandjes et al., 1996; Scotti et al., 2015). Manure incorporation into soil forms a detritosphere abundant in organic carbon (OC) and nutrients (Moore et al., 2004). It is beneficial for improvement of soil quality and crop production (Butler et al., 2013; Calleja-Cervantes et al., 2015; Zaller et al., 2004).

The application strategy is an important aspect of manure management (Webb et al., 2010; Thomsen, 2005). It affects soil-plant-microbial interactions by determining the locations of nutrients or altering soil properties (moisture, O₂ diffusion, bulk density) (Acosta-Martínez and Waldrip, 2014; Zhu et al., 2015). As a consequence, responses of plants and microorganisms vary depending on the manure application strategy. For instance, mixing of manure into soil increased soil microbial biomass (Lovell and Jarvis, 1996; Malik et al., 2013), but no response of soil microbial biomass was observed when manure pats were placed on the soil surface (Lovell and Jarvis, 1996; Cai et al., 2014). Although remarkable increases in plant production have been reported after either incorporating manure into soil (Malik et al., 2013) or broadcasting manure on the soil surface (Aarons et al., 2009; Matilla, 2006), a direct comparison of plant production under various manure application strategies is still lacking.

Enzymes, excreted by both plants and microbes, are early indicators of soil quality and the main mediators of organic matter decomposition (Nannipieri et al., 2007; Sinsabaugh et al., 2008). Assays of enzyme activities have been widely used to investigate the influence of manure application on soil nutrient cycling and microbial activities. Most studies observed significantly increased enzyme activities in soils amended with livestock manures (Liang et al., 2014; Calleja-Cervantes et al., 2015; Bell et al., 2006). However, the study of spatial and temporal responses of enzyme activities requires advanced visualization technology (Acosta-Martínez and Waldrip, 2014).

On the Tibetan Plateau, yaks are one of the main species of livestock, and around 40% of their manure is used as fertilizer for cropland and pastures (FAO, 2003; Wang, 2009).

However, the impact of yak manure application strategies on the growth of Tibetan barley – a staple crop – and on soil enzyme activities remains unknown. Such knowledge could lead to better manure application strategies. We used soil from the Tibetan Plateau for better consideration of local nutrient conditions and soil properties, and in the context of prevalent ecosystem degradation (Babel et al., 2014; Hafner et al., 2012).

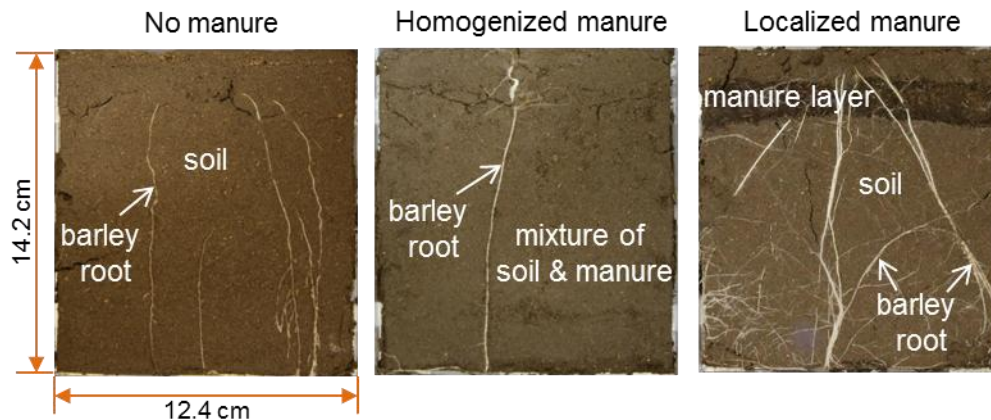


Figure 1 Rhizoboxes with barley growing under three manure application strategies: No manure (left), manure homogenized with the whole soil (middle), and manure localized in the soil layer between 1.0 and 2.5 cm below the soil surface (right).

Here we used direct soil zymography (Razavi et al., 2016) to investigate the impact of different yak manure application strategies on the growth of Tibetan barley (*Hordeum vulgare L.*) and on the temporal and spatial patterns of enzyme activities in Tibetan soil. We compared manure application strategies using three treatments (Fig. 1): 1) Localized manure: manure application as a layer in the upper soil; 2) Homogenized manure: mixing manure throughout the soil; and 3) No manure: a control without manure application. Our objectives were to investigate the effects of manure application strategy on plant shoot and root biomass and on the spatial and temporal patterns of soil enzyme activities. Direct soil zymography was used to visualize and quantify the spatial and temporal distribution of enzyme activity for the three enzymes: β -glucosidase, phosphomonoesterase and N-acetylglucosaminidase. β -glucosidase is responsible for catalyzing the hydrolysis of terminal 1, 4-linked β -D-glucose residues from β -D-glucosides (German et al., 2011) and is involved in the carbon (C) cycle. Phosphomonoesterase, which catalyzes the hydrolysis of organic phosphorus (P) compounds to inorganic P (Eivazi and Tabatabai, 1977; Malcolm, 1983), is involved in

the P cycle. N-acetylglucosaminidase (chitinase), which accomplishes the decomposition of chitin to yield low molecular weight chitooligomers (Hamid et al., 2013), is responsible for C- and nitrogen (N) -acquisition.

The considerable addition of labile organic compounds and nutrients in manure are expected to greatly influence plant and microorganism activities, and therefore soil enzyme activities. We hypothesized - H1: weaker enzyme activities at the root-soil interface as compared with a strong increase of enzyme activities in the manure-induced detritosphere; H2: stronger stimulation of plant growth by the homogenized manure application strategy.

2.5.3 Materials and methods

2.5.3.1 Soil and yak dung sampling

Soil was sampled at the research station “*Kobresia* Ecosystem Monitoring Area” (KEMA), which was established by Prof. Georg Mieke with the support of the VW foundation, and which now belongs to the Tibet University and the Institute of Tibetan Plateau Research (31°16'45"N 92°59'37"E, 4410 m a.s.l.) in Nagqu. The soil was classified as a *Stagnic Eutric Cambisol (Humic)* (WRB, 2014) with a texture of 50% sand, 33% silt and 17% clay. The pH value (H₂O) was 6.9 ± 0.03 and soil bulk density was 0.92 g cm⁻³. Yak dung was collected from Nangqian town, Yu Shu Prefecture (32°04'N, 96°31'E, 3600 m a.s.l.). Before being sampled, dung was piled and composted in the field.

In total, 10 soil core samples (25 cm deep, 5 cm diameter) were taken within an area of ca. 100 m². All the samples were hand-mixed and roots and stones were removed. The composite soil and composted yak dung samples were stored in ziplock bags at 4 °C, transported to the laboratory of the University of Göttingen and passed through a 2 mm sieve in preparation for incubation. Daily mean temperature during the sampling month ranged from 3.2 °C to 21.3 °C, so the temperature used for transportation was not uncommon and would not strongly affect soil and manure characteristics.

Additional soil and dung samples were oven-dried at 60 °C for 48 hours to measure carbon (C) and nitrogen (N) content. Initial water content was measured by oven-drying samples at 105 °C. Soil C and N contents were $3.4 \pm 0.11\%$ and $0.3 \pm 0.01\%$, respectively. The yak dung contained $37 \pm 0.3\%$ C and $1.3 \pm 0.04\%$ N.

2.5.3.2 Experimental set-up

Experimental samples were prepared to simulate the following manure applications (Fig. 1): 1) Localized manure: manure application as a layer buried in the upper soil; 2) Homogenized manure: mixing manure into the soil. Homogenized manure application was comparable to fertilizer broadcasting and plowing; and 3) No manure: a control without manure application. For the localized manure application, 110 g fresh soil (water content: 10 %) was first added to a rhizobox (14.2×12.4×1.0 cm) and then 5 g of composted yak dung (water content: 94%) was evenly spread across the soil surface in a 1.5 cm layer. A small quantity of soil was then spread above the manure to form a shallow soil layer (~1 cm) to ensure plant growth. For the homogenized manure strategy, 110 g fresh soil and 5 g composted yak dung were mixed homogeneously and placed in rhizoboxes (mixture: 4.5 % C and 0.3 % N; water content: 11 %). The third treatment only included 110 g soil and was the control (“No manure”). Each application strategy had three replicates, so a total of nine rhizoboxes were prepared. Tibetan barley seeds (*Hordeum vulgare L.*) were germinated on filter paper for 72 h to ensure plant growth, to avoid fungal contamination and errors caused by seedling difference. One seedling was planted in each rhizobox at a depth of 5 mm. Yak dung (5 g) was added to 110 g soil to meet the optimal C/N ratio for barley growth, taking into consideration the low plant density used in this study (i.e. one seedling for each rhizobox) (Aarons et al., 2009; Liu et al., 2013). The rhizoboxes were placed in an incubation chamber set to 20 °C, with photosynthetically active radiation intensity of $300 \mu\text{mol m}^{-2} \text{s}^{-1}$ and 14 hours daytime, which is within the range of the field conditions during the growing season.

Plants grew for 45 days, after which the roots completely occupied the rhizoboxes. During growth, the rhizoboxes were kept inclined at an angle of 45°, so that the roots grew along the lower wall of the rhizoboxes. The soil water content was maintained at

65% of the water holding capacity by maintaining the rhizobox at constant weight with distilled water.

After the incubation was stopped at day 45, the barley plants were destructively sampled. All visible roots were also picked out from the soil. The roots were washed with distilled water to remove soil particles and plant biomass was oven-dried at 60 °C for 48 hours. Shoot and root biomass were then weighed.

2.5.3.3 Soil zymography and imaging procedure

Zymography was performed after 5, 25 and 45 days as an *in situ* non-destructive technique to study the spatial and temporal patterns of enzyme activities as affected by manure applications. We made the first zymograms at day 5 (at early stage of growth) to avoid strong effects of roots and physical disturbances. We followed the protocol proposed by Spohn and Kuzyakov (2013) and improved by Razavi et al. (2016). Membranes saturated with 4-methylumbelliferone (MUF) substrates were used for visualization of enzyme activities. The substrates become fluorescent when enzymatically hydrolyzed by the corresponding enzyme (Dong et al., 2007). 4-Methylumbelliferyl- β -D-glucoside (MUF-G) was used as substrate to detect β -glucosidase activity; 4-methylumbelliferyl-phosphate (MUF-P) to detect phosphomonoesterase activity; and 4-methylumbelliferyl-N-acetyl- β -D-glucosaminide (MUF-C) to detect chitinase activity. Each of these substrates was separately dissolved to a concentration of 10 mM in universal buffer (MES buffer, pH: 6.7) (Koch et al., 2007) (Sigma-Aldrich, Germany). Polyamide membrane filters (Tao Yuan, China) with a diameter of 20 cm and a pore size of 0.45 μ m were cut to fit the rhizoboxes. Membranes were saturated with the substrate solution for each enzyme. The rhizoboxes were opened from the lower, rooted side and the saturated membranes were applied directly to the soil surface (Razavi et al., 2016). After incubation for 1 h, the membranes were carefully lifted off the soil surface and any attached soil particles were gently removed using tweezers. One hour of incubation time was selected based on preliminary experiments and previous studies (Hoang et al., 2016).

To quantify the zymogram images, a standard calibration that relates the activities of various enzymes to zymogram fluorescence (i.e. fluorescence of the saturated membrane) is required. The calibration was based on zymography of 2×2 cm membranes soaked in a solution of MUF – the fluorescent tag attached to each substrate proxy – with concentrations of 0.01, 0.05, 0.1, 0.5, 1, 3, 6, 8, 10 mM. The amount of MUF on an area basis was calculated from the solution volume taken up by the membrane and its size. The membranes used for calibration were photographed (EOS 5D, Canon) under UV light and analyzed in the same way as for the samples (Razavi et al., 2016).

2.5.3.4 Image processing and analysis

Fluorescence of the zymograms under UV light shows the areas where substrate has been enzymatically degraded. The intensity of fluorescence is proportional to the activity of the enzyme. To get quantitative information, we processed the zymogram images in Matlab, according to Razavi et al. (2016). Briefly, zymograms were transformed to 16-bit grayscale images as matrices and corrected for light variations and camera noise (Menon et al., 2007; Zarebanadkouki et al., 2012). Then, all zymograms were referenced based on the grayvalue of a reference object embedded in all the zymograms. The scaled black flat field identical in all images was considered as a background (reference object) during the whole image processing. We used the grayvalue obtained from these black sides of the sample as the referencing point. After referencing the zymograms, we calculated an average background grayvalue through the zymograms of calibration lines at concentration of zero and subtracted this value from all the zymograms. The grayvalue of each zymography pixel was converted to enzyme activity using the calibration function obtained for each enzyme (Razavi et al., 2016).

The processed 16-bit grayscale images were used for further analysis. To assess the response of plant roots to the manure application strategies in the context of enzyme activities, the average enzyme activities of the rhizoplane were compared with the activities of soil hotspots. Entirely visible, non-overlapping roots at the soil surface were selected. Hotspots were considered to be areas in which the grayvalues of five adjacent

pixels (each equals 0.1×0.1 mm) all exceeded the average greyvalue of the whole image (i.e. >0.7, represented by red in Fig. S1). Twenty squares (each 50×50 pixels) were randomly arranged on these hotspots and the average grayvalue of these squares (G_H) was calculated to represent the average for soil hotspots. The roots distinguishable on a zymogram were segmented and the average grayvalues of the segments (G_R) were calculated. G_R and G_H were then converted to respective enzyme activities: E_R and E_H . The ratio of E_R to E_H was used to compare enzyme activities on the rhizoplane with that in the soil hotspots. Only the ratios at days 25 and 45 were considered in this study, as plant roots were not recognizable for most images at day 5.

To represent the vertical extension of enzyme activities in the localized manure application, the standardized grayvalues were plotted against the depth (cm) from the top of the rhizobox. Briefly, a segmented vertical line was drawn through the image from the top to bottom, and the grayvalues of all the pixels on this line were extracted. All grayvalues were then standardized to the maximal grayvalue. Consequently, all the values ranged from 0 to 1.0. In total, 20 separate vertical lines were randomly selected from each image and the average standardized grayvalues of these replicates were plotted against depth. Five-parameter Weibull regression in Sigmaplot (v. 12.5) was used to correlate the relative units with depth. The depth from the manure application to the constant level of the regression curve was considered as the detritusphere extension of enzyme activity.

Effects of manure application on enzyme activities were quantified as effect sizes:

$$\text{Effect size} = (E_M - E_{CON}) / E_{CON} \quad (1)$$

where E_M is the enzyme activity with manure application (homogenized or localized), and E_{CON} is the enzyme activity of the control. An effect size greater than zero indicates that the manure application strategy had a positive effect on enzyme activity.

To confirm the boundaries of categories of enzyme activities during soil hotspots consideration, one-way analysis of variance (ANOVA) was applied to assess significant differences between independent variables (mean values of five adjacent pixels, i.e. equal to 0.1 mm). The significant results were then considered as a boundary of each

category (from very low activity to hotspot) (Fig. S1). Differences in enzyme activity and plant biomass between the three treatments (no manure, homogenized manure and localized manure) were also tested with ANOVA, where $p < 0.05$ from Tukey's HSD test indicated significance. Normality of the values and homogeneity of variance were tested using Shapiro-Wilk's W test and Levene's test. When data did not meet the normality requirement (e.g. shoot biomass data), the data were transformed by logarithm or square root. All these analyses were performed in STATISTICA 12.0 (StatSoft Inc.).

2.5.4 Results

2.5.4.1 Manure application strategies affected temporal patterns of enzyme activity

Enzyme activities increased from day 5 to day 25 after manure application, but decreased after 25 days (Fig. 2, 3, S2 and S3). Phosphomonoesterase, β -glucosidase and chitinase activities were 47-104 % higher on day 25 than on day 5. However, their activities had decreased 10-27 % by day 45 relative to the activities on day 25. In the control, these enzyme activities had increased 40-72 % by day 25 compared with their activities on day 5, but showed no significant changes between days 25 and 45 (-12 % - +9 %, $p > 0.05$).

All enzyme activities increased with manure application relative to the control (Fig. 4). Homogenized manure generally induced larger increases than localized manure. Homogenized manure increased phosphomonoesterase, β -glucosidase and chitinase activity by 6-41 % in comparison with the control (Fig. 4). In contrast, localized manure induced an increase of phosphomonoesterase and chitinase activities by 7-29 % compared with the control. Localized manure also increased β -glucosidase activity by 16 and 37 % on days 5 and 25, but its activity was 8 % lower than the control on day 45 ($p > 0.05$).

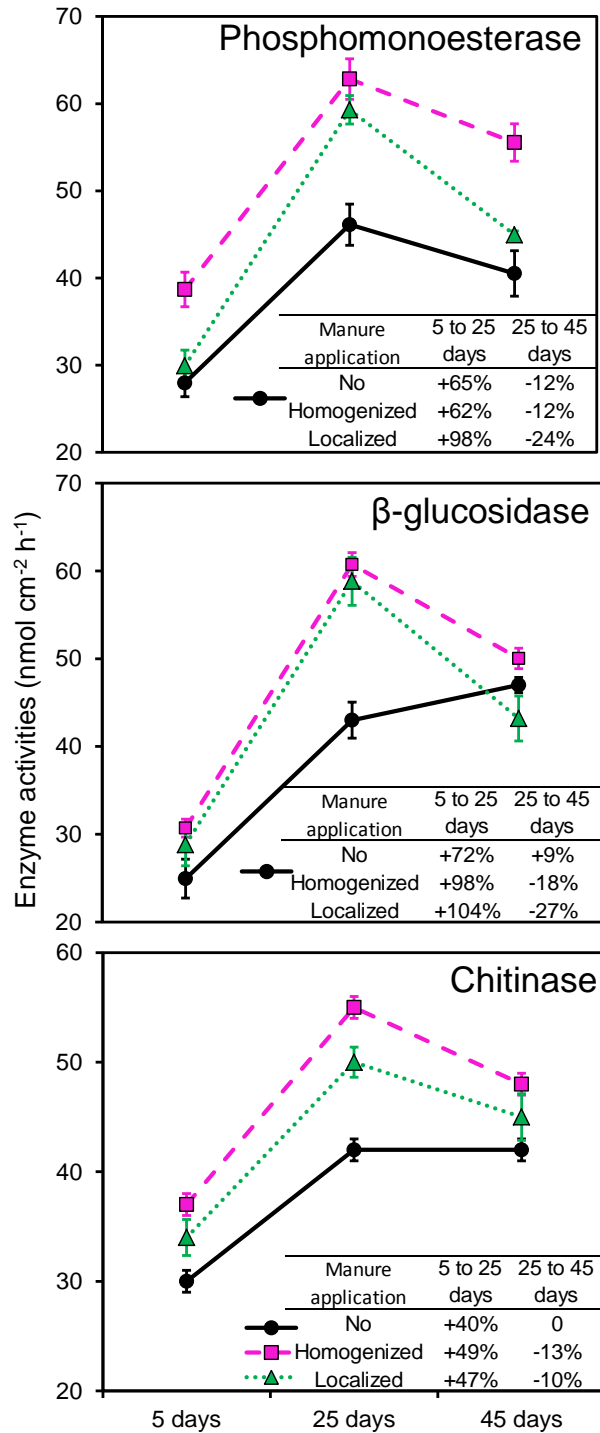


Figure 2 Response of phosphomonoesterase (top), β -glucosidase (middle) and chitinase (bottom) activities to manure application strategies over time. The embedded tables show relative changes of enzyme activities between 5 and 25 days, and 25 and 45 days. Error bars represent standard deviations (\pm SD).

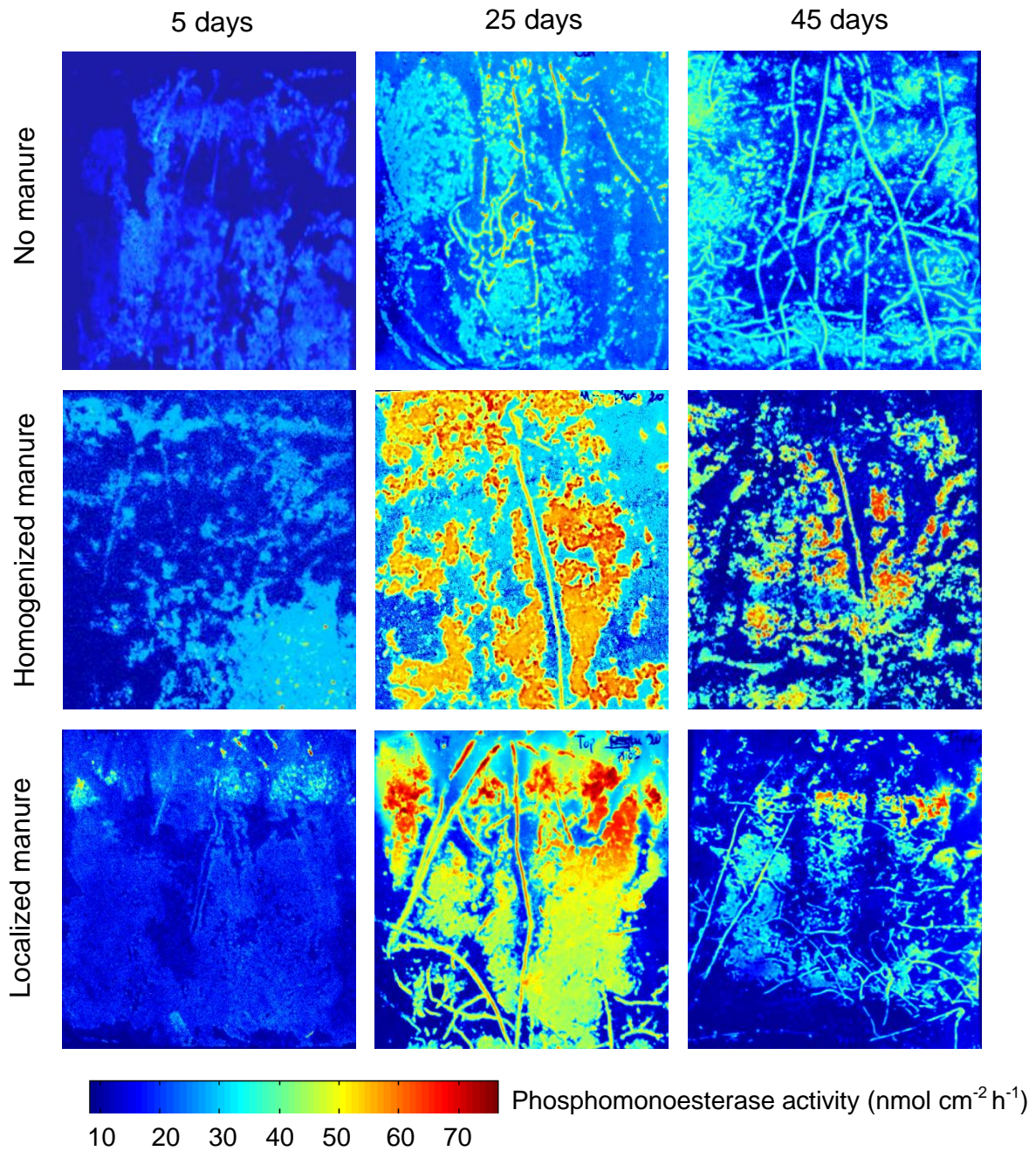


Figure 3 Examples of zymograms for phosphomonoesterase activities. Three rows represent response of activities to three manure application strategies: 1) No manure, 2) Homogenized manure and 3) Localized manure. Figures from left to right are the measurements at days 5, 25 and 45. The color bar corresponds to phosphomonoesterase activity ($\text{nmol cm}^{-2} \text{h}^{-1}$).

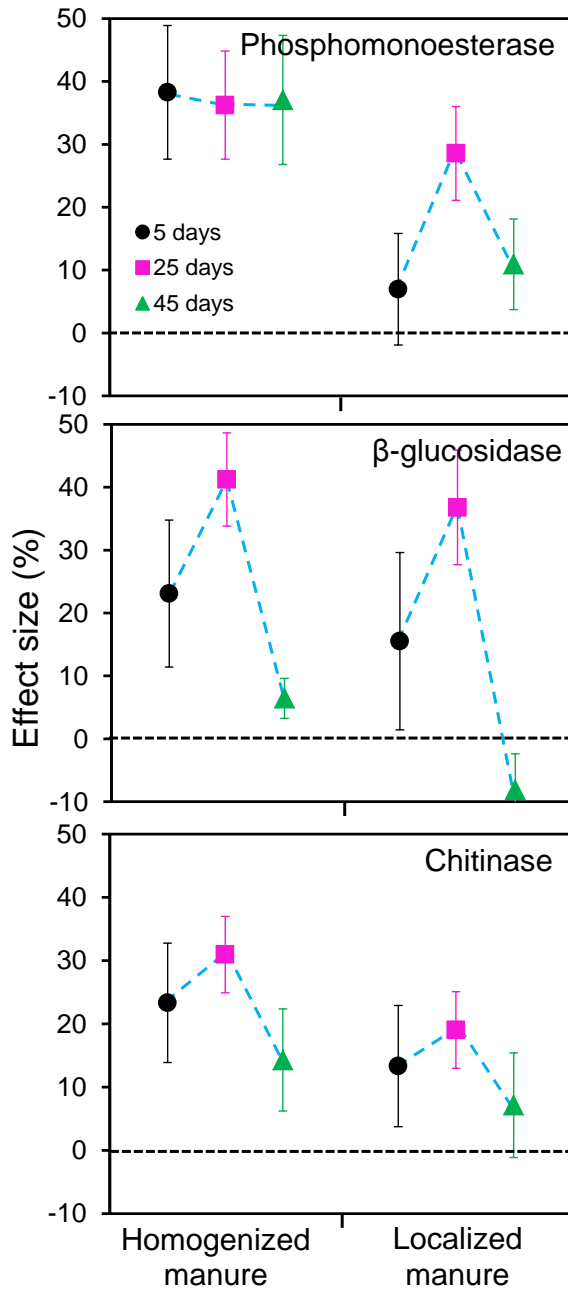


Figure 4 Effects of manure application strategies on phosphomonoesterase (top), β -glucosidase (middle) and chitinase (bottom) activities in the whole soil. The effect size (Eq. 1) shows the change of enzyme activities in soil with homogenized or localized manure addition compared to the control. Error bars represent standard deviations (\pm SD).

2.5.4.2 Detritosphere extension of enzyme activities

A clear downward extension of enzyme activities from the manure layer into the underlying soil was observed with localized manure application (Fig. 5). This extension was enzyme-specific: for example, phosphomonoesterase activity extended from 3.1 cm on day 5 to 9.2 cm on day 25 and finally exceeded 10 cm depth on day 45. In comparison, the extension of β -glucosidase activity was less (3.1 cm on day 5, 4.7 cm on day 25 and 7.0 cm on day 45). Such extension was not seen for chitinase (data not

shown). All distances were measured from the top of the rhizobox and included the depth of the manure layer.

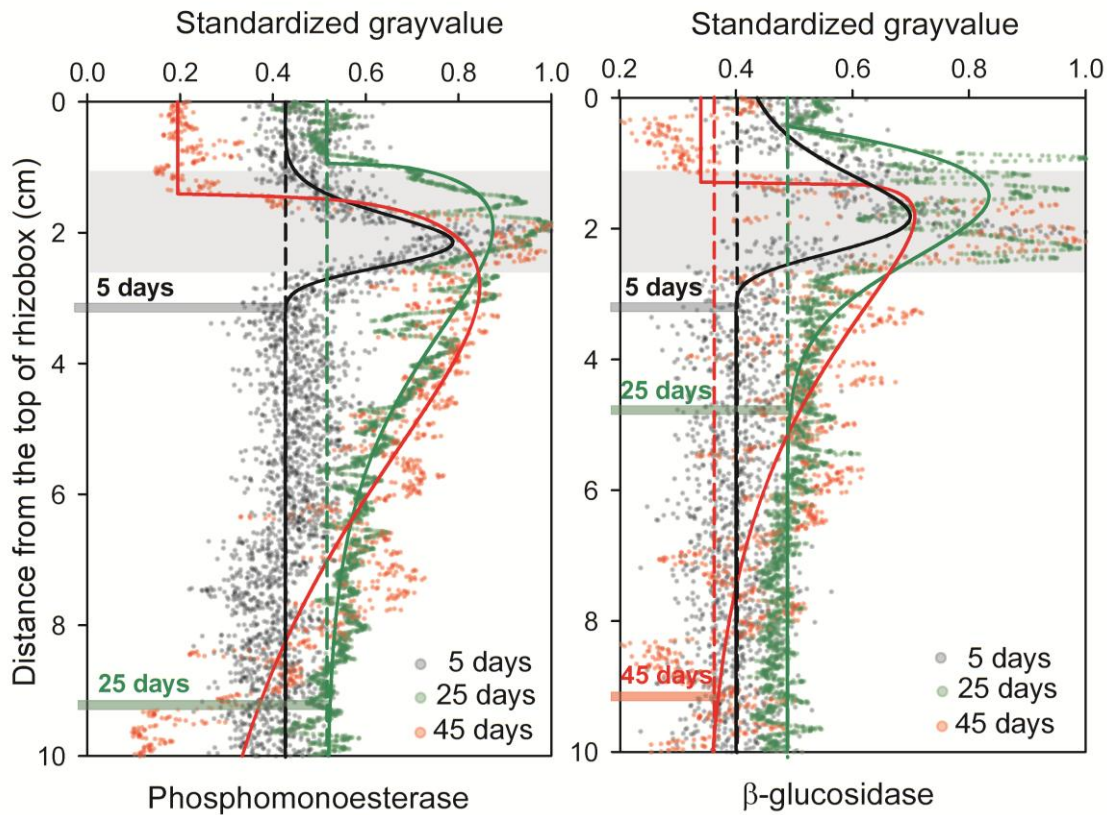


Figure 5 The detritosphere extension for phosphomonoesterase (left) and β -glucosidase activities (right) from the initial manure layer at the top (presented as the shaded area between 1.0 and 2.5 cm) over time. The depth from the manure application to the constant level of the regression curve was considered as the detritosphere extension of enzyme activity. This distance at days 5 and 25 was marked by semitransparent strips (black for 5 days and green for 25 days). Due to the limited rhizobox size, the roots started to grow laterally once they reached the bottom, after around 10-15 days of growth, inducing very high root densities at the bottom (ca. 2-3 cm). To avoid artefacts from high root densities, we used only the upper 10 cm of the membrane. According to the regression, the depth at day 45 already exceeded the membrane boundary (> 10 cm) and thus was not presented. Five-parameter Weibull regression was used to fit enzyme activities with the distance from the top of the rhizobox.

2.5.4.3 Response of plants to manure application strategies

The ratio of E_R to E_H (enzyme activities on the rhizoplane to that in soil hotspots) were all below 1.0 following manure application (Fig. 6, $p < 0.05$), indicating that average enzyme activities on the rhizoplane were lower than the activities in manure-induced soil hotspots. This ratio did not change over time for homogenized manure application. Phosphomonoesterase and β -glucosidase activities on the rhizoplane were both around 10% lower than that in the soil hotspots, while chitinase activity was 15% lower. In

contrast to the homogenized manure, when localized manure was applied, the E_R to E_H ratio decreased from day 25 to day 45. For instance, the ratio of phosphomonoesterase activities decreased from 0.89 to 0.74, while that of β -glucosidase decreased from 0.79 to 0.68. For chitinase, this ratio had the highest change (from 0.98 to 0.75). For the control, this ratio was always around 1.0, except for that of phosphomonoesterase at day 25 (~1.13).

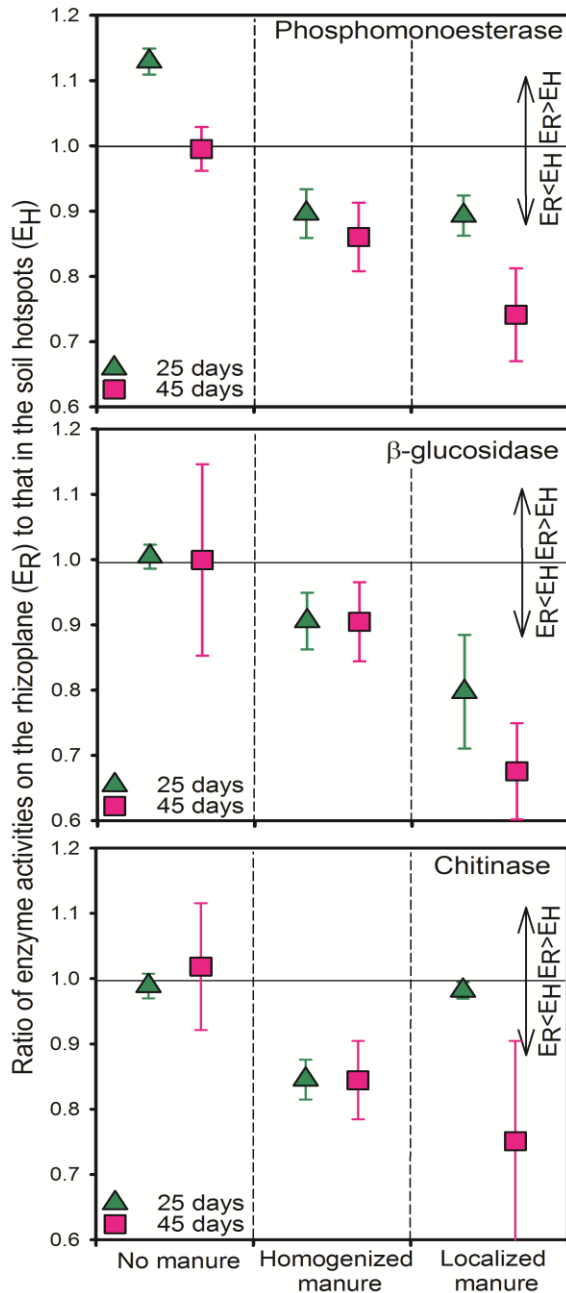


Figure 6 Ratio of E_R to E_H for phosphomonoesterase (top), β -glucosidase (middle) and chitinase (bottom). E_R and E_H are the average enzyme activities on the rhizoplane and in the soil hotspots, respectively. The values above 1.0 reflect higher enzyme activities around the roots than in hotspots in root-free soil areas. Error bars represent standard deviations (\pm SD).

Manure application strategy had significant impact on shoot and root biomass of barley (Fig. 7). Localized manure produced the highest shoot and root biomass (respectively, 3.1 and 6.7 times higher than for homogenized manure, $p < 0.05$). Localized manure significantly decreased the shoot/root ratio from 2.7 to 1.1 ($p < 0.05$), indicating that manure application strategies modified the trade-off between shoot and root biomass.

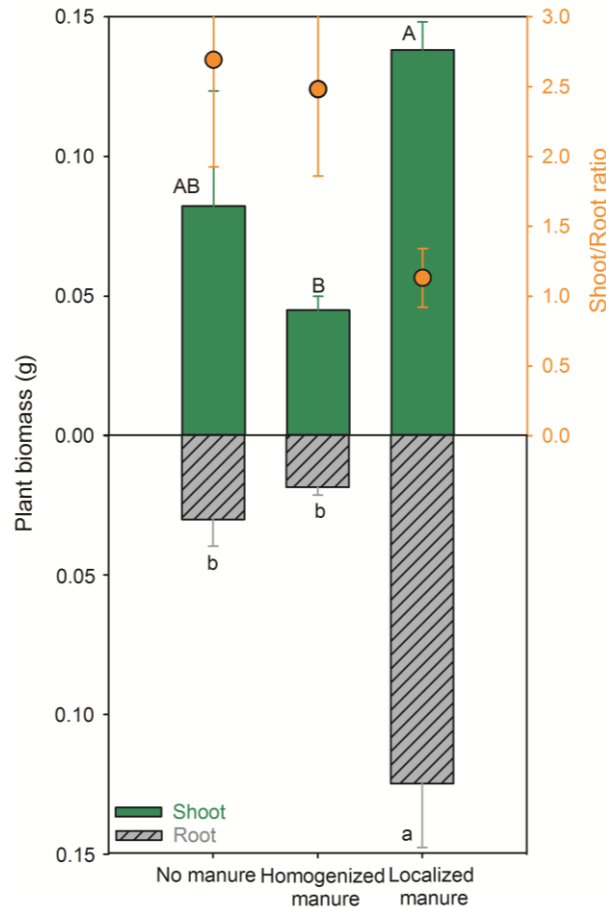


Figure 7 Plant biomass and shoot/root ratio under three manure application strategies: 1) No manure, 2) Homogenized manure and 3) Localized manure. The capital and lower-case letters show significant differences between application strategies ($p < 0.05$). Error bars represent standard deviations (\pm SD).

2.5.5 Discussion

2.5.5.1 Temporal response of enzyme activities to manure application strategy

The capability of manure to regulate soil biological processes was controlled by the manure application strategy. Homogenized manure induced higher activities of C-, N-, and P-acquisition enzymes than localized manure (Fig. 4). Three mechanisms drove these differences in response to manure application strategies. The first two

mechanisms were manure-induced changes to soil physico-chemical properties (Haynes and Naidu, 1998; Dungait et al., 2009). First, by mixing into soil, manure directly loosened the soil, decreased the bulk density and increased the soil porosity (Celik et al., 2004). Second, labile organic compounds and nutrients in the manure were also sufficiently mixed with soil following homogenized manure application. The third mechanism was the loading of indigenous enzymes and microbes from manure into the soil (Dinesh et al., 1998; Criquet et al., 2007; Tiquia et al., 2002). These mechanisms provided a favorable environment for soil microbial proliferation and activity in the rhizoboxes with homogenized manure. In contrast, localized manure affected biological processes through gradual leaching of soluble organic substances and mineral nutrients into the soil (Dickinson et al., 1981). Transport of indigenous enzymes from the manure layer into the soil was negligible due to strong adsorption by soil particles (Poll et al., 2006). Consequently, the combined effects of abiotic (e.g. loose soil structure) and biotic factors (e.g. organic carbon, nutrients, enzymes and microbes) induced higher enzyme activities in the rhizoboxes with homogenized manure.

Activities of all tested enzymes demonstrated a consistent pattern over time for both manure application strategies: i) All enzyme activities increased in the first 25 days. Most enzyme activities in the homogenized and localized manure applications were higher than in the control (Fig. 2). ii) Enzyme activities decreased from day 25 to day 45 in the homogenized and localized manure applications. In contrast, all enzyme activities in the control remained stable during this period. This indicated that the heightened enzyme activities in the homogenized and localized manure applications were mainly caused by the manure-induced detritusphere. Indeed, manure added quite substantial amounts of labile organic substances to the soil, thereby increasing microbial activity and thus nutrient demand and enzyme expression. Over time, these substances were completely decomposed, resulting in lower microbial activity and thus reductions in enzyme activity. Similarly, studies based on destructive methods demonstrated such short-term acceleration of microbial processes induced by sewage sludge (Criquet et al., 2007; Pascual et al., 2002).

Furthermore, the stable enzyme activities from day 25 to day 45 in the control (with only the rhizosphere effect of barley, Fig. 8) demonstrated that the duration of hot moments in the rhizosphere was at least 20 days. This was much longer than the lifetime (only a few days) of hotspots initiated by single releases of root exudate, as evidenced by time-resolved ^{14}C imaging after $^{14}\text{CO}_2$ pulse labeling of *Lolium perenne* (Pausch and Kuzyakov, 2011). Therefore, we conclude that continuous inputs of labile organics due to root growth prolonged the duration of hot moments in the rhizosphere.

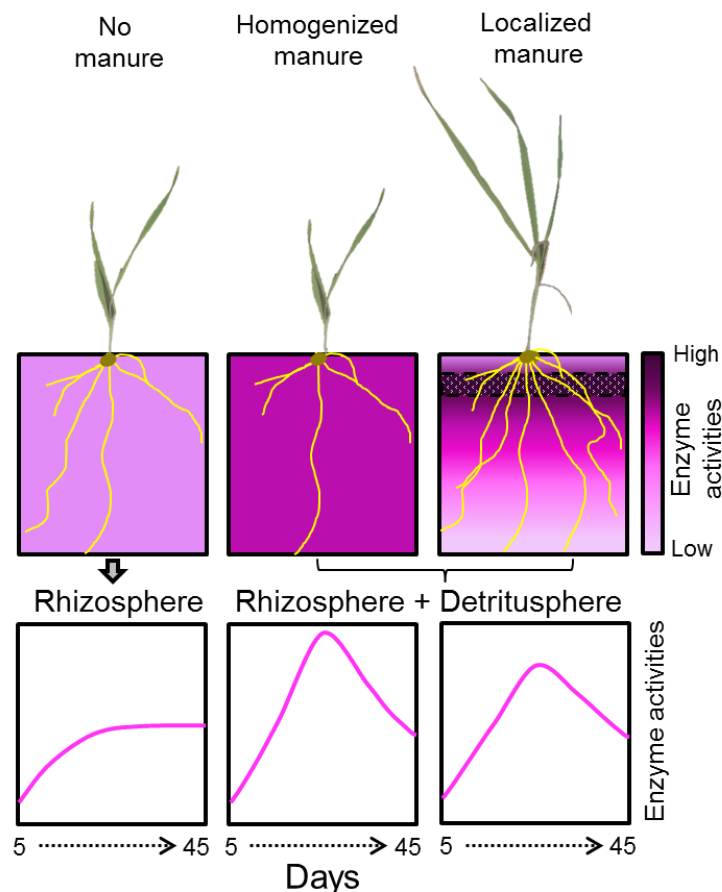


Figure 8 General responses and localization of soil enzyme activities to manure application strategies over time. A clear detritosphere extension of enzyme activities was observed below the localized manure. The manure-induced detritosphere stimulated larger increases of enzyme activities than the “No manure” treatment (i.e. only the rhizosphere effect of barley), although the increase lasted less than 45 days. Homogenized manure elevated enzyme activities more than localized manure, while localized manure induced higher shoot and root biomass than homogenized manure

2.5.5.2 Spatial response of enzyme activities to manure application strategies

The spatial distribution of enzyme activities was noticeably affected by manure application strategy. In localized manure application, enzyme activities in the top

manure layer were higher than in the control and in the soil below this top manure layer (Fig. 3, S2 and S3), which was in accordance with our first hypothesis (H1) about the strong increase of enzyme activities in the detritosphere compared with the root-soil interface below the manure layer. This means that manure itself had higher enzyme and microbial activities, in support of the mechanism that manure-derived enzymes or microorganisms contributed to the increased enzyme and microbial activities (Calleja-Cervantes et al., 2015; Dinesh et al., 1998). Though indigenous enzymes of manure were all concentrated in the localized manure layer, the nutrients in this layer could be leached downward. Leaching of available nutrients and available organics from the manure layer stimulated microorganisms, and consequently enzyme activities, in the soil below the layer (Kang et al., 2009). Therefore, enzyme activities extended downwards over time because of the redistribution of nutrients and organics (Fig. 5). Such extension indicated a gradual influence of manure on soil biochemical processes and this influence was also enzyme-specific. For instance, phosphomonoesterase exhibited deeper and faster downward extension (Fig. 5). In contrast, this extension was narrower for β -glucosidase. The significantly higher ratio of E_R to E_H for phosphomonoesterase (~ 1.13) in the control also demonstrated that phosphomonoesterase activity on the rhizoplane was 13 % higher than in the soil hotspots, suggesting that the soil was P-deficient (Ren et al., 2016) and thus the plant secreted more phosphomonoesterase to obtain inorganic P for its growth (Hunter et al., 2014). In comparison, β -glucosidase, which is mostly involved in the degradation of cellulose, showed a narrower extension. The wider extension of phosphomonoesterase compared to β -glucosidase activities has also been observed in the rhizosphere (Razavi et al., 2016). In the present study, the detritosphere extension of enzyme activities was much wider than the rhizosphere extension observed in other studies (e.g. Razavi et al., 2016; Tarafdar and Jungk, 1987; Sauer et al., 2006). This is explained by the direction of water fluxes: to the roots in the rhizosphere, but from the manure layer downwards. Consequently, extension of enzyme activities was much faster and wider in the detritosphere than in the rhizosphere, due to vertical diffusion and leaching processes.

2.5.5.3 Response of plants to manure application strategies

Following manure application, enzyme activities in the manure-induced detritosphere were higher than on root surfaces. This – in accordance with our first hypothesis (H1) - indicated that the detritosphere became more attractive to microbes than the rhizosphere, because high microbial activities tended to be in the hotspots of bulk soil instead of being balanced between the rhizoplane and soil hotspots, as in the control ($E_R \approx E_H$). Furthermore, though enzyme activities on the rhizoplane were lower, the reason for this may differ between homogenized and localized manure applications. For the homogenized manure application, tough competition for inorganic and organic nutrients between microbes and roots was initiated as soon as manure-derived microbes and labile substrates were introduced by mixing manure into the soil (Kuzyakov and Blagodatskaya, 2015; Malik et al., 2013; Xu et al., 2006, 2011). This may temporarily reduce plant nutrient availability, depress root growth and explain the lower enzyme activities on the root surface for homogenized manure application. In contrast, with localized manure application, the pre-existing and newly mineralized nutrients were easily leached downward and competition between microbes and plant roots within the localized manure layer was weaker than for the homogenized manure application. This spatial niche differentiation for the manure microbial community and roots decreased their competition for nutrients and simultaneously increased nutrient uptake, and so, the plant biomass. Both situations were also reflected in the shoot and root biomass at day 45: shoot and root biomass with localized manure application were respectively 3.1 and 6.7 times higher than for homogenized manure application, and so our second hypothesis (H2) was rejected. Compared to the control, the relatively low plant biomass in the homogenized manure application also indicated that strong competition between microbes and roots existed when manure was homogenized with soil. This significant difference demonstrated that localized manure was more advantageous for barley growth than homogenized manure.

This is especially important on the Tibetan Plateau, because soils have been very seriously degraded in the last 30-50 years due to intensive human activities (e.g. overgrazing) and climate change (Chen et al., 2013). This has induced large soil

organic carbon and nutrient losses and thus considerably decreased soil fertility. Localized manure application has been found to increase soil ammonium and nitrate concentrations in soils of the Tibetan Plateau (Cai et al., 2014; He et al., 2009). However, manure application at the soil surface leads to ammonia volatilization, involving significant nitrogen losses and negative effects on the environment. This is especially important on the Tibetan Plateau, because the solar radiation is much higher compared with other regions around the world (Liu et al., 2012), which increases the temperature of manure and accelerates the ammonia volatilization. Alternatively, homogenized manure application may reduce nitrogen losses by avoiding the impact of solar radiation. Therefore, to thoroughly investigate the impact of both manure application strategies, the effects on nitrogen emissions and leaching should be considered.

2.5.6 Conclusions

For the first time, we elucidated and visualized the impacts of different manure application strategies on enzyme activities in soil *in situ*, spatially and temporally. The manure-induced detritosphere increased enzyme activities more than the rhizosphere effect of barley alone. Manure-induced hotspots also showed higher enzyme activities than the rhizoplane. Together, these findings demonstrate that microbial activities in the detritosphere are much more stimulated than on the root-soil interface (i.e. rhizosphere and rhizoplane). The detritosphere's vertical extension of phosphomonoesterase activity from the localized manure application was much faster than that of β -glucosidase activity. Overall, homogenized manure increased enzyme activities more than localized manure. However, localized manure induced 3.1 and 6.7 times higher shoot and root biomass, respectively. We conclude that localized manure application decreases competition for nutrients between microorganisms and roots and simultaneously increases plant performance.

2.5.7 Acknowledgements

The authors thank Ingrid Ostermeyer for laboratory assistance and Yanling Shang for sampling assistance. We acknowledge the China Scholarship Council (CSC) for financial support of SL and Erasmus mundus (Experts4Asia) for supporting MM. The

contribution of BSR was supported by DAAD and EB by the Russian Science Foundation (project N^o 14-14-00625). This study was supported by the German Research Foundation (DFG) within the project 'Root exudation and the biophysics of the rhizosphere' (KU 1184/33-1) and the National Science Foundation of China (NSFC; grant number: 41671253).

2.5.8 References

- Aarons, S.R., O'Connor, C.R., Hosseini, H.M., Gourley, C.J.P., 2009. Dung pads increase pasture production, soil nutrients and microbial biomass carbon in grazed dairy systems. *Nutrient Cycling in Agroecosystems* 84, 81-92. DOI: 10.1007/s10705-008-9228-5.
- Acosta-Martínez, V., Waldrip, H.M., 2014. Soil enzyme activities as affected by manure types, application rates, and management practices. In: He, Z., Zhang, H. (Eds.), *Applied Manure and Nutrient Chemistry for Sustainable Agriculture and Environment*. Springer Netherlands, pp 99-122, DOI: 10.1007/978-94-017-8807-6_6.
- Babel, W., Biermann, T., Coners, H., Falge, E., Seeber, E., Ingrisch, J., Schleuß, P.M., Gerken, T., Leonbacher, J., Leipold, T., Willinghöfer, S., Schützenmeister, K., Shibistova, O., Becker, L., Hafner, S., Spielvogel, S., Li, X., Xu, X., Sun, Y., Zhang, L., Yang, Y., Ma, Y., Wesche, K., Graf, H.F., Leuschner, C., Guggenberger, G., Kuzyakov, Y., Miehe, G., Foken, T., 2014. Pasture degradation modifies the water and carbon cycles of the Tibetan highlands. *Biogeosciences* 11, 6633-6656. DOI: 10.5194/bg-11-6633-2014.
- Bell, J.M., Robinson, C.A., Schwartz, R.C., 2006. Changes in soil properties and enzymatic activities following manure applications to a rangeland. *Rangeland Ecology & Management* 59, 314-320. DOI: 10.2111/05-172R1.1.
- Brandjes, P.J., de Wit, J., van der Meer, H.G., 1996. Environmental impact of animal manure management. *Food and Agriculture Organization of the United Nations*. Available at (2017/1/3): <http://www.fao.org/wairdocs/lead/x61113e/x61113e00.htm#Contents>.
- Butler, T.J., Weindorf, D.C., Han, K.J., Muir, J.P., 2013. Dairy manure compost quality effects on corn silage and soil properties. *Compost Science & Utilization* 17(1), 18-24. DOI: 10.1080/1065657X.2009.10702395.
- Cai, Y.J., Wang, X.D., Tian, L.L., Zhao, H., Lu, X.Y., Yan, Y., 2014. The impact of excretal returns from yak and Tibetan sheep dung on nitrous oxide emissions in an alpine steppe on the Qinghai-Tibetan Plateau. *Soil Biology & Biochemistry* 76, 90-99. DOI: 10.1016/j.soilbio.2014.05.008.
- Calleja-Cervantes, M.E., Fernández-González, A.J., Irigoyen, I., Fernández-López, M., Aparicio-Tejo, P.M., Menéndez, S., 2015. Thirteen years of continued application of composted organic wastes in a vineyard modify soil quality characteristics. *Soil Biology & Biochemistry* 90, 241-254. DOI: 10.1016/j.soilbio.2015.07.002.
- Celik, I., Ortas, I., Kilic, S., 2004. Effects of compost, mycorrhiza, manure and fertilizer on some physical properties of a Chromoxerert soil. *Soil & Tillage Research* 78, 59-67. DOI: 10.1016/j.still.2004.02.012.
- Chen, H., Zhu, Q., Peng, C., Wu, N., Wang, Y., Fang, X., Gao, Y., Zhu, D., Yang, G., Tian, J., Kang, X., Piao, S., Ouyang, H., Xiang, W., Luo, Z., Jiang, H., Song, X., Zhang, Y., Yu, G., Zhao, X., Gong, P., Yao, T., Wu, J., 2013. The impacts of climate change and human activities on biogeochemical cycles on the Qinghai-Tibetan Plateau. *Global Change Biology* 19, 2940-2955. doi: 10.1111/gcb.12277.
- Criquet, S., Braud, A., Nèble, S., 2007. Short-term effects of sewage sludge application on phosphatase activities and available P fractions in Mediterranean soils. *Soil Biology & Biochemistry* 39, 921-929. DOI: 10.1016/j.soilbio.2006.11.002.
- Dickinson, C.H., Underhay, V.S.H., Ross, V., 1981. Effect of season, soil fauna and water content on the decomposition of cattle dung pats. *New Phytologist* 88, 129-141. DOI: 10.1111/j.1469-8137.1981.tb04576.x.
- Dinesh, R., Dubey, R.P., Prasad, G.S., 1998. Soil microbial biomass and enzyme activities as influenced by organic manure incorporation into soils of a rice-rice system. *Journal of Agronomy and Crop Science* 181(3), 173-178. DOI: 10.1111/j.1439-037X.1998.tb00414.x.
- Dong, S.F., Brooks, D., Jones, M.D., Grayston, S.J., 2007. A method for linking *in situ* activities of hydrolytic enzymes to associated organisms in forest soils. *Soil Biology & Biochemistry* 39(9), 2414-2419. DOI: 10.1016/j.soilbio.2007.03.030.
- Dungait, J.A.J., Bol, R., Bull, I.D., Evershed, R.P., 2009. Tracking the fate of dung-derived carbohydrates in a temperate grassland soil using compound-specific stable isotope analysis. *Organic Geochemistry* 40, 1210-1218. DOI: 10.1016/j.orggeochem.2009.08.001.
- Eivazi, F., Tabatabai, M.A., 1977. Phosphatases in soils. *Soil Biology & Biochemistry* 9, 167e172. DOI: 10.1016/0038-0717(77)90070-0.

- FAO., 2003. The Yak (second edition). Available at (2017/1/3): <http://www.fao.org/docrep/006/ad347e/ad347e0l.htm#bm21.9>.
- German, D.P., Weintraub, M.N., Grandy, A.S., Lauber, C.L., Rinkes, Z.L., Allison, S.D., 2011. Optimization of hydrolytic and oxidative enzyme methods for ecosystem studies. *Soil Biology & Biochemistry* 43, 1387-1397. DOI: 10.1016/j.soilbio.2011.03.017.
- Hafner, S., Unteregelsbacher, S., Seeber, E., Xu, X., Li, X., Guggenberger, G., Miehe, G., Kuzyakov, Y., 2012. Effect of grazing on carbon stocks and assimilate partitioning in Tibetan montane pasture revealed by ¹³C₂ pulse labeling. *Global Change Biology* 18(2), 528-538. DOI: 10.1111/j.1365-2486.2011.02557.x.
- Hamid, R., Khan, M.A., Ahmad, M., Ahmad, M.M., Abdin, M.Z., Javed, S., 2013. Chitinase: An update. *Journal of Pharmacy & BioAllied Sciences* 5(1), 21-29. DOI: 10.4103/0975-7406.106559.
- Haynes, R.J., Naidu, R., 1998. Influence of lime, fertilizer and manure applications on soil organic matter content and soil physical conditions: a review. *Nutrient Cycling in Agroecosystems* 51, 123-137. DOI: 10.1023/A:1009738307837.
- He, Y.X., Sun, G., Liu, L., Luo, P., Wu, N., Luo, G.R., 2009. Effect of yak dung on high-frigid meadow soil nutrition in northwestern Sichuan, China. *Chinese Journal of Applied and Environmental Biology* 15: 666-671. (in Chinese with English abstract)
- Hoang, D.T.T., Razavi, B.S., Kuzyakov, Y., Blagodatskaya, E., 2016. Earthworm burrows: Kinetics and spatial distribution of enzymes of C-, N- and P- cycles. *Soil Biology & Biochemistry* 99, 94-103. DOI: 10.1016/j.soilbio.2016.04.021.
- Hunter, P.J., Teakle, G.R., Bending, G.D., 2014. Root traits and microbial community interactions in relation to phosphorus availability and acquisition, with particular reference to Brassica. *Frontiers in Plant Science* 5, 27. DOI: 10.3389/fpls.2014.00027.
- Kang, H., Kang, S., Lee, D., 2009. Variations of soil enzyme activities in a temperate forest soil. *Ecological Research* 24, 1137-1143. DOI: 10.1007/s11284-009-0594-5.
- Koch, O., Tschirko, D., Kandeler, E., 2007. Temperature sensitivity of microbial respiration, nitrogen mineralization, and potential soil enzyme activities in organic alpine soils: temperature sensitivity in alpine soils. *Global Biogeochemical Cycles* 21(4), GB4017. DOI: 10.1029/2007GB002983.
- Kuzyakov, Y., Blagodatskaya, E., 2015. Microbial hotspots and hot moments in soil: Concept & review. *Soil Biology & Biochemistry* 83, 184-199. DOI: 10.1016/j.soilbio.2015.01.025.
- Liang, Q., Chen, H., Gong, Y., Yang, H., Fan, M., Kuzyakov, Y., 2014. Effects of 15 years of manure and mineral fertilizers on enzyme activities in particle-size fractions in a North China Plain soil. *European Journal of Soil Biology* 60, 112-119. DOI: 10.1016/j.ejsobi.2013.11.009.
- Liu, G.Y., Nima, Z.X., Nima, Z.X., Song, G.Y., 2013. The study on barley production under different nitrogen levels. *Tibet Journal of Agricultural Sciences* 35, 17-20. (in Chinese with English abstract)
- Liu, J.D., Liu, J.M., Linderholm, H.W., Chen, D.L., Yu, Q., Wu, D.R., Haginoya, S., 2012. Observation and calculation of the solar radiation on the Tibetan Plateau. *Energy Conversion and Management* 57, 23-32. DOI: 10.1016/j.enconman.2011.12.007.
- Lovell, R.D., Jarvis, S.C., 1996. Effect of cattle dung on soil microbial biomass C and N in a permanent pasture soil. *Soil Biology & Biochemistry* 28(3), 291-299. DOI: 10.1016/0038-0717(95)00140-9.
- Malcolm, R.E., 1983. Assessment of phosphatase activity in soils. *Soil Biology & Biochemistry* 15, 403e408. DOI: 10.1016/0038-0717(83)90003-2.
- Malik, M.A., Khan, K.S., Marschner, P., Fayyaz-ul-Hassean., 2013. Microbial biomass, nutrient availability and nutrient uptake by wheat in two soils with organic amendments. *Journal of Soil Science and Plant Nutrition* 13 (4), 955-966. DOI: 10.4067/S0718-95162013005000075.
- Matilla, P.K., 2006. Ammonia emissions from pig and cattle slurry in the field and utilization of slurry nitrogen in crop production. Doctoral Dissertation. *Agrifood Research Reports* 87. Available at (2017/1/3): <http://www.mtt.fi/met/pdf/met87.pdf>.
- Menon, M., Robinson, B., Oswald, S.E., Kaestner, A., Abbaspour, K.C., Lehmann, E., Schulin, R., 2007. Visualization of root growth in heterogeneously contaminated soil using neutron radiography. *European Journal of Soil Science* 58, 802-810. DOI: 10.1111/j.1365-2389.2006.00870.x.
- Moore, J.C., Berlow, E.L., Coleman, D.C., de Ruiter, P.C., Dong, Q., Hastings, A., Johnson, N.C., McCann, K.S., Melville, K., Morin, P.J., Nadelhoffer, K., Rosemond, A.D., Post, D.M., Sabo, J.L., Scow, K.M., Vanni, M.J., Wall, D.H., 2004. Detritus, trophic dynamics and biodiversity. *Ecology Letters* 7, 584-600. DOI:10.1111/j.1461-0248.2004.00606.x.
- Nannipieri, P., 1994. The potential use of soil enzymes as indicators of productivity, sustainability and pollution. In: Pankhurst, C.E., Doube, B.M., Gupta, V.V.S.R., Grace, P.R. (Eds.), *Soil Biota: Management in Sustainable Farming Systems*. CSIRO, East Melbourne, pp 238-244.
- Nannipieri, P., Ascher, J., Ceccherini, M.T., Landi, L., Pietramellara, G., Renella, G., Valori, F., 2007. Microbial diversity and microbial activity in the rhizosphere. *Ciencia del suelo* 25, 89e97.
- Pascual, J.A., Moreno, J.L., Hernández, T., García C., 2002. Persistence of immobilized and total urease and phosphatase activities in a soil amended with organic wastes. *Bioresource Technology*, 82(1): 73-78. DOI: 10.1016/S0960-8524(01)00127-4

- Pausch, J., Kuzyakov, Y., 2011. Photoassimilate allocation and dynamics of hotspots in roots visualized by ^{14}C phosphor imaging. *Journal of Plant Nutrition and Soil Science* 174, 12-19. DOI: 10.1002/jpln.200900271.
- Poll, C., Ingwersen, J., Stemmer, M., Gerzabek, M.H., Kandeler, E., 2006. Mechanisms of solute transport affect small-scale abundance and function of soil microorganisms in the detritosphere. *European Journal of Soil Science* 57, 583-595. DOI: 10.1111/j.1365-2389.2006.00835.x.
- Razavi, B.S., Zarebanadkouki, M., Blagodatskaya, E., Kuzyakov, Y., 2016. Rhizosphere shape of lentil and maize: Spatial distribution of enzyme activities. *Soil Biology & Biochemistry* 96, 229-237. DOI: 10.1016/j.soilbio.2016.02.020.
- Ren, F., Yang, X.X., Zhou, H.K., Zhu, W.Y., Zhang, Z.H., Chen, L.T., Cao, G.M., He, J.S., 2016. Contrasting effects of nitrogen and phosphorus addition on soil respiration in an alpine grassland on the Qinghai-Tibetan Plateau. *Scientific Reports* 6, 34786. DOI: 10.1038/srep34786.
- Risse, L.M., Cabrera, M.L., Franzluebbers, A.J., Gaskin, J.W., Gilley, J.E., Killom, R., Radcliffe, D.E., Tollner, W.E., Zhang, H., 2006. Land application of manure for beneficial reuse. In: Rice, J.M., Caldwell, D.F., Humenik, F.J. (Eds.), *Animal agriculture and the environment: National Center for Manure and Animal Waste Management white papers*. American Society of Agricultural and Biological Engineers, St. Joseph, pp 283–316.
- Sauer, D., Kuzyakov, Y., Stahr, K., 2006. Spatial distribution of root exudates of five plant species as assessed by ^{14}C labelling. *Journal of Plant Nutrition and Soil Science* 169, 360-362. DOI: 10.1002/jpln.200621974.
- Scotti, R., Bonanomi, G., Scelza, R., Zoina, A., Rao, M.A., 2015. Organic amendments as sustainable tool to recovery fertility in intensive agricultural systems. *Journal of Soil Science and Plant Nutrition* 15(2), 333-352. DOI: 10.4067/S0718-95162015005000031.
- Sinsabaugh, R.L., Lauber, C.L., Weintraub, M.N., Ahmed, B., Allison, S.D., Crenshaw, C., Contosta, A.R., Cusack, D., Frey, S., Gallo, M.E., Gartner, T.B., Hobbie, S.E., Holland, K., Keeler, B.L., Powers, J.S., Stursova, M., Takacs-Vesbach, C., Waldrop, M.P., Wallenstein, M.D., Zak, D.R. and Zeglin, L.H., 2008. Stoichiometry of soil enzyme activity at global scale. *Ecology Letters* 11, 1252–1264. DOI:10.1111/j.1461-0248.2008.01245.x.
- Spohn, M., Kuzyakov, Y., 2013. Distribution of microbial- and root-derived phosphatase activities in the rhizosphere depending on P availability and C allocation-Coupling soil zymography with ^{14}C imaging. *Soil Biology & Biochemistry* 67, 106-113. DOI: 10.1016/j.soilbio.2013.08.015.
- Tarafdar, J.C., Jungk, A., 1987. Phosphatase activity in the rhizosphere and its relation to the depletion of soil organic phosphorus. *Biology and Fertility of Soils* 3, 199-204. DOI: 10.1007/BF00640630.
- Thomsen, I.K., 2005. Crop N utilization and leaching losses as affected by time and method of application of farmyard manure. *European Journal of Agronomy* 22(1), 1-9. DOI: 10.1016/j.eja.2003.10.008.
- Tiquia, S.M., 2002. Evolution of extracellular enzyme activities during manure composting. *Journal of Applied Microbiology* 92, 764-775. DOI: 10.1046/j.1365-2672.2002.01582.x.
- Wang, Q., 2009. Prevention of Tibetan eco-environmental degradation caused by traditional use of biomass. *Renewable and Sustainable Energy Reviews* 13, 2562-2570. DOI: 10.1016/j.rser.2009.06.013.
- Webb, J., Pain, B., Bittman, S., Morgan, J., 2010. The impacts of manure application methods on emissions of ammonia, nitrous oxide and on crop response-A review. *Agriculture, Ecosystems and Environment* 137, 39-46. DOI: 10.1016/j.agee.2010.01.001.
- WRB., 2014. *World Reference Base for Soil Resources*. FAO, World Soil Resources Reports 106, Rome.
- Xu, X., Ouyang, H., Kuzyakov, Y., Richter, A., Wanek, W., 2006. Significance of organic nitrogen acquisition for dominant species in an alpine meadow on the Tibet plateau, China. *Plant and Soil* 285, 221-231. DOI: 10.1007/s11104-006-9007-5.
- Xu, X., Ouyang, H., Richter, A., Wanek, W., Cao, G., Kuzyakov, Y., 2011. Spatio-temporal variations determine plant-microbe competition for inorganic nitrogen in an alpine meadow. *Journal of Ecology* 99, 563-571. DOI: 10.1111/j.1365-2745.2010.01789.x.
- Zaller, J.G., Köpke, U., 2004. Effects of traditional and biodynamic farmyard manure amendment on yields, soil chemical, biochemical and biological properties in a long-term field experiment. *Biology and Fertility of Soils* 40, 222-229. DOI: 10.1007/s00374-004-0772-0.
- Zarebanadkouki, M., Kim, Y.X., Moradi, A.B., Vogel, H.J., Kaestner, A., Carminati, A., 2012. Quantification and modeling of local root water uptake using neutron radiography and deuterated water. *Vadose Zone Journal* 11. DOI: 10.2136/vzj2011.0196.
- Zhu, K., Bruun, S., Larsen, M., Glud, R.N., Jensen, L.S., 2015. Heterogeneity of O_2 dynamics in soil amended with animal manure and implications for greenhouse gas emissions. *Soil Biology & Biochemistry* 84, 96-106. DOI: 10.1016/j.soilbio.2015.02.012.

2.5.9 Supporting information

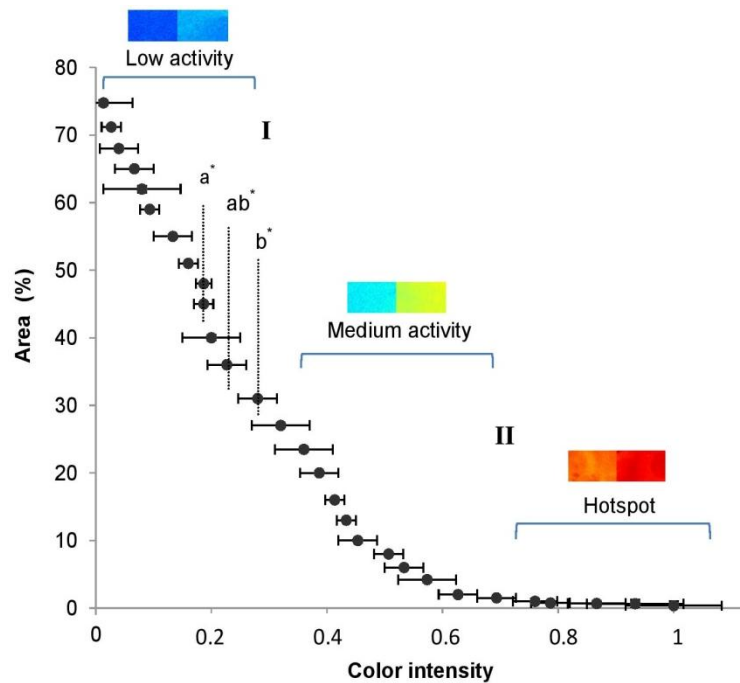


Figure S1 Example of detecting the boundaries of three categories of enzyme activities: Low activity, Medium activity, and Hotspots. The percentage of the area of MUF concentration in the total image was considered as a function of color intensity. Data points depict means calculated from five adjacent pixels. Asterisks indicate significant differences between the mean values of five adjacent pixels.

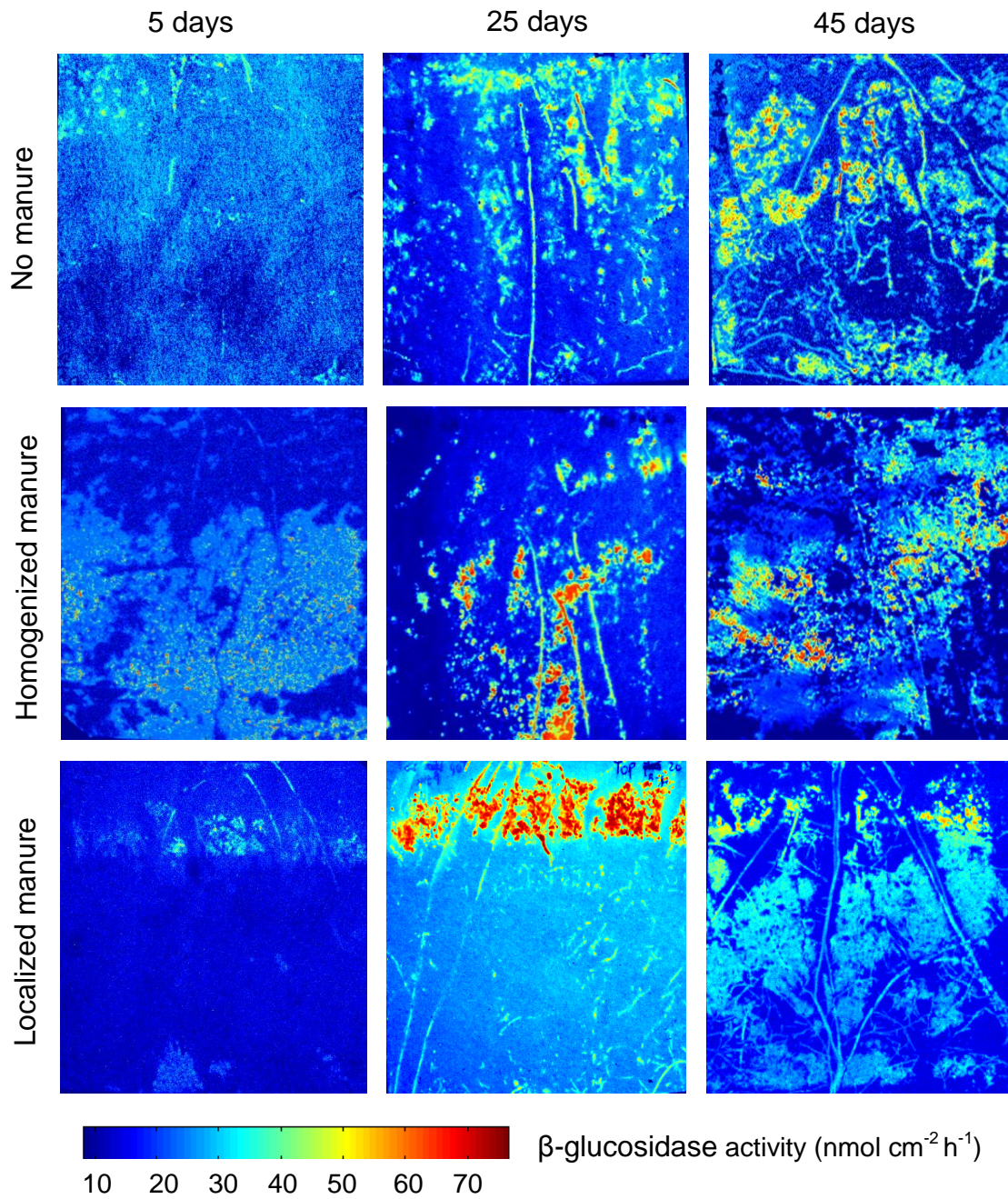


Figure S2. Examples of zymograms for β -glucosidase activity. Three rows represent response of activities to three manure application strategies: 1) No manure, 2) Homogenized manure and 3) Localized manure. Figures from left to right are the measurements at days 5, 25 and 45. The color bar corresponds to β -glucosidase activity ($\text{nmol cm}^{-2} \text{h}^{-1}$).

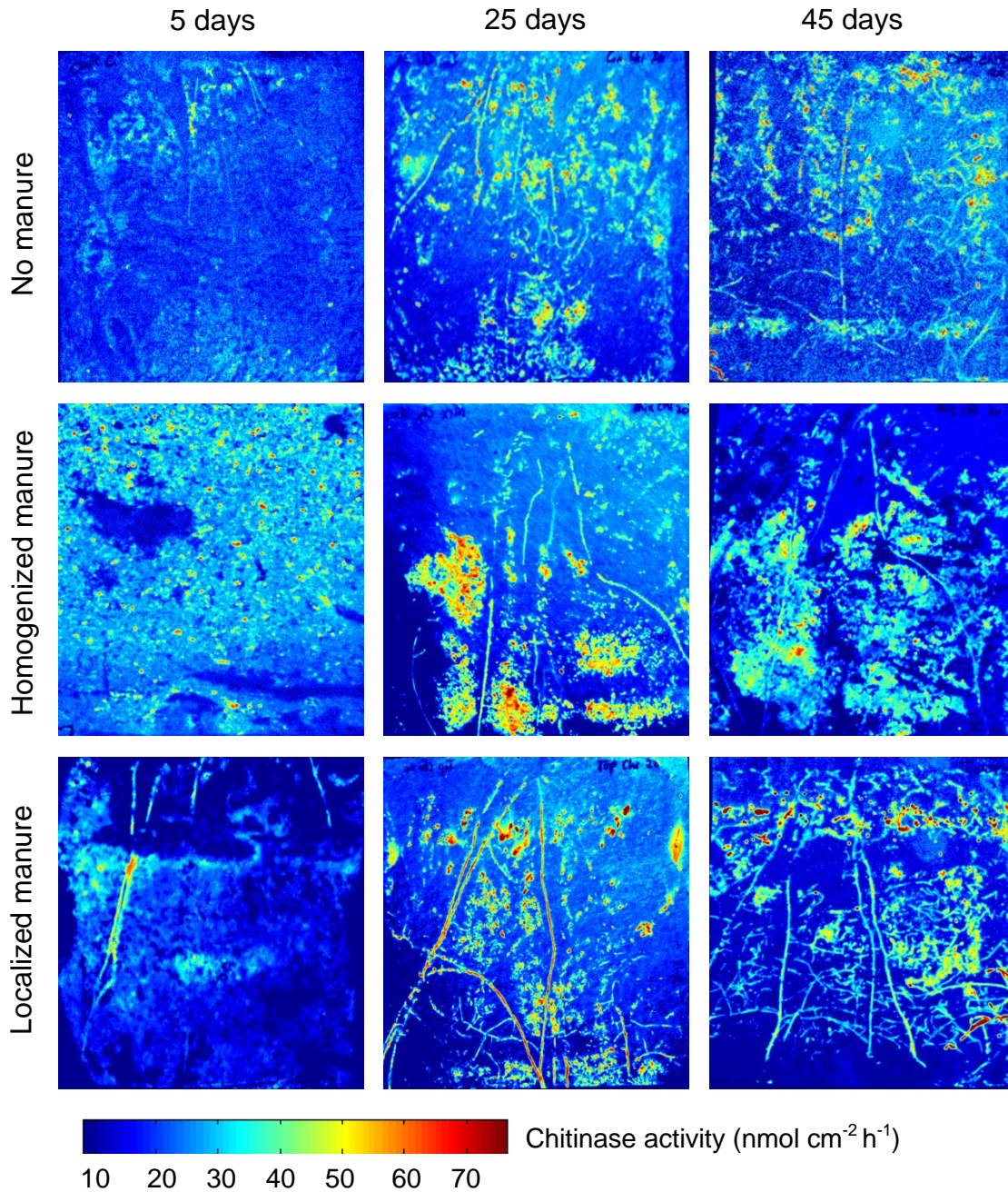


Figure S3 Examples of zymograms for chitinase activity. Three rows represent response of activities to three manure application strategies: 1) No manure, 2) Homogenized manure and 3) Localized manure. Figures from left to right are the measurements at days 5, 25 and 45. We speculated that the higher chitinase activity at the rhizoplane in soil with localized manure at day 25 may be induced by the interactions between roots and mycorrhizal fungi. The color bar corresponds to chitinase activity ($\text{nmol cm}^{-2} \text{h}^{-1}$).

3 Abstracts of additional studies

3.1 The *Kobresia pygmaea* ecosystem of the Tibetan highlands – origin, functioning and degradation of the world’s largest alpine pastoral ecosystem

Submitted to *Ecological Monographs*

Georg Mieke¹, Per-Marten Schleuss², Elke Seeber^{1,3*}, Yun Wang³, Lukas Lehnert¹, Tobias Biermann⁴, Wolfgang Babel⁵, Johannes Ingrisich⁶, Tobias Gerken⁷, Sandra Willinghöfer⁸, Silke Hafner², Sebastian Unteregelsbacher⁹, **Shibin Liu**², Maika Holzapfel¹⁰, Heinz Coners⁸, Sabine Mieke¹, Christoph Leuschner⁸, Georg Guggenberger¹¹, Yakov Kuzyakov^{2,12,13}, Xingliang Xu^{2,14}, Sandra Spielvogel^{2,15}, Thomas Foken⁵, Hans-F. Graf¹⁶, Yaoming Ma¹⁷, Yongping Yang¹⁸, Shuren Zhang¹⁹, Henry J. Noltie²⁰, Lars Opgenoorth²¹, Joachim Schmidt²², Martin Braendle²¹, Zhongping Lai²³, Volker Mosbrugger¹⁰, Fahu Chen²⁴, Jianquan Liu²⁵, Karsten Wesche^{3,26}

¹ Philipps-University of Marburg, Faculty of Geography, Marburg, Germany

² University of Göttingen, Department of Soil Science of Temperate Ecosystems, Göttingen, Germany

³ Senckenberg Museum Görlitz, Department of Botany, Görlitz, Germany

⁴ Lund University, Centre for Environmental and Climate Research, Lund, Sweden

⁵ University of Bayreuth, Department of Micrometeorology, Bayreuth, Germany

⁶ University of Innsbruck, Institute of Ecology, Innsbruck, Austria

⁷ Montana State University, Department of Land Resources and Environmental Sciences, Bozeman, MT, USA

⁸ University of Göttingen, Department of Plant Ecology and Ecosystem Research, Göttingen, Germany

⁹ Institute of Meteorology and Climate Research, Atmospheric Environmental Research (IMK-IFU), Karlsruhe Institute of Technology (KIT), Garmisch-Partenkirchen 82467, Germany

¹⁰ Senckenberg Research Institute and Natural History Museum, 60325 Frankfurt am Main, Germany

¹¹ Leibniz Universität Hannover, Institute for Soil Science, Hannover, Germany

¹² University of Göttingen, Department of Agricultural Soil Science, Göttingen, Germany

¹³ Institute of Environmental Sciences, Kazan Federal University, Kazan, Russia

¹⁴ Chinese Academy of Sciences, Institute of Geographical Sciences and Natural Resources Research, Beijing, China

¹⁵ University of Bern, Institute of Geography, Soil Science, Bern, Switzerland

¹⁶ University of Cambridge, Department of Geography, Centre for Atmospheric Science, Cambridge, United Kingdom

¹⁷ Chinese Academy of Sciences, Institute of Tibetan Plateau Research, Key Laboratory of Tibetan Environment Changes and Land Surface, Processes, Beijing, China

¹⁸ Chinese Academy of Sciences, Institute of Tibetan Plateau Research, Laboratory of Alpine Ecology and Biodiversity, Beijing, China

¹⁹ Chinese Academy of Sciences, Laboratory of Systematic and Evolutionary Botany, Institute of Botany, Beijing, China

²⁰ Royal Botanic Garden Edinburgh, Edinburgh, United Kingdom

²¹ Philipps-University of Marburg, Department of Ecology, Marburg, Germany

²² University of Rostock, Institute of Biosciences, General and Systematic Zoology, Rostock, Germany

²³ China University of Geosciences, State Key Lab of Biogeology and Environmental Geology, School of Earth Sciences, Wuhan 430074, China

²⁴ Lanzhou University, MOE Key Laboratory of West China’s Environmental System, School of Earth and Environment Sciences, Lanzhou, China 730000

²⁵ Lanzhou University, State Key Laboratory of Grassland Agri-ecosystem, College of Life Science, Lanzhou, China 730000

²⁶ German Centre for Integrative Biodiversity Research (iDiv) Halle–Jena–Leipzig, Germany

3.1.1 Abstract

Kobresia pastures in the eastern Tibetan highlands occupy an area of 450000 km² and form the world's largest pastoral alpine ecosystem. The main constituent is an endemic dwarf sedge, *Kobresia pygmaea*, which forms a lawn with a durable turf cover anchored by a felty root mat, and occurs from 3000 m to nearly 6000 m a.s.l. The existence and functioning of this unique ecosystem and its turf cover have not yet been explained against a backdrop of natural and anthropogenic factors, and thus its origin, drivers, vulnerability or resilience remain largely unknown. Here we present a review on ecosystem diversity, the reproduction and ecology of the key species, pasture health, cycles of carbon (C), water and nutrients, and on the paleo-environment. The methods employed include molecular analysis, grazing exclusion, measurements with micro-lysimeters and gas exchange chambers, ¹³C and ¹⁵N labelling, eddy-covariance flux measurements, remote sensing and atmospheric modelling.

The following combination of traits makes *Kobresia pygmaea* resilient against disturbance and highly competitive under grazing: dwarf habit, predominantly below-ground allocation of photoassimilates, mixed reproduction strategy with both seed production and clonal growth, and high genetic diversity. For an unknown period *Kobresia* pastures have been co-limited by low rainfall during the short growing season and livestock-mediated nutrient withdrawal. Overstocking has caused pasture degradation, yet the extent remains debated. In addition to the grazing-driven changes, we newly describe natural autocyclic processes of turf erosion initiated through polygonal cracking of the turf cover, and increased by soil-dwelling endemic small mammals. The major consequences of the deterioration of the vegetation cover and its turf include: (1) the release of large amounts of C and nutrients and earlier diurnal formation of clouds resulting in decreased surface temperatures with likely consequences for atmospheric circulation on large regional and, possibly global, scales.

Paleo-environmental reconstruction, in conjunction with grazing experiments, suggests that the present grazing lawns of *Kobresia pygmaea* are synanthropic since the onset of pastoralism. The traditional migratory rangeland management was largely sustainable and possibly still offers the best strategy to conserve, and possibly increase, the C stocks in the *Kobresia* turf, as well as its importance for climate regulation.

Keywords: alpine meadow, alpine plant ecology, carbon cycle and sequestration, grazing ecology, hydrological cycle, *Kobresia pygmaea*, nutrient cycle, Paleo-environment, Qinghai-Tibet Plateau, rangeland management.

Corresponding author: Elke Seeber, seeber.elke@gmx.net

3.2 Mechanisms and consequences of Tibetan grassland degradation

In preparation for resubmission to *Nature Geoscience*

Per-Marten Schleuss¹, Lukas Lehnert², Georg Miehe², Felix Heitkamp³, Elke Sebeer^{2,4}, **Shibin Liu¹**, Yun Wang⁴, Sandra Spielvogel⁵, Xingliang Xu⁶, Karsten Wesche⁴, Jörg Bendix², Georg Guggenberger⁷ and Yakov Kuzyakov^{1,8*}

¹. Department of Soil Science of Temperate Ecosystems, University of Göttingen, Büsgenweg 2, 37077 Göttingen, Germany

². Faculty of Geography, University of Marburg, Deutschhausstraße 10, 35032 Marburg, Germany

³. Section of Physical Geography, Faculty of Geoscience and Geography, Georg-August-Universität Göttingen, Goldschmidt Straße 5, 37077 Göttingen, Germany

⁴. Department of Botany, Senckenberg Museum Görlitz, Am Museum 1, 02826 Görlitz, Germany

⁵. Institute of Geography, University of Bern, Hallerstraße 12, 3012 Bern, Switzerland

⁶. Key Laboratory Ecosystem Network Observation and Modeling, Institute of Geographic Science and Natural Resources Research, Chinese Academy of Science, 11A Datun Road, 100101 Beijing, China

⁷. Institute of Soil Science, Leibniz University of Hannover, Herrenhäuser Straße 2, 30419 Hannover, Germany

⁸. Department of Agricultural Soil Science, University of Göttingen, Büsgenweg 2, 37077 Göttingen, Germany

3.2.1 Abstract

Kobresia grasslands store tremendous amounts of soil organic carbon (SOC), are an important grazing ground for local herdsman, host a major portion of the regional terrestrial biodiversity, and supply large areas of SE Asia with water – all threatened by large-scale soil degradation on the Tibetan Plateau. Nonetheless, the patterns and mechanisms of pasture degradation, visible across the entire Tibetan Plateau, remain unknown.

Here we (a) provide a novel degradation concept combining anthropogenic and natural impacts and (b) demonstrate the mechanisms for associated SOC loss. We show that soil drought and frost lead to polygonal cracking of the *Kobresia* turf, already weakened by overgrazing. This induces gradual erosion by wind and water, extends the cracks and removes the upper carbon-enriched soil. Erosion-derived SOC loss amounts to 5 kg C m⁻² and is aggravated by decreasing root C-input and increasing SOC mineralization (ca. 2.5 kg C m⁻² combined). Mineralization-driven SOC loss was reflected in a negative δ¹³C shift of SOC going from intact to severely degraded stages, and was caused by a relative enrichment of ¹³C-depleted lignin. In sum, degradation triggered high SOC loss from this ecosystem with profound consequences for carbon sequestration, atmospheric CO₂, water quality and ecosystem stability.

Corresponding author: Yakov Kuzyakov, kuzyakov@gwdg.de

Appendix

Curriculum vitae

Name: Shibin Liu **Email:** sliu3@gwdg.de **Tel:** +49 157 5118 4720

Date of Birth: 02.04.1987 **Place of Birth:** Xinxiang **Nationality:** China

Education career:

2013 - 2017: PhD student, Georg-August-University of Göttingen, Germany;

2010 - 2013: MSc. student, Northwest Agricultural and Forestry University, China;

2006 - 2010: BSc. student, North China University of Water Resources and Electric Power, China;

2002 - 2006: High school period

Expertise:

Nutrient cycling in soil, C sequestration, Zymography, Isotope labelling, Enzyme activities, Soil hydraulic properties analyses, Statistical analyses

Publications/Presentations:

Liu S.B.*, Schleuss P.-M., Kuzyakov Y. 2016. Carbon and nitrogen losses from soil depend on degradation of Tibetan *Kobresia* pastures. *Land Degradation & Development* (Impact factor: 8.1), DOI: 10.1002/ldr.2522.

Razavi B.S.*, Liu S.B.*, Kuzyakov Y. 2017. Hot experience for cold-adapted microorganisms: temperature sensitivity of soil enzymes. *Soil Biology & Biochemistry* (Impact factor: 4.1), 105: 236-243. DOI: 10.1016/j.soilbio.2016.11.026.

Liu S.B.*, Schleuss P.-M., Kuzyakov Y. 2017. Responses of degraded Tibetan *Kobresia* pastures to N addition. *Land Degradation & Development* (Impact factor: 8.1), DOI: 10.1002/ldr.2720.

Liu S.B.*, Razavi B.S., Su X., Maharjan M., Blagodatskaya E., Kuzyakov Y. 2017. Spatio-temporal patterns of enzyme activities after manure application reflect mechanisms of niche differentiation between plants and microorganisms. *Soil Biology & Biochemistry* (Impact factor: 4.1), 112:100-109.

Liu S.B., Li Y.*, He C.S., 2013. Spectral analysis and estimations of soil salt and organic matter contents. *Soil Science*, 178, 138-146.

Li Y.*, Liu S.B., Liao Z.H., He C.S., 2012. Comparison of two methods for estimation of soil water content from measured reflectance. *Canadian Journal of Soil Science*, 92(6), 845-857.

Liu S.B.*, Li Y., Robert H., 2013. Hydraulic parameters and horizontal infiltration characteristics of hydrophobic soils, 31 (11), 1000-1006. (in Chinese with English abstract)

Liu S.B.*, Schleuss P.-M., Zamanian K., Zarebanadkouki M., Kuzyakov Y. 2017. Degradation of Tibetan grasslands: Consequences for carbon and nutrient cycles. *Agriculture, Ecosystems and Environment* (submitted).

Conference papers:

Liu S.B., Schleuss P.M., Kuzyakov Y. 2016. *Kobresia pygmaea* pasture degradation and its response to increasing N deposition. *Geophysical Research Abstracts*, 18: 10071. **(oral presentation)**

Liu S.B., Schleuss P.M., Kuzyakov Y. 2015. Rewetting effects on soil CO₂ flux and nutrients leaching in alpine *Kobresia* pasture on the Tibetan Plateau. *Geophysical Research Abstracts*, 17: 733. **(poster presentation)**

Liu S.B., Razavidezfuly B., Kuzyakov Y. 2016. Hot experience for cold-adapted microorganisms: temperature sensitivity of soil enzymes. *Geophysical Research Abstracts*, 18: 6922. **(poster presentation)**

Liu S.B., Schleuss P.M., Kuzyakov Y. 2017. Degradation of Tibetan grasslands: Consequences for soil organic carbon and nutrients losses. *Geophysical Research Abstracts*, 19: 16372. **(oral presentation)**



(Signature)

25/07/2017

(Date)

Declarations

1. I, hereby, declare that this Ph.D. dissertation has not been presented to any other examining body either in its present or a similar form.

Furthermore, I also affirm that I have not applied for a Ph.D. at any other higher school of education.

Göttingen,

.....

(Signature)

2. I, hereby, solemnly declare that this dissertation was undertaken independently and without any unauthorized aid.

Göttingen,

.....

(Signature)